Fachbereich Chemie der Universität Dortmund

4´-Methylterpyridine, 1-Deazaadenine and 1-Deazapurine as Potential Artificial Nucleobases for Metal-Mediated Base Pairing

Fabian-Alexander Polonius

Dem Fachbereich Chemie der Universität Dortmund
zur Erlangung des akademischen Grades eines
Doktors der Naturwissenschaften
vorgelegte Dissertation.

Referent:	Prof. Dr. Bernhard Lippert
Korreferent:	PD Dr. Andrea Erxleben
Tag der mündlichen Prüfung:	11/08/2006

In the time from August 2002 till August 2006 this work came into being at the Lehrstuhl für Anorganische Chemie III des Fachbereichs Chemie der Universität Dortmund.

My appreciation and my thanksgiving belong to

Dr. Jens Müller

and

Prof. Dr. Bernhard Lippert

for taking care of my scientific advance,
for the academic and human engagement, commitment and cooperation.

I thank PD Dr. Andrea Erxleben for taking over the part of the second examiner.

Further I thank greatly:

- Dr. Gabriele Trötscher-Kaus to tear apart my thesis in record time (Do not worry, I put it back together! By the way, I owe you a dinner!),
- the unique Dipl. Chem. Dominik Böhme for being the indescribable "Domme"
- my trainees, Sonja Humpert and Jacqueline Ksienczyk, for their help in the laboratory, especially Jacqueline Ksienczyk, who has done a splendid job,
- my research trainees, Oliver Gerbersmann, Frank Hölter, Philipp von Grebe, Dominik Megger and Martina Gatys, for their scientific (social) contribution,
- group assistant, Nicole Düpre (Good luck on my desk and keep Dommes heart beating at a low rate!),
- Michaela Markert and Birgit Thormann for their help and the funny conversations,
- all the members of the working group for the interesting conversations,
- the ex-members Dr. Martita and Dr. Pablo,
- Christine Klimek, Alex Klauke, Christian Nowak and Thorsten Grund,
- Markus Hüffner for carrying out the elemental analyses,
- Lcda. con grado Maria Elisa Gil Bardaji, Dr. Eva Freisinger and Dr. Michael Roitzsch for measuring and solving my crystal structures,
- Prof. Dr. Burkhard Costisella, Annette Danzmann and Christa Nettelbeck for the vast amount of NMR measurements,
- PD Dr. Claus Czeslik und Dr. Dahabada Lopes for their help with the CD-spectroscopy measurements,
- Dipl. Chem. Patrick Lax for the DFT-calculations,
- the Niemeyer group for their rapid response when I ring the bell (and the good conversations with the girls),
- my team from the most successful teamsport in German history (for sometimes giving me a break),
- Björn, Matze, Samuel and the Doc,
- my girl friend Myriam and my family for their continuous support, help and love.

I shall walk with strength, power and confidence,

to put down my own special footprint on this earth

and to help and teach others,

to listen to and to follow

the ideas of respect, freedom and love.

And soon they will walk themselves

with strength, power and confidence,

so that they may step into my footprint

and make it bigger.

This work is dedicated to

Jan-Felix Polonius and Sarah Teichmann

on the occasion of their marriage.

Table of Contents

A Introduction

B Aim

C Results and Discussion

Chapter I

Chapter II

Abbreviations

A (C, G, T)	Adenine- (cytosine-, guanine- and thymine-) derivatives
AMA	Ammonia/Methylamine
br	broad
n-BuLi	n-Buthyllithium
c	concentration
χ	mole fraction
CD	Circular Dichroism
d	doublet
δ	chemical shift
DFT	Density Function Theory
DMAP	4-Dimethylaminopyridine
DMSO-d_6	Deuterated dimethylsulphoxide
DMTr	4,4´-Dimethoxytrityl
DNA	2´-Deoxyribonucleic acid
ε	extinction coefficient /elipticity
ESI-MS	Electo Spray Ionisation Mass Spectrometry
h	hours
HPLC	High-Pressure(Performance)-Liquid Chromatography
IUPAC	International Union of Pure and Applied Chemistry
LDA	Lithium diisopropylamine
m (NMR)	multiplet
MeDP	Methyldeazapurine or 1-deaza-9-methylpurine
MHz	Mega Hertz
1-mimi	1-methylimidazole
m	mass
M	Molar mass
MALDI-TOF	Matrix-Assisted Laser Desorption/Ionisation Time-Of-Flight
min	minutes

M^{n+}	M = metal and n =charge of the metal
MOPS	4-Morpholinepropanesulfonic acid
1-mtet	1-methyltetrazole
1-mtetate	1-methyltetrazolate
NMR	Nuclear Magnetic Resonance
NOESY	Nuclear Ovehauser Enhancement Spectroscopy
ppm	parts per million
q	quartet
RNA	Ribonucleic acid
r.t.	room temperature
s	singulet
TEEA	Triethylammonium acetate
TLC	Thin Layer Chromatography
TMS	Tetramethylsilane
TSP	Sodium-3-(trimethylsilyl)-propanesulfonate
trpy	2,2´:6´,2´´-Terpyridine
T	Temperature
T_m	Melting temperature
UV	Ultraviolet
Vis	Visible

A Introduction

1 DNA

The DNA (2´-deoxyribonucleic acid) exists of two complementary strands[1-3] that bind together through π-stacking and H-bonding as the two stabilising forces. These two strands are not linear, but are twisted into a helix. A single strand consists of chains of five-membered-ring sugars linked by phosphate groups, the so called sugar phosphate backbone. The anomeric carbon of each sugar is connected to a N of a nucleobase by a β-glycosidic linkage. The backbone on the outside is wrapped around the nucleobases in the inside.[4-7]

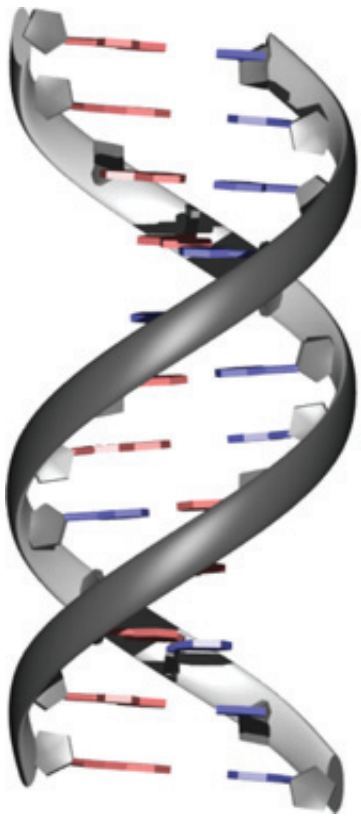

Figure 1: Example of a DNA structure; blue and red represent nucleobases, grey the sugar phosphate backbone.[7]

There are only four bases in DNA: adenine (A), cytosine (C), guanine (G) and thymine (T). A and G are substituted purines and C and T are substituted pyrimidines and they are linked to the sugar over N9 and N1, respectively. It should be mentioned that RNA (ribonucleic acid) differs from DNA by one additional OH-group at the 2´-position of the sugar and RNA has uracil as base instead of thymine. Uracil does not possess a CH_3-group at the 5-position in comparison to thymine.

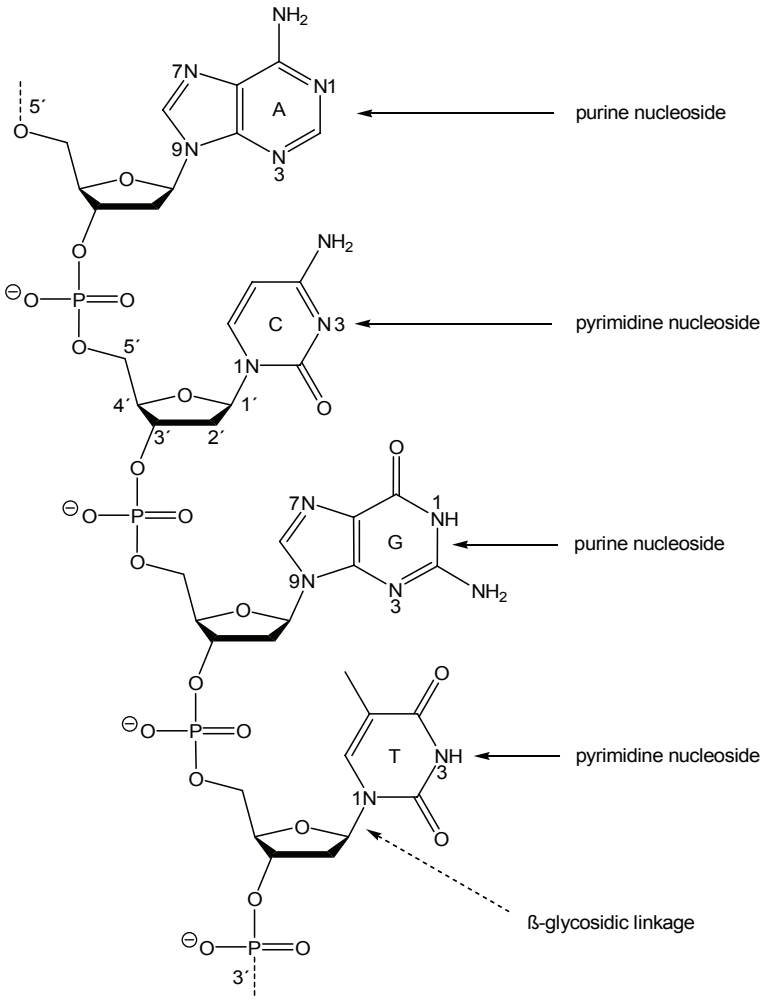

Figure 2: Schematic diagram of an oligonucleotide strand with the four natural nucleobases found inside DNA.

The Watson-Crick base pairs[1] are shown in Figure 3. It can be seen that A-T forms two and C-G three hydrogen bonds. The base pairs are planar. It should be noticed that the H-bonds that hold the base pairs together are all of a length of about 2.9(1)Å.

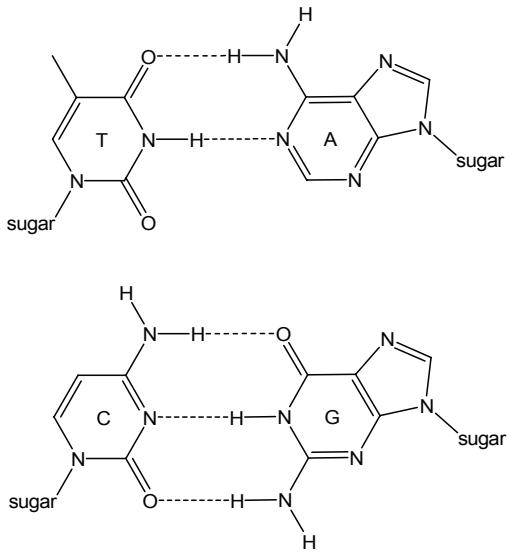

Figure 3: Watson-Crick base pairing of the four natural nucleobases.

There are additional stacking interactions that are stronger between two purines than two pyrimidines. Important for this, again, is the planarity of the base pairs. Although these are very weak interactions, when added together they have a large contribution to the stability. There are also other sides, where the base pairing on the nucleobases can take place, such as the Hoogsteen side[8,9] shown in Figure 4 for an A-T base pair.[4-7]

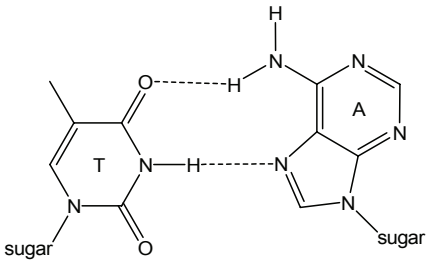

Figure 4: Hoogsteen base pairing of two natural nucleobases.

Each strand has a direction, for example, 5´ to 3´ or 3´ to 5´. Always A-T and C-G base pairs are formed, but the direction of the single strands in a double helix can be parallel (5´-3´and 5´-3´) or anti parallel (5´-3´and 3´-5´), as usually found in natural DNA. There are also two kinds of grooves because of the backbone twisting around

the nucleobases in the inside. They are called major and minor groove. These grooves are used by enzymes, proteins, metals and many more as docking station to get to the inside of the DNA or only to stabilise the backbone.

There are some common types of naturally occurring DNA: A-DNA, B-DNA and Z-DNA. Next to those other helical forms exist. The A- and B-DNA are right-handed helices, the Z-DNA is left-handed. The B-DNA is the most common form in living organisms and in aqueous solution. For A-DNA nonpolar solvents and for Z-DNA regions with a high content of G-C base pairs are necessary. A-T base pairs have a highly destabilising effect for the formation of Z-DNA. The Z-DNA is longer and thinner than the B-DNA, which itself is longer and slightly thinner than A-DNA. Helices in general can be looked at by the amount of bases per 360° turn, which is also a measure for the π-stacking interactions, and the diameter of the double helix, which gives rise to the thickness of the helix and the space present for an H-bonding pair.

A-DNA	**B-DNA**	**Z-DNA**
right handed	right handed	left handed
26Å diameter	20Å diameter	18Å diameter
2.9Å helix rise	3.4Å helix rise	3.7Å helix rise
11 bases/turn	10 bases/turn	12 bases/turn

Table 1: Common helical forms and their structural properties.[7]

Next to the double helices, higher order structures such as triple and quadruple helices are also found in nature. The resolution of DNA structures in general is done via NMR and X-ray diffraction methods, though this is not always trivial and does not always lead to the wanted accurate results. Another important fact is that DNA, a polynucleotide, is also a polyanion, due to the negative charges on the phosphates. This negative charge can be compensated by polyamines or through metal ions by the counter-ion condensation.[7] Water molecules are also present through the spin of hydration in the minor groove and can surround positions at the nucleobases and the phosphate groups. For the formation of Z-DNA metal ions, such as Mg^{2+}, are also of

great importance, since they stabilise the structure greatly. In general, soft metals tend to coordinate to the nucleobases (N-positions), whereas hard metals usually bind to the backbone (O-positions).

The organism's complete genetic information is stored and the growth and the division of the cell are controlled by DNA. Its highly specific self association is one interesting aspect for scientists. DNA has a potential as template for preparations of newly functionalised molecular architecture and bioinorganic and organic nano building blocks. Nowadays sciences find more uses for DNA, one example are the DNAzymes.[10]

Historical background:[4-6]

The DNA was first isolated in 1869 from the nuclei of white blood cells and because it was found to be acidic, it was called nucleic acid. Around 1900 it was possible to define nucleic acids as containing four different nucleotides. These could each get divided into phosphate, sugar and heterocyclic base. Although it was found a few years later that all nuclei of cells contained DNA, it took until 1944 to conclude that the DNA was a carrier of genetic information. At that time it was also found by Chargaff that the amount of a certain nucleobase present was dependent on another nucleobase being present; A = T and C = G. This was a first indication of complementarities. Also Pauling published his DNA model in 1953 before Watson and Crick[1], the latter came the nowadays excepted model very close. The proposed structures were underlined by crystallography findings by Wilkins[2] and Franklin[3]. It shall be mentioned that while Watson had his PhD already for two years, Crick was a graduate student while he worked at the prior work that brought Watson, Wilkins and him the Nobel Prize in 1962. Then the scientific interest became greater and in 1957 the triple helix and in 1962 the quadruple helix were postulated. Hoogsteen[8,9] suggested in 1959 additionally to the Watson-Crick base pairing a different way of base pairing, named after him. In 1999 the first pentaplex was published, though it was synthesised and not found in nature.[7]

2 Modifications of DNA

Due to the fascinating properties of DNA scientists are not only interested in understanding more about DNA, but also to copy the properties for their own purposes. Therefore many scientists have been working on modifying DNA to obtain more interesting and useful properties, but also to further understanding of its behaviour. As already mentioned, a nucleotide contains a phosphate, a sugar and a nucleobase unit. These are the first three categories of DNA modifications:

I Modifications on the phosphate backbone:

The phosphate backbone can be modified by substitution of an O atom with a CH_3 group or an S atom. Both free O atoms can also be substituted by S atoms. Modifications can alter the negative charge at the backbone of an oligonucleotide. Having a CH_3 group present instead of an O atom, deletes the negative charge on the backbone. This oligonucleotide is no longer a polyanion. Also S is a softer atom than an O atom and might bind different metals or avoid the binding to metals, which would have been bound by the O atom.

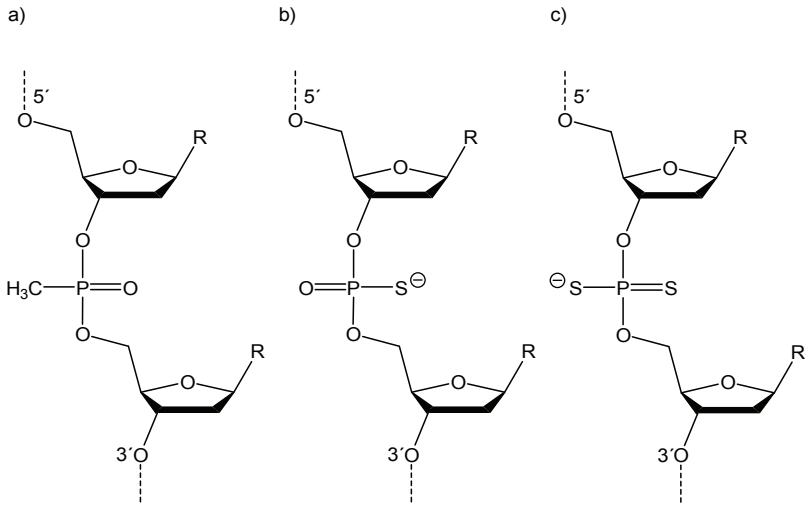

Figure 5: Modifications at the phosphate backbone: a) Substitution of an O atom by a CH_3 group, b) an O atom by a S atom, c) two O atoms by two S atoms (R = a base).

II Modifications on the sugar:

The five-membered-ring sugar can be modified by adding groups at the free 2´- or 4´-positions,[11] substituting the O atom in the ring by an S atom or by a NH_2 functional group[12] or by replacing the 3´-OH or 5´-OH groups by thiol, amine or alkylthiol functional groups.[13,14] Adding a $SeCH_3$ group, for example, at the 2´-position can be used for improved X-ray crystallography measurements.[15]

Next to the simple changes in atoms there are some interesting changes in bonds and other structural features that can be used for modifications. The TNA, threofuranosyl nucleic acid by Eschenmoser,[16,17] that is a simple nucleic acid derived from a tetrose sugar has been shown to support Watson-Crick base pairing, to form antiparallel duplexes and to crosspair with DNA and RNA. Simplification of the sugar phosphate backbone to improve the synthetic accessibility of artificial duplexes while containing the properties is the aim. The introduction of a C_3-backbone instead of the sugar ring was found to be of great stability.[18-20] It is called GNA, glycol nucleic acid, and the thoughts that a duplex needs a sugar ring for helix formation are proved wrong.

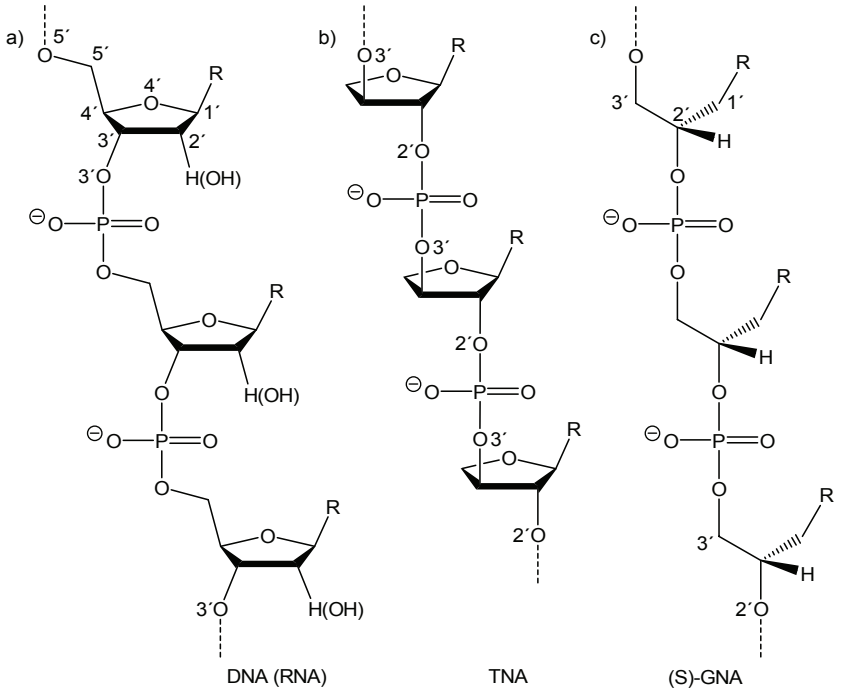

Figure 6: Modifications on the sugar unit of a) DNA (RNA): b) TNA and c) (S)-GNA (R = a base), numbering in analog to a) and b).[18]

One interesting substitution of the complete sugar phosphate backbone is done in so called PNA, peptide nucleic acid. As can be seen in Figure 7, the sugar phosphate backbone is replaced by a peptide, an amino acid chain. The two chains are held together by C-G base pairs and by four histidines coordinating a metal ion.[21] With Zn^{2+} a melting point and double strand formation were observed. For Cu^{2+}, however, only bonding to two histidines of one strand and therefore no double strand formation could be observed. By now, many examples of PNA, with and without metal ions coordinating, are known.[22-25]

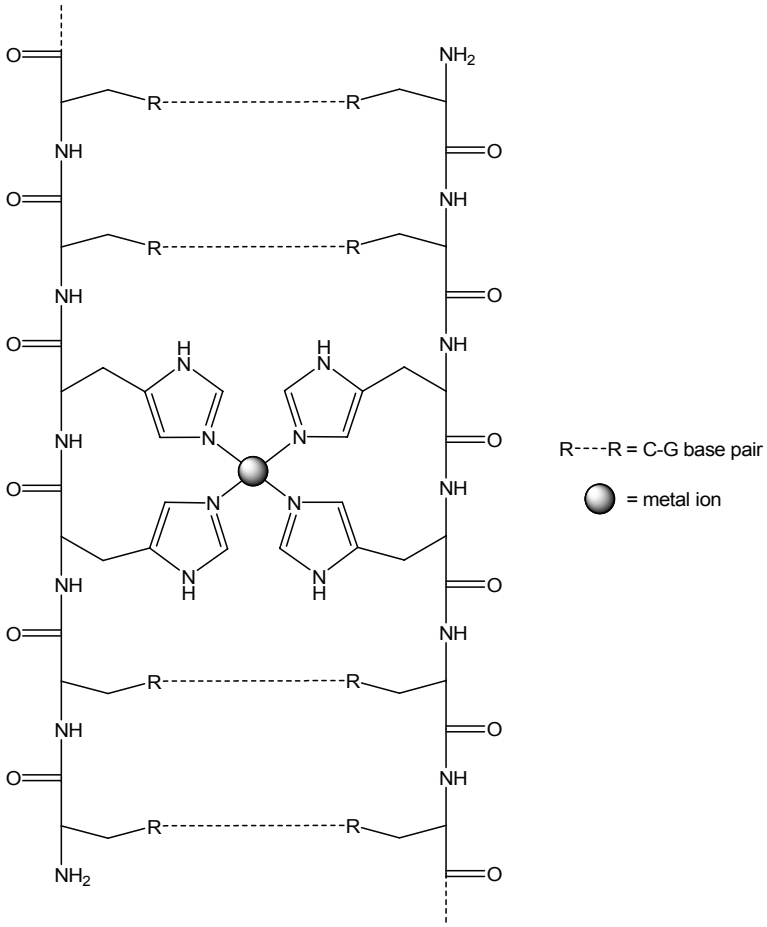

Figure 7: Idealised representation of two strands based on a peptide backbone connected via four C-G base pairs and four histidines binding one metal ion.[21]

There are other examples of complete substitution of the backbone using chains of mostly aromatic organic molecules to bring the base pairs in the right position for binding. H-bonding base pairs are formed, but the backbone is not necessarily twisted around the nucleobases.[26-29]

III Modifications on the nucleobase:

The third modification region are the nucleobases that can be divided in three categories of modifications on the nucleobases.[30-32] The first category is the simple modification of the four natural nucleobases by adding or substracting functional groups. The actual H-bonding and the π-stacking interactions, as stabilising forces, are not changed.

One example of this modification is the extension of natural nucleobases by fusion with a benzo ring and therefore the increase in size of the formed double helix.[33-36] Due to the increase in size of the nucleobases and the raised strain in the backbone, the oligonucleotides turned out to be less stable than unmodified oligonucleotides with the same sequence of natural nucleobases, if the base pairing partner is another nucleobase with increased size. The opposite is the case, if the base pairing partner is a natural nucleobase.

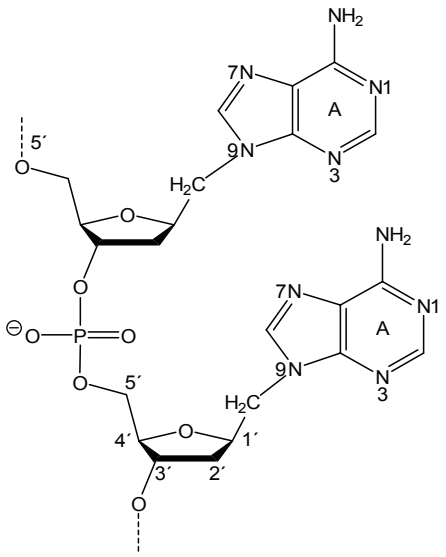

Figure 8: Introduction of a methylene group between the sugar ring and the base.[37]

Another example is the extension of the glycosidic bond between the sugar ring and the nucleobase by a methylene group, as can be seen in Figure 8.[37] This imposes an extra degree of conformational flexibility in comparison to the normal glycosidic bond being present.

Exchanging the N atom at the 3-position in an adenine with a C atom and adding a NO_2-group at that 3-position lead to other interesting properties of modified natural nucleobases.[38] The melting behaviour and the stability of an oligonucleotide containing such a modified adenine nucleobase differ only marginal from an oligonucleotide containing adenine itself. Though, the NO_2 group was shown to allow photo induced strand cleavage.
Many other modifications on the functional groups of natural nucleobases can be found in the literature.[39-42]

The second modification of nucleobases is the replacement of important functional groups (NH_2 or CO) of natural nucleobases by the substitution of those functional groups or by the introduction of artificial nucleobases.[43,44]
Taking for example an indole nucleoside and introducing it into a self complementary oligonucleotide the formation of a stable duplex was observed. The introduction of a fluorinated hydrocarbon gave an even more stable double helix. This shows that not only H-bonding is important for double helix formation and stability. Also π-stacking interactions, although a weak stabilising force, can have a high contribution to the stability, when many of them are present without interruption.

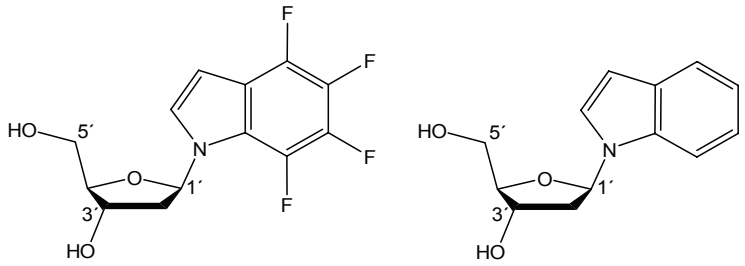

Figure 9: An example of artificial nucleobases that can be introduced into DNA; in the benzo ring fluorinated indole nucleoside and indole nucleoside (on the left and the right, respectively).[43,44]

Many other examples of this modification type can be found in the literature.[20,45-49] These are mainly artificial nucleosides with large aromatic systems. A high amount of π-stacking ability is present in those systems and therefore these systems have

been used as opposites for abasic sites. Although there is no possibility of H-bonding, the large aromatic systems can contribute with their large amount of π-stacking interactions to the stabilisation forces that are responsible for the formation of a double helix of two oligonucleotides.[50] These aromatic systems can be larger than a natural nucleobase, when present opposite an abasic site, since more space is available.

The third modification of nucleobases is reached through the introduction of a third stabilising interaction, the metal ion ligand interaction, hence the formation of metal-mediated base pairs. By designing completely new nucleobases, by extending natural nucleobases by functional groups or by using natural nucleobases, metals can be brought into the inside of oligonucleotides, forming double helices.[30,31] A possible [1+1]-, [2+2]- and [3+1]-coordination of the metal ion has been found to be successful. In Figure 10 an example of a [3+1]-coordination is shown.[51] Introduction of pyridine-2,6-dicarboxamide and pyridine as artificial nucleobases in opposite positions in two complementary oligonucleotide strands and addition of Cu^{2+} as metal ion showed an increase in stabilisation of the double helix structure. The melting temperature was even higher by introducing four artificial nucleobases in a row into two complementary strands.

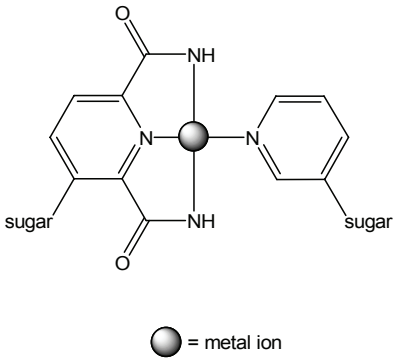

Figure 10: The tridentate pyridine-2,6-dicarboxamide and the monodentate pyridine nucleobase build a metal-mediated base pair in the presence of Cu^{2+}.[51]

Another example of metal-mediated base pairing is shown in Figure 11.[52] By exchanging the NH_2 group of an adenine with a pyridine, a 6-(2´-pyridyl)-purine

metallo base pair could be formed with Ni^{2+} selectively inside a double helix. A stabilisation of the double helix structure by an increase in melting temperature of 6°C was observed. This is an example of changing a functional group of the adenine nucleobase for the purpose of introducing a M^{n+} inside two complementary oligonucleotides forming an helix.

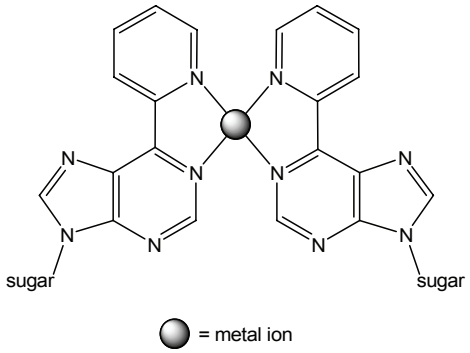

Figure 11: The two bidentate 6-(2´-pyridyl)-purine nucleobases form a metallo base pair with Ni^{2+}.[52]

The use of a metal-mediated base pair in a double helix to form a catalyst that is used for many organic reactions can be seen in the example in Figure 12.[53]

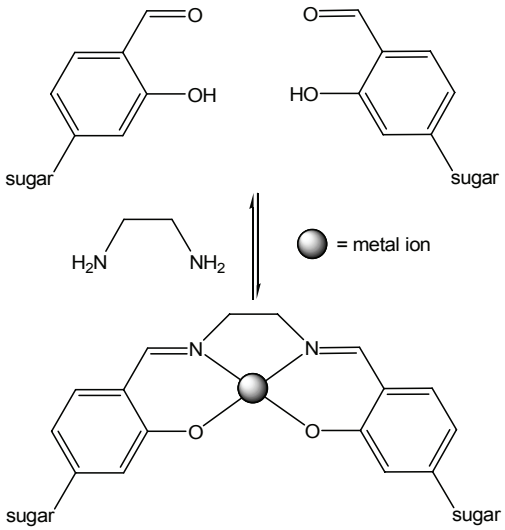

Figure 12: Formation of a metal-salen base pair.[53]

The artificial nucleobases can only build a metal-salen base pair upon the addition of two components, the ethylene diamine and Cu^{2+} or Mn^{2+}. A Schiff-base is formed and the reaction is reversible in water. Through the formation of this metal-mediated base pair the double helix of the two complementary oligonucleotides is highly stabilised.

Many other examples of artificial nucleobases that have been brought forward as possible candidates for the introduction into an oligonucleotide or that have already been built into oligonucleotides are listed in Figure 13.[54-65] The number of possible artificial nucleobases for metal-mediated base pairing increases steadily.

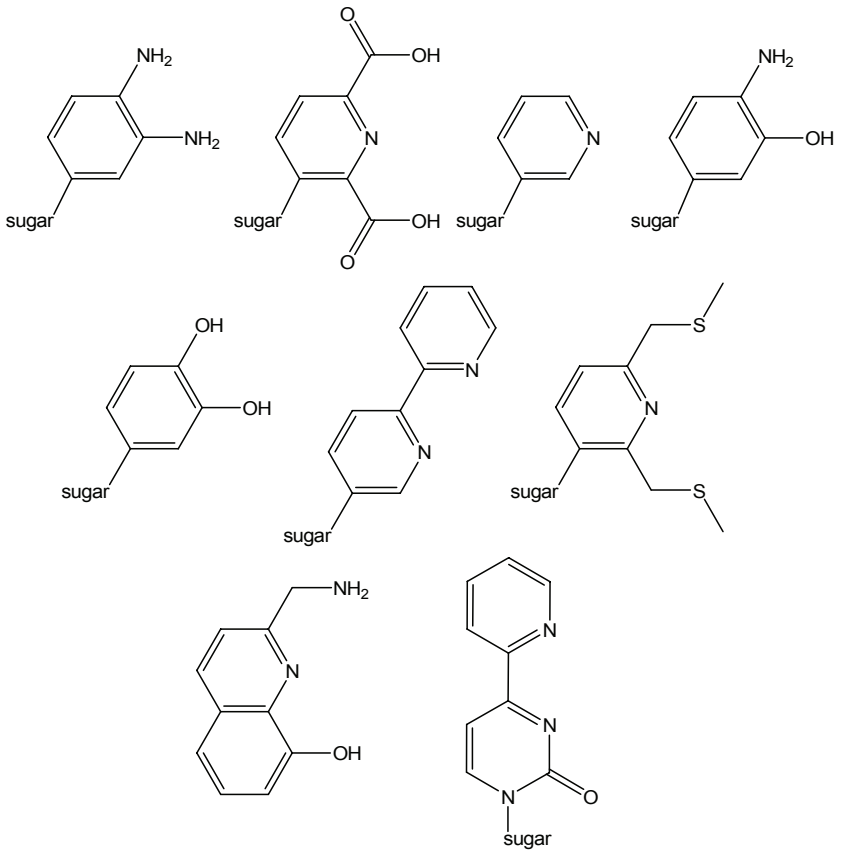

Figure 13: Examples of possible artificial nucleobases for metal-mediated base pairing from the last six years only. Except one (bottom left) all have been introduced into oligonucleotides.[54-65]

There are some rules that have to be considered when designing new artificial nucleobases for metal-mediated base pairing:[30]

- The artificial nucleobases or modified natural nucleobases need to be of comparable size and form with the natural nucleobases.
- The nucleobases should build planar complexes with the metal ions.
- The artificial nucleobases as chelating donors should have a higher metal affinity to metal ions than natural nucleobases.
- The preparation of the oligonucleotides should be possible with a standardised and automatic method.

These rules are actually more or less important guidelines. For example, the base pairs formed in nature by H-bonding are not always completely planar. Some kind of flexibility is present in the base pairs. This flexibility exists for metal-mediated base pairs, too.

Through the introduction of artificial nucleobases into oligonucleotides that can act as chelating donors and bind metal ions a third stabilising interaction has been found, next to the H-bonding and π-stacking interactions. A third stabilising effect opens up many more possibilities of modifying oligonucleotides and perhaps later DNA, too. The fascinating properties of DNA itself, such as the self association, made scientists become interested in this topic. Through the increasing number of modification possibilities present, one now has to look at the potential uses of artificial nucleobases binding metal ions inside the double helices.

Next to the general interest in gaining a better understanding of interactions inside DNA, the aim is also to use the third stabilising effect to change the properties of oligonucleotides, where it is wanted, without losing existing properties. The possibility of using metal ions to stabilise artificial base pairs means that next to the four naturally occurring nucleobases as building blocks, new building blocks can be introduced. This can result in an enlargement of the genetic alphabet.

The construction of new oligonucleotide structures and functions can lead to interesting magnetic properties.[66,67] In this example, the metal ions show spin-spin interactions, which shows that the metal ions are close to each other (3.7 ± 0.1Å). Figure 14 shows the most metal ions bonded inside a double helix and stacked in a row that has been published by now.

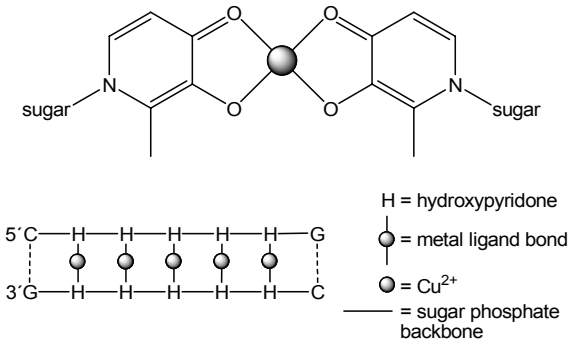

Figure 14: Schematic representation of Cu^{2+}-mediated base pairs inside an anti-parallel double helix.[66,67]

It has to be mentioned that not many examples of metal ions aligned in a linear fashion can be found in solution, unlike in the solid state, where there are many examples. Five Cu^{2+} sit above each other, which is not only giving rise to novel magnetic properties, but also to possible electrical properties of such a double helix. If it is possible to align many metal ions above each other and close enough to each other there should be a possibility of observing electrons moving through the inside of a double helix.[32] So it has been shown that M-DNA, metal ion containing DNA, can have fast electron transfer in comparison to DNA. The first evidence of metalliclike conduction was observed by Rakitin et. al.[68] The introduction of Zn^{2+} into A-T and C-G base pairs is shown in Figure 15.

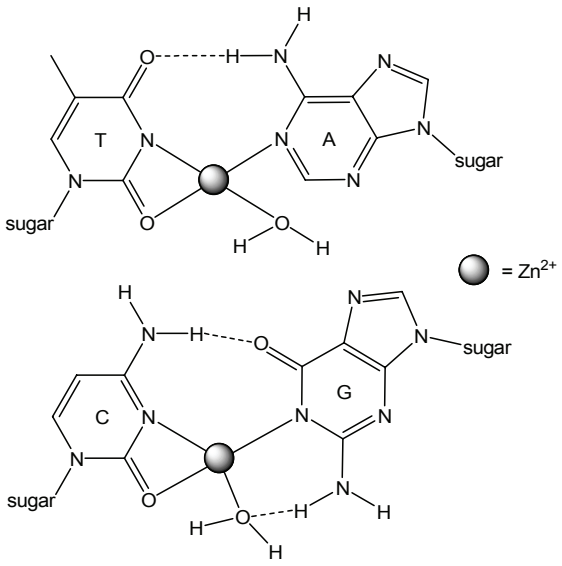

Figure 15: Schematic representation of postulated base pairs in M-DNA formed by the natural nucleobases.[68]

A one dimensional chain of metal ions inside a double helix that is bound through artificial nucleobases that self associate with the help of metal ions and the sugar phosphate backbone as structural template outside gives a strong indication of a possible use as DNA nanowire and as self-assembling electronic circuit.[69,70]

B Aim

The aim of this work is the synthesis of oligonucleotides containing new artificial nucleobases that are able to build artificial planar metal-mediated base pairs without disturbing the geometry of the backbone and therefore partially or fully exchange H-bonding and π-stacking interaction through covalent metal ligand interactions. Through the synthesis of these new systems further information about the structure and the bonding behaviour shall be studied.

1 4´-Methyl-2,2´:6´,2´´-terpyridine (Chapter I)

Different ways of introducing metal ions into the inside of a double helix using artificial base pairs have been developed. Next to the [1+1]- and the [2+2]-coordination, the [3+1]-coordination has been found successful. The tridentate heterocyclic ligand, 4´-methyl-2,2´:6´,2´´-terpyridine, is known to have a high metal affinity and additionally the ability of participating in π-stacking interactions. Using either imidazole or tetrazole, two monodentate ligands, as base pairing partners, the possibility of having stabilising interactions and a planarity in these possible artificial base pairs shall be looked at. This can be done with model structures containing a 2,2´:6´,2´´-terpyridine, a metal ion and either 1-methylimidazole or 1-methyltetrazole. The synthesis of a 4´-methyl-2,2´:6´,2´´-terpyridine nucleoside can also help characterising and gaining information about the behaviour of this ligand inside an oligonucleotide. This can be done, for example, by obtaining a crystal structure or by measuring the pK_a value to exclude the possibility of a concurrent protonation reaction to the wanted metallation. The 4´-methyl-2,2´:6´,2´´-terpyridine is meant to be connected via the 4´-methyl group to the sugar ring, which gives rise to a methylene group that links the artificial nucleoside with the sugar ring. As explained in the Modifications of DNA (I) section this methylene bridge shall introduce an extra degree of conformational flexibilitx to the system. For simplification reasons the nucleoside will be named 4´-methyl-2,2´:6´,2´´-terpyridine nucleoside.

Imidazole or tetrazole as the two monodentate ligands shall be looked at, since there could also be a possibility of 4´-methyl-2,2´:6´,2´´-terpyridine being not only able to build artificial base pairs selectively with one other monodentate ligand, but with two or three different monodentate ligands (one at a time), depending on the strength of the metal ligand interaction. For example, the imidazole could be exchanged by the tetrazole, since this might give a stronger complex with the terpyridine ligand and a metal ion and vice versa. This could be an advantage to the natural nucleobases, because they only have one binding partner. The adenine binds with thymine and cytosine with guanine. Another advantage could be the variety of different metal ions that can be bound strongly by 4´-methyl-2,2´:6´,2´´-terpyridine and that therefore different metal-mediated base pairs could be found. Metal ions could be prevented to bind at other positions within the oligonucleotide, such as the backbone or natural nucleobases, due to the high metal affinity of 4´-methyl-2,2´:6´,2´´-terpyridine.

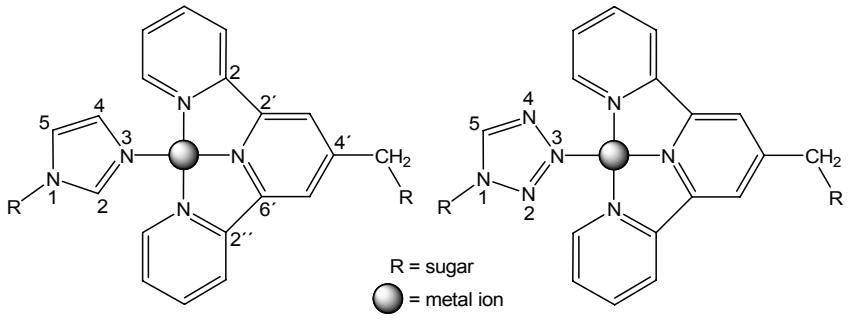

Figure 16: Possible [3+1]-coordination of a 4´-methyl-2,2´:6´,2´´-terpyridine nucleoside with an imidazole or tetrazole nucleoside.

Primarily model structures with 2,2´:6´,2´´-terpyridine, a metal ion and the either of the two different monodentate ligands, 1-methylimidazole or 1-methyltetrazole, shall be synthesised and characterised.

Secondarily, the 4´-methyl-2,2´:6´,2´´-terpyridine nucleoside shall be synthesised to start gaining further information about the possible systems, as mentioned above. For the synthesis of this artificial nucleoside a C-glycosidic bond formation is necessary.

2 1-Deazapurine and 1-Deazaadenine (Chapter II)

Whereas the potential artificial nucleoside in chapter I would contain of a C-glycosidic bond, in chapter II of the thesis potential artificial nucleosides with a N-glycosidic bond shall be looked at. Also another strategy in the actual binding possibilities of a possible artificial nucleobase with metal ions shall be explored. Instead of taking new ligand systems and employing them into oligonucleotides, the natural nucleobases can be altered by adding or subtracting binding sites. At the natural nucleobase adenine an N atom could be substituted by a CH group and the NH_2 group could be abstracted to give a 1-deazapurine, which would only have one potential binding site for H-bonding left. The N7 atom left could bind to a thymine using H-bonding. This is overall expected to be destabilising for this artificial base pair.

At the natural nucleobase adenine one could also only substitute one N atom by a CH group to give 1-deazaadenine, so that Watson-Crick base pairing, again, is hindered and any possible binding sites are at the Hoogsteen side.

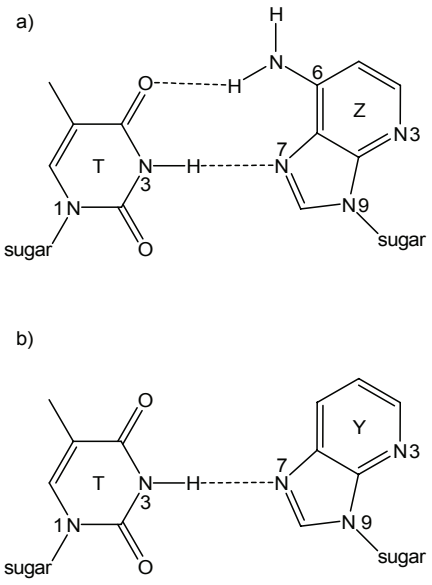

Figure 17: The possible binding of 1-deazaadenine, a), and 1-deazapurine, b), with thymine over the Hoogsteen side without metal ions being present.

This would mean that the then resulting 1-deazaadenine would build out two and the 1-deazapurine one H-bond to the natural base pairing partner thymine. But upon the addition of a metal ion, metal-mediated base pairing could be induced.

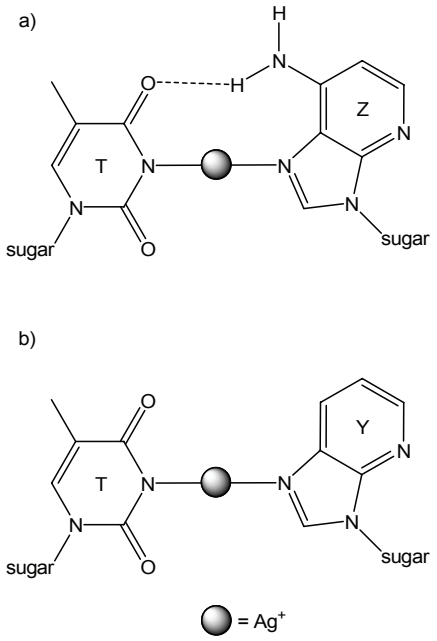

Figure 18: Possible metal-mediated base pairs between thymine and 1-deazaadenine, a), and thymine and 1-deazapurine, b).

So the destabilising effect of minimising the H-bonding in this system could eventually be overcome by additional metal ligand interactions that normally are stronger than H-bonds. Although alterations on the adenine change the possibility of H-bonding, the π-stacking interactions should not be affected largely. [1+1]-coordination on a metal ion, one additional H-bond and π-stacking interactions would give a system with the two traditional and natural interactions and the metal ligand interaction as third stabilisation effect inside an oligonucleotide. However, properties, such as the self assembling, might be influenced greatly. To find out about this and other possible changes in properties of oligonucleotides containing these artificial nucleobases, one has to examine these systems more closely. One can study them by synthesising possible model structures, the artificial nucleosides, themselves, and by introducing them into oligonucleotides. Comparison between

these systems, for example, could give information about the strength of the extra H-bond present in 1-deazaadenine compared to 1-deazapurine.

Primarily, model structures of the 1-deazapurine nucleoside (sugar unit replaced by a methyl group, for example, as in 1-deaza-9-methylpurine) in addition to the actual 1-deazapurine and 1-deazaadenine nucleosides shall be synthesised to start gaining information about the coordination systems, such as the probability of protonation reactions that can be in concurrence to metal binding. The stoichiometry and the strength of metal binding in comparable model structures shall be measured.
Secondarily, the artificial nucleoside shall be introduced in oligonucleotide strands and the synthesis standardised.
Thirdly, the oligonucleotide strand shall be subjected to thermal melting with different metal ions and base pair partners to prove the possibility of metal-mediated base pairing with these systems and to gather further information about these systems.

C Results and Discussion

Chapter I

1 4´-Methyl-2,2´:6´,2´´-terpyridine

1.1 Introduction

Aryl C-nucleosides are analogues of natural nucleosides where the bases have been replaced with aromatic moieties. The use of 4´-methyl-2,2´:6´,2´´-terpyridine as an artificial nucleobase inside an oligonucleotide is thought to induce a high metal affinity. As the opposite monodentate artificial base imidazole and tetrazole are possibilities. Though, these should not give rise to steric hindrance. The planarity of those systems that is essential for the introduction into double helices, as already mentioned in the introduction, can be visualised with the help of model structures between 1-methylimidazole and 1-methyltetrazole with 2,2´:6´,2´´-terpyridine coordinated by metal ions such as Pd^{2+} and Pt^{2+}. These metal ions should build strong complexes that can be used for crystallisation. Also DFT calculations can give a rough idea about the amount of energy needed to bring these [3+1]-coordination systems into a planar form. Additionally to the covalent M-L bonds the heterocyclic systems could induce π-stacking in a great amount, since it has three pyridine rings being able to stack, which is another advantage compared to other [3+1]-coordination systems, known by now.

Next to the preparation of those model structures and the following interpretation, the synthesis of the 4´-methyl-2,2´:6´,2´´-terpyridine nucleoside is a great challenge and needs discussion. The methyl group is meant to function as linker between the 4´-methyl-2,2´:6´,2´´-terpyridine and the sugar, giving the system some kind of flexibility and freedom. The synthesis of C-glycosidic bonds is described in the literature, but under still changing reaction conditions and routes, depending on the artificial nucleobase used. The different approaches to reach this goal will be discussed and analysed. New ways of synthesising the nucleoside are put forward.

1.2 Model Structures

For the model structures 1-methylimidazole (1-mimi) (**1**) and 1-methyltetrazole (1-mtet) (**2**) are needed. **1** was commercially available and **2** had to be synthesised. After the reaction route by Koren et al.[71] did not produce product **2**, another route was chosen[72] and successful. Deprotonation of tetrazole using NaH followed by methylation with MeI and finally a distillation over a ball-tube ("Kugelrohr") distillation gave the wanted product **2** and as side product 2-methyltetrazole (2-mtet) (**3**). The product ratio was 2:1 and the yields were low and did not compete with the literature values.

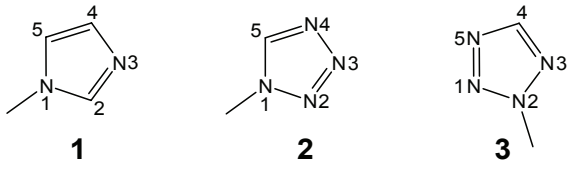

Figure 19: Schematic diagram of 1-methylimidazole (1-mimi) (**1**), 1-methyltetrazole (1-mtet) (**2**) and 2-methyltetrazole (2-mtet) (**3**).

Next, [(trpy)PdCl]Cl · $2H_2O$ (**4**) was prepared analogous to the synthesis of [(trpy)PtCl]Cl · $2H_2O$ (**5**) that was prepared similar to the synthesis by Annibale et al,[73] starting of from the 1,5-cyclooctadiene precursors[74]. The difference in reaction of **4** was the lower reaction temperature (r.t.) and the excellent yield. The yield for **5** is lower than described in the literature.

For the synthesis of the [(trpy)Pd(1-mtet)]$(ClO_4)_2$ (**6**) the [(trpy)PdCl]Cl · $2H_2O$ (**4**) is stirred with two equivalents of $AgNO_3$ and 5 equivalents of 1-methyltetrazole (**2**) for one day, whereby one Cl^- is displaced by NO_3^- and the other by **2**. The produced AgCl is taken off, the pH raised to 9 and the NO_3^- is displaced by ClO_4^-. The resulting Pd^{2+} complex (**6**), however, could not be crystallised. As shown later with the help of NMR spectroscopy, complex 6 probably is [$(trpy)_2Pd_2$(1-mtetate)]$(ClO_4)_3$.[75]

The synthesis of the [(trpy)Pt(1-mtetate)](ClO_4) (**7**) complex is analogous to **6**, but due to the Pt^{II} being more inert in comparison longer reaction times and higher reaction

temperatures are necessary. Both syntheses were done analogous to the synthesis by B. Lippert et al.[76]

Since the obtained side product 2-methyltetrazole (**3**) could also show a binding behaviour that one could compare with the other structures, it was tried to synthesise [(trpy)Pd(2-mtet)]$(ClO_4)_2$ (**8**) and [(trpy)Pt(2-mtet)]$(ClO_4)_2$ (**9**) using the same procedures as for **6** or **7.** But only the starting compound was found after the reaction, showing that this was not easily synthesised. This is a first indication that it is not possible to use **3** as opposite artificial nucleoside inside DNA. This could be due to steric reasons of the methyl group of **3** or due to electronic reasons. Different reaction conditions, however, might allow binding.

Using the same procedures as for **6** or **7**[76] with **1** as ligand, two complexes can be obtained, the [(trpy)Pd(1-mimi)]$(ClO_4)_2$ (**10**) and [(trpy)Pt(1-mimi)]$(ClO_4)_2$ (**11**).

Having synthesised all four complexes (**6**, **7**, **10** and **11**) it is important to realise, that the monodentate ligand can bind over different atoms in the heterocyclic ring. The possible coordination sites of 1-methyltetrazole inside **6** and **7** are shown in Figure 20.

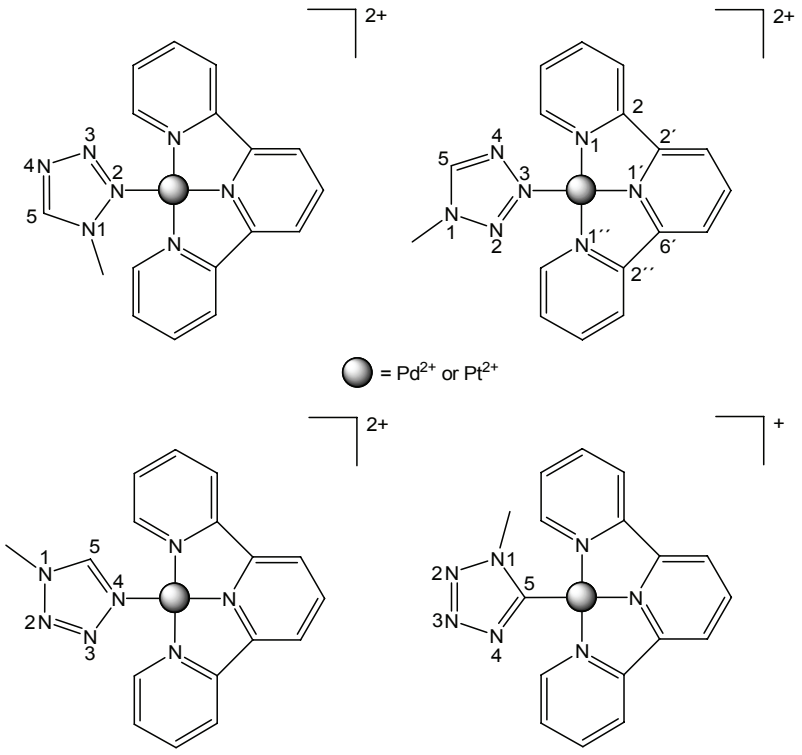

Figure 20: Schematic diagram of possible structures of the cations of **6** and **7**.

For the 1-methyltetrazole (**2**) four possible coordination sides can be found for each metal ion. On the one hand it can coordinate at the three different N atoms; on the other hand it could bind over the C atom, if it is deprotonated. For the Pt^{2+} complex (**7**) a crystal structure was obtained, but at first the complex was analysed using NMR and elemental analysis. Looking at the ^{1}H-NMR spectrum one could not find a signal for the H5 proton, which could be due to the deprotonation of this proton and binding over the C5 atom. Though, it could not be surely said that it is not hidden underneath the heteroaromatic proton signals of the 2,2´:6´,2´´-terpyridine. Additionally in the ^{1}H, ^{1}H-NOESY spectrum a cross-peak between the H6 and H6´´ protons with the methyl group of the 1-methyltetrazole (**2**) was observed. This shows that the methyl group lies close to the H6 and H6´´ protons. A coordination of **2** over N3 or N4 can therefore be excluded. Now, looking at the elemental analysis one can differentiate between the N2 and C5 linked complexes formed, since the number of counter ions (ClO_4^-) differs by one. The elemental analysis showed that there is only one ClO_4^- in the structure ruling out the coordination over the N2 position. Another observation that has been made in the NMR spectra is the movement of H6 and H6´´ to higher field. This could be the case, if **7** has its hetero aromatic ring of the 1-methyltetrazole perpendicular to the plane of the 2,2´:6´,2´´-terpyridine. The ring current effect of the 1-mtet would act on the two protons and move them to higher field.

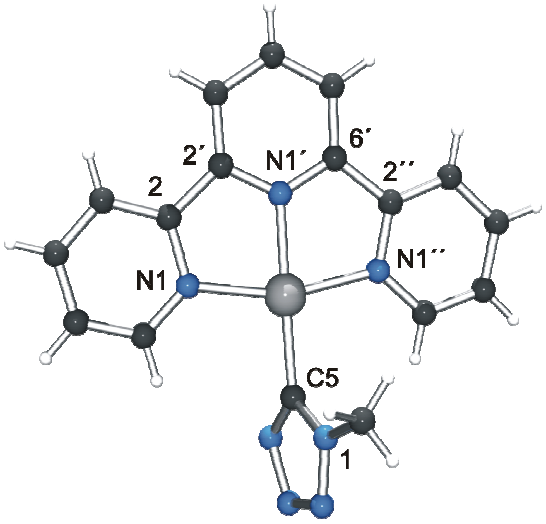

Figure 21: Crystal structure of the cation of [(trpy)Pt(1-mtetate)](ClO_4) (**7**).

Indeed, all the interpretations on the complex were correct, as can be seen in Figure 21. The 1-methyltetrazolate (1-mtetate) binds over the deprotonated C5 atom, probably because a fast deprotonation-equilibrium is present. The 1-methyl-tetrazolate (1-mtetate) is not planar, but on the way of being perpendicular to the metal ion terpyridine plane. The measured angle between the Pt-N_3C plane and the 1-mtetate coordination plane is 67.0(2)°. It should be mentioned that the Pt-N and Pt-C distances are all between 1.98 and 2.03Å. Looking at the bond lengths inside the tetrazole ring in **7**, only one short bond length and four nearly equal bond lengths were observed. This shows that there is a double bond between N2 and N3 in the tetrazole ring, but the second double bond, as shown in Figure 20, cannot be located. One could think that the charge might be delocalised or that N4 has a negative charge, however this could not be proven. Though, looking at other tetrazole containing complexes this phenomenon of only one short bond was often found.

Distances (Å) and angles (°)	**7**
M-C5	2.006(5)
M-N1	2.034(4)
M-N1´	1.981(4)
M-N1´´	2.023(4)
MN_3C-L	67.0(2)

Table 2: Selected distances and angles of the crystal structure of [(trpy)Pt(1-mtetate)](ClO_4) (**7**).

In Figure 22 it can be seen nicely that the plane of tetrazole ring is close to being perpendicular to the metal ion terpyridine plane. Only one ClO_4^- has been found since the deprotonated C5 is negatively charged, and therefore balancing one positive charge of the metal ion.

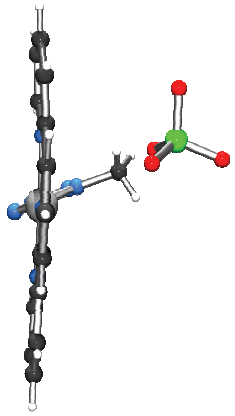

Figure 22: Crystal structure of [(trpy)Pt(1-mtetate)](ClO_4) (**7**).

In expectation of the tetrazole ring to bind over the N3 position DFT-caculations[77] were performed. The calculations show that in the comparable Pd^{2+} complex (**6**) that binds 1-mtet over N3 the energy difference between the calculated structure with a relaxed geometry (MN_4-L = 27.9°) and the geometry optimised planar structure (MN_4-L = 0.1°) lies at 0.8kJ/mol. This is a very low energy barrier and gives rise to the possibility of having a planar [3+1]-coordination system. However, it should be tried now, to coordinate the 1-methyltetrazole (**2**) over the N3-position by avoiding the deprotonation of C5. Bonding through the N3-position could stabilise the planarity of that system by having additionally to the metal ion coordination H-bonds via C6-H6···N4 and C6´´-H6´´···N2.

The Pd^{2+} complex (**6**) was also synthesised, but it could not be crystallised. Analysis of the structure using ^{1}H-NMR showed two sets of signals (1:1) of the 2,2´:6´,2´´-terpyridine ligand in the aromatic region. Now, this could give rise to equal amounts of two different products, having the tetrazole ring coordinated over two different coordination sites to two Pd^{2+}. Another explanation would be an asymmetrical 2,2´:6´,2´´-terpyridine bound to two different Pd^{2+}. Both, however, do not fit to the integration value of the methyl group of the 1-methyltetrazole ligand. The methyl group has three protons, but then, the aromatic protons count up to 22 and one 2,2´:6´,2´´-terpyridine only has 11 protons. This is a ratio of one methyl group to two 2,2´:6´,2´´-terpyridines. This data put forward the idea of the 1-methyltetrazole ring acting as a bridge between two Pd^{2+} each bound to a 2,2´:6´,2´´-terpyridine. The

question arising from this idea is then, over which atoms the 1-methyltetrazole ring binds to each of the two Pd^{2+}.

These are not easily identified using NMR spectroscopy. Crystallisation attempts have been made, but by now no suitable single crystal could be obtained. A crystal structure could identify, of course, the whole structure with all its bond lengths and angles.

For the 1-methylimidazole complexes (**10** (M = Pd^{2+}) and **11** (M = Pt^{2+})) a deprotonation of a C atom is much less likely (different pK_a value) and it is expected that the 1-methylimidazole coordinates over the N3 position.

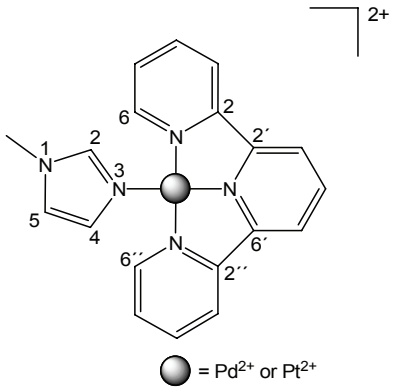

Figure 23: Schematic diagram of the possible structures of the cations of **10** (M = Pd^{2+}) and **11** (M = Pt^{2+}).

Indeed, it has been found through the use of NMR spectroscopy and elemental analysis that the 1-methylimidazole binds over the N3 position in both complexes. In the ^{1}H-NMR spectra for both complexes a ring current effect on the H6 and H6´´ of the 2,2´:6´,2´´-terpyridine could again be observed giving rise to a perpendicular position of the 1-methylimidazole ligand. Additionally, crystals were obtained that were suitable for X-ray crystallography.

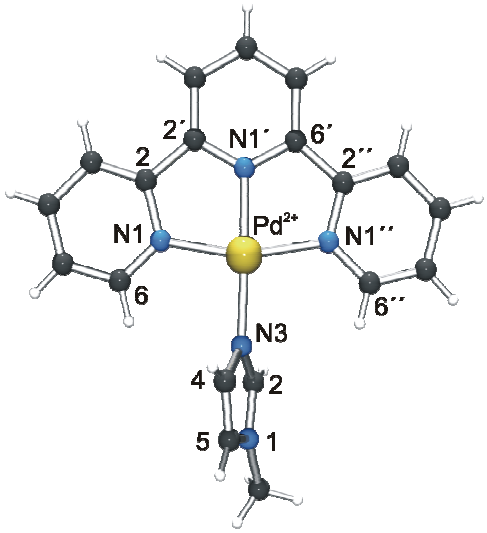

Figure 24: Crystal structure of the cation of [(trpy)Pd(1-mimi)]$(ClO_4)_2$ (**10**).

It can be seen that the imidazole ring is out of the Pt-N_4 plane and nearly perpendicular with 73.9(3)°. The 1-methylimidazole is connected via N3 and the bond distances to the metal ions are between 1.94 and 2.02Å. There is a great similarity to the Pt^{2+} complex (**11**), since nearly all distances and angles are identical.

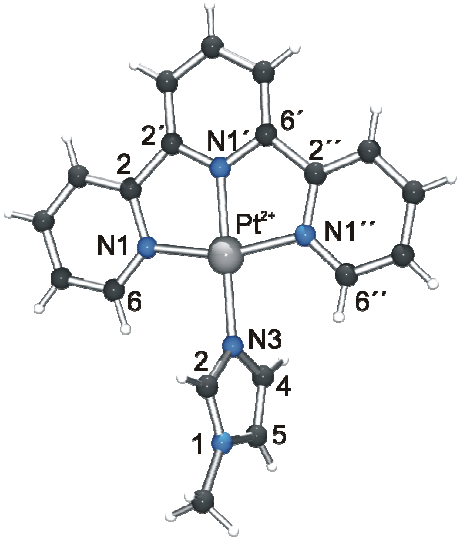

Figure 25: Crystal structure of the cation of [(trpy)Pt(1-mimi)]$(ClO_4)_2$ (**11**).

One reason for the non planar structure is the fact that the H2 and H4 protons of the 1-methylimidazole and the H6 and H6´´ protons of the 2,2´:6´,2´´-terpyridine would be very close to each other and interference between them hinders the planarity. In the [(trpy)Pt(1-mtetate)](ClO_4) (**7**) the angle between the planes is smaller, which could be due to the N4 atom of the 1-methyltetrazolate wanting to build an H-bond with H6 or H6´´ of the 2,2´:6´,2´´-terpyridine and therefore pushing the aromatic ring further to planarity. But, the methyl group of the 1-methyltetrazolate hinders this greatly for obvious steric reasons. In **10** and **11** there is no driving force to planarity. Both, H2 and H4 of 1-methylimidazole, are looking for the sterically least strained position.

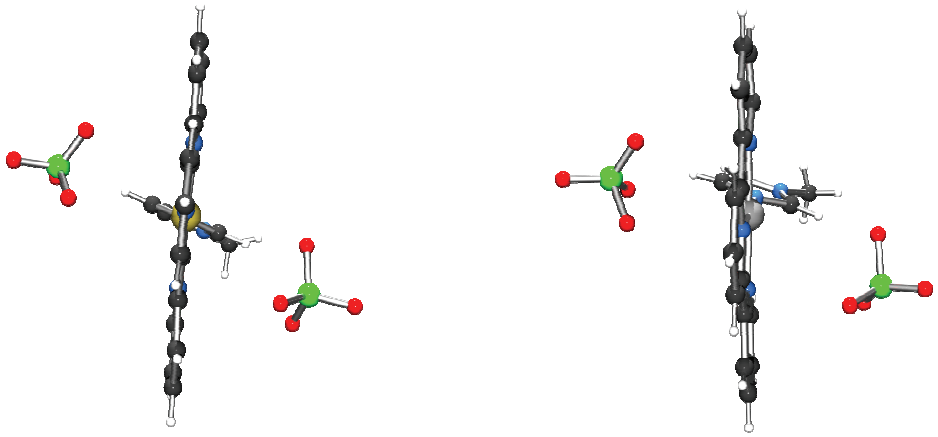

Distances (Å) and angles (°)	**10 (M = Pd^{2+})**	**11 (M = Pt^{2+})**
M-N3	2.023(5)	2.029(5)
M-N1	2.019(6)	2.032(5)
M-N1´	1.940(5)	1.943(4)
M-N1´´	2.006(5)	2.026(5)
MN_4-L	73.9(3)	74.0(2)

Figure 26 and Table 3: Pictures and selected distances and angles of the crystal structures of **10** (M = Pd^{2+}) and **11** (M = Pt^{2+}).

It has been shown in DFT calculations[77] for [(4´-methyl-2,2´:6´,2´´-terpyridine)Pd(1-methylimidazole)]$^{2+}$ that there is a great energy difference between the relaxed

geometry and an optimised planar geometry of around 81kJ/mol. The distances in the relaxed geometry of the Pd-N bonds are similar to the distances obtained in the crystal structure, thus, having an angle of 89.9° between the plane of the PdN_4 and the imidazole ring. In the planar structure the Pd-N distances are all increased by around 0.05-0.2Å. Whereas the H2 and H4 of 1-methylimidazole are far away from the H6 and H6´´ of the 2,2´:6´,2´´-terpyridine in the crystal structure and the relaxed geometry in the calculation, in the planar geometry the distances would be small giving rise to the sterical strain. From this the large amount of energy needed to force 1-methylimidazole into planarity can be explained. It can therefore be said, that the probably most successful system for the introduction into oligonucleotides, since it easily goes to planarity, is the system with the 1-methyltetrazole bound to Pd^{2+} or Pt^{2+} over N3. The N2- and N4-positions of the 1-methyltetrazole give the possibility of H-bonding via C6-H6···N4 and C6´´-H6´´···N2 and therefore a stabilising force for the planarity. Complete planarity, however, is not necessary for the formation of H-bonds. The methyl group does not hinder the formation of planarity, since it is then far enough away from the 2,2´:6´,2´´-terpyridine. It should also be recognised that planarity is essential for the formation of such a metal-mediated base pair inside an oligonucleotide, but that also in nature the base pairs are found to be twisted or tilted slightly.[5,7] Therefore the angle between the $Pt\text{-}N_4$ plane and the tetrazole ring should be close to zero.

1.3 Nucleoside

Starting with the esterification of 3-methylpentanedioic acid (**12**) to give dimethyl 3-methylpentanedioate (**13**) and following this with a substitution reaction that results in 1,5-bis(2-pyridyl)-3-methylpentane-1,5-dione (**14**), yellow 4´-methyl-2,2´:6´,2´´-terpyridine (**15**) was obtained after a ring closure reaction, as can be seen in Figure 27.[78]

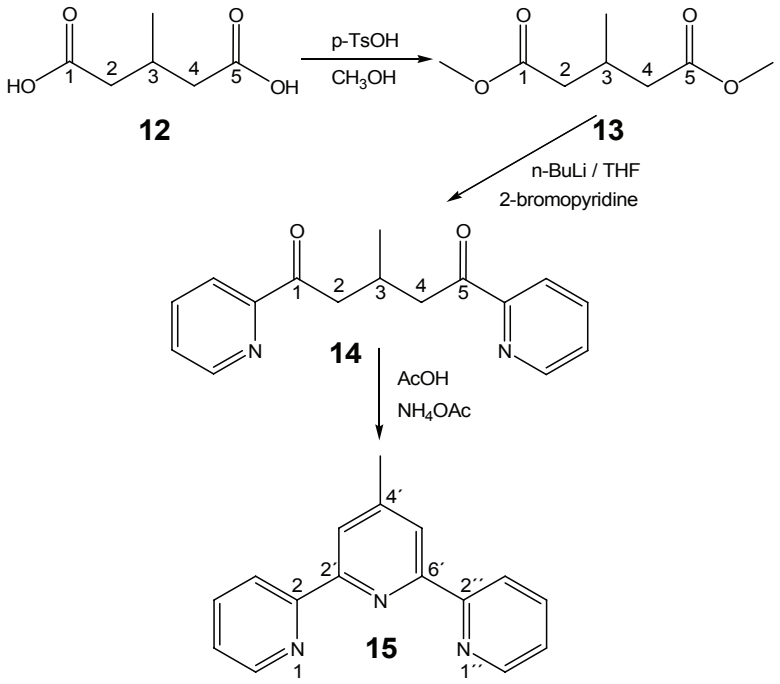

Figure 27: Schematic diagram of the synthesis of 4´-methyl-2,2´:6´,2´´-terpyridine (**15**).[78]

It needs mentioning that primarily a different route was taken with a 4´-thiomethyl-2,2´:6´,2´´-terpyridine intermediate.[79] But this route left us with the problem of having to separate 4´-methyl-2,2´:6´,2´´-terpyridine (**15**) and 4´-thiomethyl-2,2´:6´,2´´-terpyridine, which was neither described in the literature, nor was an easy way found to do this separation.

For the first synthesis step higher yields were obtained than described in the literature.[78] Difficulties were experienced with the substitution reaction of dimethyl 3-methylpentanedioate (**13**) with 2-bromopyridine using n-BuLi to give 1,5-bis(2-

pyridyl)-3-methylpentane-1,5-dione (**14**). The purification turned out to be more challenging than described in the literature.[78] Especially the purification by flash chromatography seemed to be responsible for the low yields obtained.

The chromatographic purification is effected by the so called diffusion. The longitudinal diffusion effects the movement for the same molecules on the stationary phase. The same molecules will have different retention times.

Therefore the length of the silica gel column was shortened and the amount of substance added to the column increased. This gave an improvement of the yield of **14**. However, the yield described in the literature could not be obtained.

Finally, the 4´-methyl-2,2´:6´,2´´-terpyridine (**15**) was synthesised using ammonium acetate and very good yields could be obtained, even better than described in the literature.[78] Since the product found after the purification steps described in the literature was not pure, attempts were undertaken to find a way of purification, such as flash chromatography and crystallisation. The first did not show an improvement and even more a loss in product. The crystallisation was found to be more successful. The extraction step with CH_2Cl_2, the drying over Na_2SO_4 and the evaporation to dryness, as described in the literature, were followed by re-crystallisation from n-heptane. The residue was dissolved in n-heptane and left in the ultrasonic apparatus for 10min at 40°C. Then the emulsion was put in the refrigerator (-18°C) for 10min. The yellow n-heptane (containing only the 4´-methyl-2,2´:6´,2´´-terpyridine) was decanted (leaving the side products in the round bottom flask) and evaporated. The work up procedure was repeated until no more 4´-methyl-2,2´:6´,2´´-terpyridine was found. Standard crystallisation with n-hexane or n-heptane was not of any satisfactory value.

Now, the synthesised 4´-methyl-2,2´:6´,2´´-terpyridine (**15**) was tried to link to a silyl-protected sugar as shown in Figure 28.[80-82] The disiloxane-protected 2-deoxy-ribonolactone (**16**) was synthesised in high purity. Then, attempts were undertaken using n-BuLi and LDA as to get the aryllithium reagent that could react with the disiloxane-protected 2-deoxyribonolactone (**16**).

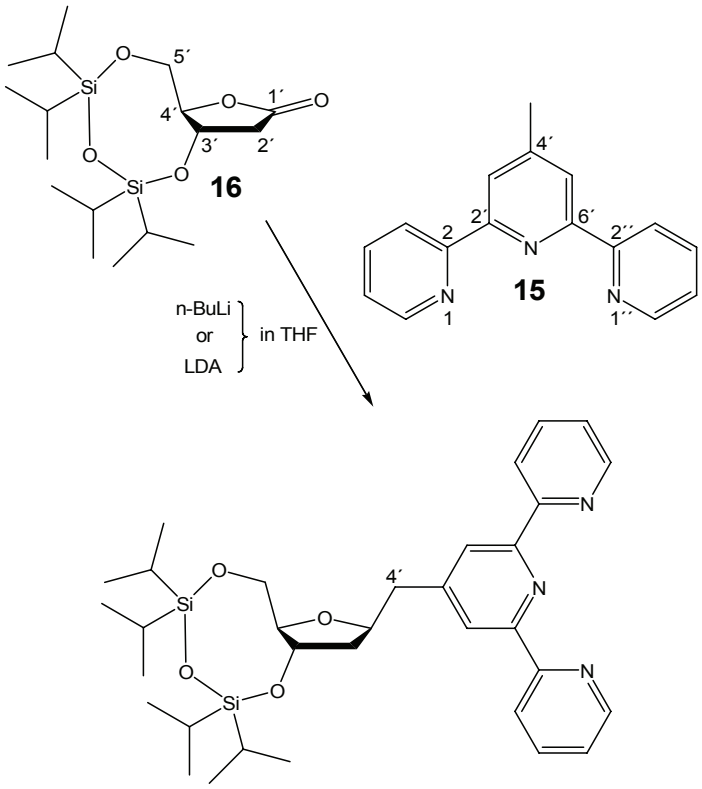

Figure 28: Schematic diagram of a possible way for the synthesis of 4´-methyl-2,2´:6´,2´´-terpyridine nucleoside.

The 4´-methyl-2,2´:6´,2´´-terpyridine nucleoside could not be synthesised after many unsuccessful attempts, with altering reaction conditions. The observation of unreacted **16** after the attempted reactions led to the idea that the terpyridyllithium reagent was not reactive enough, maybe due to sterical hindrance, or more likely, has not been formed. Therefore, at first, the reaction is repeated with acetone instead of the disiloxane-protected 2-deoxyribonolactone (**16**). Acetone is smaller than **16** and is expected to find the reactive terpyridyl species more easily. But the observation in the ^{1}H NMR spectrum after the reaction showed no chemical shift change of the CH_3 group protons of 4´-methyl-2,2´:6´,2´´-terpyridine upon the possible formation of a methylene group. Also no change in intensity upon integration (3H to 2H) was found in the spectrum. Therefore the sterical hindrance and the lack of reactivity as reasons could be excluded. To find out, whether the terpyridyllithium species was actually built, the reaction was repeated with D_2O. But as before the ^{1}H NMR spectrum after the reaction showed no chemical shift change of the CH_3-group protons of 4´-methyl-

2,2´:6´,2´´-terpyridine, no change in intensity upon integration (3H to 2H) and no change in complexity of the singlet that would be expected, due to a formation of a CH_2D group. Therefore one can conclude that the terpyridyllithium species has not been formed. This could be due to the lack of reactivity of the the CH_3-group of 4´-methyl-2,2´:6´,2´´-terpyridine.

Therefore a new strategy had to be found to synthesise the 4´-methyl-2,2´:6´,2´´-terpyridine nucleoside. To increase the reactivity of the 4´-methyl-2,2´:6´,2´´-terpyridine (**15**) a Br should be introduced at the 4´-methyl group.

For that **15** needs at first to be oxidised to 4´-carboxyaldehyde-2,2´:6´,2´´-terpyridine (**17**).[79] Reduction of **17** gives the 4´-hydroxymethyl-2,2´:6´,2´´-terpyridine (**18**).[83] Then the Br can be introduced at the C4´ position of **18** to obtain the target molecule 4´-bromomethyl-2,2´:6´,2´´-terpyridine (**19**)[83] as show in Figure 29.

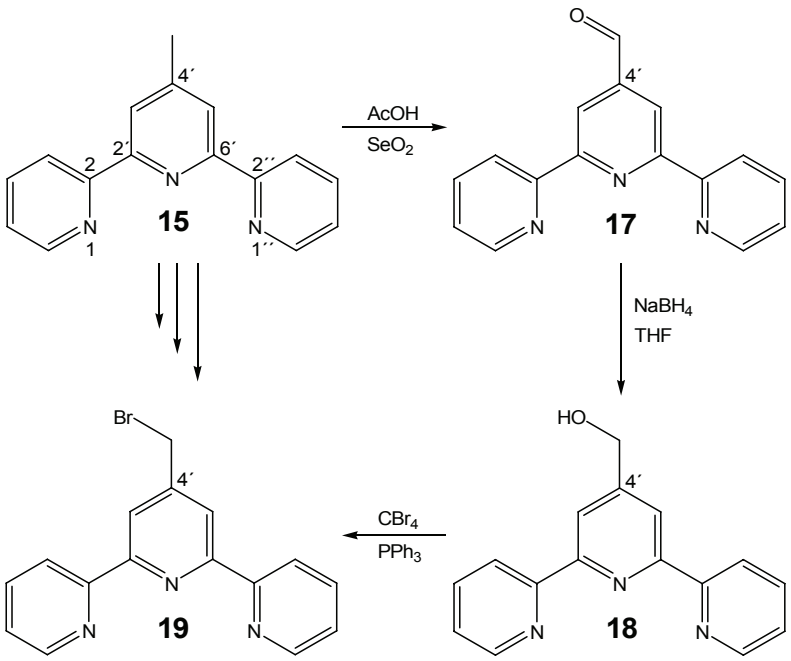

Figure 29: Schematic diagram of the synthesis of 4´-bromomethyl-2,2´:6´,2´´-terpyridine (**19**).

The oxidation reaction was done with SeO_2, as described in the literature,[79] but the produced Se metal could not be filtered off completely after the reaction, so that chelating resin was used to clear the solution. Yet again, the final crystallisation with

n-hexane did not have any success on purifying the product. A mixture of the wanted product 4´-carboxyaldehyde-2,2´:6´,2´´-terpyridine (**17**) and the starting material 4´-methyl-2,2´:6´,2´´-terpyridine (**15**) was obtained. Another synthesis route by J.-P. Collin et al.[84] did not lead to any product formation at all. Since neither another way of synthesising **17**, nor of separating **15** from **17** was found, the further reaction steps had to be done with a mixture of both. Thus, an starting material/product ratio from 4:1 clearly shows that the oxidation reaction was not very efficient.

Using $NaBH_4$ the 4´-carboxyaldehyde-2,2´:6´,2´´-terpyridine (**17**) can be reduced to the 4´-hydroxymethyl-2,2´:6´,2´´-terpyridine (**18**).[83] More importantly, one was able to recover most of the unreacted 4´-methyl-2,2´:6´,2´´-terpyridine (**15**). For this the purification of the product (**18**) had to be done differently. To the residue n-heptane was added and it was placed in the ultrasonic apparatus for 10min at 40°C. Then the suspension was left in the refrigerator for 10min. The slightly yellow n-heptane was decanted and evaporated to give **15**. To the residual solid CH_2Cl_2 was added and the suspension centrifuged. The solution was decanted and the solid again extracted with CH_2Cl_2. The CH_2Cl_2 phases were combined and evaporated. The extraction with n-heptane, as described above, was done four times, whereby the last two times the n-heptane was not decanted, but filtered off. Although this way **18** could be purified and **15** recovered, the actual yield is low.

The last step for the synthesis of 4´-bromomethyl-2,2´:6´,2´´-terpyridine (**19**) was done as stated in the literature with CBr_4.[83] Again the purification had to be optimised, since the described way gave a loss of product on the silica gel column. So we shortened the silica gel column and used different solvents to obtain **19** in a yield comparable to the literature.

Now the 4´-bromomethyl-2,2´:6´,2´´-terpyridine (**19**) can be connected with a DMTr-(S)-glycidol (**20**) to get a sugar mimic using a Grignard. The C_3-backbone sugar mimic was chosen, since it is nowadays accepted as useful artificial backbone[18-20] and the epoxide should be more reactive, since it has a strained three membered ring, than the carboxy group of the disiloxane-protected 2-deoxyribonolactone (**16**).[80-82] It is synthesised by reacting (R)-glycidol with DMTr-Cl.[85] Another advantage is the already integrated DMTr protecting group, since one further protection step would give the building block for an oligonucleotide.

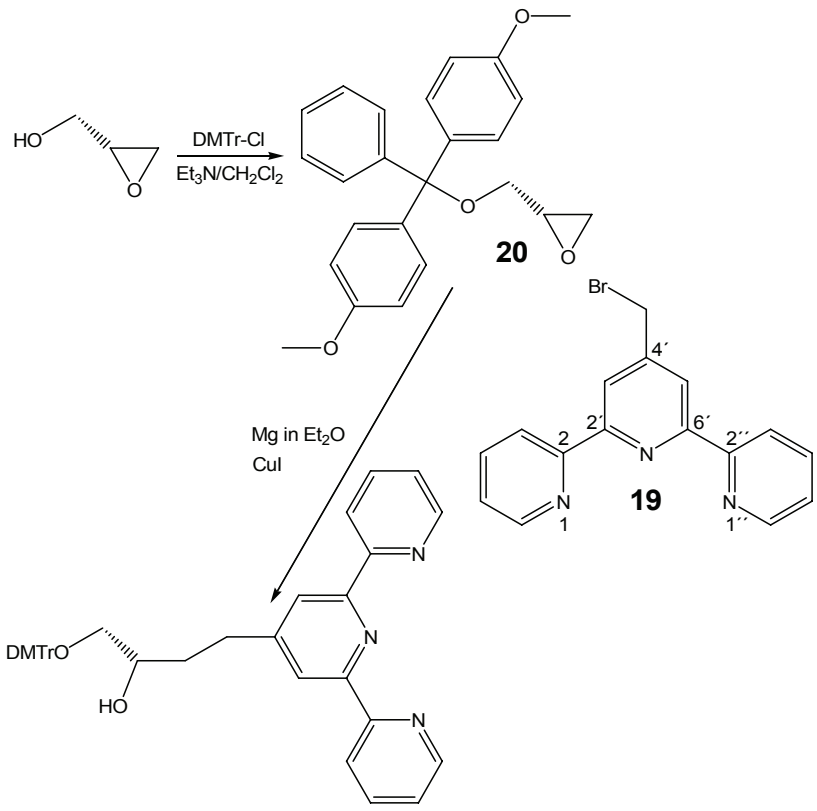

Figure 30: Schematic diagram of a possible way for the synthesis of 4´-methyl-2,2´:6´,2´´-terpyridine-DMTr-C_3-backbone.

This way of synthesis was not successful. One reason could be that the used CuI has not reacted, since it has been complexed by the terpyridine ring of 4´-bromomethyl-2,2´:6´,2´´-terpyridine (**19**). The Cu ion is needed for the formation of a Gilmour reagent during the reaction.

Other strategies therefore have to be developed. One suggestion is to connect a pyridine ring first to the sugar moiety, since the pyridine does not have such a high metal affinity as a terpyridine ring and would not be expected to bind Cu ions during the reaction. A 2,4,6-halogenated pyridine ring could be linked to a sugar moiety via the C4 position at the ring leaving the C2 and C6 positions to connect the other two pyridine rings by using a Negishi or Stille-type cross-coupling reaction.[86-90] These reactions have already been used to synthesise bipyridines and terpyridines. However, it has to be shown that under these conditions the sugar moiety does not undergo a reaction, too. The 2,4,6-halogenated pyridine could be synthesised from a 2,6-chloro-4-aminopyridine that is available for purchase.[91]

1.4 Summary and Discussion

The model structures with 2,2´:6´,2´´-terpyridine as possible tridentate ligand and the 1-methylimidazole (1-mimi) (**1**) and 1-methyltetrazole (1-mtet) (**2**) as monodentate ligands have been synthesised and analysed. Whereas the $[(trpy)Pd(1\text{-}mimi)](ClO_4)_2$ (**10**) and $[(trpy)Pt(1\text{-}mimi)](ClO_4)_2$ (**11**) showed no tendency for planarity due to steric hindrance of certain protons, one can argue that the Pd^{2+} complex (**6**) and [(trpy)Pt(1-mtetate)](ClO_4) (**7**) could give rise to planarity, if 1-methyltetrazole is bound over the N3 atom to the metal ion. The possibility of H-bonds in addition to the metal ion coordination could drive the tetrazole ring close to planarity, as it has been shown by DFT calculations. Even bound about C5 to the Pt^{2+}, which means that planarity is sterically hindered due to the methyl group being close to the terpyridine rings, 1-methyltetrazolate had an angle between the planes (PtN_3C-L) that was smaller than for 1-methylimidazole in **10** and **11**, which is possibly because of the N4 wanting to form an H-bond with a proton from the terpyridine ring. Though, to finally prove the formation of H-bonds and herewith the resulting planarity, the two complexes with the 1-methyltetrazole bound over N3 should be synthesised. A decrease in pH during the reaction should leave the C5 of the tetrazole ring protonated. This means that it could bind over N3. Also for the Pd^{2+} complex (**6**) a change in pH could influence the outcome, so that only one Pd ion is bound, instead of possible two.

In attempts to synthesise the 4´-methyl-2,2´:6´,2´´-terpyridine nucleoside, it has been tried to connect not just the 4´-methyl-2,2´:6´,2´´-terpyridine (**15**), but also the more reactive 4´-bromomethyl-2,2´:6´,2´´-terpyridine (**19**) to the different sugar moieties **16** and **20**, as shown in Figure 28 and 30. It was neither possible to deprotonate the 4´-methyl group of **15** with the reagents available in the laboratory, nor to use metal ions (i.e CuI) in the reactions possibly due to the terpyridine immediately complexing them.

The idea of introducing two new artificial nucleobases, having the ability of planar [3+1]-coordination with metal ions, into oligonucleotides has been strengthened by the results of the model structures and DFT calculations. Therefore there is a great necessity of finding a possible way of synthesising a 4´-methyl-2,2´:6´,2´´-terpyridine

building block for the automated DNA synthesiser, so that it can be introduced into an oligonucleotide. A route of synthesis, building the three terpyridine rings after having connected part of it to a sugar moiety, has been suggested and now needs to be tested for functionality. The tetrazole nucleoside has already been synthesised.[92]

Chapter II

1 Introduction

By systematic subtraction of functional groups or through the exchange of N atoms with C atoms the binding possibilities of adenine become limited. As mentioned before (Aim section), adenine builds a Watson-Crick base pair with thymine (T), but without the N1 atom, a possible binding over this side is hindered, as is shown in Figure 31 for 1-deazaadenine (Z). Without the N1 atom and the NH_2 group binding over this side is even excluded, as for 1-deazapurine (Y).

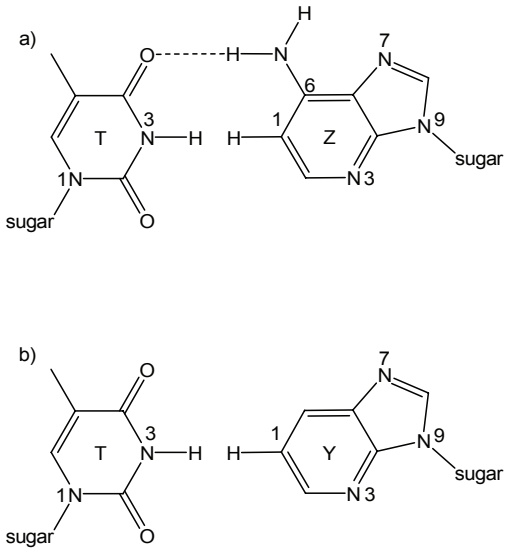

Figure 31: Binding possibilities over the Watson-Crick side for the base pairs T-Z, a) and T-Y, b).

The exchange of the N1 atom by a C atom, hence, the formation of 1-deazaadenine, hinders one of the H-bonds to form. The rotation of the 1-deazaadenine over the N-glycosidic bond can lead to the formation of a Hoogsteen or a reverse Hoogsteen base pair with thymine. Under certain conditions it is also possible for adenine to build Hoogsteen base pairs, but 1-deazaadenine is more or less forced to do so, since

the possibility of formation of Watson-Crick base pairs is limited. In size the adenine and the 1-deazaadenine are quite similar. This is an important fact for the recognition process during the self association process. An oligonucleotide containing 1-deazaadenine has already been published to show melting behaviour with a thymine containing complementary strand, but the actual melting temperature, T_m, is only 15°C.[93] The measured oligonucleotide was a 20mer and this shows that the strand should not be any shorter, since otherwise no melting behaviour will be observed. The authors state that this double helix is of parallel orientation.

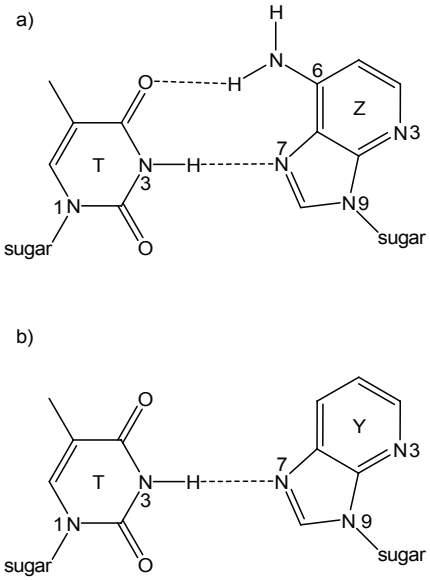

Figure 32: Binding possibilities over the Hoogsteen side for the base pairs T-Z, a) and T-Y, b).

The idea is to introduce metal ions that can linearly coordinate at the N3 atom of thymine and at the N7 atom of 1-deazaadenine. This should raise the T_m, since an additional stabilising force is present. A self assembling double helix with three stabilising forces, H-bonding, π-stacking interaction and covalent metal-ligand bonds, and binding over the Hoogsteen side would be built. There are reports of Hoogsteen base pairs blocking the information flow from Watson-Crick duplex DNA to mRNA by simply building out a triple helix.[93] The possibility of Hoogsteen base pairs opens up many other binding possibilities.

Subtracting the NH_2 group from the 1-deazaadenine will hinder the H-bonding over the Watson-Crick side completely, as can be seen in Figure 31. Over the Hoogsteen side one H-bond could be built. This could prevent self association, but upon the addition of metal ions there is still a possibility of forming a stable double helix. A comparison of the T_m and melting behaviour of a strand with 1-deazapurine and a strand with 1-deazaadenine, each binding to a thymine strand, could give information about the strength of H-bonding. One would also be able to gain knowledge about the co-operativity of H-bonding and M^{n+}-binding.

The 1-deazapurine could also be able to act as monodentate ligand in a [1+1]-coordination system. Either with itself or with natural nucleobases as base pairing partner, 1-deazapurine could build a metal-mediated base pair. It has been used in first attempts of expanding the genetic alphabet,[94] and it has been suggested that it might be formed in vivo.[95]

The size of 1-deazapurine, although having lost the NH_2 group, is still suitable for binding. But only building out one H-bond, it is probably not strong enough for self association. Introduction in a strand with only natural nucleobases around will show the destabilising effect of a single mispairing or non pairing 1-deazapurine. The stabilising effect with linearly coordinating metal ions could then give information about the strength of a single metal-mediated base pair in such a system.

2 Nomenclature

Unlike the compounds in chapter I, the compounds in chapter II have many possible and often used names. Therefore it is essential for the understanding of this work and for comparison reasons with other work to explain the nomenclature that is used throughout this thesis.

In Figure 33 a purine is shown. All related derivatives of purine are named using this purine nomenclature.

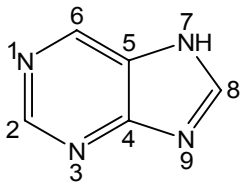

Figure 33: Numbering of purine.

One exception is the 1-deaza-6-aminopurine that will be named 1-deazaadenine and another exception is the 1-deaza-6-aminopurine-N9-β-2´-deoxyribonucleoside that will be named 1-deazaadenine-N9-β-2´-deoxyribonucleoside or 1-deazaadenine nucleoside for simplification and for comparison reasons with adenine, shown in Figure 34. This is also no problem, since the numbering of the two is identical. Nucleoside will always be used as shortage for 2´-deoxyribonucleoside, since in this thesis non of the sugar moieties has an OH group and it is exclusively written about DNA.

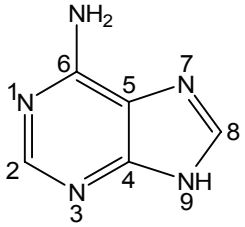

Figure 34: Nomenclature for adenine.

If a sugar ring is present the molecules will be named in order of the sugar numbering. The example in Figure 35 will be explained.

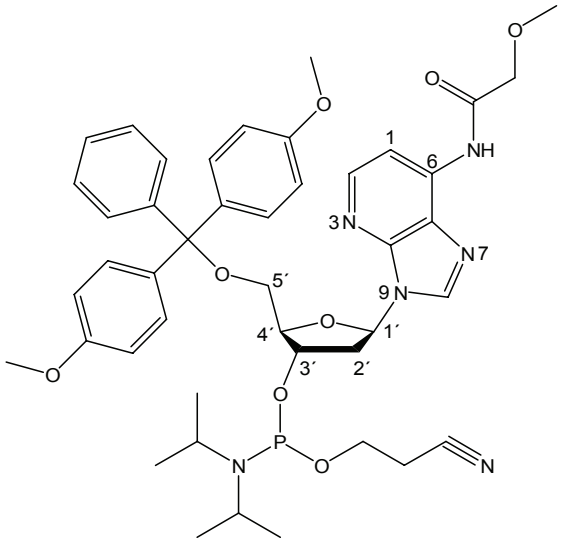

Figure 35: 1-deaza-(6-methoxyacetylamino)-purine-N9-β-[2´-deoxy-3´-O-(2-cyanoethyl)-N,N-diisopropylphosphoramidite-5´-O-(4,4´-dimethoxytrityl)-ribonucleoside] as example for the numbering and the nomenclature in this thesis.

One starts of at the C1´ position of the sugar with the 1-deaza-(6-methoxy-acetylamino)-purine. The purine is linked to the C1´ position via N9 and it is the beta-anomer. The C2´ position is named 2´-deoxy, since it has no OH group present. At the C3´ position a protecting group is linked at the O atom and therefore this bit is named 3´-O-(2-cyanoethyl)-N,N-diisopropylphosphoramidite. No extra functional group is found at the 4´-position; hence, no further name is required. At the C5´ position on the O atom another protecting group is found and it is named 5´-O-(4,4´-dimethoxytrityl). Finally the sugar is named: ribonucleoside.

One names this molecule therefore: 1-deaza-(6-methoxyacetylamino)-purine-N9-β-[2´-deoxy-3´-O-(2-cyanoethyl)-N,N-diisopropylphosphoramidite-5´-O-(4,4´-dimethoxytrityl)-ribonucleoside].

Throughout the thesis the positions, where reactions or other changes take place, will be numbered again for clarity.

3 1-Deazapurine

3.1 Model Structures

As a suitable model for a 1-deazapurine nucleobase interacting with a metal ion in an oligonucleotide N9-methyl-1-deazapurine has been taken as the monodentate ligand.[96] The sugar ring has been substituted through a methyl group to avoid binding of the free OH groups with metal ions. As metal ion Hg^{2+} was taken, because mainly, although it can adopt many other coordination geometries, it prefers linear coordination with nucleobases.[97,98] This linear coordination is, as mentioned before, also from great necessity for the coordination inside the oligonucleotide.[30] There are only three examples of Hg^{2+} binding two nucleobase derivatives, although the coordination behaviour with nucleic acids of the Hg^{2+} has been studied over a period of time;[97,99,100] a bis(methylthyminato-N3) complex,[101] a bis(9-methyladeninium-N7) complex[102] and a bis(8-azahypoxanthinato-N9) complex,[103] that is not actually useful for the introduction into DNA, since in DNA the metal can not coordinate over N9. There are several other examples of methylmercury[99,104] and $HgCl_2$ adducts[105] to nucleobases.

First of all, synthesis of 1-deazapurine (**21**) was done in good yield as described in the literature,[106] starting from purchased 2,3-diaminopyridine, but although using a liquid-liquid extractor over night, instead off extracting by hand, the yield could not be raised any further. However, the use of the liquid-liquid extractor was essential for getting these good yields. Other descriptions of this synthesis did not raise the expectations of getting higher yields.[107,108]

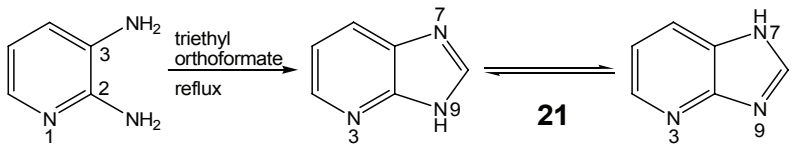

Figure 36: Schematic diagram of the synthesis of 1-deazapurine (**21**) from 2,3-diaminopyridine.

The methylation of 1-deazapurine (**21**) using methyl iodide gave the 1-deaza-9-methylpurine (**22**) and the isomeric 1-deaza-7-methylpurine (**23**) as side product, which could be separated by flash chromatography.[96] The synthesis used is analogous to the synthesis of methylpurines.[109] In the literature other routes of obtaining the two methyl-1-deazapurines or derivatives of them are described using different starting materials and reactions conditions.[110-112] 1-Deaza-9-methylpurine (**22**) and the isomeric 1-deaza-7-methylpurine (**23**) could be distinguished with the help of ^{1}H,^{1}H NOESY experiments, which gave rise to two cross-peaks involving the methyl group in the second case (close contacts to H6 and H8) and one cross-peak only in the first case (close contact to H8). The relative amount of **22** and **23** is probably influenced by the reaction solvent, as has been reported for the methylation of purine, where the N9-isomer was favoured in DMSO and equal amounts of N7- and N9-isomer were found in H_2O. This is thought to be due to the H_2O building H-bonds with the N7-anomer and therefore stabilising it.[109,113]

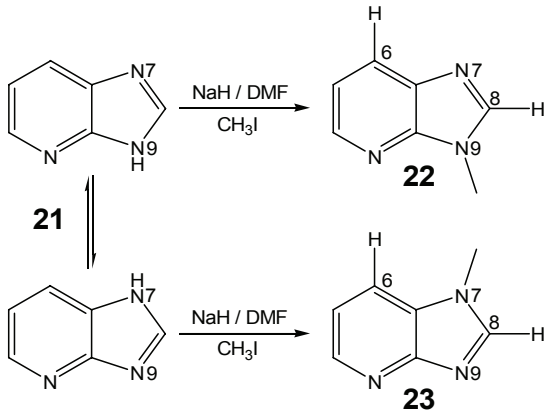

Figure 37: Schematic diagram of the synthesis of 1-deaza-9-methylpurine (**22**) and the 1-deaza-7-methylpurine (**23**) from 1-deazapurine (**21**).

For the reaction with Hg^{2+} any possible competition between protonation and metalation of the ligand had to be ruled out beforehand. Therefore the pK_a values had to be evaluated in order to verify pK_a values determined spectrophotometrically more than 40 years ago.[112] pD-dependent ^{1}H chemical shifts of the aromatic protons have been measured and gave a pK_a value (corrected for H_2O) of 3.67(5) for 1-deaza-

9-methylpurine (**22**). The isomeric 1-deaza-7-methylpurine (**23**) was found to be slightly less acidic; its pK_a amounts to 3.83(5). A good correlation with the photometrically determined values[112] (3.93 and 4.10, respectively) was found. Therefore no competing effect of protonation should be expected when performing the metalation reaction at pH values higher than 5.

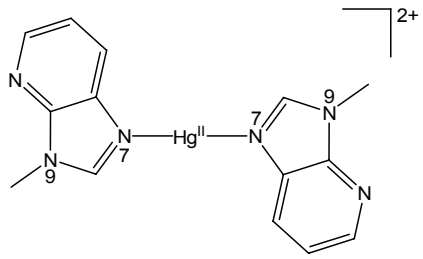

Figure 38: Schematic picture of the cation of $[Hg(9\text{-MeDP})_2](NO_3)_2 \cdot H_2O$ (**24**).

To a solution of 1-deaza-9-methylpurine (**22**) and half an equivalent of Hg^{2+}, $NaNO_3$ was added to give colourless crystals of $[Hg(9\text{-MeDP})_2](NO_3)_2 \cdot H_2O$ (**24**). The crystals turned out to be suitable for X-ray crystallography and the crystal structure is shown in Figure 39. With Ag^+, as another linear coordinating metal ion, no clean reaction was observed and the product seemed to have a low solubility. From that it was not possible to obtain crystals.

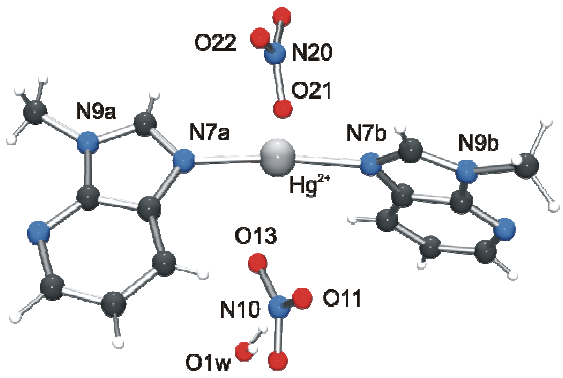

Figure 39: Crystal structure of $[Hg(9\text{-MeDP})_2](NO_3)_2 \cdot H_2O$ (**24**).

The Hg^{2+} is bound to the N7 positions of two 1-deaza-9-methylpurine (**22**) ligands that are arranged approximately trans to each other (173.1(1)°) and are orientated nearly perpendicular at a dihedral angle of 82.98(7)°. Due to the lack of coordination sites on the Watson-Crick side, the N7 position on the Hoogsteen side is the available free binding position for metal-mediated base pairing. This is also the case in a triple helix.[114]

The Hg–N distances of 2.073(3) and 2.075(3)Å are in the range of those typically found in complexes between ligands coordinated via trans orientated endocyclic nitrogen atoms and Hg^{2+}. Examples for these typically found bond lengths of around 2.07Å are complexes with 1-methylthymine (2.04Å), 9-methylguanine (2.06(1)Å, 2.08(1)Å) or ,thirdly, 1-methylcytosine (2.07(1)Å, 2.08(1)Å).[101,102,105,115,116] However, the intermetallic distance between two neighbouring mercuric ions of 5.402(1)Å is too long to account for a metal-metal interaction. In an oligonucleotide the backbone could, however, bring the metal ions bound in different base pairs closer to each other. This could lead to interactions between these metal ions and then possibly to interesting magnetic and electrical properties. But for the use inside an oligonucleotide there is a necessity of planarity for the base pairs. In Figure 40 it can clearly be seen that this is not the case for the model structure.

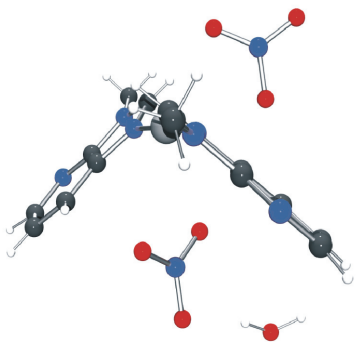

Figure 40: Crystal structure of $[Hg(9\text{-MeDP})_2](NO_3)_2 \cdot H_2O$ (**24**) looking along the N7a-Hg-N7b axis.

But next to the important features of the crystal in comparison with 1-deaza-9-methylpurine (**22**) as a potential artificial nucleobase in an oligonucleotide, the

crystal has further interesting aspects.[96] In Table 4 selected interatomic distances and angles are listed.

Hg–N7a	2.075(3)	**N7a–Hg–N7b**	173.1(1)
Hg–N7b	2.073(3)	**N10–O11–Hg**	92.5(3)
Hg–O11	2.985(4)	**N10–O13–Hg**	104.1(3)
Hg–O13	2.747(3)	**N20–O21–Hg**	98.2(2)
Hg–O21	2.716(3)	**N20–O22–Hg**	96.1(3)
Hg–O22	2.774(3)	**N20a–O21a–Hg**	99.0(2)
Hg–O21a	2.758(2)	**N20a–O23a–Hg**	94.8(3)
Hg–O23a	2.856(3)	**Hg···Hga**	5.402(1)
Hg···O1w	6.065(5)		

Table 4: Selected interatomic distances (Å) and angles (°)

It is known that mercuric complexes can contain distant bonded atoms in addition to the close bonded atoms[98]. This can be seen for $[Hg(9\text{-MeDP})_2](NO_3)_2 \cdot H_2O$ (**24**), too. Using a van der Waals radius of 1.70Å for mercury, which is the lower limit of the values suggested in the literature[117] and 1.40Å for oxygen, the Hg–O contacts between the metal ion and nitrate oxygen atoms in the title compound (Hg–O: 2.716(3) – 2.985(4)Å) can surely be considered as bonding interactions.

In addition, bonds exist to two symmetry-generated nitrate oxygen atoms from a neighbouring unit cell (Hg–O: 2.758(2)Å, 2.856(3)Å). The Hg^{II} coordination sphere is completed by six longer contacts to three nitrate ions oriented more or less perpendicular to the N–Hg–N plane (65.2(2)°, 72.8(3)° and 72.8(3)°). All nitrate moieties in $[Hg(9\text{-MeDP})_2](NO_3)_2 \cdot H_2O$ (**24**) can be considered symmetrically bidentate, when applying certain criteria.[118] Around the metal ion a distorted hexagonal bipyramidal geometry is present. The sum of inner angles within the distorted hexagonal plane should deviate only slightly from that of an ideal hexagon (720°). The sum amounts to 696° and is very close to the wanted 720°. This kind of arrangement of nitrate ions has previously only been observed for cadmium and tin

complexes.[119-121] It has to be said, though, that that strictly seen the nitrate ions in the cadmium complex are asymmetrically bidentate.

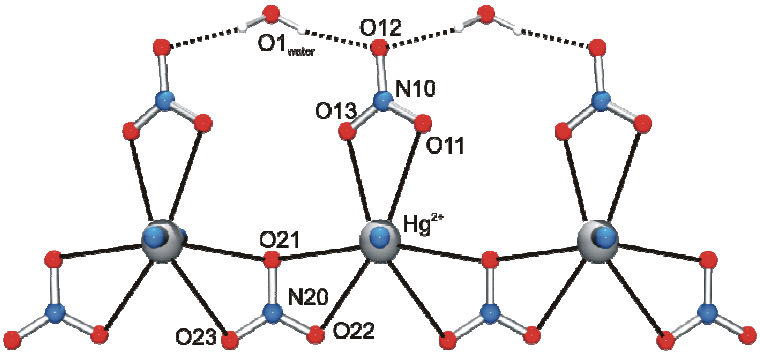

Figure 41: Honeycomb-like chain structure of $[Hg(9\text{-MeDP})_2](NO_3)_2 \cdot H_2O$ (**24**).

As the nitrate ion comprising N20, O21, O22 and O23 is bridging two neighbouring mercuric ions, an unprecedented honeycomb-like chain structure of nitrate moieties is generated that is held together by Hg^{II} ions positioned inside the combs. Usual bond lengths are observed for the nitrate N–O bonds (1.229(4)–1.258(4)Å). The water of crystallisation bridges neighbouring nitrate ions that are present in a nitrate chain via O1w–H···O12 hydrogen bonds (O1w···O12: 2.964(6)Å, O1w···O12a: 2.928(6)Å). There is no contact of the water of crystallisation with the mercuric complex (Hg···O1w: 6.065(5)Å).

3.2 Synthesis of the Nucleoside

For the synthesis of the 1-deazapurine-N9-β-2´-deoxyribonucleoside the 1-deazapurine (**21**) was deprotonated with NaH and Hoffer´s chlorosugar (**25**)[122-124] was added to get 1-deazapurine-N9-β(α)-[2´-deoxy-3´,5´-di-O-(p-toluoyl)-ribonucleoside] (**26b** and **26a**), as product and 1-deazapurine-N7-β(α)-[2´-deoxy-3´,5´-di-O-(p-toluoyl)-ribo-nucleoside] (**27b** and **27a**), as side product.

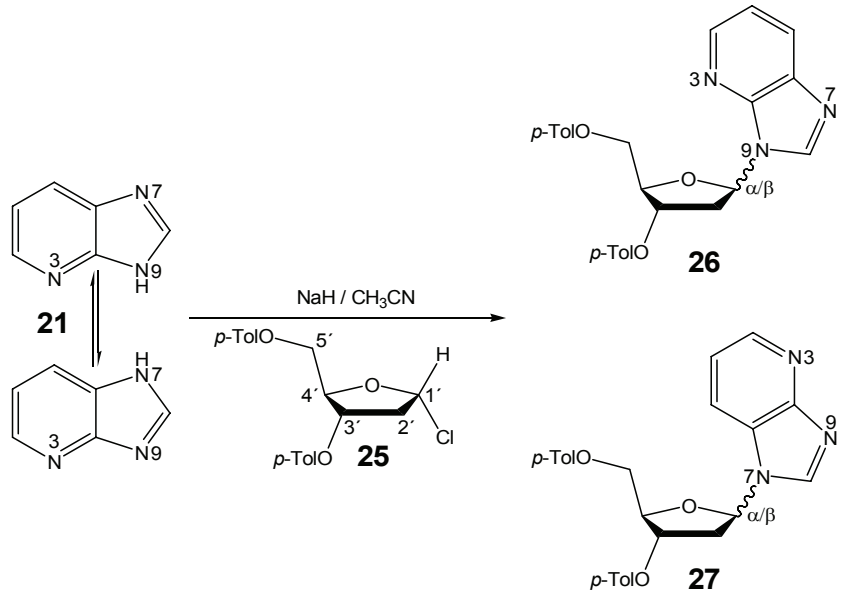

Figure 42: Schematic diagram of the synthesis of 1-deazapurine-N9-β(α)-[2´-deoxy-3´,5´-di-O-(p-toluoyl)-ribonucleoside] (**26b** and **26a**) and 1-deazapurine-N7-β(α)-[2´-deoxy-3´,5´-di-O-(p-toluoyl)-ribonucleoside] (**27b** and **27a**).

The appearance of both, the N9 (**26**) and N7 (**27**) product (no N3 coordination) is thought to be due to the possible tautomeric structure of the 1-deazapurine (**21**) as described by T. Wenzel and F. Seela.[113] The ratio of N9 (**26**) to N7 (**27**) product can be influenced by the reaction temperature and the reaction solvent;[109] the lower the temperature (down to 0°C), the more N9 product (**26**) was found; the higher the temperature (up to 60°C), the more N7 product (**27**) was found. At a reaction temperature of 0°C the ratio of 2:1 (N9:N7) and the yields are comparable to those

from T. Wenzel and F. Seela,[113] though they synthesised the two products using five equivalents of powdered KOH and TDA-1 as catalyst, instead of NaH, and got additionally mono protected products. Other reaction routes have been suggested for the synthesis of the nucleoside or its derivatives, though, they did not appear more successful than the chosen one.[125,126] However, not many observed the formation of alpha- and beta-anomers (**26a** and **26b**, **27a** and **27b**), especially not in the latter publications. While in the literature the formation of the alpha-anomer has not been reported for the formation of N-glycosidic bonds, all our reactions still gave both anomers. This could be due to the fact, that Hoffer´s chlorosugar (**25**) rapidly turned from the alpha-anomer, from which the beta nucleoside is formed, to the beta-anomer in solution. The synthesis was not always successful; the yields were low in comparison with the literature and changing permanently. Nevertheless Hoffer´s chlorosugar (**25**) could be stored under vacuum for up to two weeks without showing any sign of decomposition or anomerisation. Indeed, it has been reported, that the alpha-anomer is stable in the solid state, but that it undergoes a decomposition-anomerisation reaction in solution.[122-124] Therefore it is more likely, that Hoffer´s chlorosugar (**25**) turned into its beta-anomer very rapidly upon the addition to the deprotonated 1-deazapurine (**21**). The N9 and N7 species (**26** and **27**) can be separated by flash chromatography. At first, only the N9 linked 1-deazapurine as nucleobase (**26**) was aimed at and regarded as useful. Due to the high amounts of N7 linked 1-deazapurine (**27**) that were synthesised, as so called side product, and due to the possibility of having a [2+2]-coordination system next to the [1+1]-coordination system of 1-deazapurine-N9-β-nucleoside (**28**), the 1-deazapurine-N7-β-nucleoside (**29**) (both shown in Figure 44) became interesting and was synthesised, too.

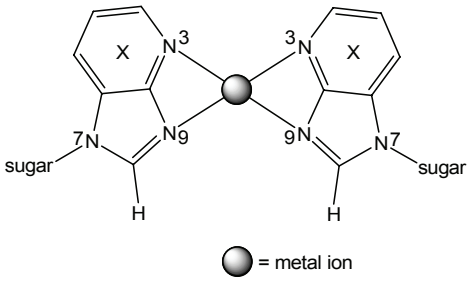

Figure 43: Example of a possible metal-mediated base pair with over N7-coordinated 1-deazapurine (X) nucleoside (**29**) binding to a metal ion over N3 and N9.

The N9 and N7 species (**26** and **27**) were deprotected using saturated NH_3/CH_3OH solution to give **28** and **29**, respectively. The reactions were monitored using TLC and the reaction times were much longer than described by T. Wenzel and F. Seela,[113] still the yields were comparable.

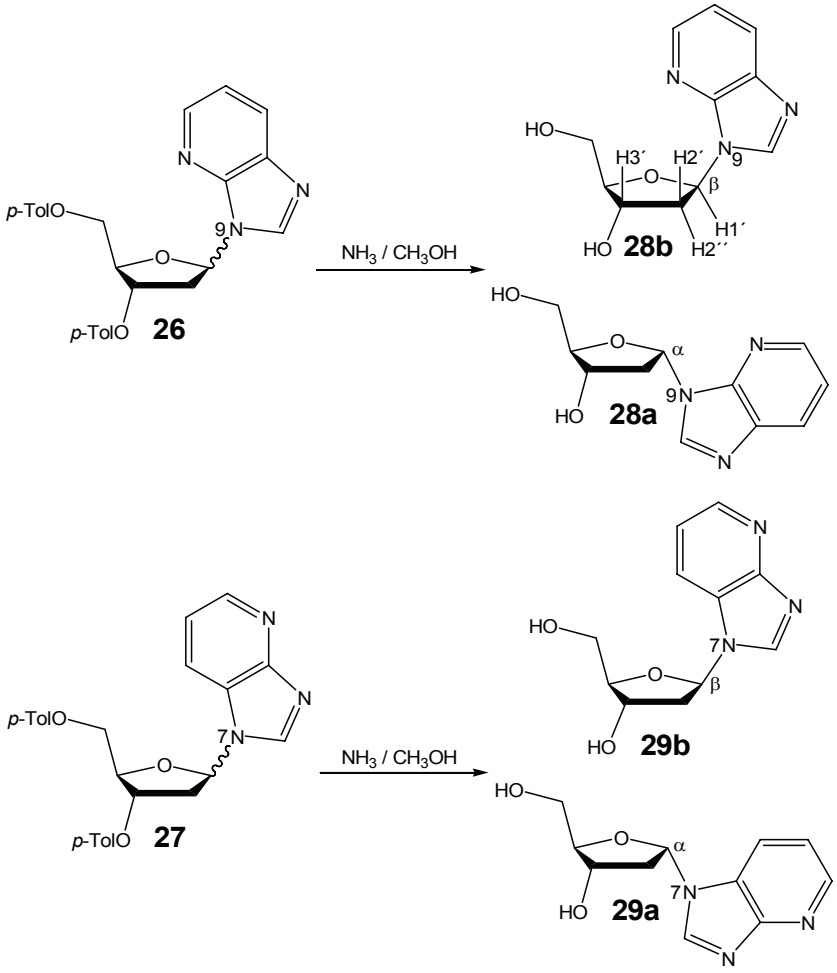

Figure 44: Schematic diagram of the syntheses of 1-deazapurine-N9-β(α)-nucleosides (**28b** and **28a**) and 1-deazapurine-N7-β(α)-nucleosides (**29b** and **29a**).

The different anomers of the N9 product (**28b** and **28a**) and the N7 product (**29b** and **29a**) can also be separated by flash chromatography and distinguished by ^1H, ^1H NOESY and by the characteristic coupling constants of the H1´ sugar proton in N-glycosides. When the two anomers are still protected (**26b**, **26a**, **27b** and **27a**), there is a very valuable observation, for distinguishing between the two anomers. The protecting group of the beta-anomer only shows chemical shifts in two regions of the

aromatic region (2 multiplets), in the alpha-anomer a third signal in-between the other two is observed. This is due to two protons on the protecting group on the O3´, which observe a high field shift, probably, because these protons experience the ring current of the heterocyclic aromatic ring of 1-deazapurine in the alpha-anomer (**26a** and **27a**).

For the 1-deazapurine-N9-β-2´-deoxyribonucleoside (**28b**) the coupling constants H1´/ H2´ and H1´/ H2´´ are almost identical (6.4 and 7.4Hz), which often gives rise to a pseudo-triplet in the ^{1}H NMR spectrum, whereas for the alpha-anomer the coupling constants are quite different (2.8 and 7.8Hz), leading more likely to a doublet of doublets. Using ^{1}H, ^{1}H NOESY experiments both anomers can easily be distinguished. The H1´ proton of 1-deazapurine-N9-β-2´-deoxyribonucleoside (**28b**) displays a strong cross-peak to H2´´, but only a week to the H2´. This is the opposite trend for the alpha-anomer. The stereospecific assignment of H2´ and H2´´ can be facilitated by comparing the intensities of their cross-peaks to the H3´ (strong and weak, respectively). Similarly the 1-deazapurine-N7-β-2´-deoxyribonucleoside (**29b**) can be distinguished from its alpha-anomer using ^{1}H, ^{1}H NOESY experiments.

3.3 Characterisation

Having synthesised the two nucleosides (**28b** and **29b**), one can characterise them and from the obtained data relate to their behaviour in oligonucleotides and possible double helix formation upon the addition of metal ions.

One was able to crystallise the 1-deazapurine-N9-β-2´-deoxyribonucleoside (**28b**) and the 1-deazapurine-N7-β-2´-deoxyribonucleoside (**29b**). Additionally, crystals of the 1,3-deazapurine-β-2´-deoxyribonucleoside (**30**) that has been synthesised in our research group[127] as another potential artificial nucleobase for metal-mediated base pairing, were obtained and all three turned out to be suitable for X-ray crystallography.

To describe the structures exactly and comparable to other nucleosides one has to define certain torsion angles. Here, the definition from the IUPAC of the year 1998 was used.[128] The five sugar torsion angles $\nu_{0\text{-}4}$ are defined as follows:

ν_0 for C4´-O4´-C1´-C2´,

ν_1 for O4´-C1´-C2´-C3´,

ν_2 for C1´-C2´-C3´-C4´,

ν_3 for C2´-C3´-C4´-O4´,

ν_4 for C3´-C4´-O4´-C1´.

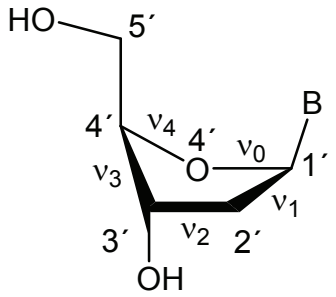

Figure 45: A nucleoside (B = base) showing $\nu_{0\text{-}4}$.

Using two equations,

$\nu_m = \nu_2/\cos P$ and $\tan P = [(\nu_4 + \nu_1) - (\nu_3 + \nu_0)]/2\nu_2(\sin 36° + \sin 72°)$,

a value for the angle of pseudorotation (P) and for the puckering amplitude (ν_m) can be calculated. Important to notice: If the value of ν_2 is negative, one has to correct the value of P by +180°. Also a negative ν_2 gives an N-type conformation of C1´-C2´-C3´-C4´, a positive value an S-type conformation, as shown in Figure 46.

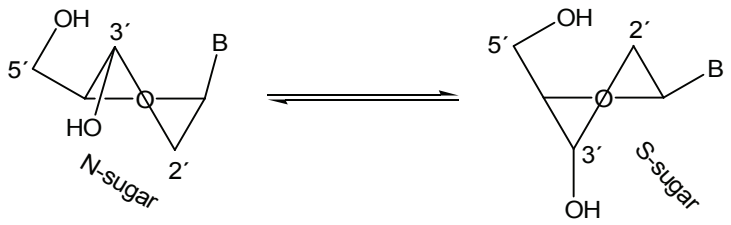

Figure 46: N-sugar (3´-endo and 2´-exo) and S-sugar (2´-endo and 3´-exo) conformations, twisted forms (T).

Knowing the value for P and using the pseudorotation cycle of the furanose ring, one can now exactly find out, whether only one atom is out of the sugar plane (envelope or E) or two atoms (twisted or T). From the value it can also be described, which atom or atoms come out of the plane (C1´, C2´, C3´, C4´or O4´), and in which direction (above the sugar plane = endo or underneath the sugar plane = exo). For example in Figure 46 both the C2´ and the C3´ are out of the sugar plane, but in Figure 45 only the C4´ is out of the plane and it would be named C4´-endo or ^{4}E. The pseudorotation cycle of the furanose ring can be found in the literature, as well as the conformational region cycle for torsion angles.[128]

There are further two important torsion angles that are described by this conformational region cycle for torsion angles, γ (O5´-C5´-C4´-C3´) (+/- synclinal (sc) or gauche), which describes the position of the C5´-O5´ compared to the sugar ring, and χ (O4´-C1´-N(base)-C4/for purine bases) (syn or anti), which describes the orientation of the nucleobase around the glycosidic bond.

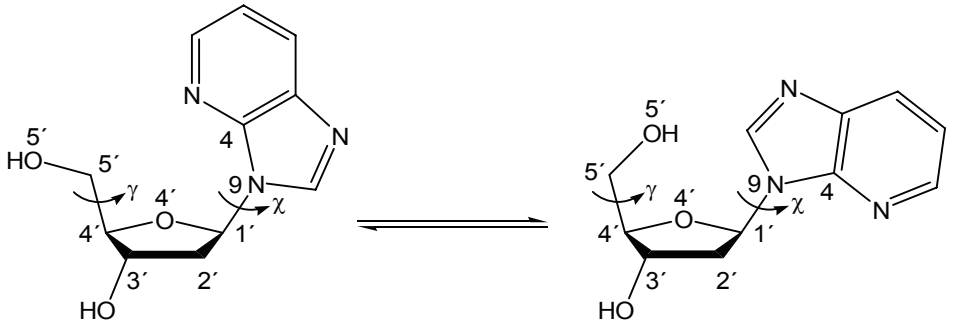

Figure 47: Picture of the two torsion angles in a nucleoside, γ (O5´-C5´-C4´-C3´) and χ (O4´-C1´-N(base)-C4/for purine bases).

Now, for the 1-deazapurine-N7-β-2´-deoxyribonucleoside (**29b**) the structure obtained was disordered at the C2´and C3´ of the sugar ring. Therefore, two different conformations can be observed. The first (**29b I**) is in the 2´-exo envelope N-type or $_2$E (N) conformation, as shown in Figure 48, which is not usually found for 2´-deoxy-ribonucleosides. The often observed conformations are of the C1´-exo (S) and C3´-exo (S) and C2´-endo (S) and C3´-endo (N) type. The second (**29b II**) (not shown) is in the 3´-exo envelope S-type or $_3$E (S) conformation. The C5´-O5´ of both are in the +gauche or +synclinal conformation compared to the sugar ring and both have the base in syn position, since this is not influenced by the disorder at C2´ and C3´.

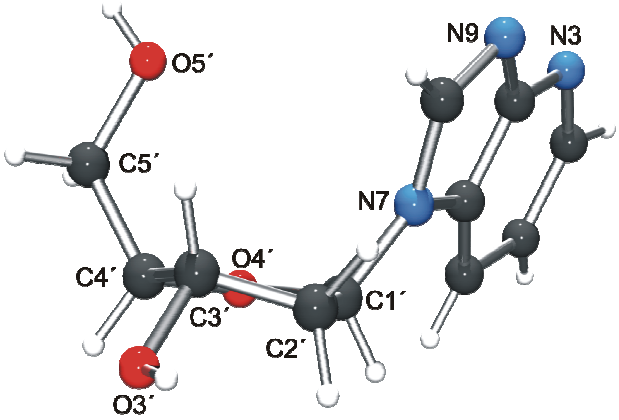

Figure 48: Crystal structure of 1-deazapurine-N7-β-2´-deoxyribonucleoside (**29b I**) in the $_2$E (N) or 2´-exo envelope (N) conformation with the base in syn position and the C5´-O5´ in +gauche or +sc.

The 1-deazapurines stack on top of each other having the N3 nearly on top of the N7 and vice versa and the N9 nearly on top of the other N9. The O5´-H5´ builds an H-bond with the N3 that lies on top of the 1-deazapurine unit that belongs to this molecule and vice versa. The length of the H-bond is 2.838(6)Å with an angle of 160.9(3)°. In one direction the 1-deazapurines stack having the sugar units lying alternating on opposite sides. The different channels of the 1-deazapurine stacking are linked by the sugar units with an H-bond over the O3´-H3´ to that of another sugar unit. However, through the disorder in the C2´, C3´and O3´ positions it is difficult to exactly find these H-bonds. The atoms do lie close enough together (≈2.8Å).

The 1-deazapurine-N9-β-2´-deoxyribonucleoside (**28b**) is present twice in one unit cell and the two nucleosides differ. Both C5´-O5´ are in the +gauche or +sc conformation. For the first (**28b I**) the sugar is in the 3´-endo envelope N-type or ^{3}E (N) conformation that is, as has been mentioned already, a typical conformation for 2´-deoxy-ribonucleosides. However, the second (**28b II**) has a C4´-exo envelope N-type or $_{4}E$ (N) conformation, as can be clearly seen in Figure 49. The C4´ can be found underneath the plane of the four other atoms in the sugar ring. Whereas the glycosidic bond angle for **28b I** can be described as syn with -82.3(5)°, the angle for **28b II** is right at the borderline between syn and anti with a value of -91.1(4)°. This could be due to the unusual conformation of **28b II**, since the sugar conformation has an influence on the glycosidic bond angle.

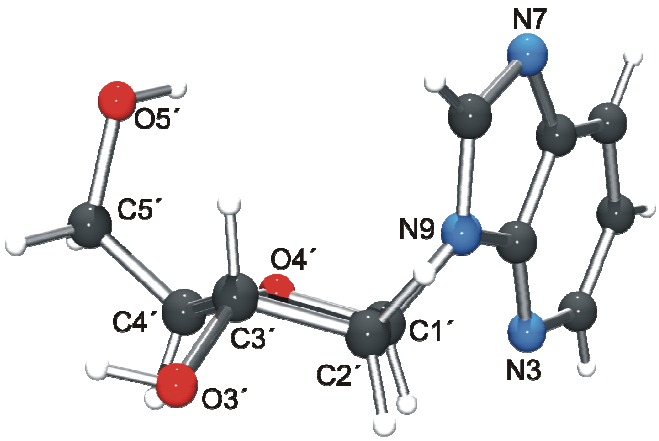

Figure 49: Crystal structure of 1-deazapurine-N9-β-2´-deoxyribonucleoside (**28b II**) in the $_{4}E$ (N) conformation with the base in syn/anti position and the C5´-O5´ in +gauche or +sc.

The deazapurine rings stack with the N3 positions over the C6 position in alternating fashion, as it was found for the 1-deaza-N3-oxidepurine (**35**). The sugar rings of two neighbouring molecules always point in opposite directions. Rows of stacking dezapurine rings can be found, where the six membered rings are completely on top of each other and the five membered rings are tilted slightly to one side in an alternating manner. Next to this, there are also channels of sugars. An H-bond between the O5´-H5´ of each sugar and an N7 of a neighbouring deazapurine is

present. The O5´-H5´···N7 bond has a length of 2.775(4)Å and an angle of 160(3)°. The interconnection of the different chains and channels, which are stabilised by stacking 1-deazapurine and an H-bond, is done by further two H-bonds. **28b I** always builds out an H-bond over its O3´-H3´ to the N3 of a **28b II** (2.800(4)Å and 170(4)°). On the other side the **28b II** builds out an H-bond over its O3´-H3´ to the O5´ of a **28b I** (2.800(5)Å and 174(4)°). Since alternating **28b I** and **28b II** are present that bind differently, one finds a tight connection between the different channels of sugar and 1-deazapurine stacking.

The crystal structure of the 1,3-deazapurine nucleoside (**30**) shows the base in the syn conformation with a glycosidic bond angle of -63.8(3)°. Again, it can nicely be seen that the C2´ atom comes of the plane of the other four atoms giving rise of a 2´-endo envelope S-type or ^{2}E (S) conformation. The C5´-O5´ points away from the ring, which shows that a –gauche or –sc conformation is present.

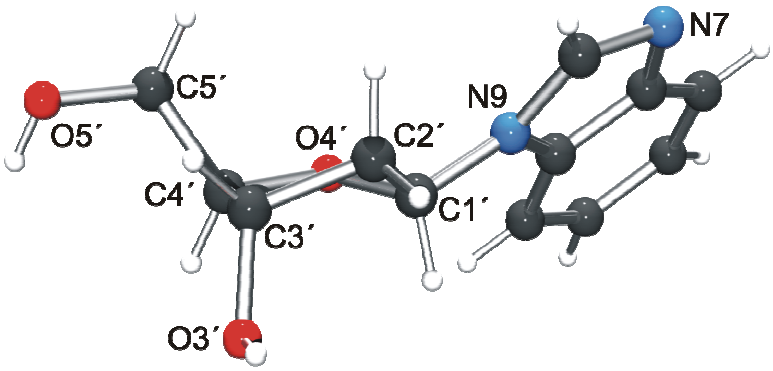

Figure 50: Crystal structure of 1,3-deazapurine-N9-β-2´-deoxyribonucleoside (**30**) in the ^{2}E (S) conformation with the base in the syn position and the C5´-O5´ in -gauche or -sc.

It has been found that there are H-bonds between O5´-H5´ and N7 from a neighbouring molecule and O3´-H3´of another neighbouring molecule to the O5´. The distances between O5´-H5´···N7 and O3´-H3´···O5´ are 2.765(3) and 2.725(2) with angles of 168(2)° and 174(2)°, respectively. These are typical values for strong H-bonds. There are one dimensional chains horizontally and vertically connected by the

H-bond O5´-H5´···N7. The one dimensional chains are like steps, but no stacking between the bases is observed. Additionally the O3´-H3´···O5´ H-bonds connect the vertical one dimensional chains with the horizontal chains and vice versa.

To be able to compare all results of the conformations of the nucleosides, the values are summarised in Table 5. Important to notice are the envelope conformation for all nucleosides, as well as the glycosidic bond angles that are all, except of one that is on the borderline, in the syn conformation. The values for the puckering amplitudes do differ slightly; however, they are all in the normal range for these values.

	29b I	**29b II**	**28b I**	**28b II**	**30**
ν_0	+20(1)°	- 2.9(5)°	+2.1(4)°	- 17.0(4)°	- 31.7(2)°
ν_1	- 40(1)°	+26(1)°	- 19.5(4)°	- 2.3(5)°	+40.8(2)°
ν_2	+40(2)°	- 35(1)°	+28.3(4)°	+19.1(4)°	- 34.0(2)°
ν_3	- 29(2)°	+35(1)°	- 27.4(4)°	- 29.1 (4)°	+16.5(2)°
ν_4	+8(1)°	- 19(1)°	+16.3(4)°	+29.0(4)°	+9.2(2)°
P	- 11°	+194°	+14°	+51°	+148°
	$_2$E (N)	**$_3$E (S)**	**^{3}E (N)**	**$_4$E (N)**	**^{2}E (S)**
ν_m	41°	36°	29°	30°	40°
γ	+44(1)°	+72(1)°	+56.4(5)°	+50.7(5)°	- 63.4(3)°
	+sc, +gauche	**+sc, +gauche**	**+sc, +gauche**	**+sc, +gauche**	**-sc, -gauche**
χ	- 74.5(6)°	- 74.5(6)°	- 82.3(5)°	- 91.1(4)°	-63.8(3)°
	syn	**syn**	**syn**	**syn/anti**	**syn**

Table 5: The endocyclic torsion angles ($\nu_{0\text{-}4}$) in the sugar ring to calculate the phase angle of pseudorotation (P) and the puckering amplitude (ν_m), the torsion angle (γ) for the conformation of the C5´-O5´ compared to the sugar ring and the glycosidic bond angle (χ) are listed (in the order as discussed).

As done before with the ligand, 1-deaza-9-methylpurine (**22**), of the model structure, $[Hg(9\text{-MeDP})_2](NO_3)_2 \cdot H_2O$ (**24**), it is important to look first at the protonation reaction of the nucleosides, to rule out an interference of this reaction with the wanted metalation. Therefore the pK_a values for the nucleosides needed to be

determined. pD-dependent ^{1}H chemical shifts of the aromatic protons of the nucleosides have been measured, as shown in Graph 1.

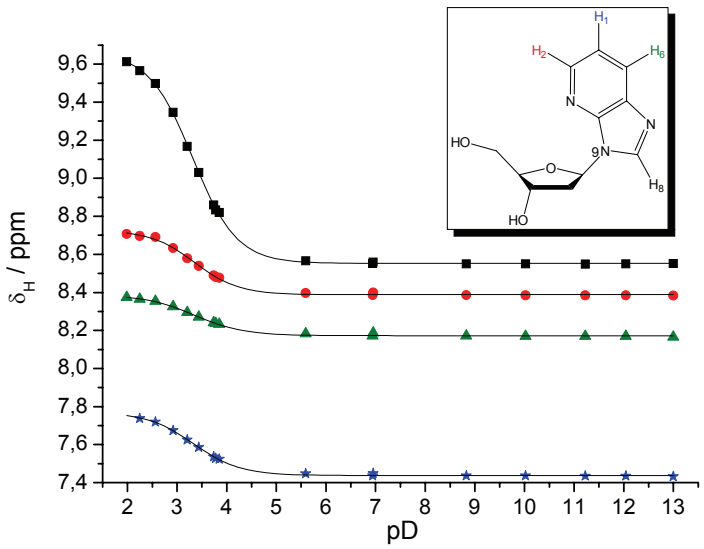

Graph 1: Chemical shift (δ) of the aromatic protons against pD-value for 1-deaza-purine-N9-β-2´-deoxyribonucleoside (**28b**).

For **28b** a pK_a value (corrected for H_2O) of 2.84(2) was calculated from the data obtained, for **29b** the pK_a value is 3.26(2). Hence, at pH values higher than 5 no competition of protonation and metalation should be expected.

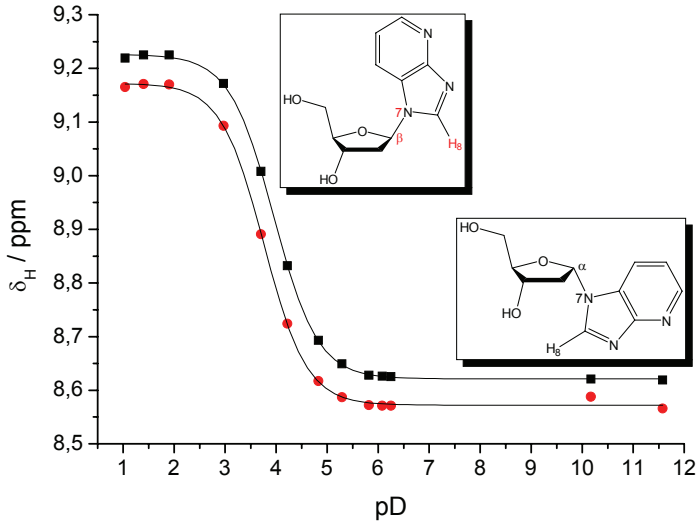

Graph 2: Chemical shift (δ_H/ppm) of the H8 protons of the β- and α-anomer against the pD-value for 1-deazapurine-N7-β(α)-2´-deoxyribonucleoside (**29b** and **29a**)

The **29b** and **29a** are slightly less acidic than **28b** and **28a**. This trend was also observed for the 1-deaza-7-methylpurine (**23**) and the 1-deaza-9-methylpurine (**22**) and for the alpha-anomers of the nucleosides in comparison with the beta-anomers. For simplification, Table 6 shows all pK_a values of the synthesised nucleosides and others for comparison.

Nucleoside	β-Anomer	α-Anomer	Methyl derivative
1,3-Deazapurine (30)	4.21 ± 0.03[127]	4.45 ± 0.03[127]	5.67 ± 0.02[129]
1-Deazapurine-N9 (28)	2.84 ± 0.02	3.15 ± 0.02	3.67 ± 0.05
1-Deazapurine-N7 (29)	3.26 ± 0.02	3.45 ± 0.02	3.83 ± 0.05
Imidazole	6.01 ± 0.05[92]	6.42 ± 0.05[92]	7.20 ± 0.02[130]
Triazole	1.32 ± 0.05[92]	1.53 ± 0.05[92]	2.31 ± 0.03[131]
Tetrazole	‹ -3	‹ -3	- 3.00[132]

Table 6: pK_a values of the synthesized nucleosides and others for comparison; the values of -3 for the tetrazoles are estimates based on the pK_a value of the corresponding 1-methyl derivative.

The methyl derivatives have in each case a less acidic pK_a value than the nucleosides[133], as is customary for nucleosides. The alpha-anomer of the nucleosides always has a less acidic pK_a value than the beta-anomer. The sugar ring of the nucleosides has a more stabilising effect on the non-protonated form than a methyl group, but the fact, that the alpha-anomer is less acidic has to be investigated further. The same trends are found for the imidazole, triazole and tetrazole nucleosides or methyl derivatives, but also an additional observation could be made. An increase of N atoms in the five membered ring gives an increase in acidity. And comparing imidazole and the 1-deazapurine-N9 or -N7 nucleosides (**28** and **29**), it can be said, that introducing a pyridine ring onto the five membered imidazole ring, which ever way around, gives also an increase in acidity. This increase is larger than through the addition of a benzene ring, as in 1,3-deazapurine (**30**). Substitution of a C atom with an N atom in the six membered ring shows the same trend as found in the five membered rings, but the effect is found to be much smaller.

Knowing, that no competition between protonation and metalation is thought to occur, it is possible to characterise the nucleosides further, especially their behaviour towards metal ions.

The ability of forming a complex with a metal ion, as well as a rough idea of the strength of such a complex and the stoichiometry can be observed with the means of a Job-Plot. The method of continuous variation was used for the Job-Plot.[134-137] The change in chemical shift ($\Delta\delta_{ppm}$) is observed with the help of ^{1}H NMR at different mole fractions (χ) of ligand (nucleoside) and M^{n+}. A Job-Plot for 1-deazapurine-N9-β-2´-deoxyribonucleoside (**28b**) with Hg^{2+} is shown in Graph 3. The change in chemical shift ($\Delta\delta$) of the aromatic protons multiplied with the mole fraction (χ) of **28b** is applied at the y-axis and the different mole fractions (χ) of **28b** at the x-axis.

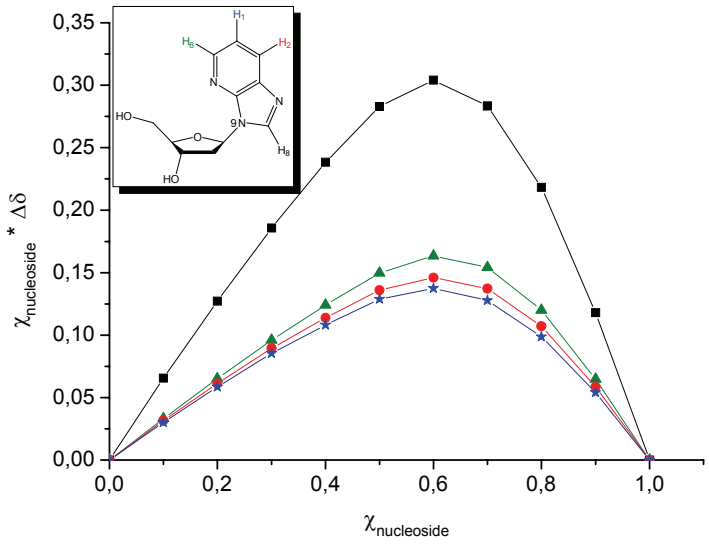

Graph 3: Job-Plot of 1-deazapurine-N9-β-2´-deoxyribonucleoside (**28b**) with Hg^{2+} at pD 5.

Graph 3 shows a maximum higher than 0.6 mole fraction (χ) of the 1-deazapurine-N9-β-2´-deoxyribonucleoside (**28b**). It can be concluded that a complex has been formed and that this result gives rise to a 2:1 complex. Two 1-deazapurine-N9-β-2´-deoxyribonucleosides (**28b**) bind to one Hg^{2+}. This correlates nicely with the model structure $[Hg(9\text{-methyl-1-deazapurine})_2](NO_3)_2 \cdot H_2O$ (**24**), which is also a 2:1 complex. The stability of the complex formed in the Job-Plot experiment could not be quantified exactly at this point, but it could be gathered that it is reasonably stable.

The sharper the change of slope the more stable the complex is found to be, the less sharp the change of slope the less stable the complex.[137] Now, in Graph 4 we can see the Job-Plot for the 1-deazapurine-N7-β-2´-deoxyribo-nucleosides (**29b**) with Hg^{2+} (^1H NMR used). It can clearly be seen that the maximum is found at 0.5 mole fractions, leading to a 1:1 complex. Further Job-Plots with Cu^{2+} and Fe^{3+} were measured with the help of UV spectroscopy (at 280nm) giving rise to a 1:1 and a 2:1 complex, respectively. It should be mentioned that those Job-Plots had a minimum and not a maximum, which is dependent on an increase or a decrease in absorbance.

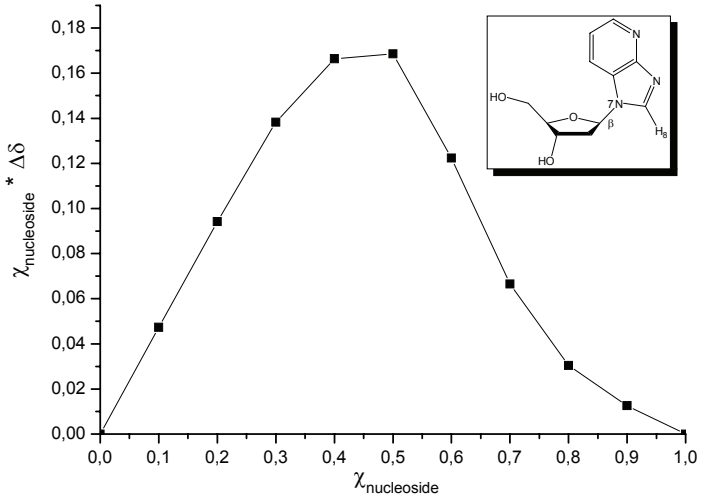

Graph 4: Job-Plot of 1-deazapurine-N7-β-2´-deoxyribonucleoside (**29b**) with Hg^{2+}.

To gather more information about the stoichiometry and the stability of the complexes, titrations with metal ions were done. The changes in chemical shift ($\Delta\delta_{ppm}$) or in absorbance (range of wavelength: 190-350nm) of the nucleosides are observed upon the addition of different equivalents M^{n+} to a fixed amount of ligand (nucleoside). For the 1-deazapurine-N9-β-2´-deoxyribonucleoside (**28b**) the titration was first done at pD 7 as shown in Graph 5. The binding of Hg^{2+} to the ligand takes place in the fast exchange limit (NMR scale). Therefore no individual signals of starting compound and product can be observed, but only the average chemical shifts. It was found that not only one, but more complexes seemed to have been built, when more Hg^{2+} was added. A 2:1 complex, a 2:3 complex and a 2:5 complex were thought to be present. A possible explanation is the formation of complexes where the Hg^{2+} binds to O atoms from the surrounding H_2O molecules.

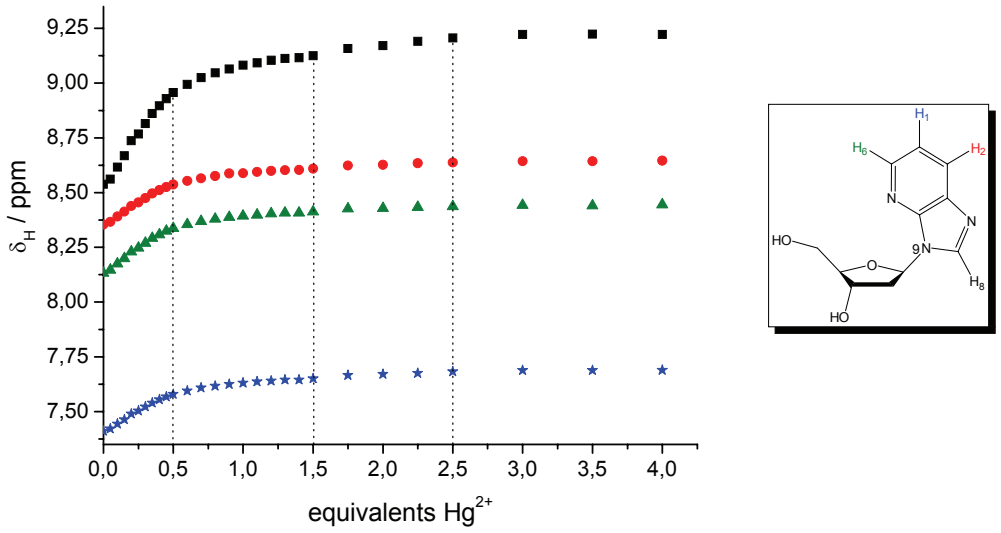

Graph 5: Titration of 1-deazapurine-N9 nucleoside (**28b**) with Hg^{2+} at pD 7.

To check the possibility of the H_2O molecules being involved in binding of Hg^{2+}, the pD was lowered down to 5. Graph 6 shows, in the first view, only the presence of a 2:1 complex. So a lower pD value cancels out the possibility of oxo bridged species being formed.

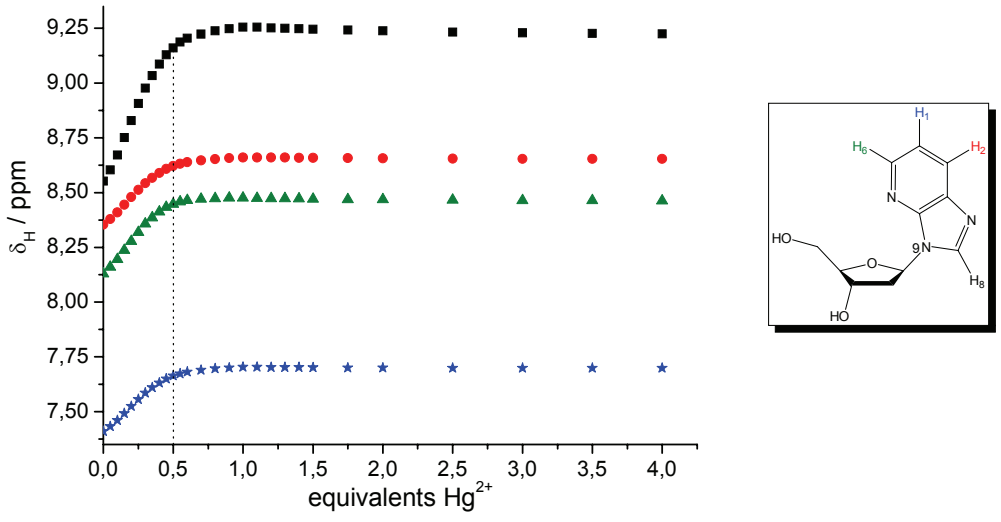

Graph 6: Titration of 1-deazapurine-N9 nucleoside (**28b**) with Hg^{2+} at pD 5.

On the second view, there is a further small change in chemical shift at 0.5 equivalents to 1.0 equivalent of Hg^{2+}. This increase is best seen at the H8 proton and the chemical shift lowers down again upon the addition of more equivalents. The reason

for this is thought to be the presence of a 1:1 complex in addition to the 2:1 complex. Both would have a similar chemical shift. At 0.5 equivalents of Hg^{2+} both the 2:1 and the 1:1 complex are present and upon the excess of equivalents of Hg^{2+}, slowly the equilibrium turns fully to the 1:1 complex side.

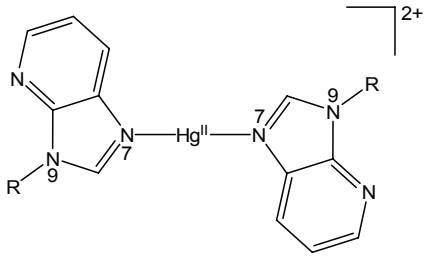

Figure 51: Schematic diagram of a possible 2:1 complex of 1-deazapurine-N9 nucleoside (**28b**) with Hg^{2+}, where R = sugar ring.

The stability of the complex formed can not be quantified exactly through a look at the titration with Hg^{2+}, but it could be gathered that it is reasonable stable, because a relatively abrupt change at 0.5 equivalents has been found, and not a broad change over a few equivalents, which would indicate a weak stability of the complex.
From the data of the titrations, the data necessary for calculating the stability constants were obtained and the stability constants were calculated using EQNMR.[138]

Nucleoside	log β_1	log β_2
1-Deazapurine-N9 (28b)	2.39 ± 0.03	5.22 ± 0.04
Imidazole	› 5[92,136]	› 10[92,136]
Triazole	1.56 ± 0.04[92]	---[92]
Tetrazole	---[92]	---[92]

Table 7: Calculated stability constants of the 1-deazapurine-N9 nucleoside **28b** for a 1:1 (log β_1) and 2:1 (log β_2) complex with Hg^{2+} and for other nucleosides for comparison.

The stability constants are calculated for the 1:1 and the 2:1 complex and it should be noticed that the individual stability constant log K_2 (log β_2 – log β_1 ≈ 2.8) is larger than log K_1 (log β_1 ≈ 2.4) for **28b**, which is also the case for the $[Ag(NH_3)_2]Cl$, for example. But examples for this are rare in the literature and the reasons for the larger value are not known. The value for the 1-deazapurine-N9-β-2´-deoxyribonucleoside (**28b**) is lower than the value for the imidazole nucleoside, though the addition of a pyridine ring to an imidazole destabilises the complex building. This can be compared with the pK_a values, where upon the addition of a pyridine ring the value also dropped. This is the same for a substitution of a C atom by an N atom. But the stability constant is higher than for triazole that only builds a 1:1 complex and tetrazole that does not build complexes with Hg^{2+}. The trend is comparable with the tendency of the individual nucleosides and their pK_a values.

Although the stability constants for the 1-deazapurine-N7 nucleoside (**29b**) were not calculated, titrations with different metal ions were done using UV-spectroscopy. Whereas for Ni^{2+}, Hg^{2+} and Cu^{2+} no change in absorption maxima upon addition of metal ions was observed, but only a small change in absorbance, for Fe^{3+} a change in both was seen. Studies by Lenarcik et al.[139] showed that there are many possible metal ions with the ability of binding 1-deazapurine (**21**) and found high stability constants for 1-dezapurine metal complexes. As described in the literature[139,140] and found in the UV-spectra there seems to be some kind of binding taking place, but it is difficult to quantify this.

3.4 Synthesis of Oligonucleotides

For the automated DNA-synthesizer protecting groups have to be introduced at the O5´-position and the O3´-position of the 1-deazapurine nucleosides (**28b** and **29b)**. This was done following standard procedures used already for the preparations of other artificial nucleosides.[42,93,141-146]

First the nucleosides (**28b** and **29b**) were protected at the O5´ with the stericly bulky DMTr group. The nucleosides were dissolved in pyridine and after the addition of DMTr-Cl and a catalytical amount of DMAP the solutions were stirred for three or four hours, respectively. After the work up yields of 63% were obtained for both, the 1-deazapurine-N9-β-[2´-deoxy-5´-O-(4,4´-dimethoxytrityl)-ribonucleoside] (**31**) and the 1-deazapurine-N7-β-[2´-deoxy-5´-O-(4,4´-dimethoxytrityl)-ribonucleoside] (**32**). It is important to avoid any acidification of the solution, because otherwise the DMTr protecting group comes off again rapidly. The pyridine, which builds pyridinium chloride with the HCl that is formed during the reaction, is supported by the DMAP, which prevents the solution to become acidic and helps the pyridine to build pyridinium chloride more rapidly. The reaction was done under exclusion of water, which would hydrolyse the DMTr-Cl and dissolve produced HCl, which could again destroy the nucleosides.

For the 1-deazapurine-N9-β-[2´-deoxy-5´-O-(4,4´-dimethoxytrityl)-ribonucleoside] (**31**) an interesting observation was made during ^{1}H NMR measurements in $CDCl_3$, where an anomerisation was observed. This anomerisation could be stopped by the addition of a catalytical amount of Et_3N. The $CDCl_3$ seemed to have catalysed the isomerisation, probably because some DCl has been built. However, for the natural nucleobases the isomerisation in the same way did not work.

The introduction of the phosphoramidite protecting group was also done following standard procedures.[42,93,141-146] The addition of $(i\text{-}Pr)_2EtN$ and chloro-(2-cyanoethoxy)-(diisopropylamino)-phosphane to the 1-deazapurine-N9- or 1-deazapurine N7-β-[2´-deoxy-5´-O-(4,4´-dimethoxytrityl)-ribonucleoside] (**31** and **32**) dissolved in dry CH_2Cl_2 and stirring for an hour at r.t. gave the two building blocks needed for the automated DNA-synthesizer, the 1-deazapurine-N9-β-[2´-deoxy-3´-O-

(2-cyanoethyl)-N,N-diisopropyl-phosphoramidite-5´-O-(4,4´-dimethoxytrityl)-ribonucleoside] (**33**) and the 1-deazapurine-N7-β-[2´-deoxy-3´-O-(2-cyanoethyl)-N,N-diisopropyl-phosphoramidite-5´-O-(4,4´-dimethoxytrityl)-ribonucleoside] (**34**). The reaction was also done under exclusion of water. No further work ups were done for two reasons; firstly, since the side product (hydrolysed chloro-(2-cyanoethoxy)-(diisopropyl-amino)-phosphane) was not visible on the TLC plates, therefore it was difficult to separate the side product from the product without a great loss of product and secondly, since the side product should not interfere with the reactions inside the DNA-synthesizers. Therefore the yield was calculated through the ratio of product to side product and the mean molar mass. Then excellent yields were obtained.

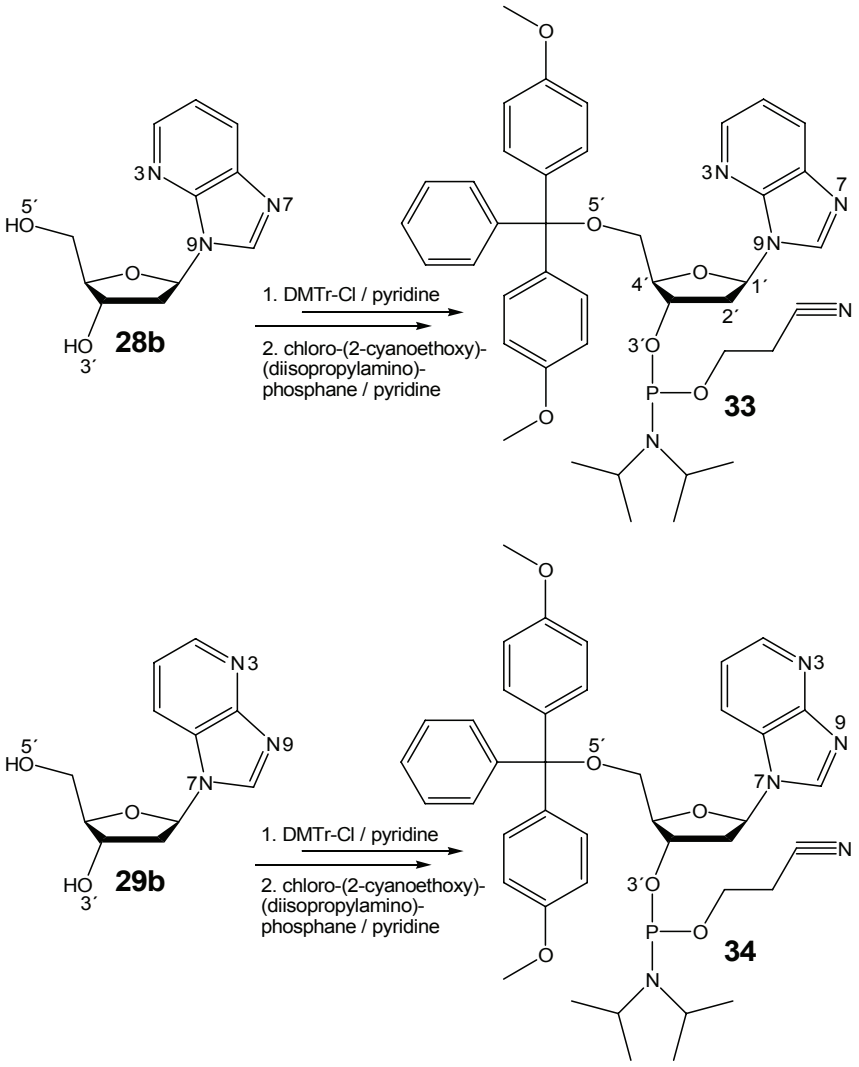

Figure 52: Schematic diagram of the synthesis of the 1-deazapurine-N9- and N7-building blocks (**33** and **34**) for the DNA-synthesizer.

The 1-deazapurine-N9- and 1-deazapurine-N7-β-[2´-deoxy-3´-O-(2-cyanoethyl)-N,N-diisopropyl-phosphoramidite-5´-O-(4,4´-dimethoxytrityl)-ribonucleoside] (**33** and **34**) could then be introduced to the automated DNA-synthesizer.

The following oligonucleotide strands were synthesised with the 1-deazapurine-N7-β-2´-deoxyribonucleoside as the artificial nucleobase (**X**):

(**a**) 5´-d(AAA AAA A**XX** **X**TT TTT TT) ‹ 1% yield

(**b**) 5´-d(AAA AAA A**XX** **XX**T TTT TTT)

(**c**) 5´-d(AAA AAA A**X**A AAA AAA)

(**d**) 5´-d(TTT TTT T**X**T TTT TTT)

The first strand (**a**) was synthesised in DMTr-off mode, deprotected, purified over an ion-exchange column (HPLC), desalted, lyophilised and the concentration was determined with the help of the Lambert-Beer Law and finally the yield was calculated. The second strand (**b**) was not purified, because the expected yield was very low and the results from measurements with the first one (**a**) were no motivation for a further engagement.

The strands (**c**) and (**d**) were synthesised in DMTr-on mode, deprotected, purified over a reversed-phase column (HPLC), deprotected with acetic acid (80%), purified again over a reversed-phase column (HPLC), lyophilised and the concentration was determined with the help of the Lambert-Beer Law. MALDI-TOF spectra though did not show any sign of the wanted oligonucleotides (**c**) and (**d**). Probably the acetic acid in the deprotection step has destroyed the oligonucleotides, since the glycosidic bonds of the used artificial nucleobases are by far not as stable as for natural nucleobases, for which these procedures have been developed for. The purification took place more than two weeks after the synthesis on the automated DNA-synthesiser Therefore another explanation could be that the purification has to be done immediately after the synthesis otherwise the oligonucleotide depurinates over time.

The following oligonucleotide strands were synthesised with the 1-deazapurine-N9-β-2´-deoxyribonucleoside as the artificial nucleobase (**Y**):

(**e**)	5´-d(C**YY YY**G)	‹ 1% yield
(**f**)	5´-d(CGC G**Y**A T**Y**C GCG)	‹ 9%
(**g**)	5´-d(AAA AAA A**Y**A AAA AAA)	‹ 6%
(**h**)	5´-d(TTT TTT T**Y**T TTT TTT)	‹ 17%
(**i**)	5´-d(**YYY YYY YYY YYY YYY Y**A)	‹ 1%

All strands with Y were synthesised in the DMTr-off mode, deprotected, purified over an ion-exchange column (HPLC), desalted, lyophilised and the concentration was determined with the help of the Lambert-Beer Law and finally the yield was calculated. The differences in the yields and the repeatedly low yields can have many possible factors. The trifluoroacetic acid (3% in CH_2Cl_2) used to take off the DMTr protecting groups in the automated DNA-synthesizer could depurinate or denature the oligonucleotide or single artificial nucleobases. The more artificial nucleosides were introduced the lower the yield, the broader the peaks in the HPLC chromatogram and therefore the more difficult to select. An especially visible effect of loss in yield was seen at changes from natural nucleobases to artificial ones. In the HPLC chromatograms for (**g**) and (**h**) peaks for three products are seen. The fact that the adenine rich strand has a lower yield than the thymine rich one has been observed many times and is comparable with the synthesis of natural nucleobases. Another obvious factor is the length of the oligonucleotides; the longer the strand, the lower the yield generally.

After the synthesis the oligonucleotide is still on a solid support. The oligonucleotide gets taken off with the help of AMA (5min / 65°C). If this step is insufficient, since the time is not long enough and only a few percent of product are taken off the solid support, one would also get generally low yields.

3.5 Melting Curves

To be able to discuss melting curves the used terminology has to be explained first. In the melting curves the absorbance at 260nm (usually used for natural nucleobases) is observed upon the change in temperature. With changing temperature the conformation of two single strands can vary between a double helix structure at lower temperatures and two single strands at higher temperatures, since the double helix structure is only stable up to a certain temperature. Above the temperature the amount of single strand goes up and the amount of double helix goes down. At a certain temperature only single strands are present in the solution, T_s. Then the absorbance is the highest and vice versa for only double helix being present. The temperature range between only single strand and only double helix being present, T_s-T_d, lies usually around 10-15°C. One then speaks of cooperative melting. If this temperature range is larger, non-cooperative melting is present.

The melting temperature, T_m, that is always stated, has the temperature value for 50% single strand and 50% double helix being present. The size of the change in absorbance upon a change in temperature differs from system to system and is quantified in percentage by the hypochromicity. At maximal absorbance only single strands are present. When a double helix is present, this value is lower. The size in hypochromicity upon the formation of a double helix gives an idea about the strength of the helix.

The oligonucleotides are always written from the 5´-end (left) to the 3´-end (right), if not stated otherwise.

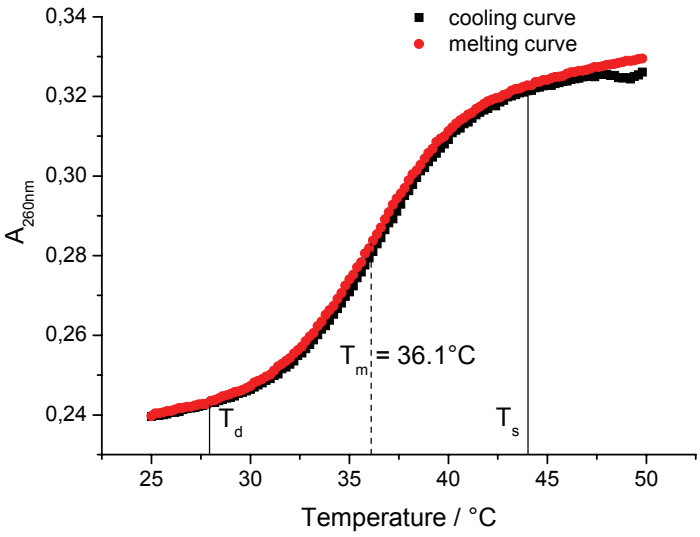

Graph 7: Example of a melting curve.

(**a**) 5′-d(AAA AAA A**XX** **X**TT TTT TT)

This strand was meant to be self complementary. The melting curves were all done at the same conditions: 5mM MOPS (pH 6.8), 150mM $NaClO_4$ and a strand concentration of 1μM. As metal ions Fe^{3+}, Cu^{2+} and Hg^{2+} were used. Without metal ions the strand (**a**) has a T_m of around 44°C, which is around 8°C higher than in the comparable A_{15}-T_{15} system. This could be due to (**a**) forming a duplex and the X not interfering, but adding to the stability by π-stacking interactions. Another explanation could be that the strand (**a**) forms a hairpin, which is known to have high melting points, although it has only seven base pairs. This could be distinguished by measuring the T_m of different concentrations. If the T_m is concentration dependent, a duplex is likely to be present, if it is not concentration dependent, a hairpin is formed. It was refrained from concentration dependent measurements, due to the low yield that was obtained. A hairpin structure is probably preferred, since in a similar strand, where X equaled a triazole nucleoside, a hairpin structure was found.[147] It was preferred to measure the change in T_m upon the addition of different metal ions, but with other metal ions (Fe^{3+}, Cu^{2+} and Hg^{2+}) no increase in T_m was observed.

(**e**) 5′-d(C**YY** **YY**G)

The strand (**e**) was primarily synthesised to test the ability of introducing Y into an oligonucleotide. The melting behaviour was observed with 5′-d(CTT TTG) as possible complementtary strand (each 1μM). As metal ions Hg^{2+} at pH 5 and pH 7 and Ag^{+} at pH 5 were used. No melting behaviour at all was found, without or with metal ions. The reason for this could be the length of the oligonucleotide (**e**). The metal ions must be strongly stabilising for the Y-T pairs in the 6-mer to get a melting behaviour. There is also a possibility of having Y-Y pairs in the 6-mer, but those do not seem to be more stable, as we did not observe any melting behaviour at all.

(**f**) 5′-d(CGC G**Y**A T**Y**C GCG)

This strand (**f**) was meant to be self complementary, as the Dickerson Drew strand. As buffer 5mM MOPS (pH 6.8) was used. But (**f**) did not show any melting behaviour, without or with Hg^{2+}, nor at different salt concentrations between 100mM and 1M $NaClO_4$. One reason for this could be the protecting groups on the C and G

nucleobases, which eventually have not been deprotected fully. The protecting groups are more robust in comparison with the protecting groups of the A and T bases that can easily be deprotected using AMA for five minutes at 65°C. The protecting groups on the nucleobases do not allow the strand (**f**) to self assembly. The nucleobases are too large and the H-bonding sites are mostly blocked. Also a reason could be the two artificial Y nucleobases, strongly destabilising the helix formation.

(**g**) 5´-d(AAA AAA A**Y**A AAA AAA) (**h**) 5´-d(TTT TTT T**Y**T TTT TTT)

It was expected that these two strands, (**g**) and (**h**), could build a double helix together, so that a possible binding of a metal ion in the inside of this helix at the artificial Y nucleobases could be observed. Next to the possibility to examine the behaviour of a Y-Y pair with a metal ion, it was also possible to have a look into the behaviour of Y-A, Y-C, Y-G and Y-T pairs. For this purpose the needed oligonucleotides, containing only natural nucleobases were bought. The melting curves were all done at the same conditions: 5mM MOPS (pH 6.8), 150mM $NaClO_4$ and each strand 1µM. These conditions are roughly standard conditions as used by other research groups, too. Sometimes higher salt or strand concentrations are used. Though, the addition of metal ions is on occasions done in an excess and not in an equimolar amount compared to the strand concentrations.[51,52,56,60,62,63,65-67] The melting curves were measured on a UV spectrometer without metal ion, with one equivalent of metal ion and with three equivalents of metal ion. The metal ion Ag^+ was used, as it, as stated before, has the tendency to build linear complexes. It was refrained from further use of Hg^{2+}, since it showed the tendency to bind to thymine.[148] It is expected that all the strands form a double helix with each other, since 14 of the 15 base pairs possible to form are natural A-T base pairs. The length of the oligonucleotides and the amount of A-T base pairs should bring the T_m in a measurable range. At temperatures less than 5°C the measurements become inaccurate due to the condensation of humidity. Sometimes this happens at even higher temperatures. For the measurements 10°C were the lower limit. Since the range of melting usually lies around 10-15°C, in which also the T_m lies, one is only able to measure T_m values down to around 18°C without getting values with high errors. On the other side measurements up to 90°C are possible. The two 15-mers in a double helix structure should melt far below this temperature.

	T_7-T-T_7	**T_7-G-T_7**	**T_7-C-T_7**	**T_7-A-T_7**	**T_7-Y-T_7**
A_7-A-A_7	36.1°C	27.6°C	24.8°C	24.1°C	24.2°C
A_7-C-A_7	26.0°C	36.9°C	20 and 33°C[a]	24.1°C	20.8°C
A_7-G-A_7	26.1°C	26.4°C	35.0°C	25.4°C	20.9°C
A_7-T-A_7	26.3°C	28.1°C	23.6°C	32.9°C	22.0°C
A_7-Y-A_7	24.2°C	18.9°C	16°C[a]	19.1°C	21.5°C

Table 8: T_m without any metal ions; [a] no cooperative melting has been observed.

Looking at Table 8 some interesting observations can be made:

- The natural base pairs A-T, T-A, C-G and G-C give the most stable duplexes, as one would expect, with T_m between *32.9* and *36.9*°C. Though, it should be noticed that interestingly the A_7-A-A_7/T_7-T-T_7 duplex is about *3.2*°C more stable than the A_7-T-A_7/T_7-A-T_7. This could be due to less efficiency in the π-stacking, because of the change between the pyrimidine and purine bases.
- This effect is also visible in A_7-A-A_7/T_7-Y-T_7 (*24.2*°C) and A_7-Y-A_7/T_7-A-T_7 (*19.1*°C), since no difference should be between the actual A-Y or Y-A, unless the structure forces the potential base pair in a more or less favoured position.
- One general point that needs mentioning is the destabilising effect of Y. Without a metal ion the T_m values are the lowest, when a Y nucleobase is present in the oligonucleotide. The destabilisation is greater than observed for mismatches of natural nucleobases, where the T_m drops roughly by *7-12*°C.
- All strands showed self assembling properties except for the T_7-C-T_7 strand with A_7-C-A_7 or A_7-Y-A_7, where no cooperative melting could be observed. The T_m values can therefore not be taken as accurate and are only written for a rough orientation.

The effect upon the addition of one equivalent Ag^+ on the 25 different systems can be seen in Table 9. One equivalent equals a 1μM concentration in solution compared to a concentration of 1μM for each strand to build a 2:1 complex. After the addition of metal ions the solution has to be heated up, so that only single strands are present. Upon slow cooling, the double helices can form with or without the metal ion inside.

	T_7-T-T_7	**T_7-G-T_7**	**T_7-C-T_7**	**T_7-A-T_7**	**T_7-Y-T_7**
A_7-A-A_7	0.6°C	3.6°C	5.7°C	0°C	1.9°C
A_7-C-A_7	4.6°C	1.3°C	a)	7.7°C	9.2°C
A_7-G-A_7	0.6°C	0.9°C	1.6°C	4.1°C	8.9°C
A_7-T-A_7	0.2°C	0.1°C	2.8°C	0.1°C	2.0°C
A_7-Y-A_7	2.5°C	11.3°C	b)	3.2°C	5.5°C

Table 9: The increase of the $T_m$with one equivalent of Ag^+, ΔT_m;
a) T_m = 32.2°C and b) T_m = 28.3°C.

- The natural base pairs A-T, T-A, C-G and G-C have negligible increases in T_m upon the addition of Ag^+.
- This is the same for the mismatching base pairs with only a few exceptions. One of those is the G-A or A-G base pair that gets slightly stabilised. Other exceptions are the base pairs with cytosine. With thymine the increase is small with *2.8* and *4.8*°C; with adenine it is larger with *5.7* and *7.7*°C. For the C-C base pair it is difficult to state a value, because of the non distinct melting without Ag^+. But it can be said that the melting curve with Ag^+ shows a distinct melting.
- For the artificial nucleobase Y only a small increase between *1.9* and *3.2*°C can be observed with adenine or thymine. The artificial base pair Y-Y shows a larger increase of *5.5*°C. Really large stabilisation effects are observed with cytosine with an increase of *9.2*°C and guanine with increases of *8.9* and *11.3*°C.
- The C-Y base pair that showed no distinct melting without Ag^+, has a nice distinct melting curve, now.

After the addition of further two equivalents of Ag^+ the T_m was not raised by a significant amount for any of the different base pairs. The differences were between *0* and *3.4*°C, whereby the higher values were for the systems that had a large increase in T_m after the addition of one equivalent Ag^+.

Looking at Graph 8, one can gain more information of the melting curves than only the T_m. The size of the hypochromicity change in the A_7-C-A_7/T_7-Y-T_7 system is at a usual value of around 22% and no change is observed upon the addition of Ag^+. The T_m, however, changes significantly by + 9.2°C, if one equivalent of Ag^+ is added. But the addition of more equivalents does not raise the T_m much further, showing the specificity in this system and that the metal ion is probably binding inside the double helix. The temperature range T_d-T_s is around 20-25°C, if no metal ions are present, but decreases upon the addition of metal ion. This shows an increase in cooperativity in the system due to the addition of Ag^+. Though, one can not state anything about the selectivity of the Ag^+ in this system. For this data of other metal ions are necessary for obvious comparison reasons.

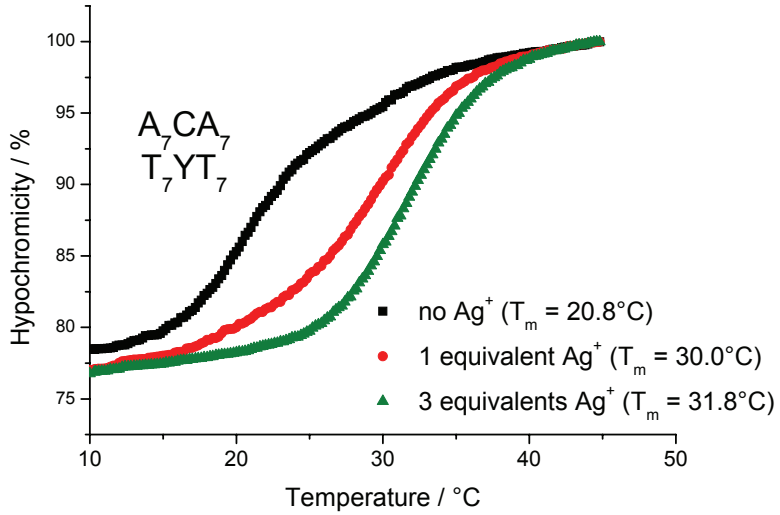

Graph 8: Melting curves of A_7-C-A_7 and T_7-Y-T_7 with different equivalents of Ag^+.

From these data it is not possible to give any structural information on the systems, neither of the oligonucleotides and their conformations, nor on the actual base pairs inside. But one can assume that the oligonucleotides build anti-parallel double helices with Watson-Crick binding between the 14 A-T base pairs. Though, it is very challenging to give a definite structure for the base pairs in the middle of the double helices from the collected data.

One can, however, put forward possible structures of the metal-mediated base pairs, for example, with Y binding over the Hoogsteen side, the only possible side for Y.

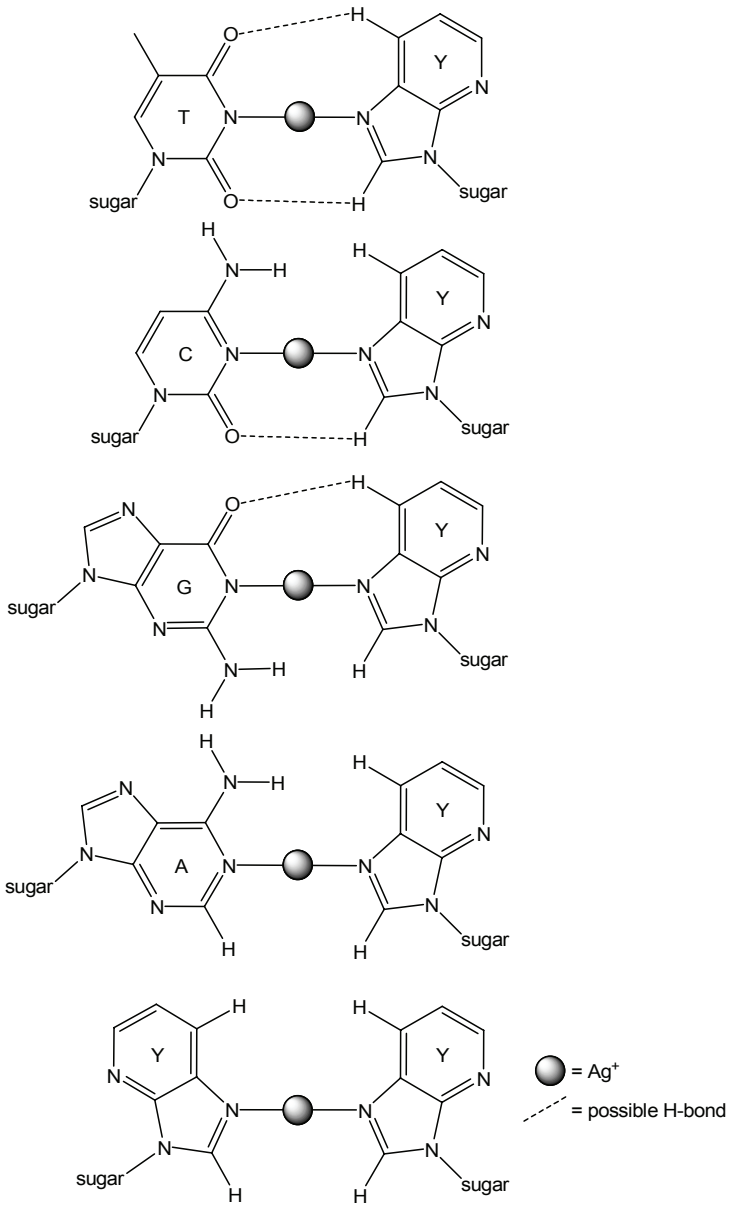

Figure 53: Schematic diagram of possible metal ion binding between the different nucleobases.

Without the metal ion present the G-Y base pair could build one or two H-bonds, but the formation of such a base pair might interrupt the π-stacking leading to the lower T_m. But in this case the A-Y base should have a lower T_m, which it has not. The addition of a metal ion stabilises then greatly through the formation of covalent metal ligand bond. But for the A-Y base pair no stabilising effect is observed. Looking at the T-Y base pair without a metal ion one could assume the formation of three H-bonds, at the most, but only one H-bond for the C-Y base pair. A possible inter-

ruption of π-stacking interactions and the difference in H-bonds present could explain why the C-Y base pair greatly destabilises the double helix. With the metal ion the C-Y base pair stabilises the double helix more than a T-Y base pair. For the Y-Y base pair there are also many binding possibilities, but probably only the N7-position is able to bind a metal ion. There are many factors influencing the bonding sides and modes of the nucleobases. The π-stacking interactions through the whole double helix and its possible disturbance through the Y nucleobase, the distances bet-ween the sugar phosphate backbones and H-bonding are the most important factors.

(**i**) 5´-d(**YYY YYY YYY YYY YYY Y**A)

Initially the strand was thought to be able to bind to a 5´-d(TTT TTT TTT TTT TTT TT) (**j**) with the help of Hg^{2+}. Coordination behaviour of Hg^{2+} with nucleic acids has been studied[97,99,100] and it is thought that Hg^{2+} can insert into base pairs by substitution of an imino proton.[149,150] As has been shown recently in the literature, the Hg^{2+} can bind selectively to thymines inside a double helix containg only thymine.[148,151] Many metal ions have been tested and only Hg^{2+} showed notable effects on the duplex stability. Ag^{+} was also tested, but no effect on the duplex stability of the used oligonucleotides was found, although Ag^{+} can bind linearly, too. However, for 5´-d(TTT TTT TTT TTT TTT TT) (**j**) self assembling in the presence of Ag^{+} was observed, as shown in Graph 9. Therefore (**j**) will not necessarily bind to (**i**) with Ag^{+}.

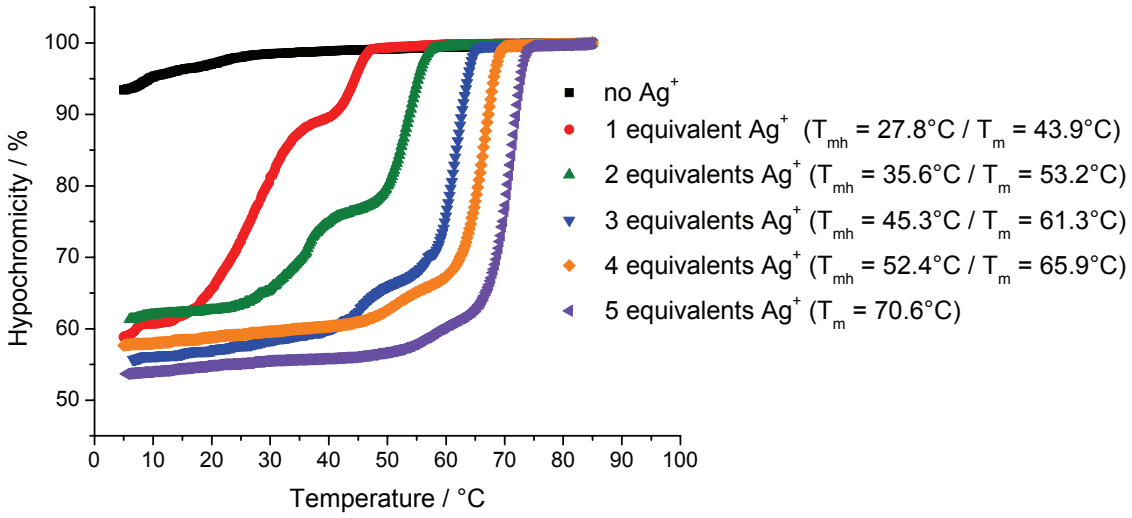

Graph 9: Melting curves of 5´-d(TTT TTT TTT TTT TTT TT) (**j**) with different equivalents of Ag^{+} (T_{mh} = melting temperature of the hairpin).

One equivalent of Ag^+ equals the amount needed to form a double helix that has one Ag^+ present in each base pair. The melting curves were measured at 5mM MOPS (pH 6.8) and 150mM $NaClO_4$ and 1µM strand concentration. The $^{5'}$-d(TTT TTT TTT TTT TTT TT) (**j**) shows no melting without Ag^+, as one would expect; only single strand is present. But upon the addition of different equivalents Ag^+ two T_m values can be observed, T_{mh} and T_m. One could be a hairpin (T_{mh}) and the other a duplex (T_m) that is favoured the more Ag^+ is added.

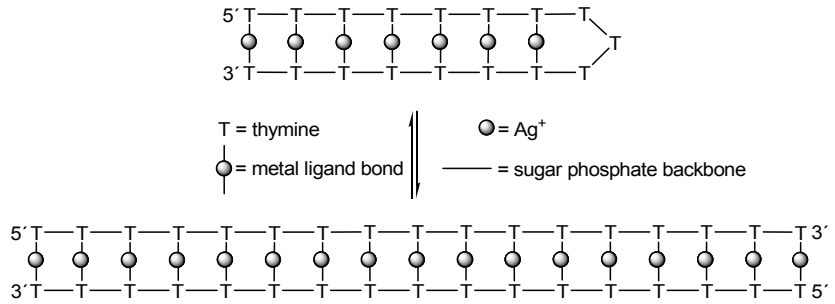

Figure 54: Possible equilibrium between hairpin and double helix structure.

Interesting was also that the cooling temperature (T_c) was always closer to the lower T_{mh}. The fact that two species are built and that even after addition of ten equivalents Ag^+ the T_m still rises shows that the melting behaviour is not very specific. When measuring at higher $NaClO_4$ concentrations the hairpin is only present until the addition of two equivalents of Ag^+, showing that the species of the higher T_m, probably a double helix, is greatly favoured. The specificity, though, has not changed and is still low. The change in hypochromicity is astonishingly large with a value of nearly 50%. Comparing the obtained data with the data in the literature it has to be said that next to the Hg^{2+}, the Ag^+ is also in favour of being a highly selective thymine nucleobase binding partner.

Due to the ability of $^{5'}$-d(TTT TTT TTT TTT TTT TT) (**j**) to bind Ag^+, the possibility of concurrent reactions can not be excluded. In Figure 55 a T-T base pair with an Ag^+ can be seen, as it would be expected from the data obtained by A. Ono and H. Togashi.[148]

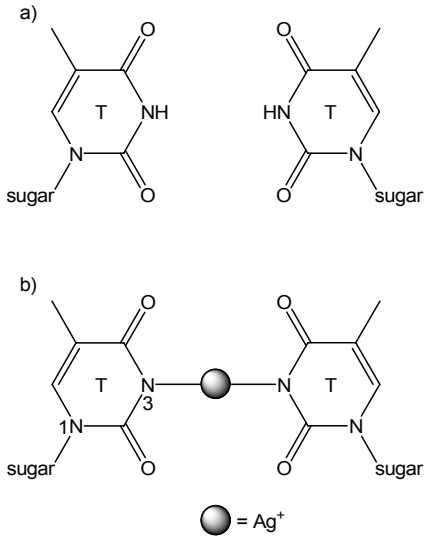

Figure 55: A T-T base pair with no H-bonds, a), and a T-T metal-mediated base pair with Ag^+, b).

Then the 5´-d(**YYY YYY YYY YYY YYY Y**A) (**i**) was measured at 5mM MOPS (pH 6.8) and 150mM $NaClO_4$ and 3µM strand concentration. The strand (**i**) is stabilised by around 17°C upon the addition of Ag^+ taking a T_m of around 28°C for the strand itself without Ag^+ for the non-cooperative melting. The melting behaviour becomes cooperative upon the addition of Ag^+. Surprisingly, the absorbance values at 80°C are not the same, as expected for only single strand being present (Graph 10).

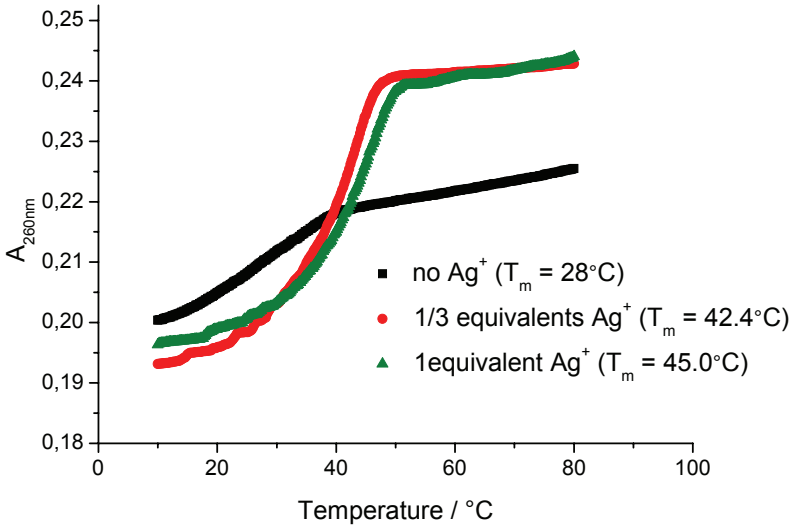

Graph 10: Melting curves of 5´-d(**YYY YYY YYY YYY YYY Y**A) (**i**) with different equivalents of Ag^+.

The melting curves were measured three times to obtain repeatable results. In Graph 11 the change in T_m with different equivalents Ag^+ is shown. An increase in T_m was observed up to an addition of roughly 0.5 equivalents Ag^+. Considering that one equivalent equals eight Ag^+ per strand, so that two strands have 16 Ag^+, 0.5 equivalents mean that 16 Ag^+ are used for four strands or eight for two. Additional equivalents of Ag^+ do not seem to have a further stabilising effect, which shows that the metal ions must have some specific purpose. The reason for only eight Ag^+ inside a double helix could be the Ag^+ not wanting to be to close to one another, because of its size or charge. Also the positions of the artificial nucleobases in such a double helix might not always be close enough for the binding of a metal ion.

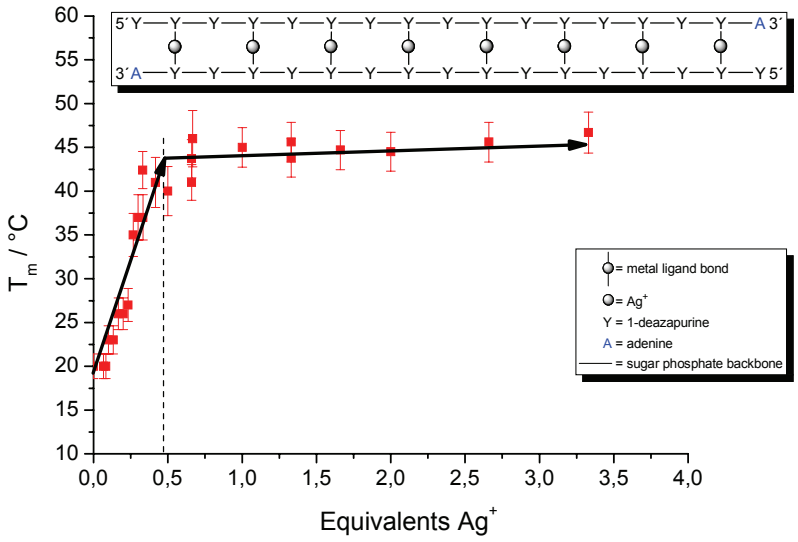

Graph 11: Change in T_m upon the addition of different equivalents of Ag^+ to (**i**).

Normally one would not expect any T_m for (**i**), but the CD-spectra showed that some kind of structure is present in the solution at 10°C and that this structure does not change upon the addition of Ag^+. So there should be some kind of structure present that shows a non-cooperative melting behaviour. One possibility would be the presence of double helices with different chain length. These would melt at different temperatures and after the melting process the single strands could again form longer double helices. Though, it can not be stated, whether these would be parallel or anti-parallel.

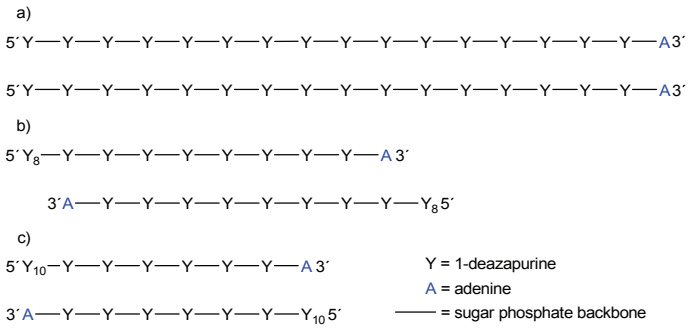

Figure 56: Possible double helix formations of (**i**).

Looking at Graph 12 it can be seen that the change in hypochromicity without metal ions is quite small. A hypochromicity effect seems to be present; hence, the hypochromicity rises upon the addition of Ag^+. The change from non-cooperative to cooperative melting upon the addition of Ag^+ can also be seen. The difference between T_s and T_d decreases from around 30°C to 10-15°C. This indicates certain specificity in the binding of the Ag^+.

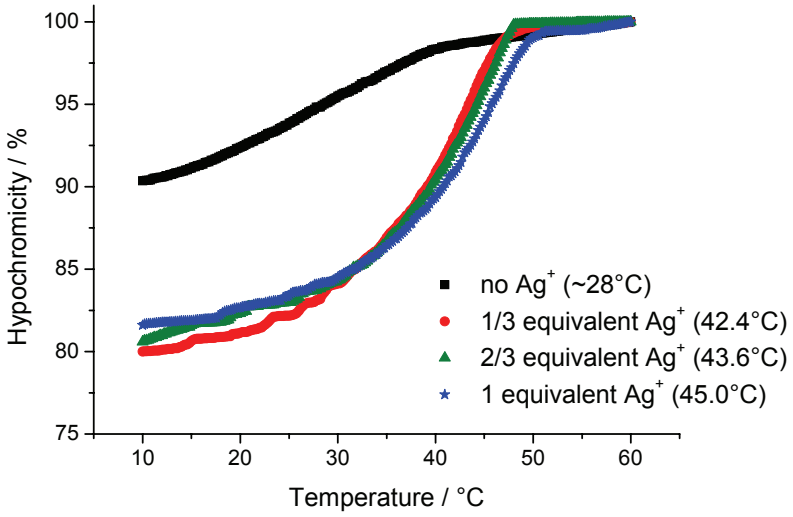

Graph 12: Melting curves of $^{5'}$-d(**YYY YYY YYY YYY YYY YA**) (**i**) with different equivalents of Ag^+.

There is an increase in T_m, a switch from non-cooperative to cooperative melting, a hypochromicity effect and an indication for specific binding of the Ag^+. But from these data one can not derive any structural knowledge of the possible double helix or eventually of the metal-mediated base pair.

3.6 CD-Spectra

The information from circular dichroism (CD) measurements is complementary to that from absorption spectra, in fact, it is even greater. The CD spectra above 210nm are influenced by the overall structure and by the nearest neighbours of the nucleic acids. This method is based on DNA and other molecules interacting differently with right and left circularly polarised light. This light is chiral and needs a chiral molecule to discriminate between its two chiral forms. One measures the change in ellipticity with the change in wavelength. The ellipticity is then converted to molar ellipticity.[152,153]

Since it was not possible to derive any structural knowledge from the melting curves of 5´-d(**YYY YYY YYY YYY YYY Y**A) (**i**), CD-spectra were measured. The buffer and salt concentrations (5mM MOPS and 150mM $NaClO_4$) were kept equal and the strand concentration was 13.5µM. At 10°C the strand was expected to be found in solution as single strand and upon the addition of Ag^+ a change in structure should be seen, if the binding of metal ions leads to a structural conformation of the oligonucleotide (**i**).

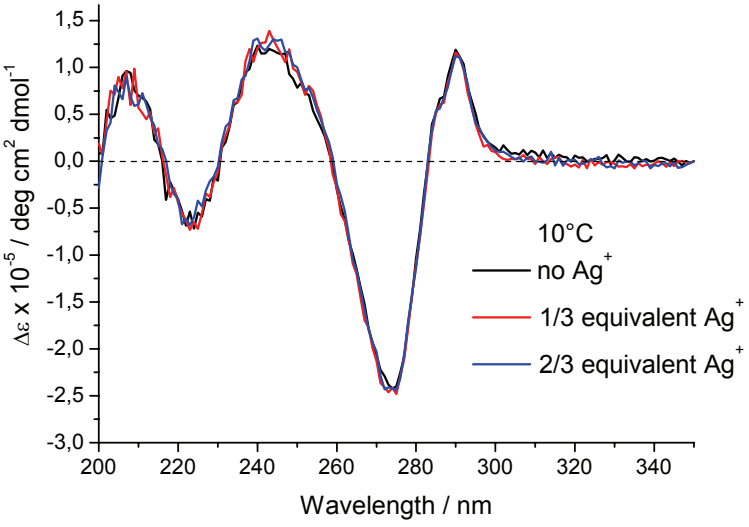

Graph 13: Δε x 10^{-5} at different wavelengths at 10°C for (**i**) upon the addition of Ag^+.

Surprisingly, no change in structure was observed, which can have two reasons. The addition of Ag^+ does not lead to defined rigid structural conformation or there could be some kind of structure present in solution at 10°C without metal ions being present. This is the case, if the CD-spectrum of the 1-deazapurine-N9-β nucleoside (**28b**) (measured under the same conditions and at the same concentration) differs significantly from the CD-spectrum of the oligonucleotide (**i**). The 1-deazapurine-N9-β nucleoside (**28b**) has a random order in solution and if the CD-spectra are similar, the oligonucleotide (**i**) does not possess a defined structural conformation.

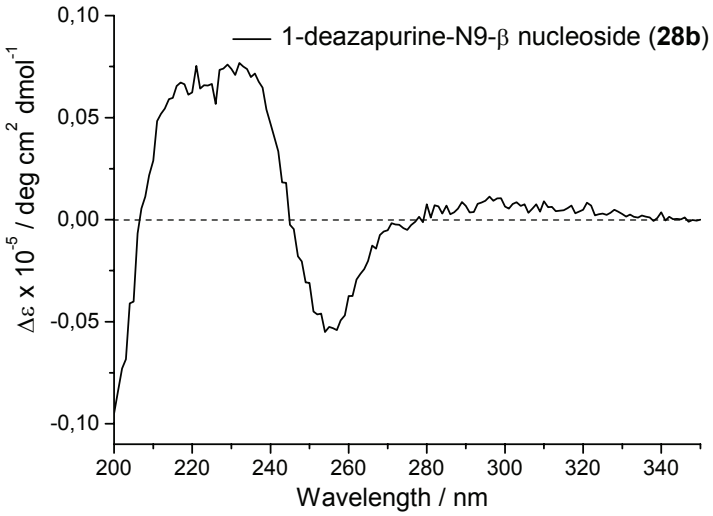

Graph 14: $\Delta\varepsilon \times 10^{-5}$ at different wavelengths at r.t. of 1-deazapurine-N9-β nucleoside (**28b**).

Only looking at the size of Δε in Graph 14 one can easily see that it is much smaller than the Δε for the oligonucleotide in Graph 13. The spectrum of the 1-deazapurine-N9-β nucleoside (**28b**) shows no significant change above 270nm, a minimum at 255nm and a broad maximum from 210nm to 240nm. For the spectrum of the oligonucleotide (**i**) (Graph 13) two minima (225nm and 275nm) and three maxima (210nm, 245nm and 290nm) are observed. Therefore the oligonucleotide (**i**) has a structural conformation even without metal ions being present and the conformation does not change upon the addition of Ag^+. The Ag^+, however, stabilises the structure by a great amount, which can be seen in the melting curves that have been shown before and the significant change in melting behaviour. If the structure is now melted

by heating up the solution to 80°C the CD-spectrum of the single strand should be seen and it should differ from the spectrum of the possible helix.

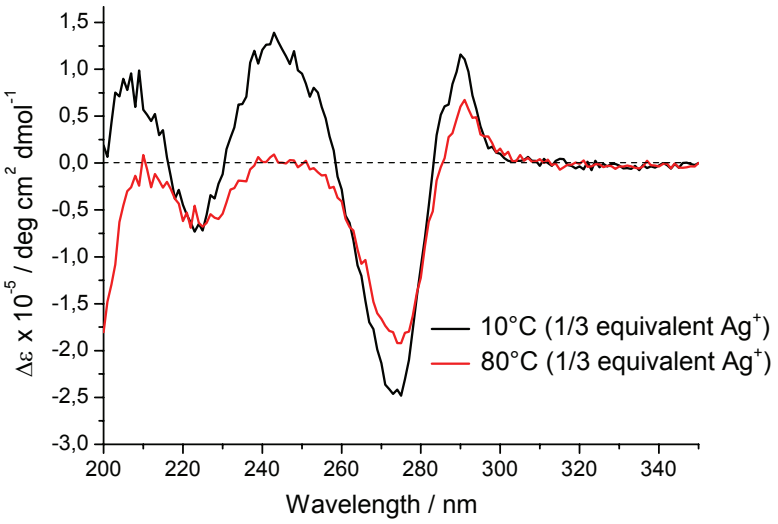

Graph 15: Δε x 10^{-5} at different wavelengths at 10°C and 80°C for (**i**) upon the addition of Ag^+.

A structural difference can clearly be seen, but it is only shown in the amount of ε and only at the already known wavelengths. So the absorption minima and maxima do not change. The changes between 10°C and 80°C are the same for the measurements with different equivalents Ag^+ and without Ag^+. This has already been observed for the unstacking of single stranded DNA. Upon an increase in temperature the near-UV CD bands decrease and the absorption at 260nm increases by around 15%. The decrease in the near-UV bands is a measure of a decrease in interaction between the neighbouring bases.[152,153] This all can be observed for (**i**), too. Even the crossover points at 265nm and 280nm do not change, which is also typical, however, these do not lie near the base line as usually. And one could say that in Graph 15 the bands of the spectrum at 80°C are slightly moved to higher wavelength. Interesting is also the unequally sized decrease in the bands upon a change in temperature, which is also unusual. In the case of some interstrand interactions it is difficult to visualise their presence in the CD spectra. The spectra of poly[A] and poly[T] strands binding are roughly the average of the single stranded poly[A] and poly[T] spectra.[152,153] At 10°C this could also be the case for (**i**), since the average of

two (**i**) equals (**i**). This is in accord with the observation of the absorption spectra having nearly exactly the same bands at the same wavelength. This leaves the questions why the Ag^+ binds so specifically. Eight Ag^+ (half an equivalent) inside two single strands maybe building a helix. If the metal ions would bind at the backbone, the binding would be much less specific and probably more than eight ions would stabilise the structure. One could propose that the structure of the strands without metal ions can stack and therefore has some kind of stability. If now a single strand can stack in such a fashion that the Y lies opposite another Y of another strand, these could bind with a metal ion stabilising the structure without any great change in structure. It would still not be possible to describe the orientation of the two strands to each other. For double helices of poly[A] with poly[T] no great structural difference was found between a parallel and an anti-parallel orientation. The position of the adenine base (A) in the oligonucleotide (**i**) is also important, but the possible positions (Figure 57) can not be distinguished with the help of the data obtained from the different measurements.

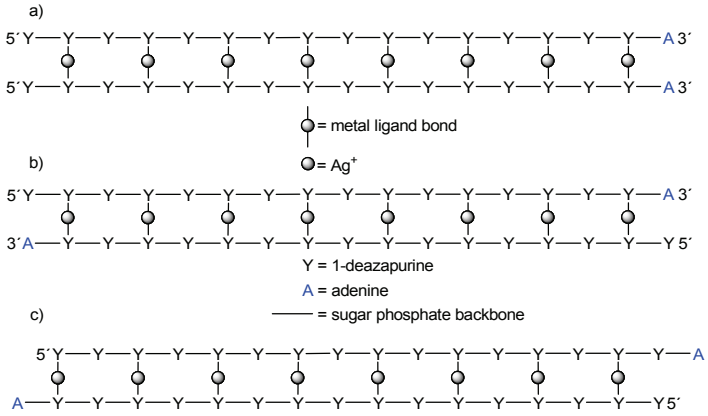

Figure 57: Possible double helix formations of $^{5´}$-d(**YYY YYY YYY YYY YYY Y**A) (**i**) with Ag^+.

So there seems to be a structure of the strand (**i**) present in solution that shows specific binding upon the addition of eight Ag^+ (half an equivalent) for two strands, a stabilisation and a hyperchromicity effect. All suggestions about the overall structure and the eventual artificial Y-Y base pairs can only be of speculative and hypothetical

nature, due to the lack of reliable information. Two possible Y-Y base pairs with Ag^+ are shown in Figure 58.

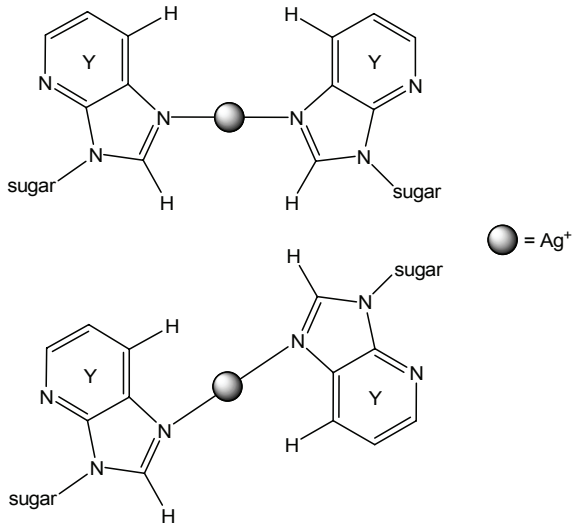

Figure 58: Schematic diagram of possible structures of an Ag^+-mediated Y-Y base pair.

Possible NMR measurements are difficult, because of the probable high symmetry, which makes the identification nearly impossible. Crystallography could be a good method to gather further information about the structure, but the amount of strand (**i**) needed for the crystallisation procedures with the generally available crystallisation kits is compared to the yields obtained much higher (factor of a thousand). A new way of actually observing the formation of a double or triple helix was recently published, using a conjugated polymer complex that wraps around a double or triple helix, since it contains positive charges that go to the negative charges of a double helix backbone. Due to the different charge balance upon single strand, double or triple helix, different colours are observed, giving raise to the actual structure.[154]

4 1-Deazaadenine

For the introduction of 1-deazaadenine in an oligonucleotide, one has to synthesise the nucleoside first and characterise it. This is then followed by the preparation of the nucleoside with protecting groups for the automated DNA-synthesizer and the work up for the oligonucleotides.

4.1 Synthesis of the Nucleoside

The synthesis of the 1-deaza-6-aminopurine-N9-β-2´-deoxyribonucleoside (1-deazaadenine nucleoside) was started at the already known 1-deazapurine (**21**), which was oxidised using H_2O_2 and refluxing for two days, giving, after the work up, 1-deaza-N3-oxidepurine (**35**) in high yields.[155]

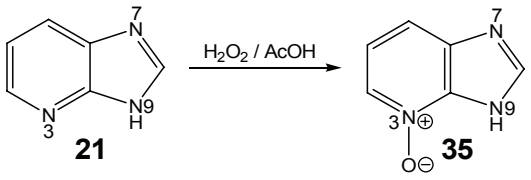

Figure 59: Schematic diagram of the synthesis of 1-deaza-N3-oxidepurine (**35**).[155]

A crystal structure could be obtained, which includes two water molecules bonding along the N-O axis of the molecule, but the resolution was not very good and the crystal data were not useable for publishing. The difficulties are due to the crystals that are thin needles and therefore difficult to be measured. Though, it can be seen that the aromatic rings show the expected planarity. The two water molecules (not shown in Figure 60) are connected via an H-bond to each other and to the O3, too. The length of the H-bonds are 2.858(1)Å and 2.850(1)Å, respectively, with bond angles of 170.63(1)° and 171.67(1)°. There is a third H-bond with a length of 2.879(1)Å and an angle of 146.22(1)° between the N7-H7⋯O3 of two different molecules. Due to

this H-bond the molecules build one dimensional chains in the unit cell. The one dimensional chains are not connected to each other and the water molecules are in the holes in-between these chains. In the unit cell two molecules stack on top of each other with the N3-O3 bonds in opposite direction and the six membered ring slightly moved on top of the five membered ring. Looking along the plane of the molecules and along the chain direction one can see that the chains are orientated like steps, one horizontally, another diagonally and so on.

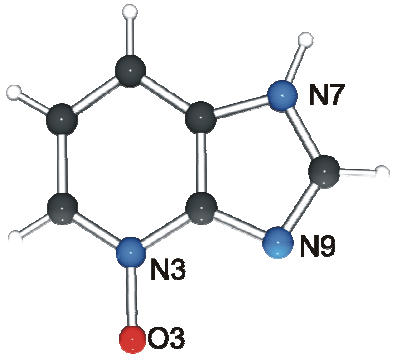

Figure 60: Crystal structure of 1-deaza-N3-oxidepurine (**35**).

Next, the 1-deaza-N3-oxidepurine (**35**) was dissolved in trifluoroacetic acid at 0°C and fuming HNO_3 (100%) was added drop wise. Important to notice here is that the reaction only worked with fuming HNO_3 (100%) and not with usual HNO_3 (90%), as described in the literature.[106,155] This could be reasoned in them using 1-deaza-N3-oxidepurine and not 1-deaza-N3-oxidepurine $2H_2O$ (**35**). The reaction was then heated for four instead of three hours under reflux and neutralised using NH_3. It was essential to keep the solution underneath 30°C and to permanently stir the solution, to obtain some product at all. Further standard work up gave then 1-deaza-N3-oxide-6-nitropurine (**36**) as a yellow solid in quantitative yield.

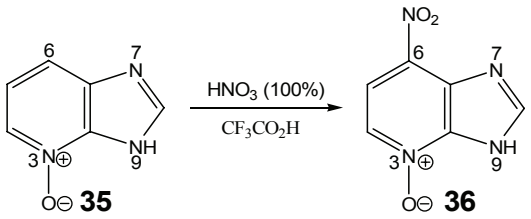

Figure 61: Schematic diagram of the synthesis of 1-deaza-N3-oxide-6-nitropurine (**36**).

To reduce the 1-deaza-N3-oxide-6-nitropurine (**36**) to 1-deaza-6-nitropurine (**37**) PCl_3 was used, but only half of the yield in the literature could be obtained.[156] This could be due to chlorination at the C4 or C5 position, as has been described in the literature for reactions with 1-deaza-N3-oxidepurines.[108]

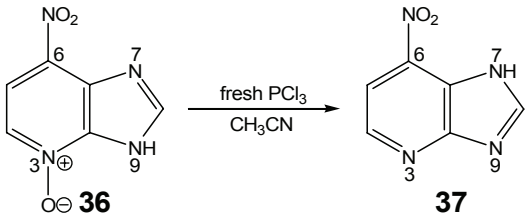

Figure 62: Schematic diagram of the synthesis of 1-deaza-6-nitropurine (**37**).

Though, red crystals were obtained that turned out to be suitable for X-ray crystallography and the crystal structure is shown in Figure 63.

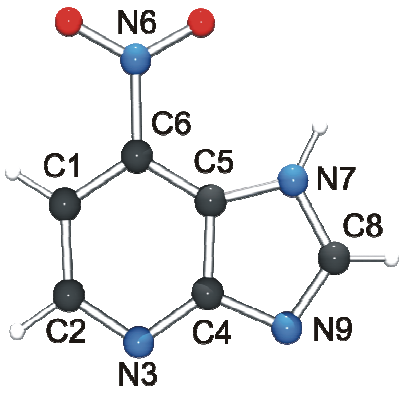

Figure 63: Crystal structure of 1-deaza-6-nitropurine (**37**).

The aromatic system is planar with the NO_2 group coming out slightly of the ring plane (7.18(17)°). The bond lengths and the angles of all bonds are in the expected ranges. In the solid state the H atom is observed at the N7 position, as it has been observed for purine, too.[157] This could be assigned by looking at the difference in the angles between C8-N9-C4 and C8-N7-C5 (103.7(2)° and 106.4(2)°, respectively). This difference is around 3° and the larger angle normally contains the protonated N atom. Also it can be said that the larger bond length of C8-N7 compared to C8-N9

(1.352(3) and 1.303(3)Å, respectively) shows nicely that the C8-N9 must contain of a double bond and vice versa. This fits well into the chemical scheme shown in Figure 61. The molecules in the crystal structure form a one dimensional chain over an H-bond N7-H7⋯ N9 of the next molecule (H7⋯ N9 = 1.88(3)Å), as can be seen in Figure 64.

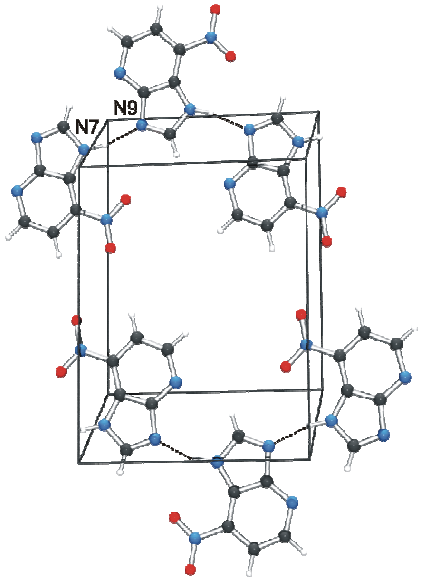

Figure 64: Unit cell of 6-nitro-1-deazapurine

Theoretical calculations with the ADF program show that in the gas phase the N7 tautomer is more stable by 14.1kJ/mol compared to the N9 tautomer. In solution there is a solvent-dependent equilibrium between the two tautomers present.[158]

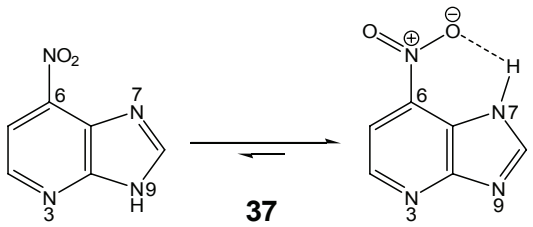

37

Figure 65: Schematic diagram of the tautomer forms of 1-deaza-6-nitropurine (**37**).

Then 1-deaza-6-nitropurine (**37**) was deprotonated with NaH and Hoffer´s chlorosugar (**25**)[122-124] was added to give 1-deaza-6-nitropurine-N9-β(α)-[2´-deoxy-3´,5´-di-O-(p-toluoyl)-ribonucleoside (**38b** and **38a**).[159]

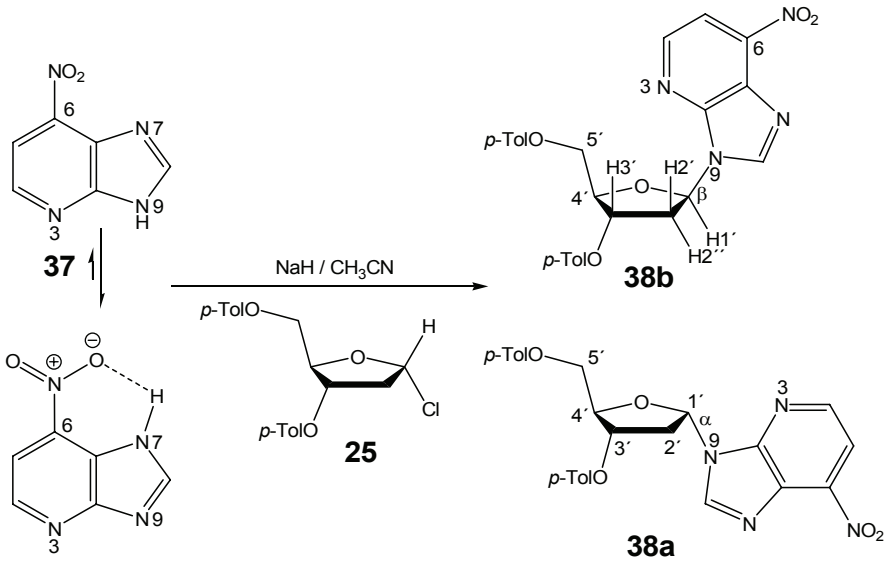

Figure 66: Schematic diagram of the synthesis of 1-deaza-6-nitropurine-N9-β(α)-[2´-deoxy-3´,5´-di-O-(p-toluoyl)-ribonucleoside] (**38b** and **38a**).

The appearance of both, the N9 and N7 product (no N3) has not been observed. There must be a reason that only the N9 product was formed. It is thought to be due to one of the tautomeric structures of **37** being more stable than the other. The preferred tautomeric structure in the equilibrium of 1-deaza-6-nitropurine (**37**), where the nitro group stabilises one form, is shown in Figure 65 (right side) and Figure 66 (bottom left). No preferred tautomeric structure was found in the equilibrium of the 1-deazapurine (**21**).[113] The low reaction temperature of 0°C could also be a reason for the presence of only N9 product, as already described for the 1-deazapurine. T. Wenzel and F. Seela,[113] though they synthesised the two products using five equivalents of powdered KOH and TDA-1 as catalyst, instead of NaH had roughly the same yield as Cristalli et. al.[159] Another glycosylation reaction was done using $SnCl_2$ as catalyst, getting, as is proposed, N9- and N3-isomers, but similar yields.[160] Further it is proposed that the yield of the reaction using NaH and Hoffer´s chlorosugar can be raised by longer reaction times. This could not be observed in the synthesis here.

There are other reaction routes to the 1-deazaadenine nucleoside and its derivatives found in the literature, though looking at the reaction conditions and the yield, they do not appear to be more successful than the one used.[161] However, the formation of alpha- and beta-anomers was not observed, previously. Therefore purification of the product and separation from its alpha-anomer with flash chromatography had to be developed. After separation of the alpha-anomer the yield was only slightly lower than in the described literature.[113,159] The reaction solvent could also be a reason for the formation of only N9-isomer, as has been described in the literature.[109]

The two anomers of the 1-deaza-6-nitropurine-N9-β(α)-[2´-deoxy-3´,5´-di-O-(p-toluoyl)-ribonucleoside] (**38b** and **38a**) can be distinguished by ^{1}H, ^{1}H NOESY, by looking at the coupling constants or by looking at the protecting groups. As already described for the 1-deazapurine nucleosides, most rapidly the anomers can be distinguished by looking in the ^{1}H NMR spectrum at the p-Tol protecting group signals of the alpha-anomer. The protecting group of the beta-anomer shows chemical shifts in only two regions of the aromatic region (2 multiplets), in the alpha-anomer a third in-between the other two is observed. This is probably due to two protons on the protecting group on the O3´, which observe a high field shift, probably, because these protons experience the ring current of the heterocyclic aromatic ring of 1-deaza-6-nitropurine in the alpha-anomer (**38a**).

For the 1-deaza-6-nitropurine-N9-β-[2´-deoxy-3´,5´-di-O-(p-toluoyl)-ribonucleoside] (**38b**) the coupling constants H1´/ H2´ and H1´/ H2´´ are almost identical (4.1 and 5.9Hz), which often gives raise to a pseudo-triplet in the ^{1}H NMR spectrum, whereas for the alpha-anomer the coupling constants are quite different (4.8 and 8.2Hz), leading more likely to a doublet of doublets. Using ^{1}H, ^{1}H NOESY experiments both anomers can easily be distinguished. The H1´ of 1-deaza-6-nitropurine-N9-β-[2´-deoxy-3´,5´-di-O-(p-toluoyl)-ribonucleoside] (**38b**) displays a strong cross-peak to H2´´, but only a week to the H2´. This is the opposite trend for the alpha-anomer. The stereospecific assignement of H2´and H2´´ can be facilitated by comparing the intensities of their cross-peaks to the H3´, which are strong and weak, respectively.

The 1-deaza-6-nitropurine-N9-β-[2´-deoxy-3´,5´-di-O-(p-toluoyl)-ribonucleoside] (**38b**) was then deprotected using saturated NH_3/CH_3OH solution to give 1-deaza-6-

nitropurine-N9-β-2´-deoxyribonucleoside (**39**). The reaction was monitored using TLC and the reaction time was much shorter than described by Cristalli et. al.,[159]. The yield, however, was found to be higher.

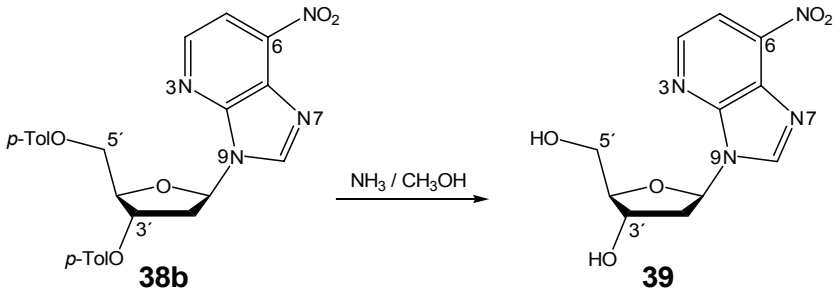

Figure 67: Schematic diagram of the synthesis of 1-deaza-6-nitropurine nucleoside (**39**).

Also a side product was found in small yields, the 1-deaza-6-methoxypurine-N9-β-[2´-deoxy-3´,5´-di-O-(p-toluoyl)-ribonucleoside]. The shorter the reaction time is, the lower the yield of the side product and the higher the yield of the product. The CH_3OH can get deprotonated and attack the slightly positively charged C6 and therefore substitute the NO_2 group. It was possible to keep the amount of side product formed during the reaction small.

It has to be mentioned that 1-deaza-6-nitropurine-N9-β-2´-deoxyribonucleoside (**39**) could also be a possible artificial nucleobase building metal-mediated base pairs in oligonucleotides. A possible base pair with cytosine is shown in Figure 68.

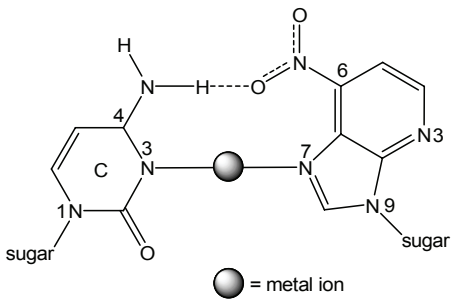

Figure 68: Possible metal-mediated base pair formation of 1-deaza-6-nitropurine nucleoside (**39**) with a cytosine.

One could already observe the 1-deazapurine building block Y in two strands, **g** (5´-d(AAA AAA AYA AAA AAA)) and **h** (5´-d(TTT TTT TYT TTT TTT)), building a base pair with cytosine in the opposite position of another strand upon the addition of a metal ion (see Section 3.5). Without the metal ion the melting behaviour was poor and no melting point could be obtained. Maybe the possible H-bond formation of this 1-deaza-6-nitropurine building block with cytosine could stabilise the double helix formation without a metal ion. Then, upon the addition of a metal ion a large increase in T_m would be expected. Also this base pair could be compared with the 1-deazadenine thymine base pair, since both would have three stabilising interactions present, the π-stacking, the H-bonding and the metal-ligand interactions.

Reduction of 1-deaza-6-nitropurine-N9-β-2´-deoxyribonucleoside (**39**) using Raney-Nickel and hydrazine hydrate gave 1-deaza-6-aminopurine-N9-β-2´-deoxyribonucleoside (**40**), also called 1-deazadenine-N9-β-2´-deoxyribonucleoside or 1-deazaadenine nucleoside. The yield was lower than described in the literature,[162] but still reasonably good. This method was used, since it is less dangerous and more easily handable than the method described in the literature, which uses H_2 in combination with pressure.[163] Crystals of the 1-deazaadenine nucleoside (**40**) could be obtained easily as needles or blocks. The unit cells and the space groups were nearly identical to the crystal structures published by F. Seela et al.[164] The solvent used for crystallisation was water instead of iso-propanol.

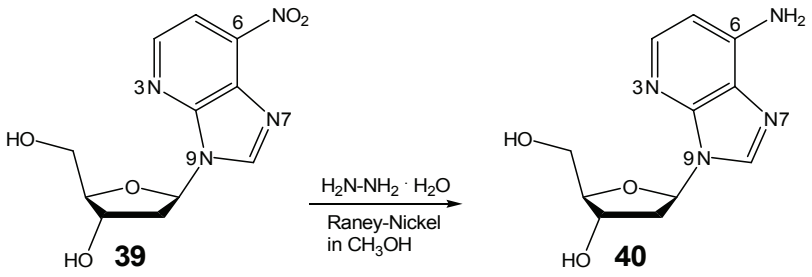

Figure 69: Schematic diagram of the synthesis of 1-deazaadenine nucleoside (**40**).

4.2 Characterisation

As done before with the ligand 1-deaza-9-methylpurine (**22**) of the model structure, $[Hg(9\text{-MeDP})_2](NO_3)_2 \cdot H_2O$ (**24**) and the 1-deazapurine nucleosides (**28b** and **29b**), it is important to look at the protonation reaction of the 1-deazaadenine nucleoside (**40**), to rule out an interference with the wanted metalation reaction. Therefore the pK_a values for the 1-deazaadenine nucleoside (**40**) needed to be determined. pD-dependent ^1H chemical shifts of the aromatic protons of the nucleoside have been measured trying to confirm the pK_a value of 4.6,[93] in comparison to the value of 4.7[111] for the 1-deazaadenenine ribonucleoside (2´-OH group present), that were obtained by UV spectroscopy. This value, however, could not be confirmed, since lowering the pD value underneath 5, lead to a fast depurination of the 1-deazaadenine nucleoside (**40**). Above a pD value of 5 no protonation reaction was observed, hence above that value we would not expect the protonation reaction to disturb the metalation reaction. Although it has been reported that the pK_a value of the nucleoside in an oligonucleotide is about 0.6 units higher than the one from the monomer,[93] working at pH 7 should rule out any competition reaction between protonation and metalation. In comparison with the 1-deazapurine nucleosides (**28b** and **29b**) this means that the additional NH_2 group has a destabilising effect on the glycosidic bond. Attempts were also undertaken to quantify the half-life of the depurination of the 1-deazaadenine nucleoside (**40**) using ^1H NMR spectroscopy, but the calculated data were too far away from the actually observed experimental data. Though the fact that the 1-deazaadenine nucleoside turned out to be very labile and easily depurinated at pH values lower than 5 is of great importance. Especially for the further synthesis this has to be considered.

But as can be seen in Graph 16, the pK_a value for 1-deazaadenine (**41**) could be measured.

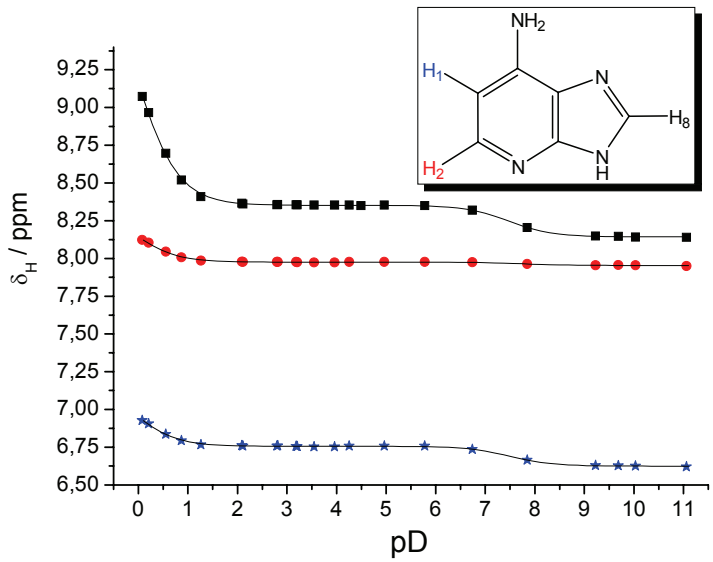

Graph 16: Chemical shift (δ_H/ppm) of the aromatic protons against pD-value for 1-deazaadenine (**41**).

The same was done for the reaction intermediates, 1-deazapurine (**21**), 1-deaza-N3-oxidepurine (**35**), 1-deaza-N3-oxide-6-nitropurine (**36**) and 1-deaza-6-nitropurine (**37**). In Table 10 the different pK_a values that have been found can be seen.

Purine derivatives	**pK_a value I**	**pK_a value II**
1-Deazapurine (21)	4.01 ± 0.03	10.87 ± 0.05
1-Deaza-N3-oxidepurine (35)	1.02 ± 0.01	8.73 ± 0.01
1-Deaza-N3-oxide-6-nitropurine (36)	‹ 0	7.19 ± 0.02
1-Deaza-6-nitropurine (37)	1.39 ± 0.02	---[a]
1-Deaza-6-aminopurine (41)	-0.53 ± 0.03	7.94 ± 0.04

Table 10: The pK_a values calculated (weighted mean of the values for the different aromatic protons) for the intermediates of the synthesis of the 1-deazaadenine nucleoside (**40**); [a] = pD values over 7 have not been determined.

The pK_a value I of 1-deazapurine (**21**) of 4.01 fits nicely to the found value of 4.1 in the literature.[139] The pK_a values I drop upon the oxidation of the N3 position and the addition of a NO_2 group (electron withdrawing) at the C6 position. A dramatic change is observed upon the addition of a NH_2 group at the C6 position. These changes are also visible in the pK_a values II, but the effects are much smaller.

Since the wanted 1-deazaadenine-thymine base pair (Z-T) needs to be planar inside the oligonucleotide for binding, DFT calculations[165] have been made to calculate the structure in the gas phase. For simplification the sugar has been replaced by a methyl group and as metal ion Hg^{2+} has been used.

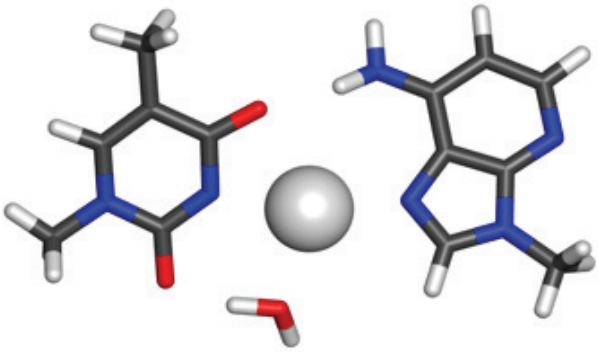

Figure 70: Calculated structure of a 1-deazaadenine-Hg^{2+}-thymine base pair (C, H, N: B3LYP/6-31 G*, metal ions: B3LYP/LanL2DZ).

A glycosidic bond distance of 11.3Å has been observed, which is slightly larger but comparable with the glycosidic bond distances observed between natural nucleobases inside DNA (in B-DNA 10.85Å).[4-6] The bases in the calculated structure are not planar, since a propeller twist of 27.2° has been found. This, however, is not unusual and can also be found in natural DNA.

4.3 Synthesis of Oligonucleotides

For the automated DNA-synthesizer protecting groups have to be introduced at the O5´-position and the O3´-position of the 1-deazaadenine nucleoside (**40**). Additionally the NH_2 group needs protection. At first the NH_2 group was protected with benzoyl chloride, followed by the standard procedures for the O5´-position and the O3´-position used already for the preparations of other nucleotides.[93,146,162,166,167] Reaction of the 1-deazaadenine nucleoside (**40**) with benzoyl chloride gave the 1-deaza-(6-benzoylamino)-purine-N9-β-2´-deoxyribonucleoside (**42**) as colourless crystals. The yield was slightly higher than found in the literature.[93,146] The crystals turned out to be suitable for X-ray crystallography and two different crystal structures (**42I** and **42II**) were obtained out of two different solvents.

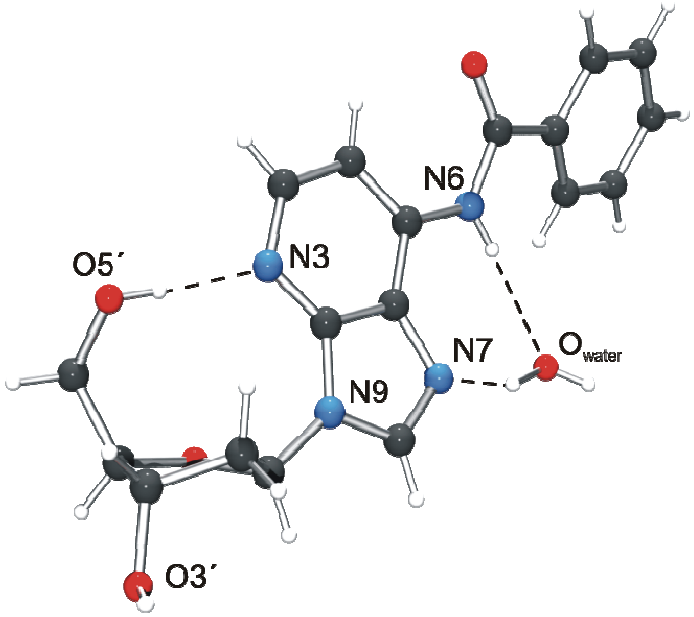

Figure 71: Crystal structure of 1-deaza-(6-benzoylamino)-purine-N9-β-2´-deoxyribonucleoside ·H_2O (**42I**).

In Figure 71 one can easily recognise the C2´-endo (^{2}E) S-type conformation. The C5´-O5´ points towards the ring and can be found in the +gauche or +sc conformation and the base is in the syn position. Three intramolecular H-bonds can be found in **42I**, O5´-H5´···N3, O_w-H_{w1}···N7 and N6-H6···O_w. The first two H-bonds have usual

lengths of 2.715(4)Å and 2.791(4)Å with bond angles of 170(3)° and 157(4)°, respectively. The third is a bit longer with 3.116(5)Å, but with an angle of 173(3)° it can still be regarded as H-bond.

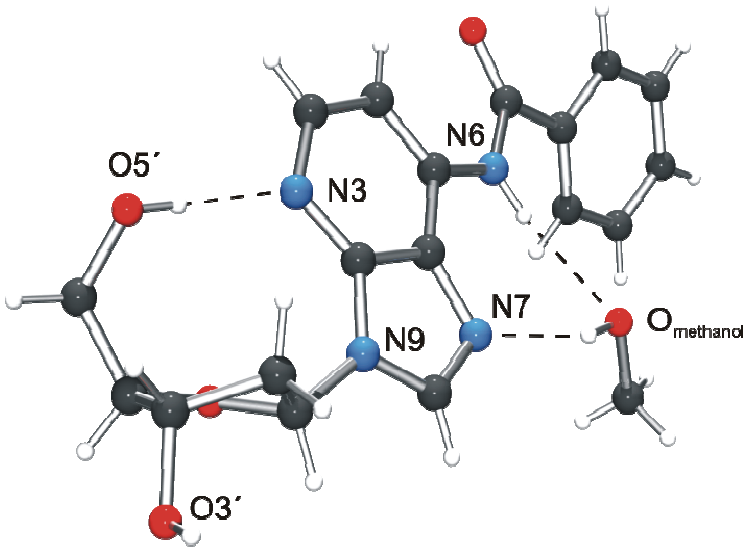

Figure 72: Crystal structure of 1-deaza-(6-benzoylamino)-purine-N9-β-2´-deoxyribonucleoside ·CH_3OH (**42II**).

The second crystal structure has identical conformations, as one would expect, since only one water molecule is substituted by one methanol. Also the same intramolecular H-bonds can be found, except that the O atom now belongs to the methanol. The O5´-H5´···N3 has a length of 2.771(5)Å with an angle of 177.5(2)° and the second H-bond, O_m-H_m···N7, a length of 2.789(5)Å, with an angle of 155.5(2)°. Again, the third H-bond, N6-H6···O_m, is a little bit longer with 3.034(5)Å and the angle is 164.9(3)°.

Interestingly, a different packing pattern of **42I** and **42II** was found. Both have alternating stacking between one 1-deazapurine ring and the phenyl e ring of another molecule. Though, for **42I** the 1-deazapurine ring and the phenyl ring of one molecule stack with a phenyl ring and a 1-deazapurine ring of another molecule. For **42II** the 1-deazapurine ring stacks with the phenyl ring of one molecule, and the phenyl ring with the 1-deazapurine of a third molecule. This leads to a zick zack of the stacking channels. The different channels build a zick zack chain and the different chains are connected through an H-bond of the O3´-H3´ with the O5´ atom of another molecule. The O3´-H3´···O5´ has a length of 2.786(5)Å and an angle of 158.1(3)°. For

42I also an H-bond between O3´-H3´and O5´ with a length of 2.818(4)Å and an angle of 178(3)° can be found. Therefore, one finds two stacking channels that are linked to other two stacking channels via the H-bonds from the sugars that are present to the left and to the right. There is connection through another H-bond, O_w-$H_{w2}\cdots$O4´, with a bonding length of 3.042(4) and an angle of 175(5)° that links the water molecule with a neighbouring sugar ring of a neighbouring stacking channel.

	42I	**42II**
ν_0	- 15.6(4)°	- 19.4(5)°
ν_1	+30.4(4)°	+34.2(5)°
ν_2	- 33.2(4)°	- 35.7(5)°
ν_3	+24.4(4)°	+25.1(5)°
ν_4	- 5.7(4)°	- 4.0(5)°
P	171°	+167°
	^{2}E (S)	**^{2}E (S)**
ν_m	34°	37°
γ	+44.4(5)°	+44.3(6)°
	+sc, +gauche	**+sc, +gauche**
χ	+57.5(5)°	+53.7(6)°
	syn	**syn**

Table 11: The endocyclic torsion angles ($\nu_{0\text{-}4}$) in the sugar ring to calculate the phase angle of pseudorotation (P) and the puckering amplitude (ν_m), the torsion angle (γ) for the conformation of C5´-O5´ compared to the sugar ring and the glycosidic bond angle (χ) are shown.

42I and **42II** have a conformation of the base in the crystal structures (N3 pointing toward the O5´ and N6 and N7 (the Hoogsteen side) pointing towards the possible base pairing partner) that is assumed to be formed in solution by 1-deazaadenine nucleoside (**40**). However, in the corresponding crystal structures of **40** this conformation could not be observed.[146,164] Also, one has to mention that the bases stand in the right position for binding over the Hoogsteen side with the water and

the methanol molecules in the position, where one wants to find a metal ion, when the 1-deazaadenine nucleoside has been introduced into an oligonucleotide.

Now the 1-deaza-(6-benzoylamino)-purine-N9-β-2´-deoxyribonucleoside (**42**) was protected at the O5´-position with the stericly bulky DMTr group. The obtained yield for the 1-deaza-(6-benzoylamino)-purine-N9-β-[2´-deoxy-5´-O-(4,4´-dimethoxytrityl)-ribonucleoside] (**43**) was with 56% much lower than the 76% in the literature.[93,146] The introduction of the phosphoramidite protecting group was, as mentioned already, done following a standard procedure. The addition of $(i\text{-}Pr)_2EtN$ and chloro-(2-cyanoethoxy)-(diisopropylamino)-phosphane to the 1-deaza-(6-benzoylamino)-purine-N9-β-[2´-deoxy-5´-O-(4,4´-dimethoxytrityl)-ribonucleoside] (**43**) dissolved in dry CH_2Cl_2 and stirring for an hour at r.t. gave the building block for the automated DNA-synthesizer, the 1-deaza-(6-benzoylamino)-purine-N9-β-[2´-deoxy-3´-O-(2-cyanoethyl)-N,N-diisopropylphosphoramidite-5´-O-(4,4´-dimethoxytrityl)-ribonucleoside] (**44**).[93,146]

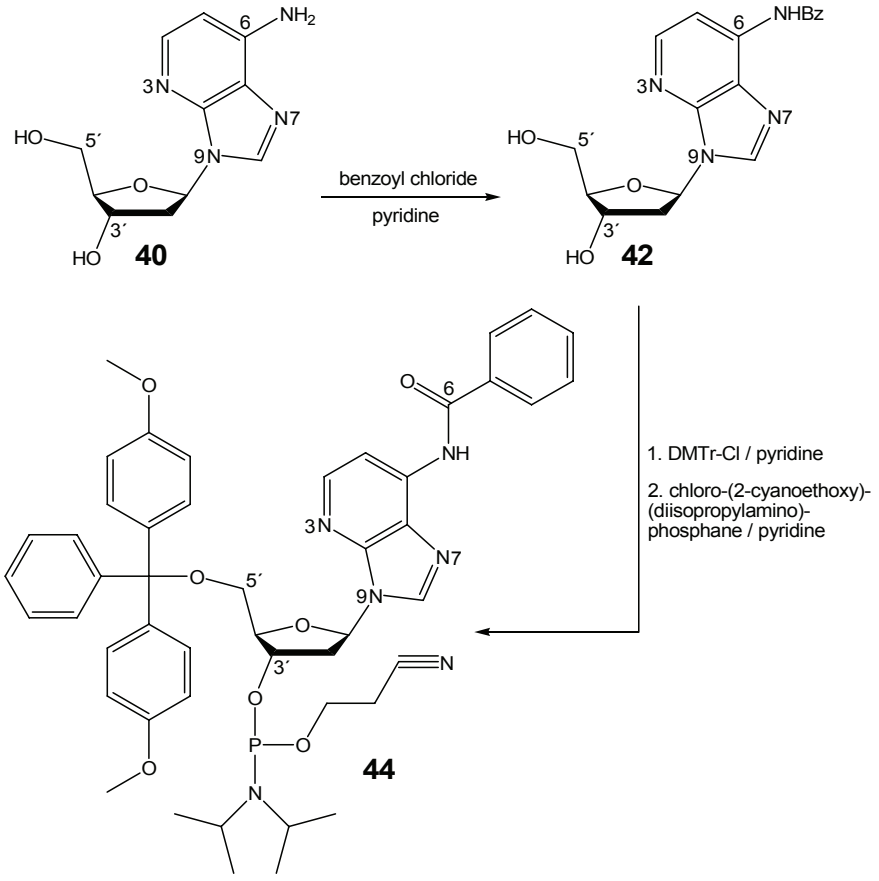

Figure 73: Schematic diagram of the synthesis of the N6, O5´ and O3´-protected 1-deazaadenine nucleotide (**44**).

No further work up was done for the same two reasons that were already mentioned for the 1-deazapurine nucleotides (**33** and **34**). Therefore the yield was calculated through the ratio of product to side product and the mean molar mass.

The 1-deaza-(6-benzoylamino)-purine-N9-β-[2´-deoxy-3´-O-(2-cyanoethyl)-N,N-diisopropylphosphoramidite-5´-O-(4,4´-dimethoxytrityl)-ribonucleoside] (**44**) could then be introduced to the automated DNA-synthesizer. The following oligonucleotide strand was synthesised with the 1-deazaadenine nucleoside as the artificial nucleobase (**Z**):

(**k**) 5´-d(A**ZZ ZZZ ZZZ** A)

The strand (**k**) was synthesised in the DMTr-off mode, deprotected, purified over a reversed phase column (no collectable peak found in the ion-exchange column) (HPLC), desalted, lyophilised and the concentrations were calculated with the help of the Lambert-Beer Law. The very low absorptions in the UV-spectra that were hardly much higher than the absorption from the salt (from the column), lead to the assumption that the synthesis has not been successful. The MALDI-TOF spectra did not show a trace of oligonucleotide. Thinking about a reason for the unsuccessful synthesis one has to look at the stability of the intermediates with the protecting groups, but especially at the stability of the 1-deaza-(6-benzoylamino)-purine-N9-β-2´-deoxyribonucleoside (**42**). It turned out to be depurinated upon the addition of trichloroacetic acid, which is used to deprotect the DMTr group during the automated DNA-synthesis. The depurination must have taken place in the matter of seconds, since in the ^{1}H NMR spectra and in the observations with TLC the 1-deaza-(6-benzoylamino)-purine-N9-β-2´-deoxyribonucleoside (**42**) in all cases was already depurinated. The known instability of the 1-deaza-(6-benzoylamino)-purine-N9-β-2´-deoxyribo-nucleoside (**42**) is a strong reason for the unsuccessful DNA-synthesis.

A new protecting group for the NH_2 group was necessary. One that protects it and does not destabilise the glycosidic bond had been found with the methoxyacetyl residue.[93,167,168] The reaction of the 1-deazaadenine nucleoside (**40**) with methoxyacetyl chloride afforded via peracylation, which was followed by selective deprotection of the sugar-protecting groups, the 1-deaza-(6-methoxyacetylamino)-

purine-N9-β-2´-deoxyribo-nucleoside (**45**). Although the purification by flash chromatography was done differently, the yield was the same as in the literature.[93,146] The 1-deaza-(6-methoxyacetylamino)-purine-N9-β-2´-deoxyribonucleoside (**45**) is stable in trichloroacetic acid for at least an hour. This could be observed by taking ^{1}H NMR spectra and doing TLC. Since the DNA-synthesiser uses the trichloroacetic acid for around two minutes to take off the DMTr protecting group, the methoxyacetyl protecting group should be suitable for our purposes.

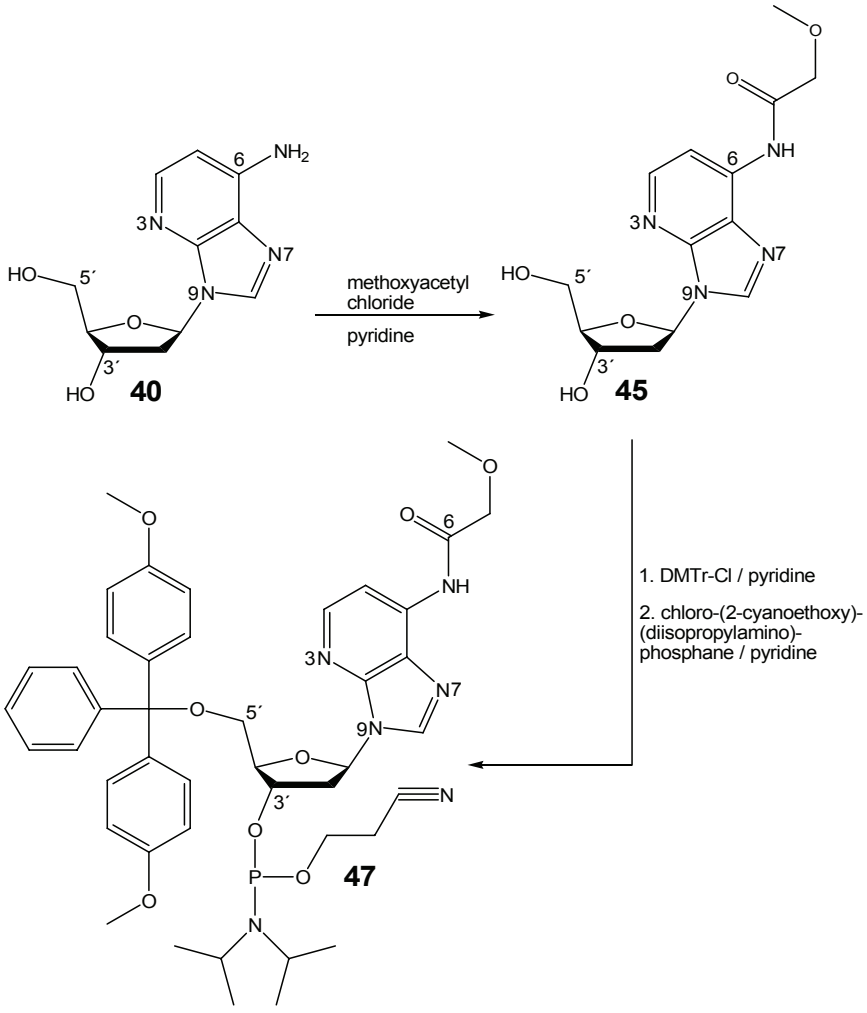

Figure 74: Schematic diagram of the synthesis of the N6, O5´ and O3´-protected 1-deazaadenine nucleotide (**47**).

Then the 1-deaza-(6-methoxyacetylamino)-purine-N9-β-2´-deoxyribonucleoside (**45**) was protected at the O5´-position with the stericly bulky DMTr group. The obtained

yield for the 1-deaza-(6-methoxyacetylamino)-purine-N9-β-[2´-deoxy-5´-O-(4,4´-dimethoxytrityl)-ribo-nucleoside] (**46**) was with 65% much lower than the 84% described in the literature, as it was found already for the 1-deaza-(6-benzoylamino)-purine-N9-β-2´-deoxyribo-nucleoside (**42**).[146] The introduction of the phosphoramidite protecting group was done following standard procedures.[146] The addition of (i-Pr)$_2$EtN and chloro-(2-cyanoethoxy)-(diisopropylamino)-phosphane to the 1-deaza-(6-methoxy-acetylamino)-purine-N9-β-[2´-deoxy-5´-O-(4,4´-dimethoxy-trityl)-ribonucleoside] (**46**) dissolved in dry CH_2Cl_2 and stirring for an hour at r.t. gave the building block for the automated DNA-synthesizer, 1-deaza-(6-methoxyacetylamino)-purine-N9-β-[2´-deoxy-3´-O-(2-cyanoethyl)-N,N-diisopropyl-phosphoramidite-5´-O-(4,4´-dimethoxytrityl)-ribonucleoside] (**47**). No further work up was done for the same two reasons that were already mentioned for the 1-deazapurine nucleotides (**33** and **34**). Therefore the yield was calculated through the ratio of product to side product and the mean molar mass.

The 1-deaza-(6-methoxyacetylamino)-purine-N9-β-[2´-deoxy-3´-O-(2-cyanoethyl)-N,N-diisopropylphosphoramidite-5´-O-(4,4´-dimethoxytrityl)-ribonucleoside] (**47**) could then be introduced to the automated DNA-synthesizer.
The following oligonucleotide strands were synthesised with the 1-deazaadenine nucleoside as the artificial nucleobase (**Z**):

(**l**) 5´-d(A**Z**A **Z**A**Z** A**Z**A) ‹ 1% yield
(**m**) 5´-d(**ZZZ ZZZ ZZZ ZZZ ZZZ ZZZ Z**A) ‹ 1%

Both strands (**l** and **m**) were synthesised in the DMTr-off mode, deprotected, purified over an ion-exchange column (HPLC), desalted, lyophilised and the concentration was determined with the help of the Lambert-Beer Law and finally the yield was calculated.
The low yields can have many possible factors. The acid used to take off the DMTr protecting groups in the automated DNA-synthesizer could depurinate or denature the oligonucleotide or single artificial nucleobases, although one has tried to avoid this. The more artificial nucleosides were introduced the lower the yield, the broader

the peaks in the HPLC chromatogram and therefore the more difficult to distinguish between product and side product and to collect the product. An especially visible effect of loss in yield was observed at changes from natural nucleobases to artificial ones, as in 5′-d(A**Z**A **Z**A**Z** A**Z**A) (**l**). Another obvious factor is the length of the oligonucleotides; the longer the strand, the lower the yield.

4.4 Melting Curves

(**l**) 5′-d(A**Z**A **Z**A**Z** A**Z**A)

The strand (**l**) was primarily synthesised to test the ability of introducing Z into an oligonucleotide using the methoxyacetyl as protecting group for the NH_2 group. The melting behaviour was observed with 5′-d(TTT TTT TTT TTT TTT) as possible complementary strand. The melting curves were done at the same buffer and strand conditions: 5mM MOPS (pH 6.8) and each strand 1µM. 150mM and 1M $NaClO_4$ salt concentrations and as metal ion Ag^+ was used. No melting behaviour at all was found, without or with Ag^+. The reason for this could be the base Z that needs to bind over the Hoogsteen side, but due to the alternating adenine and 1-deazaadenine nucleobases (A and Z) it is very unlike to turn to that way. Another reason for this could be the length of the oligonucleotide. The metal ions must be strongly stabilising for the Z-T pairs in the 9-mer to get a melting behaviour in the detectable temperature range. The T_m for a thymine 15-mer with an adenine 15-mer is only 36.1°C and considering the loss of six base pairs and a destabilising effect of the Z, due to the loss of a H-bond, the two strands are not necessarily expected to bind.

(**m**) 5′-d(**ZZZ ZZZ ZZZ ZZZ ZZZ ZZZ Z**A)

(**m**) should build out Z-T base pairs with a thymine 20-mer (**n**), as shown in Figure 75

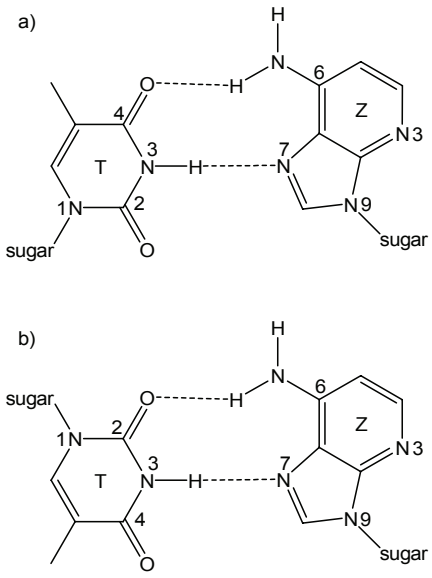

Figure 75: Hoogsteen, a), and reverse Hoogsteen, b), binding of a Z-T base pair.[93,146]

and in the literature.[93,146,167] Due to the missing N1 in Z, binding over the Hoogsteen side was expected to be favoured. But under the standard conditions we used (5mM MOPS (pH6.8), 1M $NaClO_4$ and each strand 1µM) and even at high salt concentrations, the two strands did not show a cooperative melting behaviour.

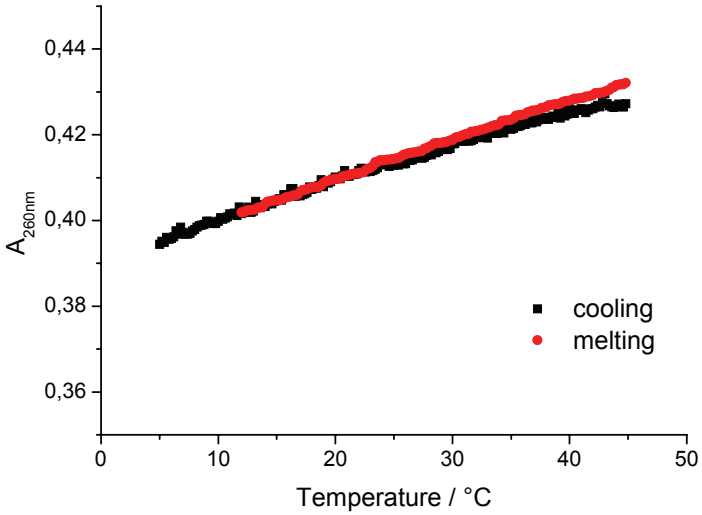

Graph 17: Cooling and melting curves for 5´-d(**ZZZ ZZZ ZZZ ZZZ ZZZ ZZZ Z**A) (**m**) and 5´-d(TTT TTT TTT TTT TTT TTT TT) (**n**).

However, the conditions chosen were comparable to the ones in the literature, except that a 5µM strand concentration was used.[93] The lower strand concentrations could be a reason for not observing a cooperative melting behaviour, since the T_m for a double helix is concentration dependent. Though, these conditions are roughly standard conditions. Sometimes lower salt (1M is on the upper limit) or higher strand concentrations, as just mentioned, are used. The two strands (**m**) and (**n**) are probably building out double helices of different lengths upon cooling, since the self assembling for Hoogsteen base pairs is not as pronounced (smaller hypochromicity) as for the formation of Watson-Crick base pairs (larger hypochromicity). Upon the temperature rising slowly, the shorter double helices melt earlier than the longer ones, giving rise to single strands being present in the solution at lower temperature. These single strands can then, again, build longer double helices, leading overall to a non-cooperative melting behaviour. But upon the addition of Ag^+, a cooperative melting behaviour starts to develop. This could be due to the Ag^+ being able to

strengthen self assembling of (**m**) and (**n**). This increase in cooperativity of the melting behaviour can be seen nicely in Graph 18.

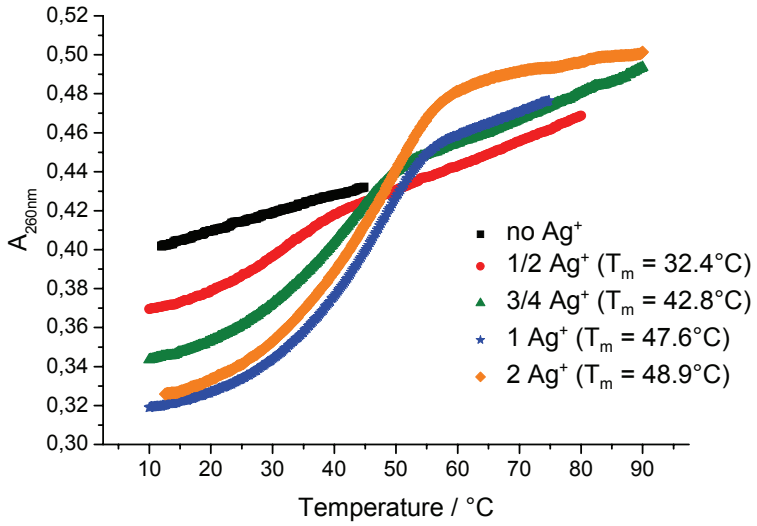

Graph 18: Melting curves of 5´-d(**ZZZ ZZZ ZZZ ZZZ ZZZ ZZZ Z**A) (**m**) and 5´-d(TTT TTT TTT TTT TTT TTT TT) (**n**) with different equivalents of Ag^+.

Upon the addition of one equivalent Ag^+ a hypochromicity effect can be observed; the hypochromocity roughly doubles. A T_m can be measured, when only half an equivalent of metal ion is present. Looking at Graph 19 it can be seen that the T_m does not rise further after the addition of one equivalent of Ag^+ showing specificity (Z-Ag^+-T) and that the Ag^+ does not bind randomly (permanent increase in T_m).

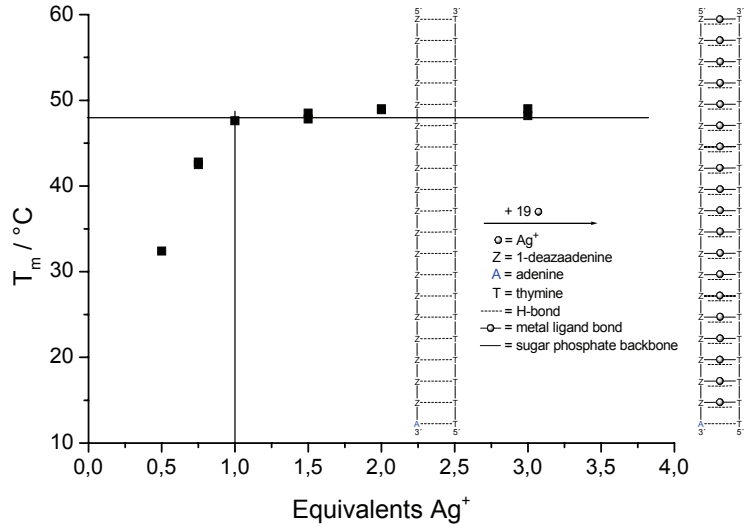

Graph 19: Change of T_m/°C upon the addition of different equivalents of Ag^+.

To gain information, whether other metal ions can also support the binding and therefore about the selectivity of Ag^+, further melting curves with different metal ions would have to be measured. The two different possibilities of binding over the Hoogsteen side, which can not be distinguished with the data present, can be seen in Figure 76.

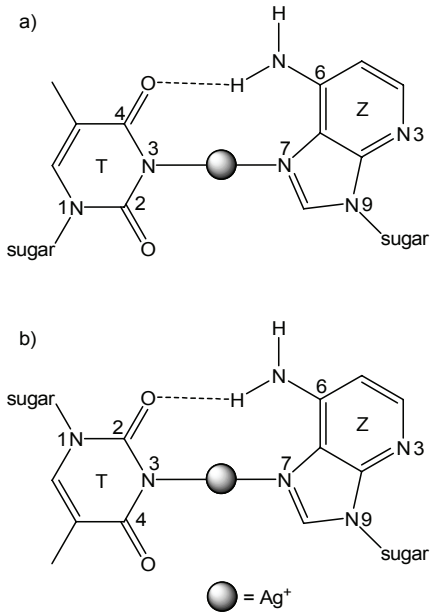

Figure 76: Hoogsteen, a), and reverse Hoogsteen, b), binding of a Z-T base pair with Ag^+.

To gather information about the structure and the actual binding more melting curves have to be taken, to exclude, for example, a self pairing of the 5´-d(**ZZZ ZZZ ZZZ ZZZ ZZZ ZZZ Z**A) (**m**)[12,146,169] or 5´-d(TTT TTT TTT TTT TTT TTT TT) (**n**) with Ag^+, as it has been observed before for 5´-d(TTT TTT TTT TTT TTT TT) (**j**). A measurement of 5´-d(TTT TTT TTT TTT TTT TTT TT) (**n**) with 5´-d(AAA AAA AAA AAA AAA AAA AA) with and without Ag^+ would show how the T_m of a system with apparent Hoogsteen base pairs compares with a system of Watson-Crick base pairs. This could show whether one apparent H-bond and a metal-ligand bond can compete with two H-bonds in a natural duplex. A rough estimation for a comparison of the two systems could be: A double helix with 15 A-T base pairs has a T_m of around 36°C. These are around 2.4°C for one A-T base pair or two H-bonds with π-

stacking interactions. A T_m of around 48°C has been found for a system with $^{5'}$-d(**ZZZ ZZZ ZZZ ZZZ ZZZ ZZZ Z**A) (**m**), $^{5'}$-d(TTT TTT TTT TTT TTT TTT TT) (**n**) and one equivalent Ag^+. These are also around 2.4°C for one Z-T base pair. However, the two T_m values have a quite important difference. The first was obtained through a measurement at a low salt concentration (150mM) and the second at a high salt concentration (1M). Therefore one would expect the Watson-Crick base pairs to be more stable.

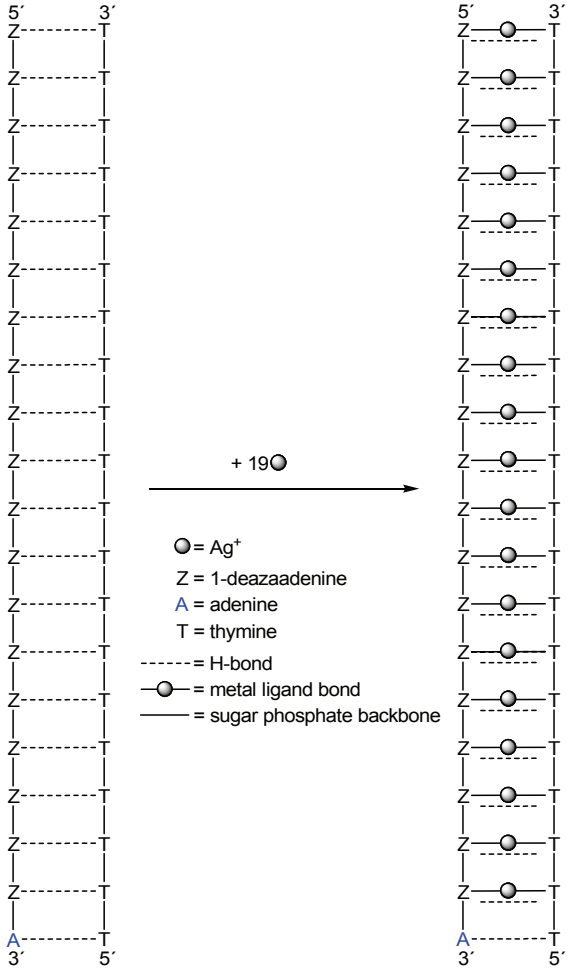

Figure 77: Possible double helix formation of $^{5'}$-d(**ZZZ ZZZ ZZZ ZZZ ZZZ ZZZ Z**A) (**m**) and $^{5'}$-d(TTT TTT TTT TTT TTT TTT TT) (**n**) without and with Ag^+.

With the data present one can not distinguish between parallel or anti-parallel binding. The one A-T base pair in the double helix is thought to bind over the Hoogsteen side, too. However, one can neither be certain of this, nor, whether a

metal ion will also bind in-between this A-T base pair, or not. If one could increase the cooperativity of the melting behaviour of **m** with **n** without metal ions, it would lead to an increase in hyperchromicity and here-with to an existing T_m. One then would expect a double helix formation as shown above in Figure 77.

For a better structural knowledge more data of this system have to be collected. CD-spectra could give more information about a possible change in structure upon the addition of Ag^+ or about the presence of a double helix without metal ions.

5 Summary and Discussion

Synthesis of the nucleosides and their introduction into oligonucleotides:

The synthesis of the two 1-deazapurine nucleosides (**28** and **29** / Figure 78), starting off with the synthesis of 1-deazapurine (**21**) and followed by the reaction with Hoffer´s chlorosugar (**25**), was achieved in good yields. The appearance of alpha- and beta-anomers, could be solved partially by separating them using flash chromatography. The appearance of unwanted alpha-anomer, though, could not be hindered or even stopped. The deprotection steps to obtain the nucleosides, and the syntheses of the protected nucleotides (**33** and **34**) for the automated DNA-synthesizer were performed smoothly.

The synthesis of the 1-deazaadenine nucleoside (**40** / Figure 78) was more challenging. The oxidation of 1-deazapurine (**21**) to the N3-oxide (**35**), the nitration and the reduction reaction gave the precursor 1-deaza-6-nitropurine (**37**). The ways of synthesising these products had to be altered and always to be done with great care to gain substantially good yields. Connecting the 1-deaza-6-nitropurine (**37**) to the Hoffer´s chlorosugar (N9-position) gave again the alpha-anomer as side product (**38a**), which was separated, but no N7 side product was observed. Deprotection and amination reactions to obtain the 1-deazaadenine nucleoside (**40**) could be done with reasonable yields. With the 1-deaza-6-nitropurine nucleoside (**39** / Figure 78) another potential artificial nucleobase was found. The protection of the NH_2 group was done using benzoyl chloride at first, but the protecting group, unlike the description in the literature, was not found to be useable for the introduction of 1-deazaadenine nucleoside into an oligonucleotide. Surprisingly, it led to depurination with trichloroacetic acid in the DNA-synthesizer.

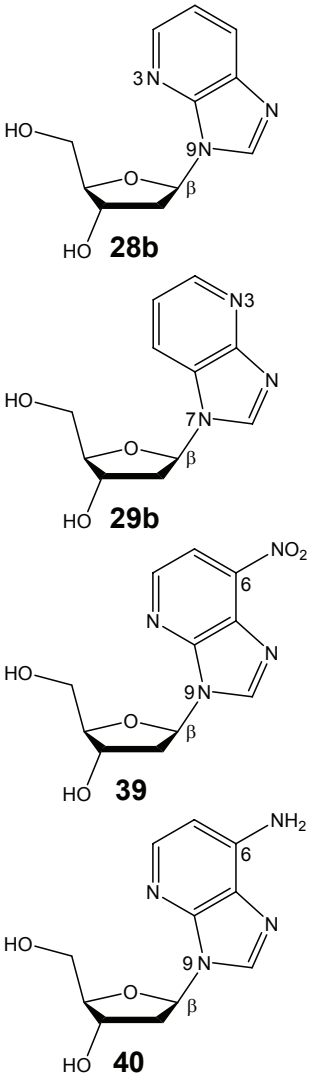

Figure 78: **28**, **29**, **39** and **40**.

Therefore methoxy acetyl chloride was used. The next two protecting steps (DMTr / phosphoramidite) were done without any further surprises to obtain the protected nucleotide (**47**).

All three nucleosides (**28**, **29** and **40**), and their derivatives showed a high acid lability or the tendency under catalytical conditions to form the alpha-anomer.

In no cases the phosphoramidites (**33**, **34** and **47**) were purified by flash chromatography due to the lack of visibility of the side product. This could be one reason for the low yields that are obtained throughout the synthesis of the oligonucleotides. Finding new ways of purifying the phosphoramidites could give higher yields. Clearing the synthesised oligonucleotides off the solid phase (5min/r.t.) and deprotecting them (5min/65°C), was done with AMA. Using AMA twice to get the oligonucleotides off the solid phase improved the yield slightly. But, as experience has shown, the deprotection step has to be done over a longer period of time to really get all protecting groups off, especially for the cytosine and guanine. That is one reason probably that the modified Dickerson Drew strand (**f**) does not show any melting behaviour.

All successfully purified oligonucleotides (**a**), (**e**)-(**i**), (**l**) and (**m**) were synthesised in the DMTr-off mode and were purified over an ion-exchange column. The problem herewith is the high salt concentration that has to be used and the broad peaks in the chromatograms that make it difficult to collect the product peak. The high salt concentrations damage the ion-exchange column, even with a protection column in front, quite rapidly, which leads to high purchasing costs. This could be avoided synthesising the oligonucleotides in the DMTr-on mode and purifying them over a reversed phase column. Attempts to synthesise in the DMTr-on mode and to use a reversed phase column were not successful. This is probably due to the 1-deazaadenine nucleoside (Z) depurinating at the deprotection step with acetic acid. Though, for the 1-deazapurines (**33** and **34**) attempts should be made to test their stability in acetic acid, since the reversed phase column is much easier to work with and the life of the column much longer. Another factor for the low yields could be the HPLC itself. It is difficult to know, when exactly the collection of a product should take place, since the length of the way from the UV-detector to the collection

point and the time taken by an oligonucleotide for this way is yet unknown. Test runs with coloured substances could give a time value for the collection.

Characterisation of the nucleosides, melting behaviour and structural knowledge:

For all three nucleosides it could be shown that no competition between protonation and metallation reaction is expected. pK_a values of 2.84 (**28**) and 3.26 (**29**) were found. Whereas the 1-deazapurine nucleosides (**28** and **29**) are stable at low pD values, the 1-deazaadenine nucleoside (**40**) undergoes depurination at pD values lower than 5. The methyl derivatives of 1-deazapurine have higher pK_a values than the α-anomers that themselves have higher values than the β-anomers.

For the 1-deazapurine nucleosides (**28** and **29**) crystal structures were obtained and compared with each other and with the crystal structures of 1,3-deazapurine nucleoside (**30**), another potential artificial nucleobase that could also be crystallised. Although all had quite different sugar conformations, it should be mentioned that the bases were always found in the syn position.

For the 1-deazapurine nucleoside (**29**) with the N7-glycosidic bond the titrations with different metal ions (Ni^{2+}, Hg^{2+} and Cu^{2+}) on the UV-spectrometer showed some changes in the absorbance, but the actual changes were quite small, so that it was difficult to say, whether bonding takes place. With Fe^{3+} a change in absorbance maxima and value was observed. Additionally the Job-Plot with Fe^{3+} shows the formation of a 2:1 complex giving rise to a possible X-Fe-X base pair (Figure 79). All other metal ions only formed a 1:1 complex. The synthesised strand, $^{5'}$-d(AAA AAA AXX XTT TTT TT) (**a**), had a melting behaviour, but upon the addition of metal ions, the T_m did not change. The actual T_m of 44°C though was larger than for an A_{15}/T_{15} duplex with around 36°C. Therefore the formation of a double helix or a hairpin structure is possible, but with these data alone it can not be distinguished between the two. A study of the change of T_m upon the change in strand concentration would give a hint, since the T_m of a double helix is concentration dependent.

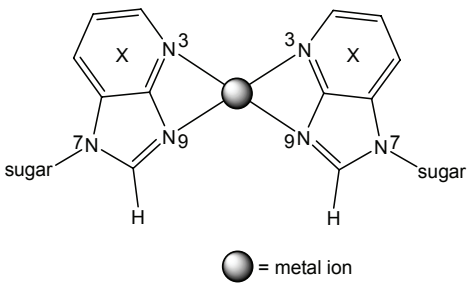

Figure 79: Possible binding of **29** with a metal ion.

For the 1-deazapurine nucleoside with the N9-glycosidic bond (**28**) the model structure $[Hg(9\text{-MeDP})_2](NO_3)_2 \cdot H_2O$ (**24**) already showed the formation of a 2:1 complex. This was shown with the help of a crystal structure. A Job-Plot and a titration with Hg^{2+} and 1-deazapurine-N9-nucleoside (**28**) confirmed this nicely. Also the stability constants for the 1:1 and the 2:1 complex were calculated and were found to be in a suitable range compared to imidazole and triazole. The strands 5´-d(AAA AAA A**Y**A AAA AAA) (**g**) and 5´-d(TTT TTT T**Y**T TTT TTT) (**h**) were synthesised. The melting behaviour was observed having, next to the 14 A-T base pairs, different binding possibilities in the middle of the strand, such as A-Y, C-Y, G-Y and T-Y. Not amazingly suprising, the T_m dropped sometimes even dramatically, when a mispair was positioned in the middle base pair, so that one could not speak of a distinct melting behaviour. Upon the addition of one equivalent of Ag^+ for cytosine, as one of the bases in a base pair, an increase in T_m was observed. For a Y-Y base pair a large increase was observed, but this increase was found to be even larger with guanine or cytosine as base pairing partner. All other nucleobases did not show a stabilising effect upon the addition of Ag^+. Further addition of Ag^+ raised the T_m of the systems only marginally. This was a first indication of Y being able to build metal-mediated base pairs (Figure 80). However, it is not possible from these data to relate neither to the conformation of the helices nor to the bonding between the nucleobases. Further research on the melting behaviour with other metal ions or with different artificial nucleobases, such as the X (**29**) or an imidazole nucleoside must be undertaken to get more information about possible artificial or natural base pairing partners and the specificity of certain metal ions for possible artificial or natural nucleobases. Taking the double helices with a large increase in T_m upon the addition of Ag^+ and measuring CD-spectra of them would give additional structural knowledge about the individual systems. One would expect the A-T base pairs to bond over the Watson-Crick side and that the strands are antiparallel, as it is common for A-T rich double helices under the used conditions.

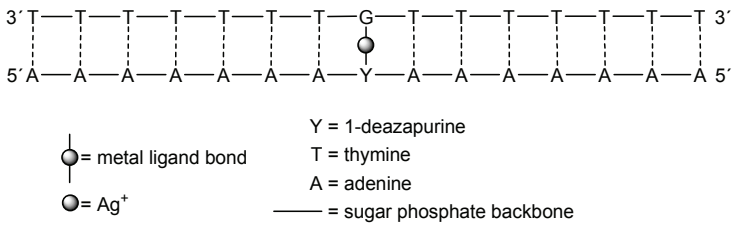

Figure 80: An example of an artificial Ag^+-mediated G-Y base pair in a 15-mer with 14 natural A-T base pairs.

Furthermore, with the 1-deazapurine-N9-nucleoside the strand $^{5'}$-d(**YYY YYY YYY YYY YYY Y**A) (**i**) was synthesised. Primarily, it was prepared to observe the behaviour of the strand with a thymine strand of equal length (**j**). This was then meant to be compared with the 1-deazaadenine nucleoside (**40**) in a 20-mer (**m**) and its melting behaviour with a thymine 20-mer (**n**). Due to the ability of $^{5'}$-d(TTT TTT TTT TTT TTT TT) (**j**) to bind Ag^+, the possibility of a competitive reaction could not be excluded. Therefore the self assembling of the strand $^{5'}$-d(**YYY YYY YYY YYY YYY Y**A) (**i**) was studied, but, as expected, in the absence of metal ions it showed no cooperative melting. Then it was looked at the melting behaviour of the strand (**i**) with Ag^+. An increase in hypochromicity, cooperativity of the melting and a T_m were found upon the addition of Ag^+. The increase in T_m of around 17°C was observed at roughly 0.5 equivalents of Ag^+ added. Addition of more equivalents did not show a further increase, which shows a certain specificity. 16 Ag^+ for four strands or 8 Ag^+ for two strands are needed to saturate the system and employ melting behaviour (Figure 81).
In the CD-spectra it was shown that there is no structural difference without and with Ag^+, showing some kind of organisation even without metal ion being present. A structural difference between the melted strands and the organised strands can be seen, but it is not a large effect. A possible explanation for all these effects is the formation of a double helix that is formed by π-stacking interactions and that is barely stable. The added Ag^+ can then bind in the middle between two Ys and stabilise the double helix. Due to possible repulsion between two Ag^+ not all base pairs have a metal ion, but every second.
The high symmetry of the system rules out possible NMR measurements, but crystallography could be a good method to gather further information about the structure, the base pairing and the position of the Ag^+ in the base pair. The limitation at this point is the low yield of this strand synthesised. The difference in melting behaviour upon the addition of different metal ions would be another interesting point.

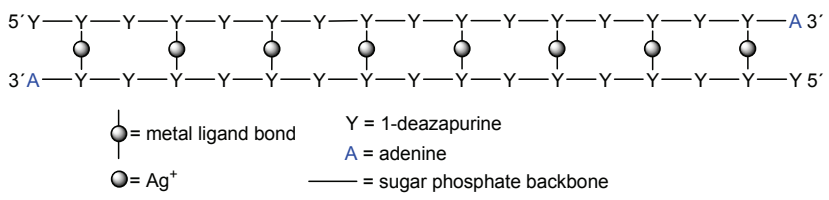

Figure 81: An example of a possible double helix with an artificial Ag^+-mediated Y-Y base pair in a 17-mer.

The 5´-d(**ZZZ ZZZ ZZZ ZZZ ZZZ ZZZ Z**A) (**m**) was synthesised in the hope to form a double helix with 5´-d(TTT TTT TTT TTT TTT TTT TT) (**n**). The 1-deazaadenine (**Z**) as nucleobase should bind over the Hoogsteen side to a thymine. The melting behaviour was measured, but no cooperative melting behaviour was observed without metal ion. Upon the addition of one equivalent Ag^+ a cooperative melting behaviour, a T_m and a hypochromicity effect could be observed. After the addition of one equivalent Ag^+ no further change in melting behaviour was observed, which shows some kind of specificity (Figure 82). Under the conditions measured the H-bonds do not seem to be strong enough to give cooperative melting, which could explain the small linear increase in the melting curve without metal ion. The two strands bind partially (a few base pairs) or fully and a slow increase in temperature breaks some of the base pairs of the partially bound strands. The single strands at lower temperatures can reorganise and form again partially or fully binding helices with more base pairs present. Hence no cooperative melting is observed. For further information about the structure (double helix, parallel or anti parallel), and the actual binding of the nucleobases (Hoogsteen or reverse Hoogsteen) other measurements are necessary. CD-spectra could give information about a possible change in structure upon the addition of metal ions. The two strands have to be tested each separately and together on their melting behaviour with metal ions. Assumable the thymine seems to bind to the Ag^+ only, if no stronger binding possibilities are present. This would mean that possibly the 5´-d(**YYY YYY YYY YYY YYY Y**A) (**i**) would show a melting behaviour with 5´-d(TTT TTT TTT TTT TTT TT) (**j**) upon the addition of Ag^+ or even Hg^{2+} and this should be looked at. The idea of introducing metal ions into the inside of a double helix, however, has been strengthened trough the results obtained.

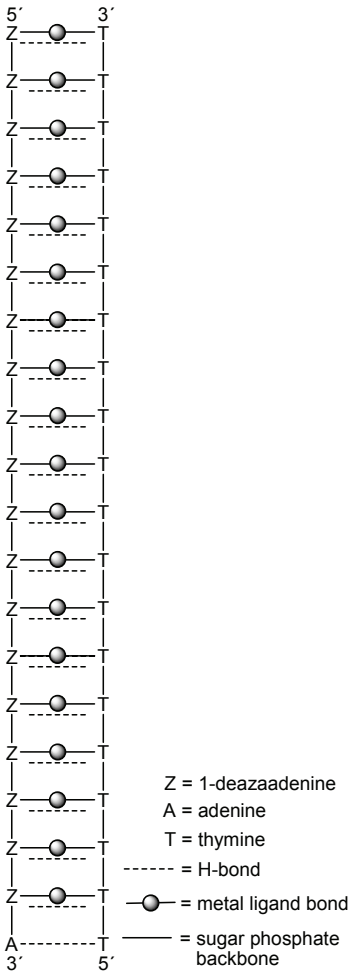

Figure 82: A possibly formed double helix
through artificial Ag^+-mediated Z-T base pairs.

D Experimental Section

1 Instrumentation and Methods

Starting materials

The chemicals used were purchased from Sigma-Aldrich, ABCR, Fluka or Acros or were present in the laboratory facilities of the University of Dortmund, if not stated otherwise.

Following oligonucleotides, containing only natural nucleobases, were purchased from EuroGenTec:

5´-d(AAA AAA ATA AAA AAA)

5´-d(AAA AAA ACA AAA AAA)

5´-d(AAA AAA AGA AAA AAA)

5´-d(CTT TTG)

5´-d(TTT TTT TAT TTT TTT)

5´-d(TTT TTT TCT TTT TTT)

5´-d(TTT TTT TGT TTT TTT)

5´-d(TTT TTT TTT TTT TTT TT)

5´-d(TTT TTT TTT TTT TTT TTT TT)

Solvents

Pyridine was dried over molecular sieves. CH_3CN, CH_2Cl_2 and $CHCl_3$ were freshly distilled over CaH_2. CH_3OH was freshly distilled over Mg. Et_2O was dried over Na. All other solvents were used as purchased by Roth, Sigma-Aldrich, ABCR, Fluka or Acros.

Flash Column Chromatography and TLC

TLC analyses were carried out with the use of pre-coated TLC plates 60 F_{254} purchased from Fluka and were visualized in UV light (254nm) and sometimes additionally a colourising agent was used (2.5g molybdophosphoric acid, 1g cerium sulphate, 6ml conc. H_2SO_4 and 94ml H_2O). The silica gel (0.040-0.063mm) used for column chromatography was purchased from Merck. The solvents for the column chromatography were used as purchased.

Elemental Analyses

Microanalyses were measured on a Leco CHNS 932 instrument.

NMR-Spectroscopy

^{1}H and ^{13}C NMR spectra were recorded on Varian Mercury 200 (200.13MHz) and Bruker DRX 400 (400.13MHz) spectrometers. ^{31}P spectra were recorded on a Varian Mercury 200 (80.98MHz) instrument and ^{195}Pt NMR and ^{199}Hg NMR spectra were recorded on a Bruker DPX 300 instrument (64.4MHz and 53.51MHz, respectively). Chemical shifts (δ in ppm) were referenced to internal sodium 3-(trimethylsilyl)-propanesulfonate (^{1}H, D_2O, δ = 0 ppm), tetramethylsilane (^{1}H, MeOD and $CDCl_3$, δ = 0 ppm), external dimethylmercury (^{199}Hg, D_2O, δ = 0 ppm) or to external K_2PtCl_6 (^{195}Pt, δ = 0 ppm). Spectra in DMSO-d_6 were referenced to residual DMSO-d_5 at 2.5ppm. All deuterated solvents were purchased from Deutero.
NOESY-spectra were recorded on Bruker DRX 400 (400.13MHZ) at 300.1K with mixing times between 0.5 and 1.5 seconds.

MS-Measurement

For the MS measurements a JOEL JMS_SX 102A was used. As matrix for the FAB measurements 3-nitrobenzylalcohol was used.

pH / pD Measurements

The pH-values of aqueous solutions were measured with a Model inoLab Level 1 made by Wissenschaftliche Technische Werkstätten (WTW) with a glas electrode Model pH Electrode SemTix 81 pH 0…14/0-100°C/3 mol/L KCl of the Wissenschaftliche Technische Werkstätten (WTW).

pD-values of D_2O solutions were obtained by adding 0.4 to the pH meter reading.[170]

The pK_a values in H_2O were calculated from the pK_a^* values according to

$$pK_a^* = 1.015pK_a + 0.45.$$[171]

For the adjustment of the pD value DNO_3 or NaOD solutions in different concentrations were added.

Job-Plots with Hg^{2+}

For the Job-Plots the method of continuous variation was used.[134-137] The change in chemical shift ($\Delta\delta_{ppm}$) was observed with the help of ^1H NMR at different mole fractions (χ) of ligand (nucleoside) and M^{n+}.

The nucleoside solution was prepared by dissolving 6.0mg (25.5µmol) 1-deazapurine-N9-β-2´-deoxyribonucleoside in 600µl buffer solution (pD 5, 100mM sodium acetate/acetic acid in D_2O/TSP) to give a 42.5mM solution. The metal ion solution was done by dissolving 25.4mg (59.5µmol) $Hg(CF_3COO)_2$ in 1400µl of the same buffer solution (pD 5, 100mM sodium acetate/acetic acid in D_2O/TSP) to give an equally molar solution.

For 1-deazapurine-N7-β-2´-deoxyribonucleoside 3.1mg (13.0µmol) were dissolved in 600µl buffer solution (pD 7, 60µl 1M triethylammonium acetate/540µl D_2O/TSP) to give a 21.7mM solution. For the metal ion solution 14.3mg (33.5µmol) $Hg(CF_3COO)_2$ were dissolved in 1528µl of the same buffer solution (pD 7, 153µl 1M triethylammonium acetate/1375µl D_2O/TSP) to give an equally molar solution.

^{1}H NMR	$\chi_{nucleoside}$	$\chi_{metal\ ion}$	$solution_{nucleoside}$	$solution_{metal\ ion}$
1	1	/	600µl	/
2	0.9	0.1	- 60µl	+ 60µl
3	0.8	0.2	- 67µl	+ 67µl
4	0.7	0.3	- 75µl	+ 75µl
5	0.6	0.4	- 86µl	+ 86µl
6	0.5	0.5	- 100µl	+ 100µl
7	0.4	0.6	- 120µl	+ 120µl
8	0.3	0.7	- 150µl	+ 150µl
9	0.2	0.8	- 200µl	+ 200µl
10	0.1	0.9	-300µl	+ 300µl

Job-Plot method

Titrations with M^{n+}

The titrations with M^{n+} were done with the help of ^{1}H NMR (400MHz) or UV spectroscopy. The changes in chemical shift ($\Delta\delta_{ppm}$) or in absorbance (range of wavelength: 190-350nm) were observed upon the addition of different equivalents M^{n+} to a fixed amount of ligand (nucleoside).

For the titration with the help of ^{1}H NMR spectroscopy, the nucleoside solution was prepared by dissolving 4.2mg (18µmol) 1-deazapurine-N9-β-2´-deoxyribonucleoside in 600µl buffer solution (pD 5.0, 100mM sodium acetate/acetic acid in D_2O/TSP) to give a 30.0mM solution.

For the measurement at pD 7.0, the nucleoside solution was prepared by dissolving 5.5mg (23µmol) 1-deazapurine-N9-β-2´-deoxyribonucleoside in 600µl buffer solution (100mM triethylammonium acetate in D_2O/TSP) to give a 39mM solution.
The metal ion solutions were prepared, so that 5µl equaled 0.05 equivalents. As metal salt $Hg(CF_3COO)_2$ was used.
For the measurements on the UV spectrometer, the nucleoside solution was prepared by dissolving 2.1mg (8.93µmol) 1-deazapurine-N7-β-2´-deoxyribonucleoside in 1000µl CH_3OH and diluting the solution by a factor of 100 gave an 89.3µM solution. The metal ion solutions were prepared, so that 20µl equaled one equivalent. Following metal salts were used: $CuCl_2•2H_2O$, $FeCl_3•6H_2O$, $HgCl_2$, $NiCl_2•6H_2O$ and $ZnCl_2$.

Stability Constants

The stability constants were calculated with the help of the EQNMR programme.[138] The data used, were the chemical shifts (δ_{ppm}), the concentration of the metal ion ($[M^{n+}]$) and the concentration of the ligand (nucleoside/[L]).

X-ray Crystallography

Crystal data were collected at 150K or at 293K on an Enraf-Nonius-KappaCCD diffractometer using graphite-monochromated $Mo_{K\alpha}$ radiation (λ = 0.71069Å). For data reduction and cell refinement, a Bruker-Nonius HKL 2000 Suite and the DENZO and SCALE-PACK[172] was used. The measurements for **28b**, **29b**, **30**, **37**, **42I** and **42II** were done by Dipl.-Chem. E. Gil Bardaji, for **7**, **10**, **11** and **35** by Dr. Eva Freisinger and for **24** by Dr. M. Roitzsch. All structures were solved by standard Patterson methods or by direct methods and were refined by full-matrix least squares methods based on F^2 using the SHELXTL PLUS,[173] SHELXL-97[174] and WinGX[175] programs. In the refinement process of the X-ray data, if not specified, all non-hydrogen atoms of the crystals were refined anisotropically.

DNA-Synthesizer

For the syntheses of the modified DNA strands a synthesizer from Beckman, Model OLIGO 1000M, was used. The reagents used were purchased from Glen Research. Columns for a 1000nM synthesis from Beckman were used and the synthesizer worked with the phosphoramidite method. The synthesizer always started synthesizing at the solid support end at the 3´-position, where a natural nucleobase sits.

The syntheses were performed in the DMTr-off mode, except for the strands $^{5'}$-d(AAA AAA AXA AAA AAA) and $^{5'}$-d(TTT TTT TXT TTT TTT) where the DMTr-on mode was used. After the synthesis the oligonucleotides were cleaved off the solid support and deprotected using 1ml of AMA (≤10% NH_4OH and ≥90% CH_3NH_2) for 5min at r.t. and for 5min at 65°C. Afterwards the AMA could be removed under vacuum.

High-Pressure (Performance)-Liquid-Chromatography (HPLC)

Two high-pressure-pumps (model 1525) and a UV-detector (model 2487) from Waters were used, as well as the software Breeze (Version 3.20). A column thermostat (Jet stream 2 Plus) from Knauer was used and it was worked with temperatures between 25°C (r.t.) and 60°C.

The ion-exchange column used was purchased from Macherey-Nagel (Model EC 125/4 Nucleogen 60-7) and a precursor column (Model CC 30/4 Nucleogen) was used to protect the ion-exchange column. The flow rate used was at 1 to 1.5ml/min and the UV-detection was done at 260nm. For the ion-exchange column the solvent A was prepared by adding 1.31g (0.02mol) of sodium acetate to 800ml of H_2O, bringing the pH down to 6 using acetic acid and adding 200ml of HPLC grade CH_3CN. Solvent A with 84.78g (2mol) of LiCl gave solvent B.

The reversed phase column used was purchased from Waters (Model Symmetry® C_{18} 5µm 4.6 x 150mm) and no precursor column was used. The flow rate was between 0.7

and 1.5ml/min and the UV-detection was done at 260nm. Solvent A was Et_3NHOAc (0.05M) at pH 7 in H_2O and solvent B was HPLC grade CH_3CN.
All solvents were filtered and degassed prior to use.

Desalting

To desalt the DNA solutions after HPLC treatment, a NAP™ 5 or NAP™ 10 column (Sephadex™ G-25 DNA Grade contains 0.15% Kathon® CG as preservative) purchased from Amersham Biosciences or a Waters OASIS® Sample Extraction Products column purchased from Waters was used.

UV/Vis-Spectroscopy

UV-spectra were recorded on a Cary 100 spectrophotometer.
To determine the concentrations of the DNA solutions, the absorption at 260 nm was used in the Lambert-Beer law ($E_{260nm} = \varepsilon\ c\ d$, where distance d = 1cm). The extinction coefficient ε of the DNA strand equals the sum of the individual extinction coefficients multiplied with the correction factor, f, for the stacking interactions (0.9 for a single stranded DNA strand).

$$\varepsilon = f * \Sigma n_i \varepsilon_i$$

The ε values for the natural nucleobases are known, but for the synthesised nucleobases this value can be calculated by measuring the absorption of a known concentration of the nucleoside.

$$\varepsilon = E_{260nm}/c$$

	ε-values
Adenine (A)	15.4cm^2/μmol
Cytosine (C)	7.3cm^2/μmol
Guanine (G)	11.7cm^2/μmol
Thymine (T)	8.8cm^2/μmol
1-Deazapurine-N7 (X)	3.3cm^2/μmol
1-Deazapurine-N9 (Y)	3.3cm^2/μmol
1-Deazaadenine (Z)	11.5cm^2/μmol

ε-values for the nucleosides

Thermal Denaturation

The melting studies were carried out in 1cm path length quartz cells from Varian (CELL STOP SMICRO/total volume 1ml; 0.9ml sample volume) on a Cary 100 spectrophotometer equipped with a thermo-programmer. Melting curves were monitored at 260nm with a heating rate of 1°C/min. Melting temperatures were calculated as the first derivatives of the heating curves.

MALDI-TOF

The MALDI-TOF spectra were measured at a Voyager-DETM Pro Biospectrometry Workstation Spectrometer from the Perseptive Biosystems Company. As matrix 3-hydroxypicolinic acid (5mg, 100μl H_2O, 100μl CH_3CN, 12.5μl ammonium citrate solution (50mg/ml)) was used.

2 General Work Description

If methods from the literature are slightly modified, it will be stated. If the methods differ from methods in the literature, the yield is stated for comparison.

2.1 Chapter I

1-Methyltetrazole and 2-Methyltetrazole (2 and 3)

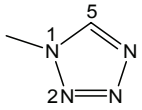

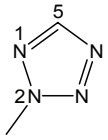

This is a slightly modified version of the synthesis in the literature.[72]

Deprotonation with NaH:

Under argon 5.27g (75.2mmol) tetrazole are dissolved in 100ml CH_3CN at 35°C. The solution is stirred and carefully 3.61g (75.2mmol) NaH (60% in oil) are added. The reaction mixture is stirred for two hours at r.t. and then evaporated to dryness to give a white solid, that is washed with 15ml n-hexane (3x). The solid is dried over night at 40°C to give 6.92g (75.2mmol) sodium tetrazolate.

^{1}H-NMR (200MHz, DMSO-d_6, δ in ppm): δ 8.01 (s, 1H, H5).

Methylation of sodium tetrazolate with CH_3I:

To a suspension of 6.92g (75.2mmol) sodium tetrazolate in 40.0ml CH_3CN, 4.66ml (75.2mmol) CH_3I are added dropwise at -15°C. The suspension is heated up to 100°C and stirred for one hour. Then the solvent is evaporated and the residue extracted with 50ml CH_2Cl_2 (3x). The solution is evaporated to dryness to give yellowish brown oil, which is purified with the help of a Kugelrohr (ball-tube) distillation under reduced pressure (oil pump). At 20-50°C a fraction of clean 2-methyltetrazole is obtained and between 50°C and 75°C a mixture of 1-methyltetrazole (**2**) and 2-methyltetrazole (**3**) is found. At temperatures higher then 75°C, 1.09g (13.0mmol) 1-methyltetrazole (**2**) are obtained (17%, ref.: 58%)[72]; **2** : ^{1}H-NMR (200MHz, DMSO-d_6, δ in ppm): 9.32 (s, 1H, H5), 4.10 (s, 3H, CH_3); **3**: 8.94 (s, 1H, H5), 4.38 (s, 3H, CH_3).

[(trpy)PdCl]Cl•2H_2O (4)

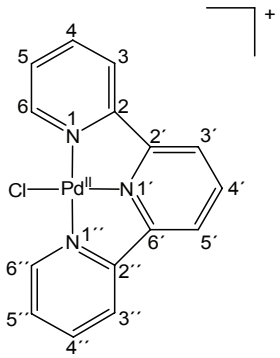

A suspension of 114mg (0.400mmol) [(COD)$PdCl_2$] in 10ml H_2O is stirred at r.t. and 94.0mg (0.403mmol) 2,2´:6´,2´´-terpyridine are added. After roughly 15min stirring not reacted [(COD)$PdCl_2$] and Pd^0 are filtered off and the solution is evaporated to dryness. The yellow brown solid is washed with 20ml Et_2O (3x) to give 174mg (0.386mmol) [(trpy)PdCl]Cl•2H_2O (98%); ^{1}H-NMR (200MHz, DMSO-d_6, δ in ppm): 8.73 (dd, 2H, H6, H6´´), 8.69-8.61 (m, 5H, H3, H3´, H3´´, H4´ and H5´), 8.47 (dt, 2H, H4, H4´´), 7.89 (dd, 2H, H5, H5´´); elemental analysis calc. (%) for $C_{15}H_{11}N_3Cl_2Pd$•2H_2O (M = 450.92g/mol): C 40.3, H 3.4, N 9.4; found: C 40.0, H 3.1, N 9.1.

[(trpy)PtCl]Cl•2H_2O (5)

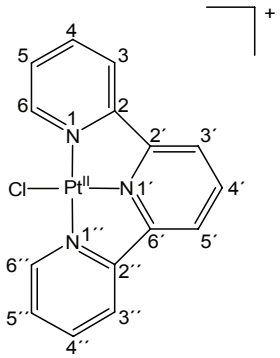

This is a slightly modified version of the synthesis in the literature.[73]

A suspension of 150mg (0.400mmol) [(COD)$PtCl_2$] in 10ml H_2O is stirred at 40-50°C and 93.6mg (0.399mmol) 2,2´:6´,2´´-terpyridine are added. After roughly 15min stirring excess [(COD)$PtCl_2$] is filtered off and the yellow red solution is evaporated to dryness. The residue is washed with 20ml Et_2O (3x) to give 155mg (0.287mmol) [(trpy)PtCl]Cl•2H_2O as a red solid (73%, ref.: 98%)[73]; ^{1}H-NMR (200MHz, DMSO-d_6, δ

in ppm): 8.91 (dd, 2H, 2 x H6), 8.69-8.62 (m, 5H, H3, H3´, H3´´, H4´ and H5´), 8.47 (dt, 2H, H4, H4´´), 7.95 (ddd, 2H, H5, H5´´); elemental analysis calc. (%) for $C_{15}H_{11}N_3Cl_2Pt•2H_2O$ (M = 539.58g/mol): C 33.7, H 2.8, N 7.9; found: C 34.1, H 2.7, N 7.8.

$[(trpy)_2Pd_2(1\text{-}mtetate)](ClO_4)_3$ (6)

To a solution of 46.1mg (0.548mmol) 1-methyltetrazole and 33.1mg (0.195mmol) $AgNO_3$ in 5ml H_2O a suspension of 47.0mg (0.105mmol) $[(trpy)PdCl]Cl•2H_2O$ in 5ml H_2O is added at r.t. The solution is then stirred in the dark for one day at 40°C. The resulting yellow suspension is filtered over celite and the pH-value of the solution is changed from 4.5 to 9.0 using a NaOH solution (0.1M). Then 5ml $NaClO_4$ solution (0.25M) are added to the yellow solution. Up to a few millilitres the solution is evaporated, whereby a slight yellow solid precipitates. For complete precipitation the solution is stored at 4°C for three days. The solid is filtered off and re-crystallised from H_2O to yield 15mg of $[(trpy)_2Pd_2(1\text{-}mtetate)](ClO_4)_3$ (27%). ^{1}H-NMR (200MHz, DMSO-d_6, δ in ppm): 8.64 (m, 6H, 2 x H3´, 2 x H4´, 2 x H5´), 8.61 (dt, 4H, 2 x H3 and 2 x H3´´), 8.44-8.39 (m, 4H, 2 x H4 and 2 x H4´´), 8.18 (m, 4H, 2 x H6 and 2 x H6´´), 7.66-7.56 (m, 4H, 2 x H5 and 2 x H5´´), 4.51 (s, 3H, CH_3).

$[(trpy)Pt(1\text{-}mtetate)](ClO_4)$ (7)

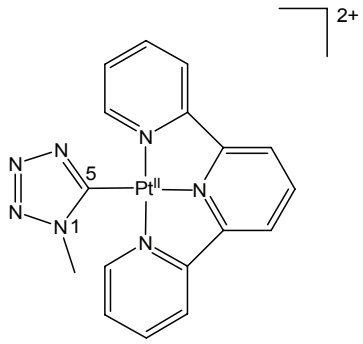

A solution containing of 18.2mg (0.216mmol) 1-methyltetrazole and 67.5mg (0.397mmol) $AgNO_3$ in 5ml H_2O is stirred at 60°C in the dark. To this solution a suspension of 108.3mg (0.202mmol) $[(trpy)PtCl]Cl•2H_2O$ in 5ml H_2O is added. The

solution is then stirred in the dark for three days at 60°C. The pH-value of the red suspension is then changed from 2.8 to 9.0 using NaOH solution (0.1M) and the suspenion is stirred in the dark for three days at 60°C. Now, the suspension is filtred over celite and 5ml $NaClO_4$ solution (0.25M) are added to the yellow solution. For precipitation of the product the solution is stored at 4°C for three days. The yellow solid, that precipitates, is filtered off and re-crystallised from H_2O to yield 10.3mg of [(trpy)Pt(1-mtetate)](ClO_4) (8%). ^{1}H-NMR (200MHz, DMSO-d_6, δ in ppm): 8.77-8.73 (m, 5H, H3, H3´, H3´´, H4´, H5´), 8.51 (dt, 2H, H4, H4´´), 8.17 (dd, 2H, H6, H6´´), 7.78 (ddd, 2H, H5, H5´´), 4.15 (s, 3H, CH_3); ^{195}Pt NMR (DMSO-d_6, δ in ppm): -2760; elemental analysis calc. (%) for $C_{17}H_{14}N_7O_4ClPt$ (M = 610.89g/mol): C 33.4, H 2.3, N 16.1; found: C 32.5, H 2.1, N 16.0.

[(trpy)Pd(2-mtet)](ClO_4)$_2$ (8)

To a solution of 16.9mg (0.2mmol) 2-methyltetrazole and 66.0mg (0.4mmol) $AgNO_3$ in 5ml H_2O a suspension of 90.1mg (0.2mmol) [(trpy)PdCl]Cl•2H_2O in 5ml H_2O is added at r.t. The solution is then stirred in the dark for one day at 40°C. The resulting yellow suspension is filtered over celite and the pH-value of the solution is changed from 4.5 to 9.0 using NaOH solution (0.1M), whereby the yellow colour becomes more intensive. Then 5ml $NaClO_4$ solution (0.25M) are added to the yellow solution. Up to a few millilitres the solution is evaporated and for complete precipitation the solution is stored at 4°C for one day. The solid is filtered off and dried over night at 40°C. The ^{1}H-NMR shows only the starting complex, [(trpy)PdCl]Cl•2H_2O, and no product at all.

[(trpy)Pt(2-mtet)](ClO_4)$_2$ (9)

A solution containing of 17.4mg (0.2mmol) 2-methyltetrazole and 67.1mg (0.4mmol) $AgNO_3$ in 5ml H_2O is stirred at 60°C in the dark. To this solution a suspension of 107.7mg (0.2mmol) [(trpy)PtCl]Cl•2H_2O in 5ml H_2O is added. The solution is then

stirred in the dark for three days at 60°C. The pH-value of the red suspension is then changed from 2.7 to 8.9 using NaOH solution (0.1M) and the suspension is stirred in the dark for a further three days at 60°C. Now, the suspension is filtered over celite and 5ml $NaClO_4$ solution (0.25M) are added to the solution, whereby a solid precipitates. For complete precipitation of the product the solution is stored at 4°C for three days. The orange red solid is filtered off and dried over night at 40°C. The ^{1}H-NMR shows only the starting complex, [(trpy)PtCl]Cl•2H_2O, and no product at all.

[(trpy)Pd(1-mimi)](ClO$_4$)$_2$ (10)

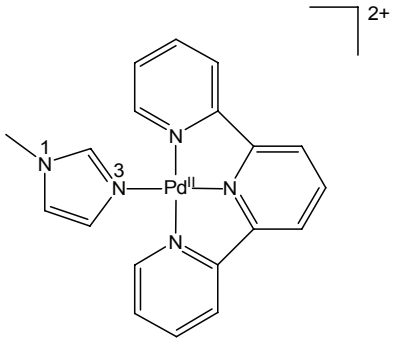

To a solution of 15.9µl (0.200mmol) 1-methylimidazole and 67.5mg (0.397mmol) $AgNO_3$ in 5ml H_2O a suspension of 89.0mg (0.200mmol) [(trpy)PdCl]Cl•2H_2O in 8ml H_2O is added at r.t. The solution is then stirred in the dark for one day at 40°C. The resulting orange suspension is filtered over celite and the pH-value of the solution is changed from 8.3 to 9.0 using NaOH solution (0.1M). The solution is evaporated to half its volume and 5ml $NaClO_4$ solution (0.5M) are added, whereby immediately a solid precipitates. For complete precipitation the solution is stored at 4°C for a couple of days. The solid is filtered off and re-crystallised in H_2O to give 57.2mg (0.092mmol) [(trpy)Pd(1-mimi)](ClO$_4$)$_2$ as compact orange cubes (46%); ^{1}H-NMR (200MHz, DMSO-d$_6$, δ in ppm): 8.73-8.71 (m, 6H, H3, H3´, H3´´, H4´, H5´) 8.64 (s, 1H, H2$_{(1\text{-mimi})}$), 8.52 (dt, 2H, H4, H4´´), 7.83-7.81 (m, 4H, H5, H5´´, H6, H6´´), 7.76 (d, 1H, H5$_{(1\text{-mimi})}$), 7.59 (d, 1H, H4$_{(1\text{-mimi})}$), 3.91 (s, 3H, CH_3); elemental analysis calc. (%) for $C_{19}H_{17}N_5O_8Cl_2Pd$ (M = 620.69g/mol): C 36.8, H 2.8, N 11.3; found: C 36.8, H 2.6, N 11.4.

[(trpy)Pt(1-mimi)]$(ClO_4)_2$ (11)

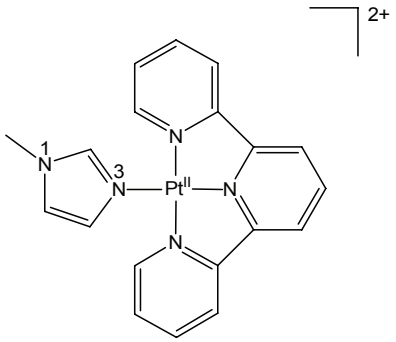

A solution containing of 7.90µl (0.100mmol) 1-methylimidazole and 33.7mg (0.198mmol) $AgNO_3$ in 5ml H_2O is stirred. To this solution a suspension of 53.5mg (0.100mmol) [(trpy)PtCl]Cl•$2H_2O$ in 5ml H_2O is added. The solution is then stirred in the dark for three days at 60°C. The pH-value of the suspension is then changed from 8.0 to 9.0 using NaOH solution (0.1M) and the suspension is stirred in the dark for a further three days at 60°C. Now, the suspension is filtered over celite and 5ml $NaClO_4$ solution (0.5M) are added, whereafter a yellow precipitates starts to form. For complete precipitation of the product the solution is stored at 4°C for one day. The yellow solid is filtered off and re-crystallised in H_2O. After a few days 23.3mg (32.8µmol) [(trpy)Pt(1-mimi)]$(ClO_4)_2$ fall out in form of yellow sticks (33%); ^{1}H-NMR (400MHz, DMSO-d_6, δ in ppm): 8.76-8.69 (m, 6H, H3, H3´, H3´´, H4´, H5´ and $H2_{(1\text{-}mimi)}$), 8.57 (dt, 2H, H4, H4´´), 8.02 (dd, 2H, H6, H6´´), 7.89 (ddd, 2H, H5, H5´´), 7.84 (d, 1H, $H5_{(1\text{-}mimi)}$), 7.63 (d, 1H, $H4_{(1\text{-}mimi)}$), 3.94 (s, 3H, CH_3); ^{195}Pt NMR (DMSO-d_6, δ in ppm): -2858; elemental analysis calc. (%) for $C_{19}H_{17}N_5O_8Cl_2Pt$ (M = 709.35g/mol): C 32.2, H 2.4, N 9.9; found: C 32.2, H 2.4, N 10.0.

Dimethyl 3-methylpentanedioate (13)

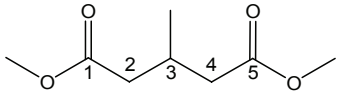

This is a slightly modified version of the synthesis in the literature.[78]

A mixture of 250mg (1.30mmol) p-TsOH, 25.0g (170mmol) of 3-methylpentanedioic acid, 8.50ml (210mmol) CH_3OH and 34.5g (340mmol) 2,2-dimethoxypropane is heated to 45°C and stirred for twelve hours. Then the solvents are evaporated and the residue is distilled under vacuum (T_m = 113°C/water pump) to give 25.7g (147mmol) dimethyl 3-methylpentanedioate as a light yellow oil (87%, ref.: 81%)[78]; ^{1}H- NMR (200MHz, $CDCl_3$/TMS, δ in ppm): 3.61 (s, 2 x 3H, 2 x $OC\underline{H}_3$), 2.50-2.10 (m, 5H, $C\underline{H}_2C\underline{H}C\underline{H}_2$), 0.96 (d, 3H, $C\underline{H}_3$); ^{13}C-NMR (200MHz, $CDCl_3$/TMS): 172.7 (C_q), 50.5 (OCH_3), 40.6 (CH_2), 27.4 (CH), 19.9 (CH_3).

1,5-Bis(2-pyridyl)-3-methylpentane-1,5-dione (14)

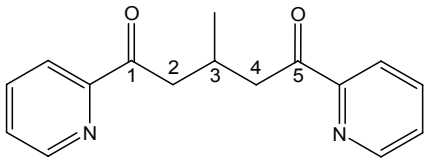

This is a slightly modified version of the synthesis in the literature.[78]

In a 500ml round bottom flask 300ml dry THF are cooled down to -78°C under an argon atmosphere. Now 20.5ml (137mmol) TMEDA are added and then 85.5ml (137mmol) n-BuLi (1.6M in hexane) are added drop wise. After further drop wise addition of 13.0ml (137mmol) 2-bromopyridine the temperature is raised to -55°C and the mixture is stirred for 30min, whereas it becomes yellow. The temperature is dropped to -78°C again and 10.0g (57.0mmol) dimethyl 3-methylpentanedioate are added and the mixture becomes red. After stirring the mixture for one hour, it is hydrolysed with 100ml H_2O and the orange mixture is evaporated to dryness. The residue is dissolved in 100ml HCl solution (20%) and washed with 100ml CH_2Cl_2. The H_2O phase is neutralised with 125ml NaOH solution (20%), whereby the product falls out as dark red oil. Then the product gets extracted with 100ml CH_2Cl_2 (4x) and the organic phase is dried over Na_2SO_4, filtered and evaporated to dryness. After flash chromatography over silica gel (12 x 7cm, CH_2Cl_2 (9) : EtOAc (1)) 4.17g

(15.5mmol) of brown 1,5-bis(2-pyridyl)-3-methylpentane-1,5-dione are obtained (27%, ref. 41%)[78]; ^{1}H-NMR (200MHz, $CDCl_3$ / TMS, δ in ppm): 8.63 (m, 2H, H6 and H6´´), 8.02 (td, 2H, H3 and H3´), 7.81 (dt, 2H, H4 and H4´), 7.44 (ddd, 2H, H5 and H5´), 3.29 (m, 4H, $C\underline{H}_2CHC\underline{H}_2$), 2.92 (septet, 1H, $CH_2C\underline{H}CH_2$), 1.10 (d, 3H, $C\underline{H}_3$).

4´-Methyl-2,2´:6´,2´´-terpyridine (15)

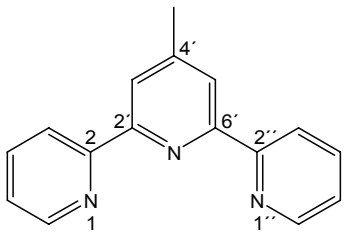

This is a slightly modified version of the synthesis in the literature.[78]

In a 500ml round bottom flask 4.17g (15.5mmol) 1,5-bis(2-pyridyl)-3-methylpentane-1,5-dione are dissolved in 215ml acetic acid (98-100%) and 10.4g (135mmol) ammonium acetate are added. The mixture is heated under reflux (120°C) for two hours, whereby the colour changes from orange over green to dark red. Then the mixture is evaporated to dryness and the residue is dissolved in 200ml NaOH solution (10%). The H_2O phase gets extracted with 150ml CH_2Cl_2 (3x) and the organic phase is dried over Na_2SO_4, filtered and evaporated to dryness. To the residue 50ml n-heptane are added and the round bottom flask is put into the ultrasonic apparatus for 10min at 40°C. Then the mixture is left in the refrigerator (-18°C) for 10min. The yellow n-heptane is decanted and evaporated. The work up procedure with the n-heptane is done six times in total and 3.51g (14.2mmol) slightly yellow 4´-methyl-2,2´:6´,2´´-terpyridine are obtained (91%, ref.: 76%)[78]; ^{1}H-NMR (200MHz, $CDCl_3$/TMS, δ in ppm): 8.71 (qd, 2H, H6 and H6´´), 8.63 (td, 2H, H3 and H3´´), 8.31 (d, 2H, H3´ and H5´), 7.87 (dt, 2H, H4 and H4´´), 7.34 (ddd, 2H, H5 and H5´´), 2.54 (s, 3H, $C\underline{H}_3$); elemental analysis calc. (%) for $C_{16}H_{13}N_3$ (M =247.30g/mol): C 77.7, H 5.3, N 17.0; found: C 76.3, H 5.5, N 16.3.

4´-(Carboxaldehyde)-2,2´:6´,2´´-terpyridine (17)

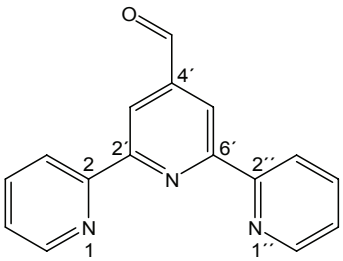

This is a slightly modified version of the synthesis in the literature.[79]

In a 500ml round bottom flask 2.17g (8.78mmol) 4´-methyl-2,2´:6´,2´´-terpyridine are dissolved in 220ml acetic acid (98-100%), 2.01g (18.1mmol) SeO_2 are added and the mixture is refluxed (120°C) for 43h. Then a tip of chelating resin is added, the mixture is filtered to remove the gray selenium metal and the solution is evaporated to dryness. The residue is neutralised with 100ml NaOH solution (20%). The aqueous phase is extracted three times with 150ml $CHCl_3$, the organic phase is dried over Na_2SO_4 and then evaporated. Then 2.50g of a dark green product are obtained (4´-methyl-2,2´:6´,2´´-terpyridine (4) : 4´-carboxyaldehyde-2,2´:6´,2´´-terpyridine (1)) and used without further workup for the preparation of **18**. ^{1}H-NMR (200MHz, $CDCl_3$/TMS, δ in ppm): 8.90 (d, 2H, H3´ and H5´), 8.76 (qd, 2H, H6 and H6´´), 8.64 (td, 2H, H3 and H3´´), 7.91 (dt, 2H, H4 and H4´´), 7.40 (ddd, 2H, H5 and H5´´), δ 5.31 (s, 1H, C<u>H</u>).

4´-(Hydroxymethyl)-2,2´:6´,2´´-terpyridine (18)

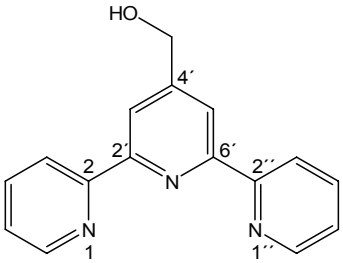

In a 250ml round bottom flask 2.50 g of a mixture of 4´-methyl-2,2´:6´,2´´-terpyridine (2.0g, 8.09mmol) and 4´-carboxyaldehyde-2,2´:6´,2´´-terpyridine (0.50g, 1.91mmol) and 240mg (6.36mmol) $NaBH_4$ are dissolved in 120ml dry THF under argon and stirred at 0°C for one hour. The solvent is evaporated and the resulting yellow solid is dissolved in 200ml EtOAc using an ultrasonic apparatus. The organic phase gets

washed with 50ml saturated NaCl solution (3x) and the aqueous phase is then washed with 100ml EtOAc. The combined organic phases are evaporated. To the residue 100ml n-heptane are added and the round bottom flask is put into the ultrasonic apparatus for 10min at 40°C. Then the suspension is left in the refrigerator (-18°C) for 10min. The n-heptane is decanted (product still in the round bottom flask) and evaporated to give 4´-methyl-2,2´:6´,2´´-terpyridine. To the residual solid 100ml CH_2Cl_2 are added and the suspension is centrifuged. The solution is decanted (product) and the solid is again extracted with 100ml CH_2Cl_2. The CH_2Cl_2 phases are combined and evaporated. To the residue 50ml n-heptane are added again and the round bottom flask is put into the ultrasonic apparatus for 10min at 40°C. Then the suspension is left in the refrigerator (-18°C) for 10min. The n-heptane is decanted (product still in the round bottom flask) and evaporated to give 4´-methyl-2,2´:6´,2´´-terpyridine. This extraction with n-heptane is done four times, whereby the last two times the n-heptane is not decanted, but filtered off. The n-heptane is evaporated to give 4´-methyl-2,2´:6´,2´´-terpyridine. The remaining orange solid is 175mg (665µmol) clean 4´-hydroxymethyl-2,2´:6´,2´´-terpyridine (35%, ref.: 85%)[83]. ^{1}H-NMR (200MHz, $CDCl_3$/TMS, δ in ppm): 8.74 (d, 2H, H3´ and H5´), 8.76 (qd, 2H, H6 and H6´´), 8.64 (td, 2H, H3 and H3´´), 7.91 (dt, 2H, H4 and H4´´), 7.40 (ddd, 2H, H5 and H5´´), 4.93 (s, 2H, C<u>H</u>$_2$).

4´-(Bromomethyl)-2,2´:6´,2´´-terpyridine (19)

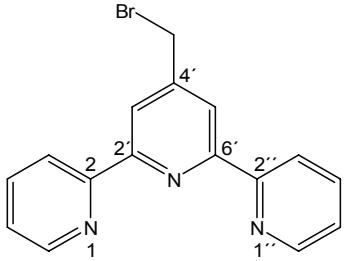

In a 50ml round bottom flask 138mg (520µmol) 4´-hydroxymethyl-2,2´:6´,2´´-terpyridine are dissolved in 4.0ml CH_2Cl_2 and to the solution 347mg (1.05mmol) CBr_4 are added. The solution is cooled to 0°C and 151mg (580µmol) triphenylphosphane are added in several portions over 15min. Then the solution is stirred for 30min at 0°C and for 30min at r.t. The solution is directly poured onto a silica gel column (6 x

2.5cm) and eluted off the column with CH_2Cl_2 and EtOAc (250ml CH_2Cl_2 / 300ml EtOAc/ flashed with CH_3OH). First the 4´-bromomethyl-2,2´:6´,2´´-terpyridine is eluted, then the triphenylphosphaneoxide. Mixed fractions are further purified with flash chromatography over silica gel (2cm x 2.5cm / 200ml fractions of only CH_2Cl_2 / CH_2Cl_2 (5) : EtOAc (1) in full steps down to 2 : 1). From the 4´-bromomethyl-2,2´:6´,2´´-terpyridine 63.2mg (190µmol) are obtained (37%, ref.: 40%)[83]. ^{1}H-NMR (200MHz, $CDCl_3$/TMS, δ in ppm): 8.71 (qd, 2H, H6 and H6´´), 8.62 (td, 2H, H3 and H3´´), 8.49 (s, 2H, H3´ and H5´), 7.87 (dt, 2H, H4 and H4´´), 7.35 (ddd, 2H, H5 and H5´´), 4.57 (s, 2H, C$\underline{H_2}$Br); ^{13}C-NMR (200MHz, $CDCl_3$ / TMS, δ in ppm): 149.0 (C6 and C6´´), 137.1 (C4 and C4´´), 124.1 (C3 and C3´´), 121.4 (C5 and C5´´), 120.9 (C3´ and C5´), 30.9 (C$\underline{H_2}$Br); elemental analysis calc. (%) for $C_{16}H_{12}N_3Br$ (M = 326.20g/mol): C 58.9, H 3.7, N 12.9; found: C 57.2, H 3.6, N 12.5.

DMTr-(S)-glycidol (20)

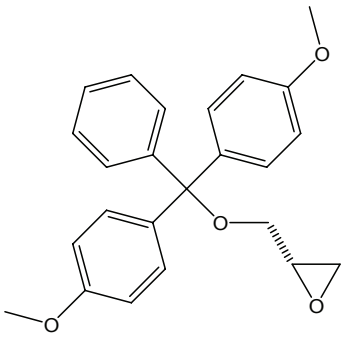

In a 50ml round bottom flask a mixture of 12.5ml dry CH_2Cl_2 and 2.0ml of Et_3N is stirred and 356µl (5.10mmol) (R)-glycidol are added. Additionally 2.11g (6.20mmol) DMTr-Cl are added. The mixture is stirred for 40min at r.t., whereby the colour of the solution changes from orange to green. Then the suspension is filtered and the solution is washed with 10ml H_2O. The organic phase is dried over Na_2SO_4, filtered off and evaporated. Chromatographic purification over silica gel (16 x 2.5cm / n-hexane (18) : EtOAc (1) : Et_3N (1)) gives 333mg (880µmol) DMTr-(S)-glycidol (17%, ref.: 65%). ^{1}H-NMR (200MHz, DMSO-d_6): 6.9 and 7.3 (m, 13H, aryl), 3.7 (s, 2 x 3H, 2 x OCH_3), 3.3 and 3.4 (2 x d, 2H, CH_2ODMTr), 3.1 (m, 1H, CH), 2.7 and 2.9 (2 x m, 2H, C$\underline{H_2}$ (endocyclic)); elemental analysis calc. (%) for $C_{24}H_{24}O_4$ (M = 376.452g/mol): C 76.6, H 6.4; found: C 75.0, H 6.5; FAB-MS calc. (M/Z): 377.175; found: 376.432.

2.2 Chapter II

1-Deazapurine (21)

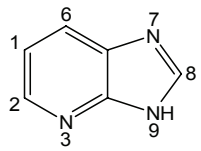

This is a slightly modified version of the synthesis in the literature.[106]

A mixture of 5.0g (46mmol) 2,3-diaminopyridine and 100ml freshly distilled triethyl orthoformate is stirred at reflux (128-130°C) for three hours. The solution is evaporated to dryness in vacuo (60°C) and the residue is stirred at reflux (ca. 50°C) for one hour after having been dissolved in 50ml of concentrated HCl. After letting the mixture cool down to r.t., it is carefully neutralized with solid $Na_2CO_3 \cdot 10H_2O$ (vigorous reaction!). Using a liquid-liquid extractor, the mixture is extracted with EtOAc over night. The organic phase gets dried over Na_2SO_4, filtered and evaporated to dryness. The residue is dissolved in 50 ml absolute CH_3CH_2OH, treated with charcoal, and heated at reflux (ca. 80°C) over night. The charcoal is filtered off and the solvent evaporated until needles start to fall out of the solution. Now the solution is stored over night at 4°C and at the next morning the slight yellow needles are filtered off and dried at 40°C to give 3.8g (32mmol) 1-deazapurine (70%, ref.: 73%)[106]; ^{1}H-NMR (200MHz, DMSO-d_6, δ in ppm): 12.94 (br, 1H, $N_{7/9}H$), 8.44 (s, 1H, H8), 8.35 (dd, 1H, H2), 8.02 (dd, 1H, H6), 7.23 (dd, 1H, H1); elemental analysis calc. (%) for $C_6H_5N_3$ (M = 119.12g/mol): C 60.5, H 4.2, N 35.3; found: C 60.2, H 3.9, N 35.0.

1-Deaza-9-methylpurine and 1-Deaza-7-methylpurine (22 and 23)

In 30ml dry DMF 1.04g (8.69mmol) 1-deazapurine and 207mg (8.63mmol) NaH (emulsion in mineral oil, washed with dry diethyl ether) are dissolved and the clear solution is cooled to 0°C and stirred for 90min. After addition of 639µl (10.1mmol) CH_3I, the reaction is allowed to proceed until the ice bath reaches ambient temperature (ca. two and a half hours). The DMF is then removed by vacuum distillation (oil pump) at 35 °C, and the crude product is purified by flash chromatography over silica gel (19 x 4cm, EtOH) to give 345mg (2.59 mmol) 1-deaza-9-methylpurine (30%) and 212mg (1.59 mmol) 1-deaza-7-methylpurine (18%). Re-crystallization from $CHCl_3$ gives hygroscopic white foams. 1-deaza-9-methylpurine: ^{1}H-NMR (200MHz, D_2O, pD 6.6, δ in ppm): 8.14 (d, 1H, H2), 8.10 (s, 1H, H8), 7.88 (d, 1H, H6), 7.20 (dd, 1H, H1), 3.71 (s, 3H, CH_3); elemental analysis calc. (%) for $C_7H_7N_3$•0.83H_2O (M = 148.11g/mol): C 56.7, H 5.9, N 28.4; found: C 56.7, H 5.9, N 28.4; 1-deaza-7-methylpurine: ^{1}H-NMR (200MHz, D_2O, pD 5.6, δ in ppm): 8.32 (d, 1H, H2), 8.19 (s, 1H, H8), 7.83 (d, 1H, H6), 7.27 (dd, 1H, H1), 3.79 (s, 3H, CH_3); elemental analysis calc. (%) for $C_7H_7N_3$•4.1H_2O (M = 207.03g/mol): C 40.6, H 7.4, N 20.3; found: C 40.6, H 6.4, N 20.0.

[Hg(1-deaza-9-methylpurine)$_2$](NO_3)$_2$•H_2O (24)

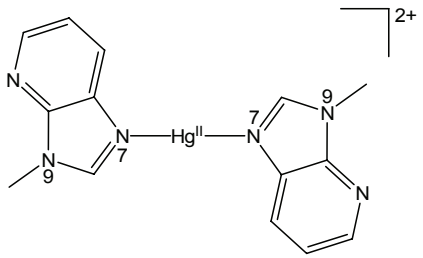

To a solution of 45.0mg (0.37mmol) 9-methyl-1-deazapurine in 1ml H_2O 250µl of a 0.74mM solution of $Hg(CF_3COO)_2$ in H_2O (0.19mmol) and 200µl of a 2.2mM solution of $NaNO_3$ in H_2O (0.44mmol) are added. After one day, colourless crystals of [Hg(1-deaza-9-methylpurine)$_2$](NO_3)$_2$•H_2O are found. Upon drying at 40 °C overnight,

[Hg(1-deaza-9-methyl-purine)$_2$]$(NO_3)_2$•H_2O looses its water of crystallization to give 54.0mg (91.0µmol) [Hg(1-deaza-9-methylpurine)$_2$]$(NO_3)_2$ (50%). ^{1}H NMR (200MHz, D_2O, pD 4.0, δ in ppm): 9.16 (s, 1H, H8), 8.72 (d, 1H, H2), 8.59 (d, 1H, H6), 7.73 (dd, 1H, H1), 4.18 (s, 3H, CH_3); ^{199}Hg NMR (53.51MHz, D_2O, pD 4.0, δ in ppm): -1948; elemental analysis calc. (%) for $C_{14}H_{14}HgN_8O_6$ (M = 484.91g/mol): C 28.5, H 2.4, N 19.0; found: C 28.3, H 2.6, N 19.0.

1-Deazapurine-N9(N7)-β(α)-[2´-deoxy-3´,5´-di-O-(p-toluoyl)-ribonucleoside] (26 and 27)

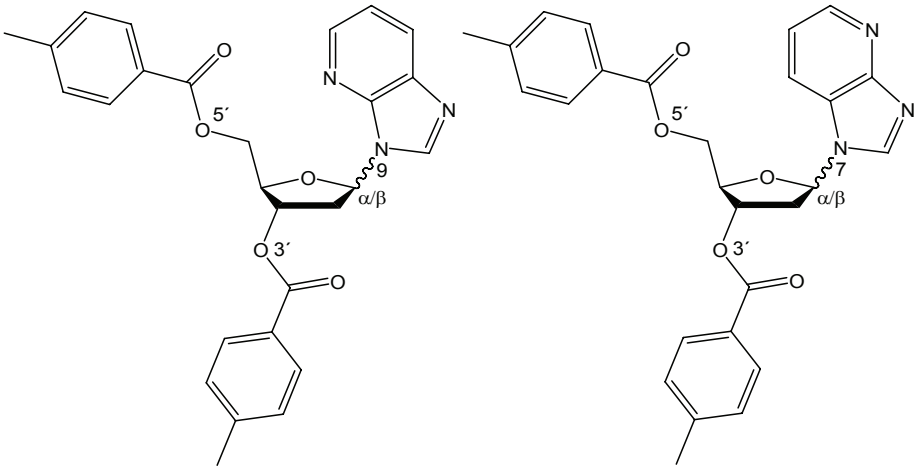

In a 250ml round bottom flask 1.97g (16.6mmol) 1-deazapurine are added to 211ml dry CH_3CN and stirred at r.t. To the yellow suspension 857mg (21.4mmol) NaH (60% in oil) are added and the reaction mixture is stirred for 30min at r.t. Now the cloudy white/yellow suspension is cooled down to 0°C and 8.25g (21.2mmol) Hoffer´s chlorosugar are added in portions within one hour. The suspension is stirred for three hours at 0°C and then the solvent is evaporated. The oily suspension is purified by flash chromatography over silica gel (25 x 2.5cm, EtOAc (20) : CH_3OH (1) : $CHCl_3$ (3)) to give 4.10g (8.70mmol) 1-deazapurine-N9-β(α)-[2´-deoxy-3´,5´-di-O-(p-toluoyl)-ribonucleoside] (53%, ref.: 48%)[113] and 2.00g (4.24mmol) 1-deazapurine-N7-β(α)-[2´-deoxy-3´,5´-di-O(p-toluoyl)-ribonucleoside] (26%, ref.: 29%)[113](overall yield: 79%, ref.: 77%)[113]; ^{1}H-NMR (200MHz, $CDCl_3$/TMS, δ in ppm) 1-deazapurine-N9-β(α)-[2´-deoxy-3´,5´-di-O-(p-toluoyl)-ribonucleoside]: 8.46 (s, 1H (only alpha), H8), 8.40 (8.40) (dd, 1H, H2), 8.25 (s, 1H (only beta), H8), 8.08 (8.11) (dd, 1H, H6), 8.02-7.89 (8.02-7.89)

(m, 4H (alpha 3H), p-Tol), 7.61 (m, 1H (only alpha), p-Tol), 7.34-7.24 (7.34-7.24) (m, 4H, p-Tol), 7.21 (7.21) (dd, 1H, H1), 6.69 (6.78) (pt, 1H, H1´), 5.83 (5.73) (m, 1H, H3´), (4.93) (m, 1H (only alpha), H4´), 4.75-4.62 (4.75-4.62) (m, 1H (only beta), H4´; 2H, H5 and H5´), 3.2-2.8 (3.2-2.8) (m, 2H, H2´ and H2´´), 2.46 and 2.43 (2.44 and 2.41) (2 x s, 2 x 3H, 2 x p-Tol C$\underline{H}_3$); ^{1}H-NMR (200MHz, $CDCl_3$/TMS, δ in ppm) 1-deazapurine-N7-β(α)-[2´-deoxy-3´,5´-di-O-(p-toluoyl)-ribonucleoside]: 8.56 (8.61) (dd, 1H, H2), 8.46 (s, 1H (only alpha), H8), 8.32 (s, 1H (only beta), H8), 8.04-7.91 (8.04-7.91) (m, 1H, H6), 8.00-7.84 (8.00-7.84) (m, 4H (alpha 3H), p-Tol), (7.74) (m, 1H (only alpha), p-Tol), 7.33-7.19 (7.33-7.19) (m, 4H, p-Tol), 7.06 (7.21) (dd, 1H, H1), 6.38 (6.47) (pt, 1H, H1´), 5.74 (5.74) (m, 1H, H3´), 4.80-4.60 (4.80-4.60) (m, 1H, H4´; 2H, H5 and H5´), 3.2-2.7 (3.2-2.7) (m, 2H, H2´ and H2´´), 2.45 and 2.42 (2.43 and 2.40) (2 x s, 2 x 3H, 2 x p-Tol C$\underline{H}_3$); elemental analysis calc. (%) for $C_{27}H_{25}N_3O_5$ (α and β) (M = 471.50g/mol); C 68.8, H 5.4, N 8.9; found: C 68.1, H 6.1, N 8.1.

1-Deazapurine-N9-β(α)-2´-deoxyribonucleoside (28b and 28a)

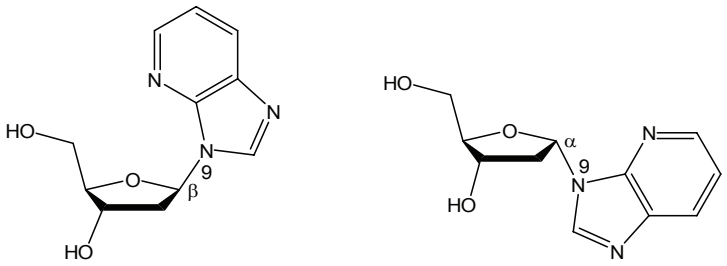

In a 250ml round bottom flask 4.1g (8.7mmol) 1-deazapurine-N9-β(α)-[2´-deoxy-3´,5´-di-O-(p-toluoyl)-ribonucleoside] are dissolved in 10ml CH_3OH and under stirring and at r.t. 65ml of a saturated NH_3/CH_3OH solution are added. The yellow solution is stirred and the reaction is monitored by TLC. After 92h and 15min the solvent is evaporated off. The oily suspension is purified by flash chromatography over silica gel (40 x 7cm, CH_2Cl_2 (9) : CH_3OH (1)) to give 920mg (3.9mmol) 1-deazapurine-N9-β-2´-deoxyribonucleoside (45%, ref.: 90%)[113] and 240mg (1.0mmol) α/β (12%) and 560mg (2.4mmol) 1-deazapurine-N9-α-2´-deoxyribonucleoside (27%) (overall yield: 84%); ^{1}H-NMR (200MHz, D_2O/TSP, pD 5.8, δ in ppm) 1-deazapurine-N9-β-2´-deoxyribonucleoside: 8.54 (s, 1H, H8), 8.36 (d, 1H, H2), 8.14 (d, 1H, H6), 7.41 (dd, 1H, H1), 6.59 (pt, 1H, H1´), 4.67 (m, 1H, H3´), 4.21 (m, 1H, H4´), 3.82 (m, 2H, H5´ and

H5´´), 2.97-2.51 (m, 2H, H2´ and H2´´); ^{1}H-NMR (200MHz, D_2O/TSP, pD 6.5, δ in ppm) 1-deazapurine-N9-α-2´-deoxyribonucleoside: 8.63 (s, 1H, H8), 8.40 (d, 1H, H2), 8.18 (d, 1H, H6), 7.44 (dd, 1H, H1), 6.60 (pt, 1H, H1´), 4.56 (m, 1H, H3´), 4.39 (m, 1H, H4´), 3.73 (m, 2H, H5´ and H5´´), 2.98 and 2.62 (m, 2H, H2´ and H2´´); elemental analysis calc. (%) for $C_{11}H_{13}N_3O_3$ (β) (M = 235.24g/mol): C 56.2, H 5.6, N 17.9; found: C 56.3, H, 5.5; N, 18.2; FAB-MS calc. value (M/Z): 236.1035; found for β: 236.1056.

1-Deazapurine-N7-β(α)-2´-deoxyribonucleoside (29b and 29a)

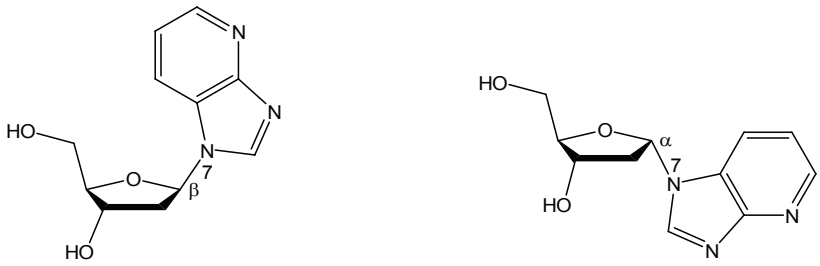

In a 100ml round bottom flask 2.0g (4.2mmol) 1-deazapurine-N7-β(α)-[2´-deoxy-3´,5´-di-O-(p-toluoyl)-ribonucleoside] are dissolved in 25ml CH_3OH and while stirring 55ml of a saturated NH_3/CH_3OH solution are added. The reaction is monitored by TLC (CH_2Cl_2 (9) : CH_3OH (1)). The yellow solution is stirred for 88h 35min and evaporated to dryness. The yellowish foam gets purified by flash chromatography over silica gel (20 x 2.5cm, CH_2Cl_2 (8) : CH_3OH (2) : Et_3N (1)) to give 419mg (1.78mmol) 1-deazapurine-N7-β-2´-deoxyribonucleoside (42%) and 315mg (1.34mmol) 1-deazapurine-N7-α-2´-deoxyribonucleoside (32%) (overall yield: 74%, ref.: 72%); ^{1}H-NMR (200MHz, D_2O/TSP, pD 5.0, δ in ppm) 1-deazapurine-N7-β(α)-2´-deoxyribonucleoside: 8.65 (8.60) (s, 1H, H8), 8.43 (8.43) (dd, 1H, H2), 8.16 (8.12) (m, 1H, H6), 7.39 (7.39) (dd, 1H, H1), 6.47 (6.47) (pt, 1H, H1´), 4.57 (4.65) (dt, 1H, H3´), 4.32 (4.15) (dt, 1H, H4´), 3.79 (3.79) (ddd, 2H, H5 and H5´), 2.90-2.54 (3.00-2.64) (m, 2H, H2´ and H2´´); FAB-MS calc. (M/Z): 236.1035; found for α and β: 236.1053.

1-Deazapurine-N9-β-[2´-deoxy-5´-O-(4,4´-dimethoxytrityl)-ribonucleoside]•0.5H_2O (31)

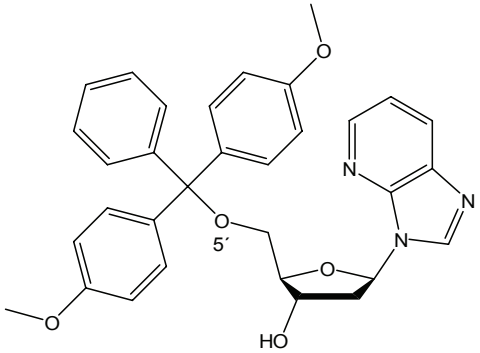

In a 50ml round bottom flask 499mg (2.12mmol) 1-deazapurine-N9-β-2´-deoxyribonucleoside are dissolved in 27.5ml dry pyridine under argon atmosphere. To the slightly yellow solution 1.37g (4.04mmol) of DMTr-Cl and a catalytical amount of DMAP are added and the orange solution is stirred for four hours at r.t. under argon atmosphere. Over the time a little bit of solid (pyridinium chloride) falls out. Then the reaction mixture is quenched by adding 41.0ml $NaHCO_3$ solution (5%) and the resulting orange solution with a white solid is extracted three times with CH_2Cl_2. The organic phase is dried over Na_2SO_4 for two hours, filtered and evaporated. The yellowish foam is purified by flash chromatography over silica gel (33 x 2.5cm, CH_2Cl_2 (95) : CH_3OH (5)) to give 729mg (1.36mmol) 1-deazapurine-N9-β-[2´-deoxy-5´-O-(4,4´-dimethoxytrityl)-ribonucleoside] as a white solid (63%); ^{1}H-NMR (200MHz, $CDCl_3$/TSP, δ in ppm): 8.39 (dd, 1H, H2), 8.36 (s, 1H, H8), 8.17 (dd, 1H, H6), 7.34 (dd, 1H, H1), 7.31-7.25 (m, 5H, $(CH_3O)_2$Tr), 7.21-7.14 (m, 4H, $(CH_3O)_2$Tr), 6.87-6.79 (m, 4H, $(CH_3O)_2$Tr), 6.46 (dd, 1H, H1´), 4.84 (m, 1H, H3´), 4.25 (dt, 1H, H4´), 3.80 (2 x s, 2 x 3H, Tr-$(OCH_3)_2$), 3.81-4.01 (m, 2H, H5´ and H5´´), 3.25-3.11 and 2.43-2.32 (m, 2H, H2´ and H2´´); elemental analysis calc. (%) for $C_{32}H_{31}N_3O_5$•0.5H_2O (M = 547.70g/mol): C 70.3, H 5.9, N, 7.7; found: C 70.4, H 5.6, N 7.6; FAB-MS calc. (M/Z): 538.2342; found: 538.2370.

1-Deazapurine-N7-β-[2´-deoxy-5´-O-(4,4´-dimethoxytrityl)-ribonucleoside] (32)

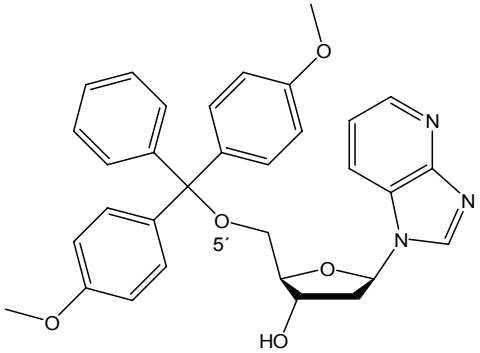

In a 50ml round bottom flask and under argon atmosphere 201mg (0.85mmol) 1-deazapurine-N7-β-2´-deoxyribonucleoside are dissolved in 11.0ml dry pyridine. Now 576mg (1.70mmol) DMTr-Cl and a catalytical amount of DMAP are added and the slightly yellow solution is stirred for three hours. Then the reaction is quenched by 16.0ml $NaHCO_3$ solution (5%) and the solution is stirred for a further 20min. Extraction with CH_2Cl_2 (1 x 50ml and 2 x 30ml), drying of the organic phase over Na_2SO_4 and evaporation give a yellowish foam, which gets purified by flash chromatography over silica gel (15 x 2.5cm, CH_2Cl_2 (95) : CH_3OH (5)) to give 290mg (0.54mmol) of 1-deazapurine-N7-β-[2´-deoxy-5´-O-(4,4´-dimethoxytrityl)-ribonucleoside] as a white foam (63.5%). ^{1}H-NMR (400MHz, $CDCl_3$/TMS, δ in ppm): 8.40 (dd, 1H, H2), 8.35 (s, 1H, H8), 7.98 (dd, 1H, H6), 7.33-7.08 (m, 9H, $(CH_3O)_2\underline{Tr}$), 6.96 (dd, 1H, H1), 6.68 (m, 4H, $(CH_3O)_2\underline{Tr}$), 6.40 (pt, 1H, H1´), 4.87 (m, 1H, H3´), 4.23 (dt, 1H, H4´), 3.67 (2 x s, 2 x 3H, Tr-(OC$\underline{H_3}$)$_2$), 3.35 (m, 2H, H5´ and H5´´), 2.57-2.78 (m, 2H, H2´ and H2´´); FAB-MS calc. (M/Z): 538.2342; found: 538.2356.

1-Deazapurine-N9-β-[2´-deoxy-3´-O-(2-cyanoethyl)-N,N-diisopropylphosphoramidite-5´-O-(4,4´-dimethoxytrityl)-ribonucleoside] (33)

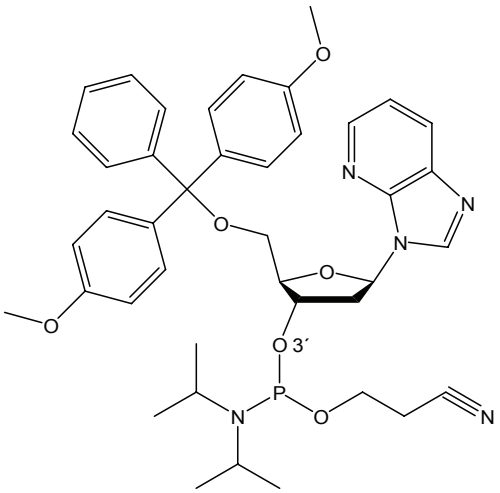

In a 100ml round bottom flask 290mg (529µmol) 1-deazapurine-N9-β-[2´-deoxy-5´-O-(4,4´-dimethoxytrityl)-ribonucleoside] are dissolved in 19.3ml dry CH_2Cl_2 under an argon atmosphere. Now, 710µl (4.08mmol) $(i\text{-}Pr)_2EtN$ and 180µl (809µmol) chloro-(2-cyanoethoxy)-(diisopropylamino)-phosphane are added and the reaction mixture is stirred for one hour at r.t. The solution is quenched with 38.0ml saturated $NaHCO_3$ solution and extracted with CH_2Cl_2. The organic solvents are dried over Na_2SO_4 for one hour, filtered and evaporated. The product was not purified further and the yield was quantitative. Yellow syrup of 1-deazapurine-N9-β-[2´-deoxy-3´-O-(2-cyanoethyl)-N,N-diisopropylphosphoramidite-5´-O-(4,4´-dimethoxytrityl)-ribo-nucleoside]; ^{1}H-NMR (200MHz, $CDCl_3$/TMS, δ in ppm): 8.48 (s, 1H, H8), 8.26 (d, 1H, H2), 7.99 (d, 1H, H6), 7.37-7.14 (m, 9H, $(CH_3O)_2\underline{Tr}$; 1H, H1), 6.71 (m, 4H, $(CH_3O)_2\underline{Tr}$), 6.52 (pt, 1H, H1´), 4.71 (m, 1H, H3´), 4.24 (m, 1H, H4´), 3.79-3.26 (m, 2H, H5´ and H5´´) 3.70 (2 x s, 2 x 3H, 2 x Tr-OC$\underline{H}_3$), 2.93-2.37 (m, 2H, H2´ and H2´´; 4H CH_2CH_2CN), 1.23-1.03 (m, 14H, 2 x $(CH_3)_2CH$); ^{31}P-NMR (80.98MHz, $CDCl_3$, δ in ppm): 149.8 and 149.7 (product), 15.3 ((2-cyanoethoxy)-(diisopropylamino)-phosphane oxide); FAB-MS calc. (M/Z): 738.3420; found: 738.3430.

1-Deazapurine-N7-β-[2´-deoxy-3´-O-(2-cyanoethyl)-N,N-diisopropyl-phosphoramidite-5´-O-(4,4´-dimethoxytrityl)-ribonucleoside] (34)

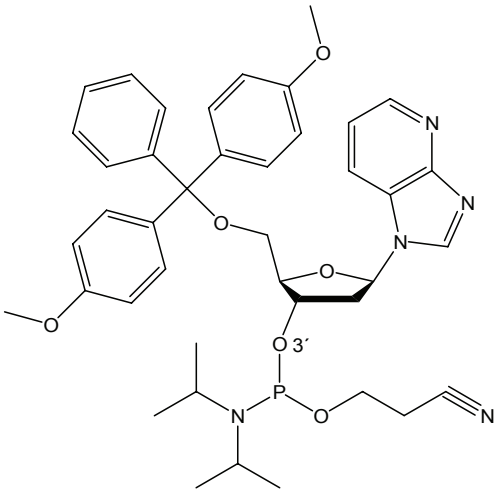

In a 50ml round bottom flask and under argon atmosphere 180mg (340µmol) 1-deazapurine-N7-β-[2´-deoxy-5´-O-(4,4´-dimethoxytrityl)-ribonucleoside] are dissolved in 12.0ml dry CH_2Cl_2. Now, 441µl (2.53mmol) $(i\text{-}Pr)_2EtN$ and 112µl (0.50mmol) chloro-(2-cyanoethoxy)-(diisopropylamino)-phosphane are added and the solution becomes slightly yellow. The solution is stirred for one hour and then diluted with 40.0ml EtOAc and quenched with 24.0ml saturated $NaHCO_3$ solution. After addition of 50.0ml CH_2Cl_2 and 20.0ml H_2O the organic phase is taken off, dried over Na_2SO_4 and evaporated. The yellow-brown oil is not worked up further. The yield of the product is calculated through the ratio of product to side product in the NMR spectra and the mean molar mass. The side product is the hydrolysed protecting group that does not interfere with the synthesis in the DNA-synthesizer.

Raw mass = 290.0mg

Ratio: product (0.59) : side product (0.41)

Mean molar mass = molar mass (product) x 0.59 + molar mass (side product) x 0.41

⇒ Mean molar mass = 534.80g/mol

⇒ Medium moles = 553µmol

Mass (product) = medium moles x molar mass (product) x ratio (product)

⇒ Mass (product) = 241mg (326µmol) (97%)

^{1}H-NMR (200MHz, $CDCl_3$/TMS, δ in ppm): 8.55 (d, 1H, H2), 8.26 (s, 1H, H8), 7.93 (d, 1H, H6), 7.26 (m, 9H, $(CH_3O)_2\underline{Tr}$), 6.99 (m, 1H, H1), 6.75 (m, 4H, $(CH_3O)_2\underline{Tr}$), 6.29 (pt, 1H, H1´), 4.73 (m, 1H, H3´), 4.29 (m, 1H, H4´), 3.80-3.30 (m, 2H, H5´ and H5´´)

3.77 (2 x s, 2 x 3H, Tr-OC$\underline{H}_3$), 2.80-2.50 (m, 2H, H2´ and H2´´; 4H, CH_2CH_2CN), 1.30-1.08 (m, 14H, 2 x $(CH_3)_2CH$); ^{31}P-NMR (80.98MHz, $CDCl_3$, δ in ppm): 149.8 and 149.7 (product), 15.3 ((2-cyanoethoxy)-(diisopropylamino)-phosphane oxide); FAB-MS calc. (M/Z): 738.3420; found: 738.3435.

Oligonucleotides (X = 1-deazapurine-N7 nucleoside)

(**a**) 5´-d(AAA AAA A**XX** **X**TT TTT TT)

(**b**) 5´-d(AAA AAA A**XX** **XX**T TTT TTT)

(**c**) 5´-d(AAA AAA A**X**A AAA AAA)

(**d**) 5´-d(TTT TTT T**X**T TTT TTT)

The 290.0mg (240.6mg / 0.326mmol product) 1-deazapurine-N7-β-[2´-deoxy-3´-O-(2-cyanoethyl)-N,N-diisopropylphosphoramidite-5´-O-(4,4´-dimethoxy-trityl)-ribo-nucleoside] are dissolved in 3.26ml dry CH_3CN to give a 100mM solution that can be used in the oligonucleotide synthesis at the DNA-synthesizer.

(**a**) 5´-d(AAA AAA A**XX** **X**TT TTT TT)

HPLC Column: ion-exchange column

Temperature: 50°C

Time (min)	Flow (ml min^{-1})	% of solvent A	% of solvent B
0.0	1.50	100	0
5.0	1.50	100	0
20.0	1.50	83	17
30.0	1.50	76	24
40.0	1.50	0	100
45.0	1.50	100	0
50.0	0.01	100	0

HPLC-method

One product was collected and desalted (2 x NAP™ 10 column).

Peak 1 at T_1 = 23.0-25.0min

After the desalting the oligonucleotide (peak 1) is lyophilised, dissolved in 1000µl and 90µl are diluted to a volume of 900µl and the absorption spectrum is taken.

$E_{(260nm)} = c * d * \varepsilon$, where $\varepsilon = f * \Sigma n_i \varepsilon_i$ (for further explanation see UV-Vis spectroscopy)

$E_{(260nm)}$ = 0.06347

Therefore concentration c (900µl) = 0.386µmol/l

Overall concentration c (1000µl) = 3.86µmol/l ⇒ Yield = 0.39%

(**b**) 5´-d(AAA AAA A**XX XX**T TTT TTT)

No further purification steps where done until now.

(**c**) 5´-d(AAA AAA A**X**A AAA AAA)

HPLC Column: reversed phase column

Temperature: 50°C

Time (min)	**Flow (ml min^{-1})**	**% of solvent A**	**% of solvent B**
0.0	1.50	100	0
25.0	1.50	90	10
30.0	1.50	50	50
35.0	1.50	50	50
40.0	1.50	100	0
41.0	0.01	100	0

HPLC-method

Three products were collected.

Peak 1 at T_1 = 10.0-11.0min

Peak 2 at T_2 = 18.8-20.5min

Peak 3 at T_3 = 28.9-30.1min

Then, for peak 1 and 2, the DMT-protecting group at the 5´-end is taken off by leaving the oligonucleotides in 2ml acetic acid (80%) for half an hour each. The acetic acid (80%) is taken off under vacuum.

Product 2 is purified further.

HPLC Column: reversed phase column

Temperature: 50°C

Time (min)	**Flow (ml min^{-1})**	**% of solvent A**	**% of solvent B**
0.0	1.00	100	0
25.0	1.00	90	10
30.0	1.00	50	50
31.0	1.00	50	50
35.0	1.00	100	0
36.0	0.01	100	0

HPLC-method

One product was collected and desalted (1 x NAP™ 10 column).

Peak 1 at T_1 = 21.2-22.3min

After the desalting the oligonucleotide (peak 1) is lyophilised, dissolved in 1000µl and 100µl are diluted to a volume of 900µl and the absorption spectrum is taken. After calculating the concentration and measuring MALDI-TOF spectra, none of the peaks showed a signal for any kind of oligonucleotide.

(**d**) 5´-d(TTT TTT T**X**T TTT TTT)

HPLC Column: reversed phase column

Temperature: 50°C

Time (min)	**Flow (ml min^{-1})**	**% of solvent A**	**% of solvent B**
0.0	1.00	100	0
25.0	1.00	81	19
30.0	1.00	60	40
35.0	0.10	100	0
36.0	0.10	100	0

HPLC-method

One product was collected.

Peak 1 at T_1 = 16.0-16.5min

Then the DMT-protecting group at the 5´-end is taken off by leaving the oligonucleotide in 1ml acetic acid (80%) for half an hour. The acetic acid (80%) is taken off under vacuum.

HPLC Column: reversed phase column

Temperature: 50°C

Time (min)	**Flow (ml min^{-1})**	**% of solvent A**	**% of solvent B**
0.0	1.00	100	0
25.0	1.00	88	12
30.0	1.00	60	40
35.0	1.00	100	0
36.0	0.01	100	0

HPLC-method

One product was collected and desalted (1 x NAP™ 5 column).

Peak 1 at T_1 = 23.0-23.6min

After the desalting the oligonucleotide (peak 1) is lyophilised, dissolved in 1000µl and 900µl are taken off and the absorption spectrum is measured. After calculating the concentration and measuring MALDI-TOF spectra, none of the peaks showed a signal for any kind of oligonucleotide.

Oligonucleotides (Y = 1-deazapurine-N9 nucleoside)

(e) 5´-d(C**YY YY**G)

The 1-deazapurine-N9-β-[2´-deoxy-3´-O-(2-cyanoethyl)-N,N-diisopropylphosphor-amidite-5´-O-(4,4´-dimethoxy-trityl)-ribonucleoside] is purified by flash chromatography over aluminium oxide (25 x 2.5cm, CH_2Cl_2 (1) : EtOAc (1)) to give 166mg (226µmol) clean 1-deazapurine-N9-β-[2´-deoxy-3´-O-(2-cyanoethyl)-N,N-diisopropylphosphor-amidite-5´-O-(4,4´-dimethoxy-trityl)-ribonucleoside], which is dissolved in 3.32ml dry CH_3CN to give a 100mM solution that can be used in the oligonucleotide synthesis at the DNA-synthesizer.

HPLC column: ion-exchange column

Temperature: r.t.

Time (min)	Flow (ml min^{-1})	% of solvent A	% of solvent B
0.0	1.50	100	0
10.0	1.50	100	0
60.0	1.50	75	25
65.0	1.50	0	100
70.0	1.50	0	100
71.0	1.50	100	0
81.0	1.50	100	0
81.5	0.01	100	0

HPLC-method

One product was collected and desalted twice (2 x OASIS®).

Peak 1 at T_1 = 47.0-48.0min

After the desalting the oligonucleotide is lyophilised, dissolved in 900 µl and the absorption spectrum is taken.

$E_{(260nm)} = c * d * \varepsilon$, where $\varepsilon = f * \Sigma n_i \varepsilon_i$ (for further explanation see UV-Vis spectroscopy)

$E_{(260nm)} = 0.376$

Therefore concentration c (900µl) = 6.51µmol/l ⇒ Yield = 0.59%

(**f**) 5´-d(CGC G**Y**A T**Y**C GCG)

(**g**) 5´-d(AAA AAA A**Y**A AAA AAA)

(**h**) 5´-d(TTT TTT T**Y**T TTT TTT)

(**i**) 5´-d(**YYY YYY YYY YYY YYY Y**A)

441mg (390mg / 529µmol product) 1-deazapurine-N9-β-[2´-deoxy-3´-O-(2-cyanoethyl)-N,N-diisopropylphosphoramidite-5´-O-(4,4´-dimethoxy-trityl)-ribo-nucleoside] are dissolved in 5.29ml dry CH_3CN to give a 100mM solution that can be used in the oligonucleotide synthesis at the DNA-synthesizer.

(**f**) 5´-d(CGC G**Y**A T**Y**C GCG)

HPLC Column: ion-exchange column

Temperature: 50°C

Time (min)	**Flow (ml min^{-1})**	**% of solvent A**	**% of solvent B**
0.0	1.50	100	0
5.0	1.50	100	0
35.0	1.50	71	29
40.0	1.50	0	100
46.0	1.50	100	0
51.0	1.50	100	0
51.5	0.01	100	0

HPLC-method

One product was collected and desalted (2 x NAP™ 10 column).

Peak 1 at T_1 = 24.7-25.0min

After the desalting the oligonucleotide (peak 1) is lyophilised, dissolved in 1000µl and 10µl are diluted to a volume of 900µl and the absorption spectrum is taken.

$E_{(260nm)} = c * d * \varepsilon$, where $\varepsilon = f * \Sigma n_i \varepsilon_i$ (for further explanation see UV-Vis spectroscopy)

$E_{(260nm)}$ = 0.110

Therefore concentration c (900µl) = 0.99µmol/l ⇒ Yield = 8.91%

MALDI-TOF

Value calc. (M/Z) for $(MH)^+$ = 3623.7; found: 3622.6.

Also peaks at larger (M/Z) values were found, which are probably due to an incomplete deprotection of the oligonucleotide.

(**g**) 5′-d(AAA AAA A**Y**A AAA AAA)

HPLC Column: ion-exchange column

Temperature: 50°C

Time (min)	**Flow (ml min^{-1})**	**% of solvent A**	**% of solvent B**
0.0	1.50	90	10
5.0	1.50	90	10
20.0	1.50	75	25
25.0	1.50	0	100
28.0	1.50	0	100
30.0	1.50	90	10
35.0	1.50	90	10
35.5	0.01	90	10

HPLC-method

One product was collected and desalted (2 x NAP™ 10 column).

Peak 1 at T_1 = 16.0-18.0min

After the desalting the oligonucleotide (peak 1) is lyophilised, dissolved in 1000µl and 10µl are diluted to a volume of 900µl and the absorption spectrum is taken.

$E_{(260nm)} = c * d * \varepsilon$, where $\varepsilon = f * \Sigma n_i \varepsilon_i$ (for further explanation see UV-Vis spectroscopy)

$E_{(260nm)} = 0.138$

Therefore concentration c (900µl) = 0.674µmol/l $\Rightarrow$ Yield = 6.07%

MALDI-TOF

Value calc. (M/Z) for $(MH)^+$ = 4494.7; found: 4489.4.

(**h**) 5´-d(TTT TTT T**Y**T TTT TTT)

HPLC Column: ion-exchange column

Temperature: 50°C

Time (min)	**Flow (ml min^{-1})**	**% of solvent A**	**% of solvent B**
0.0	1.50	100	0
5.0	1.50	100	0
35.0	1.50	50	50
40.0	1.50	0	100
41.0	1.50	100	0
51.0	1.50	100	0
51.5	0.01	100	0

HPLC-method

One product was collected and desalted (2 x NAP™ 10 column).

Peak 1 at T_1 = 16.8-17.7min

After the desalting the oligonucleotide (peak 1) is lyophilised, dissolved in 1000µl and 10µl are diluted to a volume of 900µl and the absorption spectrum is taken.

$E_{(260nm)} = c * d * \varepsilon$, where $\varepsilon = f * \Sigma n_i \varepsilon_i$ (for further explanation see UV-Vis spectroscopy)

$E_{(260nm)}$ = 0.225

Therefore concentration c (900µl) = 1.862µmol/l ⇒ Yield = 16.75%

MALDI-TOF

Value calc. (M/Z) for $(MH)^+$ = 4620.9; found: 4618.7.

(**i**) $^{5'}$-d(**YYY YYY YYY YYY YYY Y**A)

HPLC Column: ion-exchange column

Temperature: 50°C

Time (min)	**Flow (ml min^{-1})**	**% of solvent A**	**% of solvent B**
0.0	1.50	100	0
5.0	1.50	100	0
20.0	1.50	83	17
45.0	1.50	66	34
55.0	1.50	0	100
60.0	1.50	100	0
65.0	1.50	100	0
66.0	0.01	100	0

HPLC-method

One product was collected and desalted (2 x NAP™ 10 column).

Peak 1 at T_1 = 34.0-36.0min

After the desalting the oligonucleotide (peak 1) is lyophilised, dissolved in 1000µl and 100µl are diluted to a volume of 900µl and the absorption spectrum is taken.

$E_{(260nm)} = c * d * \varepsilon$, where $\varepsilon = f * \Sigma n_i \varepsilon_i$ (for further explanation see UV-Vis spectroscopy)

$E_{(260nm)}$ = 0.185

Therefore concentration c (900µl) = 1.028µmol/l ⇒ Yield = 0.93%

MALDI-TOF

Value calc. (M/Z) for $(MH)^+$ = 5006.9; found: 5007.5.

1-Deaza-N3-oxidepurine•2H_2O (35)

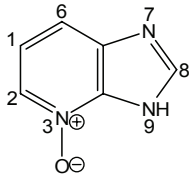

To a mixture of 1.60g (13.4mmol) 1-deazapurine and 12.0ml acetic acid (98-100 %), 2.45ml H_2O_2 (30%) are added and the solution is stirred for 24h at 80°C. The solution is cooled down to r.t., further 2.45ml H_2O_2 (30%) are added and the solution is stirred at 80°C for another 24h. Upon cooling down to r.t., a yellow solid precipitates. The solid is filtered off and dried at 40°C. On evaporation of more solvent, further solid precipitates, giving in total 1.77g (10.3mmol) of 1-deaza-N3-oxidepurine•2H_2O (77%); ^{1}H-NMR (200MHz, DMSO-d_6, δ in ppm): 8.40 (s, 1H, H8), 8.18 (dd, 1H, H2), 7.60 (dd, 1H, H6), 7.20 (dd, 1H, H1); elemental analysis calc. (%) for $C_6H_5N_3O$•2H_2O (M = 171.15g/mol): C 42.1, H 5.3, N 24.6; found: C 42.2, H 4.9, N 24.8.

1-Deaza-N3-oxide-6-nitropurine (36)

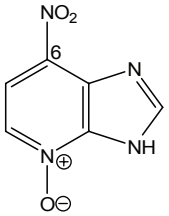

A solution of 1.0g (5.8mmol) 1-deaza-N3-oxidepurine•2H_2O in 7.8ml of trifluoroacetic acid is cooled to 0°C and in a dropwise fashion, 4.3ml HNO_3 (100%) are added in the duration of an hour. The mixture is stirred at 90°C for four hours, cooled and poured into a round bottom flask with crushed ice. Neutralisation is done with concentrated NH_3, while keeping the temperature below 30°C, which is essential for high yields. At pH 5 a yellow solid starts to precipitate. At pH 7 the solid is filtered off, washed with ice water and dried at 40°C to give 990mg (5.5mmol) of 1-deaza-N3-oxide-6-nitropurine as a yellow solid (95%, ref.: 75%)[106]; ^{1}H-NMR (200MHz, DMSO-d_6, δ in ppm): 14.02 (br, 1H, $N_{7/9}$H), 8.61 (s, 1H, H8), 8.33 (d, 1H, H1), 8.09 (d, 1H, H2); elemental analysis calc. (%) for $C_6H_4N_4O_3$ (180.12g/mol): C 40.0, H 2.2, N 31.1; found: C 35.5, H 2.3, N 28.3.

1-Deaza-6-nitropurine (37)

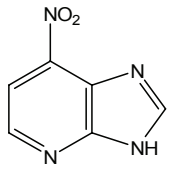

This is a slightly modified version of the synthesis in the literature.[156]

A solution of 1.3g (7.2mmol) 1-deaza-N3-oxide-6-nitropurine in 25ml dry CH_3CN is stirred and over the duration of one hour 5.5ml fresh PCl_3 are added drop wise, while cooling the round bottom flask with ice water. The produced suspension is refluxed for two hours at 80 °C and then cooled down to r.t. The round bottom flask is allowed to stand in the fume hood, so that the fumes can steam off. After roughly 15min the solid is filtered off and washed with Et_2O and saturated Na_2CO_3 solution (careful, vigorous reaction! do not use vast amounts, otherwise loss in yield!) and dried at 40°C to give 1-deaza-6-nitropurine as a yellow-brownish solid. After re-crystallization in water 610mg yellow blocks are found (52%, ref.: 82%)[156]; ^{1}H-NMR (200MHz, DMSO-d_6, δ in ppm): 13.69 (br, 1H, $N_{7/9}H$), 8.78 (s, 1H, H8), 8.70 (d, 1H, H1), 8.01 (d, 1H, H2); elemental analysis calc. (%) for $C_6H_4N_4O_2$ (M = 164.12g/mol); C 43.9, H 2.5, N 34.1; found: C 43.6, H 2.4, N 34.8.

1-Deaza-6-nitropurine-N9-β(a)-[2´-deoxy-3´,5´-di-O-(p-toluoyl)-ribonucleoside] (38b and 38a)

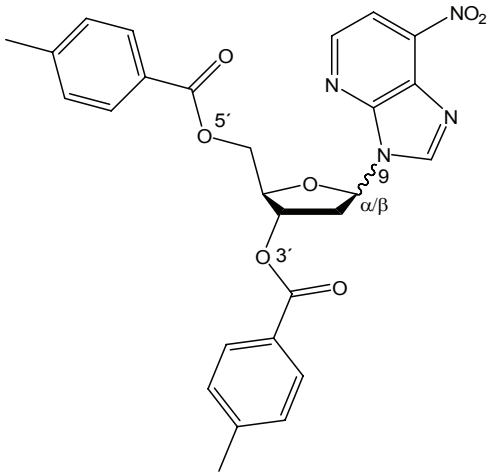

This is a slightly modified version of the synthesis in the literature.[159]

A suspension of 978mg (5.96mmol) 1-deaza-6-nitropurine in 20.5ml dry CH_3CN is stirred under argon. After addition of 260mg (6.50mmol) NaH (60% in oil) the reaction mixture is stirred for 30min at r.t. and under argon. Then the reaction mixture is cooled to 0°C and over the duration of 15min 3.50g (9.00mmol) Hoffer´s chlorosugar are added in small portions. For further three hours the reaction mixture is stirred at 0°C under argon. The insoluble material is filtered off (mainly Na salt) and the solution evaporated. The oily residue is purified by flash chromatography over silica gel (25 x 2.5cm, n-hexane (100) : EtOAc (60) : CH_2Cl_2 (4)) to give 1.26mg (2.44mmol) 1-deaza-6-nitropurine-N9-β-[2´-deoxy-3´,5´-di-O-(p-toluoyl)-ribonucleoside] (41% beta, ref.: 60% beta)[159] and 227mg (0.44mmol) 1-deaza-6-nitropurine-N9-α-[2´-deoxy-3´,5´-di-O-(p-toluoyl)-ribonucleoside] (7%) and 138.0mg (0.267mmol) α/β-mixture (4%) (overall yield: 52%); ^{1}H-NMR (200MHz, $CDCl_3$/TSP, δ in ppm) 1-deaza-6-nitropurine-N9-β(α)-[2´-deoxy-3´,5´-di-O-(p-toluoyl)-ribonucleoside]: (8.69) (only alpha, s, 1H, H8), 8.56 (8.57) (d, 1H, H1), 8.50 (only beta, s, 1H, H8), 8.00-7.84 (8.00-7.84) (m, 4H (alpha 3H), p-Tol; d, 1H, H2), (7.58) (only alpha, m, 1H, p-Tol), 7.31-7.14 (7.31-7.14) (m, 4H, p-Tol), 6.69 (6.80) (dd, 1H, H1´), 5.84 (5.73) (m, 1H, H3´), (4.96) (only alpha, m, 1H, H4´), 4.84-4.63 (4.84-4.63) (m, 2H, H5´ and H5´´; only beta, m, 1H, H4´), 3.24-2.85 (3.24-2.85) (m, 2H, H2´ and H2´´), 2.45 and 2.40 (2.43 and 2.39) (2 x s, 2 x 3H, 2 x p-Tol-C$\underline{H_3}$); elemental analysis calc. (%) for $C_{27}H_{24}N_4O_7$ (β) (M = 516.50g/mol): C 62.8, H 4.7, N 10.9; found: C 62.7, H 4.7, N 10.6; FAB-MS calc. (M/Z): 517.1723; found for β: 517.1749.

1-Deaza-6-nitropurine-N9-β-2´-deoxyribonucleoside (39)

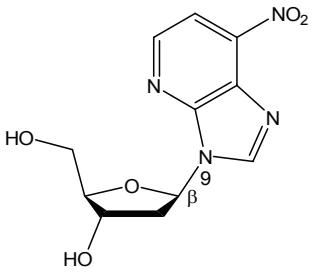

This is a slightly modified version of the synthesis in the literature.[159]

To a round bottom flask with 1.58g (3.06mmol) 1-deaza-6-nitropurine-N9-β-[2´-deoxy-3´,5´-di-O-(p-toluoyl)-ribonucleoside] 50.0ml of a saturated NH_3/CH_3OH

solution are added. Immediately a reddish solution with an oily residue is formed. After 10-15min the oil is gone into the pink solution and a white solid precipitates, which itself dissolves within the next five minutes to then give a yellow solution. The reaction is monitored by TLC. After 10h the reaction is finished and therefore the solution is evaporated to give an orange-reddish oil. The oil is purified by flash chromatography over silica gel (19 x 2.5cm, $CHCl_3$ (88) : CH_3OH (10) : NH_3 (2)) to give 534mg (1.91mmol) 1-deaza-6-nitropurine-N9-β-2´-deoxyribonucleoside (62%, ref.: 55%)[159]; ^{1}H-NMR (200MHz, D_2O/TSP, pD 7.47, δ in ppm): 8.87 (s, 1H, H8), 8.67 (d, 1H, H1), 8.14 (d, 1H, H2), 6.69 (pt, 1H, H1´), 4.69 (m, 1H, H3´), 4.21 (m, 1H, H4´), 3.83 (m, 2H, H5´ and H5´´), 3.02-2.58 (m, 2H, H2´ and H2´´); elemental analysis calc. (%) for $C_{11}H_{12}N_4O_5$ (280.24g/mol); C 47.1, H 4.3, N 20.0; found: C 46.8, H 4.7, N 20.2; FAB-MS calc. (M/Z): 281.0886; found: 281.0876.

1-Deaza-6-aminopurine-N9-β-2´-deoxyribonucleoside (1-Deaza-2´-deoxyadenosine) (40)

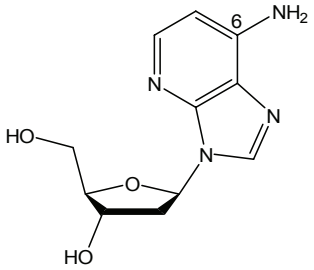

This is a slightly modified version of the synthesis in the literature.[167]

To a solution of 190mg (0.678mmol) 1-deaza-6-nitropurine-N9-β-2´-deoxyribonucleoside in 47.5ml CH_3OH (yellow solution), 3.57ml H_2N-NH_2•H_2O and 1.20g of activated Raney-Nickel are added at r.t. to give a black suspension. After the solution becomes colourless (ca. 90min) the solid is filtered off (Careful, Raney-Nickel ignites immediately up on drying!) and the solution is evaporated to give a yellow oil. Flash chromatography over silica gel (17 x 2.5cm, CH_2Cl_2 (8) : CH_3OH (2)) gives 115mg (0.460mmol) of 1-deaza-6-aminopurine-N9-β-2´-deoxyribonucleoside (68%, ref.: 87%)[167]; ^{1}H NMR (200MHz, D_2O/TSP, pD 9.52, δ in ppm): 8.13 (s, 1H, H8), 7.79 (d, 1H, H2), 6.49 (d, 1H, H1), 6.35 (dd, 1H, H1´), 4.50 (m, 1H, H3´), 4.04 (m, 1H, H4´), 3.65 (m, 2H, H5´ and H5´´), 2.79-2.31 (m, 2H, H2´ and H2´´); elemental analysis

calc. (%) for $C_{11}H_{14}N_4O_3$ (M = 250.25g/mol): C 52.8, H 5.6, N 22.4; found: C 52.4, H 5.6, N 22.7; FAB-MS calc. for (M/Z): 251.1144; found 251.1132.

1-Deaza-(6-benzoylamino)-purine-N9-β-2´-deoxyribonucleoside•H_2O (42)

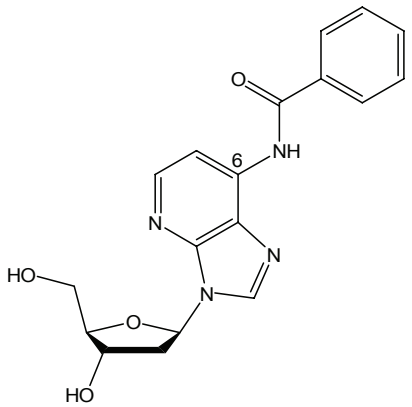

This is a slightly modified version of the synthesis in the literature.[167]

In a round bottom flask 250mg (999µmol) 1-deaza-6-aminopurine-N9-β-2´-deoxyribonucleoside are dried by co-evaporation with dry pyridine (2 x 6ml). The round bottom flask is set under argon and the 1-deaza-6-aminopurine-2´-deoxyribonucleoside is dissolved in 15.0ml dry pyridine. To the slightly yellow solution 642µl (5.06mmol) Me_3SiCl are added and the solution is stirred for 15min at r.t. Then 579µl (4.99mmol) benzoyl chloride are added to the yellow solution and the solution is stirred at r.t. under argon, whereby a white solid (probably pyridinium chloride) falls out after five minutes. After two hours the yellow solution is cooled down to 0°C within 15min and hydrolysed with 1.0ml H_2O. Having stirred the solution for five minutes at 0°C, it is quenched with 2.0ml NH_3 (25%), whereby a solid falls out (NH_4Cl), and stirred for another 30min at 0°C. The solvent is evaporated to give a yellowish oil, which is co-evaporated with toluene and acetone. The oil is dissolved in CH_3OH and purified by flash chromatography over silica gel (26 x 2.5cm, CH_2Cl_2 (9) : CH_3OH (1)) to give 640mg of a mixture of 1-deaza-(6-benzoylamino)-purine-N9-β-2´-deoxyribonucleoside and benzoyl hydroxide. Crystallisation in CH_3OH gives 300mg (806µmol) 1-deaza-(6-benzoylamino)-purine-N9-β-2´-deoxyribonucleoside as colourless crystals (81%, ref.: 77%)[167]; ^{1}H-NMR

(200MHz, DMSO-d_6, δ in ppm): 10.42 (br, 1H, C6-N<u>H</u>), 8.64 (s, 1H, H8), 8.32 (d, 1H, H2), 7.52-8.05 (m, 1H, H1; 4H, Ph), 6.51 (dd, 1H, H1´), 5.34 (t, 1H, C3´-O<u>H</u>), 5.18 (t, 1H, C5´-O<u>H</u>), 4.45 (m, 1H, H3´), 3.91 (m, 1H, H4´), 3.71-3.48 (m, 2H, H5´ and H5´´), 2.88-2.27 (m, 2H, H2´ and H2´´); elemental analysis calc. (%) for $C_{18}H_{18}N_4O_4 \bullet H_2O$ (M = 372.38g/mol): C 58.1, H 5.4, N 15.0; found: C 57.8, H 5.5, N 14.9.

1-Deaza-(6-benzoylamino)-purine-N9-β-[2´-deoxy-5´-O-(4,4´-dimethoxytrityl)-ribonucleoside] (43)

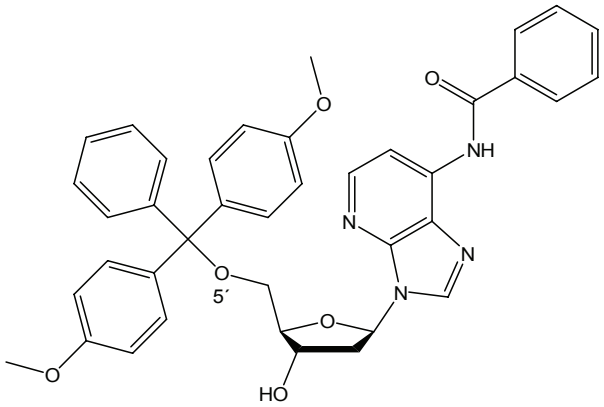

This is a slightly modified version of the synthesis in the literature.[167]

In a 50ml round bottom flask 116mg (312µmol) 1-deaza-(6-benzoylamino)-purine-N9-β-2´-deoxyribonucleoside are dissolved in 4.20ml dry pyridine under argon. To the slightly yellow solution 210mg (620µmol) DMTr-Cl are added and the solution is now stirred for two hours at r.t. The solution is then quenched with $NaHCO_3$ solution (5%) and extracted with 40ml CH_2Cl_2 (3x). The organic phase is dried over Na_2SO_4 and evaporated. The resulting oil is dissolved in CH_2Cl_2 (9) and CH_3OH (1) and purified by flash chromatography over silica gel (33 x 2.5cm , CH_2Cl_2 (95) and CH_3OH (5)) and the product fraction is dissolved in 3.0ml CH_2Cl_2 and poured in 6.0ml of a n-hexane (1) / Et_2O (1) mixture to give 115mg (175µmol) 1-deaza-(6-benzoylamino)-purine-N9-β-[2´-deoxy-5´-O-(4,4´-dimethoxytrityl)-ribonucleoside] as a white solid (56%, ref. 76%)[167]. ^{1}H-NMR (200MHz, DMSO-d_6, δ in ppm): 10.39 (br, 1H, C6-N<u>H</u>), 8.53 (s, 1H, H8), 8.26 (d, 1H, H2), 8.05-6.75 (m, 1H, H1, 4H, Bz; 13H, $(CH_3O)_2$<u>Tr</u>), 6.53 (pt, 1H, H1´), 5.39 (t, 1H, C5´-O<u>H</u>), 4.52 (m, 1H, H3´), 4.01 (m, 1H,

H4´), 3.71 and 3.69 (2 x s, 2 x 3H, 2 x Tr-OC<u>H</u>$_3$), 3.40-3.20 (m, 2H, H5´ and H5´´), 3.03-2.33 (m, 2H, H2´ and H2´´).

1-Deaza-(6-benzoylamino)-purine-N9-β-[2´-deoxy-3´-O-(2-cyanoethyl)-N,N-diisopropylphosphoramidite-5´-O-(4,4´-dimethoxytrityl)-ribo-nucleoside] (44)

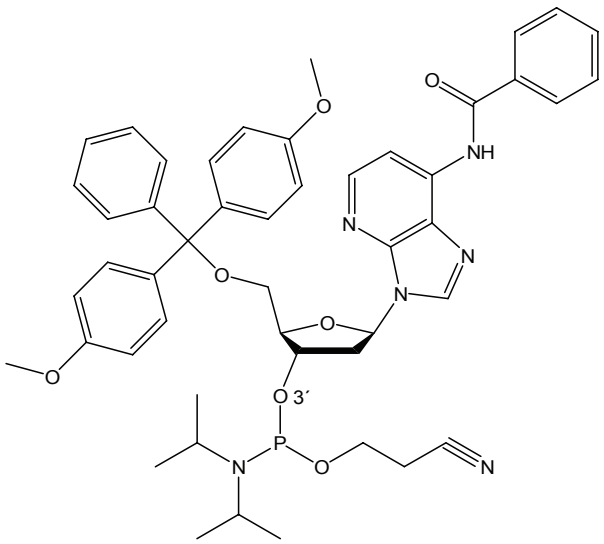

This is a slightly modified version of the synthesis in the literature.[167]

In a 50ml round bottom flask 135mg (206µmol) of 1-deaza-(6-benzoylamino)-purine-N9-β-[2´-deoxy-5´-O-(4,4´-dimethoxytrityl)-ribonucleoside] are dissolved in 4.50ml dry pyridine under argon. To the solution 108µl (633µmol) (i-Pr)$_2$EtN and 135µl (605µmol) chloro-(2-cyanoethoxy)-(diisopropylamino)-phosphane are added at r.t. and the solution is stirred for one hour. Then the solution gets quenched with 4.50ml of $NaHCO_3$ solution (5%), extracted with 10ml CH_2Cl_2 (4x) and the organic phase is dried over Na_2SO_4. The CH_2Cl_2 is evaporated off to give 345mg of a side product to product mixture. The product was not purified further and the yield was quantitative. Yellow-brown syrup of 1-deaza-(6-benzoylamino)-purine-N9-β-[2´-deoxy-3´-O-(2-cyanoethyl)-N,N-diisopropylphosphoramidite-5´-O-(4,4´-dimethoxy-trityl)-ribonucleoside]; ^{1}H-NMR (200MHz, $CDCl_3$/TMS, δ in ppm): 9.08 (br, 1H, C6-N<u>H</u>), 8.48 (s, 1H, H8), 8.09 (d, 1H, H2), 7.97-7.14 (m, 1H, H1; 4H, Bz; 13H, (CH$_3$O)$_2$<u>Tr</u>), 6.50 (pt, 1H, H1´), 4.72 (m, 1H, H3´), 4.01 (m, 1H, H4´), 3.70 and 3.69 (2 x s, 2 x 3H, 2 x OC<u>H</u>$_3$), 3.30-4.30 (m, 2H, H5´ and H5´´), 3.00-2.50 (m, 2H, H2´ and H2´´; 4H,

CH_2CH_2CN), 1.30-1.10 (m, 14H, 2 x $(CH_3)_2CH$); ^{31}P-NMR (80.98MHz, $CDCl_3$, δ in ppm): 149.8 and 149.7 (product), 15.3 ((2-cyanoethoxy)-(diisopropylamino)-phosphane oxide); FAB-MS calc. (M/Z): 857.3792; found: 857.3763.

Oligonucleotides (Z = 1-Deazaadenine nucleoside)

(**k**) 5´-d(A**ZZ ZZZ ZZZ** A).

The 345mg (177mg/206µmol product) 1-deaza-(6-benzoylamino)-purine-N9-β-[2´-deoxy-3´-O-(2-cyanoethyl)-N,N-diisopropylphosphoramidite-5´-O-(4,4´-dimethoxy-trityl)-ribonucleoside] are dissolved in 2.0ml dry CH_3CN to give a 100mM solution that can be used in the oligonucleotide synthesis at the DNA-synthesizer.

HPLC Column: reversed phase column
Temperature: r.t.

Time (min)	Flow (ml min^{-1})	% of solvent A	% of solvent B
0.0	1.50	100	0
10.0	1.50	90	10
40.0	1.50	80	20
43.0	1.50	50	50
48.0	1.50	50	50
53.0	1.50	100	0
53.5	0.01	100	0

HPLC-method

Three products were collected at different times and desalted (desaltation column).
Peak 1 at T_1 = 9.7min (OASIS®)
Peak 2 at T_2 = 10.4min (NAP™ 5 column)
Peak 3 at T_3 = 14.5min (OASIS®)

After the desalting the oligonucleotides (peaks 1-3) are lyophilised, dissolved in 900µl and 100µl are taken off and filled up to 900µl with H_2O. The absorption spectrum is taken. After calculating the concentration and measuring MALDI-TOF spectra, none of the peaks showed a signal for any kind of oligonucleotide.

1-Deaza-(6-methoxyacetylamino)-purine-N9-β-2´-deoxyribonucleoside•0.5H_2O (45)

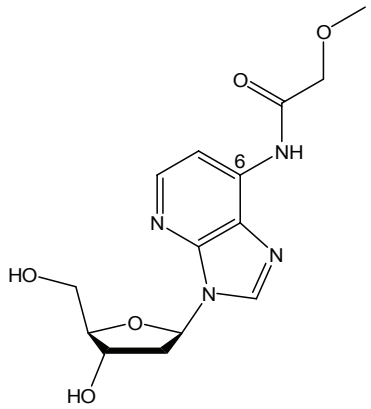

This is a slightly modified version of the synthesis in the literature.[167]

In a 100ml round bottom flask 305mg (1.22mmol) 1-deaza-6-aminopurine-N9-β-2´-deoxyribonucleoside are co-evaporated twice with 15.2ml dry pyridine and then dissolved in 30.0ml dry pyridine under argon. To the slightly yellow solution 800µl (8.75mmol) methoxyacetyl chloride are added and immediately the solution becomes yellow and a solid precipitates. After five minutes the solution is red and nearly all solid has disappeared. The solution gets stirred for two hours at r.t.. Then, to destroy excess methoxyacetyl chloride, 1.50ml H_2O are added and the solution is stirred for further 25min, before it gets evaporated. The red oil is then dissolved in 30ml CH_2Cl_2 and washed with 20ml $NaHCO_3$ solution (5%/3x) and 20ml H_2O (1x) and dried over Na_2SO_4. The CH_2Cl_2 is evaporated off to give a reddish-brown oil. To this oil 20ml of a solution containing Et_3N (1), pyridine (1) and H_2O (3) are added and the resulting brown solution is stirred for 30min at r.t. Evaporation and co-evaporation with 50ml toluene (2x) and 50ml acetone (2x) gives an orange-brown oil. Flash chromatography over silica gel (30.5 x 2.5cm, CH_2Cl_2 (19) : MeOH (1)) gives 314.1mg (948µmol) of 1-

deaza-(6-methoxyacetylamino)-purine-N9-β-2´-deoxyribonucleo-side•0.5H_2O as a white foam (78%, ref.: 78%)[167]. ^{1}H-NMR (200MHz, CH_3OD/TMS, δ in ppm): 8.50 (s, 1H, H8), 8.27 and 8.22 (2 x d, 1H, H2; 1H, H1), 6.54 (pt, 1H, H1´), 4.60 (m, 1H, H3´), 4.16 (s, 2H, C$\underline{H_2}$OCH_3), 4.01 (m, 1H, H4´), 3.90-3.64 (m, 2H, H5´ and H5´´), 3.56 (s, 3H, CH_2OC$\underline{H_3}$), 2.95-2.37 (m, 2H, H2´ and H2´´); elemental analysis calc. (%) for $C_{14}H_{18}N_4O_5$•0.5H_2O (M = 331.33g/mol): C 50.8, H 5.8, N 16.9; found: C 50.7, H 5.7, N 16.8; FAB-MS calc. (M/Z): 323.1355; found: 323.1379.

1-Deaza-(6-methoxyacetylamino)-purine-N9-β-[2´-deoxy-5´-O-(4,4´-dimethoxytrityl)-ribonucleoside] (46)

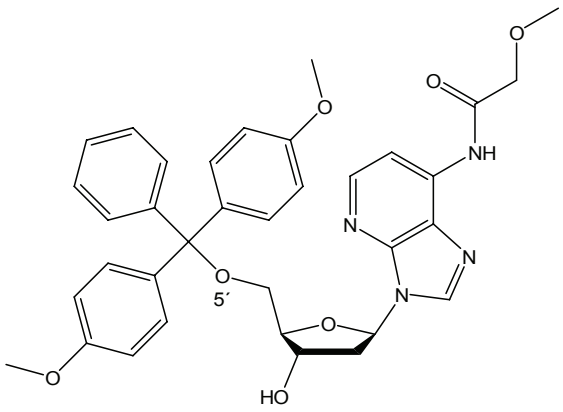

This is a slightly modified version of the synthesis in the literature.[146]

In a 50ml round bottom flask 305mg (921µmol) 1-deaza-(6-methoxyacetylamino)-purine-N9-β-2´-deoxyribonucleoside•0.5H2O are co-evaporated twice with 5.0ml dry pyridine and then dissolved in 5.0ml dry pyridine under argon. To the light yellow solution 385mg (1.139mmol) DMTr-Cl are added and the solution immediately turns orange. The solution is stirred for three hours at r.t. under argon, whereby a solid precipitates (pyridinium chloride). Then 800µl CH_3OH are added and the solution is stirred for a further 30min, whereby the solid dissolves slowly. The solution is evaporated to half of its volume and 32.0ml CH_2Cl_2 are added. The organic phase is washed with 16ml $NaHCO_3$ solution (5%/2x) and 16ml saturated NaCl solution (1x) and dried over Na_2SO_4. Evaporation and co-evaporation with 30ml toluene gives an orange-brown oil. Flash chromatography over silica gel (10.0 x 2.5cm, CH_2Cl_2 (8) : acetone (2)) gives 372mg (596µmol) of 1-deaza-(6-methoxyacetylamino)-purine-N9-β-

2´-deoxyribonucleoside as a white solid (65%, ref. 84%)[146]. ^{1}H-NMR (200MHz, $CDCl_3$/TMS, δ in ppm): 9.49 (br, 1H, H1´), 8.28 (br, 1H, H2; 1H, H8), 7.99 (s, 1H, H1), 7.31-7.14 (m, 9H, $(CH_3O)_2\underline{Tr}$), 6.90-6.80 (m, 4H, $(CH_3O)_2\underline{Tr}$), 6.41 (dd, 1H, H1´), 4.83 (m, 1H, H3´), 4.25 (m, 1H, H4´), 4.12 (s, 2H, $C\underline{H}_2OCH_3$), 4.03-3.80 (m, 2H, H5´ and H5´´), 3.80 (2 x s, 2 x 3H, 2 x Tr-$OC\underline{H}_3$), 3.57 (s, 3H, $CH_2OC\underline{H}_3$), 3.30-2.27 (m, 2H, H2´ and H2´´); elemental analysis calc. (%) for $C_{35}H_{36}N_4O_7$ (M = 624.68g/mol): C 67.3, H 5.8, N 9.0; found: C 66.3, H 4.4, N 8.1; FAB-MS calc. for (M/Z): 625.2663; found: 625.2692.

1-Deaza-(6-methoxyacetylamino)-purine-N9-β-[2´-deoxy-3´-O-(2-cyano-ethyl)-N,N-diisopropylphosphoramidite-5´-O-(4,4´-dimethoxytrityl)-ribonucleoside] (47)

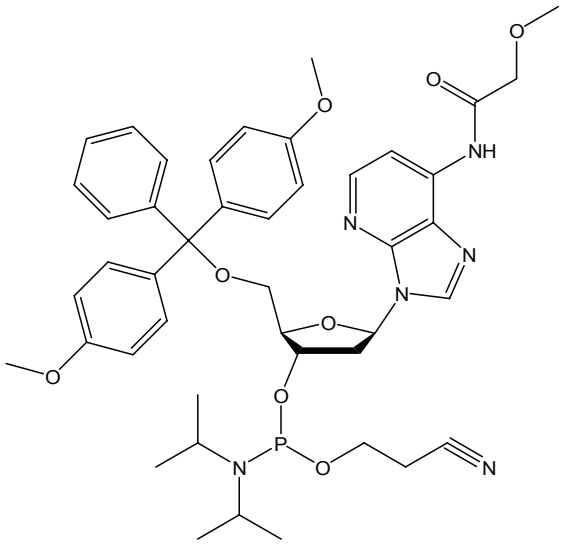

This is a slightly modified version of the synthesis in the literature.[146]

In a 100ml round bottom flask 372mg (596µmol) 1-deaza-(6-methoxyacetylamino)-purine-N9-β-2´-deoxyribonucleoside are dissolved in 22.0ml dry CH_2Cl_2 under argon. To the solution 199µl (1.14mmol) $(i\text{-}Pr)_2EtN$ and 199µl (0.89mmol) chloro-(2-cyanoethoxy)-(diisopropylamino)-phosphane are added at r.t. and the solution is stirred for 20min under argon. Now 22.0ml CH_2Cl_2 are added and the light yellow solution is washed with 15ml $NaHCO_3$ solution (5% / 2x) and 15ml saturated NaCl solution and the organic phase is dried over Na_2SO_4. The CH_2Cl_2 is evaporated off

and the resulting yellow oil is co-evaporated twice with dry CH_2Cl_2 to give 555mg of a side-product-product mixture.

The yellow oil is not worked up further. The yield is calculated through the ratio of product to side product and the mean molar mass.

Raw mass = 555.3mg

Ratio: product (0.6) : side product (0.4)

Mean molar mass = molar mass (product) x 0.6 + molar mass (side product) x 0.4

⇒ Mean molar mass = 582.23g/mol

⇒ Medium moles = 954µmol

Mass (product) = medium moles x molar mass (product) x ratio (product)

⇒ Mass (product) = 472mg (572µmol) (96%, ref. 87%)[146]

^{1}H-NMR (200MHz, $CDCl_3$/TMS, δ in ppm): 9.41 (br, 1H, C6-NH), 8.55 (s, 1H, H8), 8.24 (d, 1H, H2), 8.14 (d, 1H, H1), 7.42-6.76 (m, 13H, $(CH_3O)_2$Tr), 6.55 (pt, 1H, H1´), 4.77 (m, 1H, H3´), 4.20 (m, 1H, H4´), 4.11 (s, 2H, CH_2OCH_3), 3.77 and 3.78 (2 x s, 2 x 3H, 2 x OCH_3), 3.56 (s, 3H, CH_2OCH_3), 4.30-3.30 (m, 2H, H5´ and H5´´), 3.00-2.50 (m, 2H, H2´ and H2´´; 4H, CH_2CH_2CN), 1.30-1.10 (m, 14H, 2 x $(CH_3)_2CH$); ^{31}P-NMR (80.98MHz, $CDCl_3$, δ in ppm): 149.8 and 149.6 (product), 15.3 ((2-cyanoethoxy)-(diisopropylamino)-phosphane oxide); FAB-MS calc. value (M/Z): 825.3741; found: 825.3716.

Oligonucleotides (Z = 1-Deazaadenine nucleoside)

(**l**) 5´-d(A**Z**A **Z**A**Z** A**Z**A)

The 178mg (104mg/126µmol product) 1-deaza-(6-methoxyacetylamino)-purine-N9-β-[2´-deoxy-3´-O-(2-cyanoethyl)-N,N-diisopropylphosphoramidite-5´-O-(4,4´-dimethoxytrityl)-ribonucleoside] are dissolved in 1.25ml dry CH_3CN to give a 100mM solution that can be used in the oligonucleotide synthesis at the DNA-synthesizer.

HPLC Column: ion-exchange column

Temperature: 50°C

Time (min)	Flow (ml min^{-1})	% of solvent A	% of solvent B
0.0	1.50	100	0
10.0	1.50	100	0
40.0	1.50	75	25
45.0	1.50	0	100
48.0	1.50	0	100
50.0	1.50	100	0
55.0	1.50	100	0
55.5	0.01	100	0

HPLC-method

Three products were collected at different times and desalted (desaltation column).

Peak 1 at T_1 = 15.2min (none)

Peak 2 at T_2 = 25.2min (none)

Peak 3 at T_3 = 28.2min (2 x NAP™ 10 column)

After the desalting the oligonucleotide (peak 3) is lyophilised, dissolved in 900 µl and the absorption spectrum is taken.

$E_{(260nm)} = c * d * \varepsilon$, where $\varepsilon = f * \Sigma n_i \varepsilon_i$ (for further explanation see UV-Vis spectroscopy)

$E_{(260nm)} = 0.717$

Therefore concentration c (900µl) = 6.48µmol/l $\Rightarrow$ Yield = 0.58%

MALDI-TOF

Value calc. (M/Z) for $(MH)^+$ = 2753.97; found: 2756.34.

(**m**) 5´-d(**zzz zzz zzz zzz zzz zzz z**A)

The 555.3mg (472.0mg/0.5722mmol product) 1-deaza-(6-methoxyacetylamino)-purine-N9-β-[2´-deoxy-3´-O-(2-cyanoethyl)-N,N-diisopropylphosphoramidite-5´-O-(4,4´-dimethoxytrityl)-ribonucleoside] are dissolved in 5.72ml dry CH_3CN to give a 100mM solution that can be used in the oligonucleotide synthesis at the DNA-synthesizer.

HPLC Column: ion-exchange column

Temperature: 60°C

Time (min)	**Flow (ml min^{-1})**	**% of solvent A**	**% of solvent B**
0.0	1.5	100	0
5.0	1.5	100	0
55.0	1.5	75	25
60.0	1.5	75	25
90.0	1.5	65	35
93.0	1.5	0	100
97.0	1.5	0	100
100.0	1.5	100	0
105.0	1.5	100	0
106.0	0.01	100	0

HPLC-method

Five products were collected at different times and desalted (desaltation column).

Peak 1 at T_1 = 62.5-65.8min (1 x NAP™ 10 column)

Peak 2 at T_2 = 66.0-68.3min (2 x NAP™ 10 column)

Peak 3 at T_3 = 68.5-71.3min (2 x NAP™ 10 column)

Peak 4 at T_4 = 71.5-74.5min (2 x NAP™ 10 column)

Peak 5 at T_5 = 75-78min (2 x NAP™ 10 column)

After the desalting the oligonucleotides (peaks 2-4) are lyophilised, dissolved in 900µl and 100µl are taken off and filled up to 900µl with H_2O. The absorption spectrum is taken. After calculating the concentration and measuring a MALDI-TOF, none of the peaks showed a clear signal.
The peaks 2-4 are joined and again treated with 1ml AMA. The AMA is taken off under vacuum.

HPLC Column: reversed phase column
Temperature: 50°C

Time (min)	**Flow (ml min^{-1})**	**% of solvent A**	**% of solvent B**
0.0	1.0	100	0
25.0	1.0	81	19
30.0	1.0	60	40
35.0	0.1	100	0
36.0	0.1	100	0

HPLC-method

One product was collected and desalted (1 x NAP™ 5 column).
Peak 2-4(II) at T_1 = 19.9-20.5min

After the desalting the oligonucleotide (peak 2-4(II)) is lyophilised, dissolved in 1000µl and 900µl are taken off and the absorption spectrum is taken. After calculating the concentration and measuring MALDI-TOF spectra, none of the peaks showed a signal for any kind of oligonucleotide.

After the desalting the oligonucleotide (peak 5) is lyophilised, dissolved in 900µl and 100µl are taken off and filled up to 900µl with H_2O. The absorption spectrum is taken.

$E_{(260nm)} = c * d * \varepsilon$, where $\varepsilon = f * \Sigma n_i \varepsilon_i$ (for further explanation see UV-Vis spectroscopy)

$E_{(260nm)} = 0.0787$

Therefore concentration c (900µl) = 0.374µmol/l $\Rightarrow$ Yield = 0.30%

MALDI-TOF

Value calc. (M/Z) for $(MH)^+$ = 6184.3; found: 6190.7.

E Summary

1 English Version

The generall aim of this work is the synthesis of oligonucleotides containing new artificial nucleobases that are able to build artificial planar metal-mediated base pairs without disturbing the geometry of the backbone and therefore partially or fully exchanging H-bonding and π-stacking interactions through covalent metal ligand interactions. Through the synthesis of these new systems further information about the structure and the bonding behaviours are studied. Four different systems with four different coordination modes ([3+1], [2+2], [1+1] and [1+1] + H-bond) are discussed in this thesis.

Chapter I

Model structures with 2,2´:6´,2´´-terpyridine, Pd^{2+} or Pt^{2+} and either of the two different monodentate ligands, 1-methylimidazole or 1-methyltetrazole, were synthesised and characterised. In $[(trpy)Pd(1\text{-}mimi)](ClO_4)_2$ and $[(trpy)Pt(1\text{-}mimi)](ClO_4)_2$ the 1-methylimidazole binds over the N3 position, as expected. Crystal structures show clearly that there is no planarity between the 2,2´:6´,2´´-terpyridine and the opposite 1-methylimidazole, due to sterical hindrance of some H atoms of the ligands. It is shown, through a crystal structure, that the $[(trpy)Pt(1\text{-}mtetate)](ClO_4)$ (Figure I) binds over the C5 atom and not over N3, again, having a sterical hindrance for planarity, this time through the methyl group. The Pd^{2+} complex probably binds similarly, except that it seems to have additional binding over the N4 or N3 to another 2,2´:6´,2´´-terpyridine-Pd entity. The binding of the C5 atom might be avoided through a change in pH and it is obvious that binding over N3 would open the possibility of H-bonding.

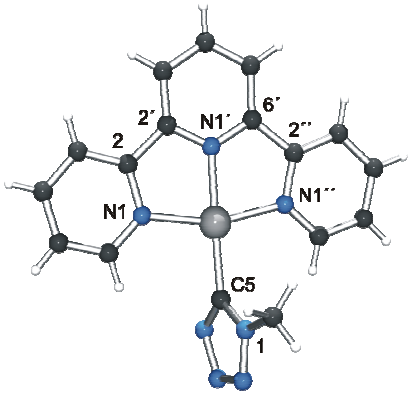

Figure I: Crystal structure of the cation of $[(trpy)Pt(1\text{-}mtet)](ClO_4)$.

In this case the N2 and N4 positions can build H-bonds to the H6 and H6´´ positions of the outer 2,2´:6´,2´´-terpyridine rings giving rise to a near planar system, which has been shown by DFT calculations. It is expected that the 1-methyltetrazole will bind a metal ion over the N3 position inside an oligonucleotide due to sterical reasons. Therefore it could be shown that having terpyridine and tetrazole as artificial nucleobases in opposite positions inside two complementary oligonucleotide strands is very promising for metal-mediated base pairing.

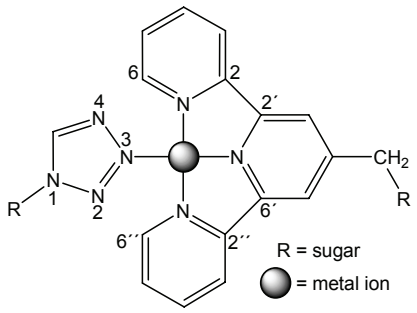

Figure II: A possible planar metal-mediated base pair with a [3+1]-coordination.

It is also shown that the 2,2´:6´,2´´-terpyridine can be a useful artificial nucleobase due to its high metal affinity, for example. The attempts that were undertaken to synthesise the 4´-methyl-2,2´:6´,2´´-terpyridine nucleoside are described. For these attempts a couple of precursors were synthesised such as the 4´-methyl-2,2´:6´,2´´-terpyridine and the 4´-bromomethyl-2,2´:6´,2´´-terpyridine. These were meant to be linked to different protected sugar moieties.

The C-glycosidic bond formation was not successful and reasons, such as the high metal affinity of the terpyridine rings, are described and discussed. A new synthetic route is proposed. This concludes the build up of the terpyridine ring after the C-glycosidic bond formation.

Chapter II

The synthesis of three different artificial nucleosides with N-glycosidic bonds that are thought to be able to form metal-mediated base pairs is described. 1-deazapurine-N7 nucleoside and 1-deazapurine-N9 nucleoside, as well as 1-deazaadenine nucleoside were synthesised and characterised. Characterisation included crystal structures of the nucleosides and synthesised model structures, comparisons with DFT calculations, pK_a value determinations, Job-Plots, titrations with different metal ions

and determination of stabilisation constants. For all three nucleosides a competitive protonation to the wanted metalation could be excluded. Especially for the 1-deazapurine-N9 nucleoside a 2:1 complex formation with Hg^{2+} (linear coordinating metal ion) could be observed and certified with a crystal structure of $[Hg(9\text{-MeDP})_2](NO_3)_2 \cdot H_2O$. Crystal structures of the 1-deazapurine nucleosides were obtained and described in detail. The further synthesis to obtain the different nucleotides and the synthesis and purification of artificial oligonucleotides are described and challenging parts, such as the high acid lability of the N-glycosidic bond, are discussed. On occasions crystal structures of intermediates were obtained and analysed.

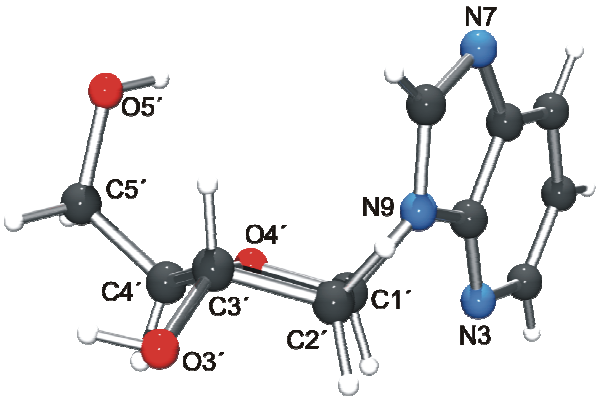

Figure III: Crystal structure of 1-deazapurine-N9-β-2´-deoxyribonucleoside.

Whereas the formation of metal-mediated base pairs with the synthesised 1-deazapurine-N7 (X) containing oligonucleotides was not succesful, the 1-deazapurine-N9 (Y) containing oligonucleotides showed some indication of the formation of those base pairs with Ag^+ (linear coordinating metal ion).

Y-A, Y-C, Y-G, Y-T and Y-Y base pairs inside a 15-mer with 14 A-T base pairs were looked at and discussed. Especially for Y-G and Y-C a metal-mediated base pair formation can be assumed because of a high increase in melting temperature (11.3°C and 9.2°C, respectively) and cooperativity of the melting.

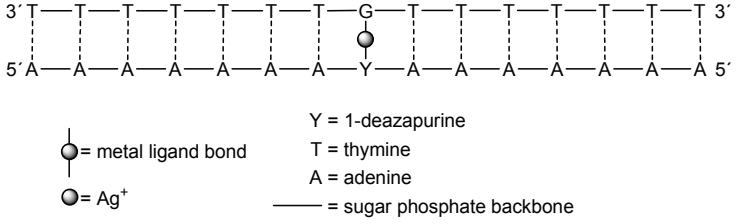

Figure IV: A possible Ag^+-mediated Y-G base pair inside a 15-mer.

Also the increase in melting temperature is specific for one equivalent of Ag^+, hence, a further addition does not give an increase in melting temperature, which excludes a possible binding at the backbone. Without Ag^+ the natural base pairs (A-T and C-G) have higher melting temperatures than the base pairs with Y, but for the natural base pairs neither an increase in melting temperature nor a change in the cooperativity of the melting is observed upon the addition of Ag^+. The results of the base pair formation with and without Ag^+ of all base pairs are discussed and the differences are pointed out.

The melting behaviour of an oligonucleotide, $Y_{16}A$ (Y = 1-deazapurine-N9 nucleoside), containing nearly only Y and maybe self assembling upon the addition of Ag^+ has been looked at. It has been found with the help of CD-spectra that even without Ag^+ a defined rigid structural conformation is present. After the addition of only half an equivalent of Ag^+, the melting temperature of around 43°C did not change further. Hence, the increase in melting temperature is specific for half an equivalent of Ag^+. Also a hypochromic effect is present and the cooperativity of the melting is significantly increased. However, the structural conformation of the possible double helix does not change upon the addition of Ag^+. Every second possible artificial base pair probably has one Ag^+ bound inside (Figure V), as in the nearest neighbour exclusion principle. Possible structural conformations of the base pairs or the double helices that are not known at the moment are suggested and discussed.

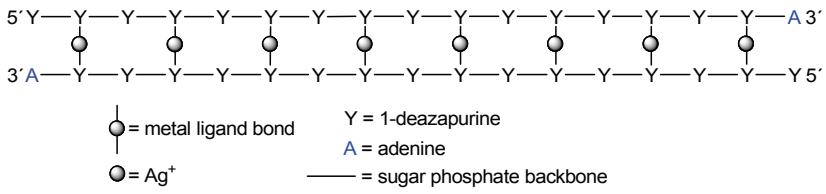

Figure V: Possible structure of a $Y_{16}A$ strand self assembling upon the addition of half an equivalent of Ag^+.

The melting behaviour of an oligonucleotide, containing 19 1-deazaadenine nucleosides (Z) and one adenine nucleoside, with a thymine 20-mer was examined. Without Ag^+ no cooperative melting has been observed. Upon the addition of Ag^+ a melting temperature of around 48°C is found. Next to the increase in cooperativity of the melting, a large hypochromic effect can be seen. The increase in melting temperature is specific for one equivalent of Ag^+, hence, a further addition does not give an increase in melting temperature, which excludes a possible binding of Ag^+ at the backbone.

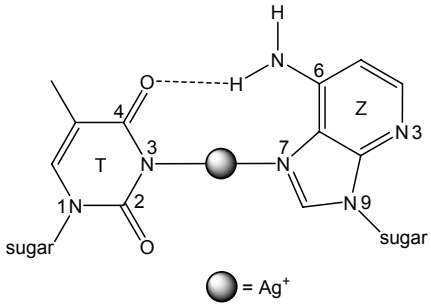

Figure VI: Possible structure of an Ag^+-mediated Z-T base pair with a [1+1]-coordination and an additional H-bond.

The possible binding over the Hoogsteen side of Z and the introduction of Ag^+ to form a stable double helix with possible 19 Ag^+ in a one dimensional chain inside, is pointed out and discussed, but up to this point could not be fully proven. Further measurements to obtain a greater knowledge about the structure of the possible double helix and the artificial metal-mediated base pair are suggested.

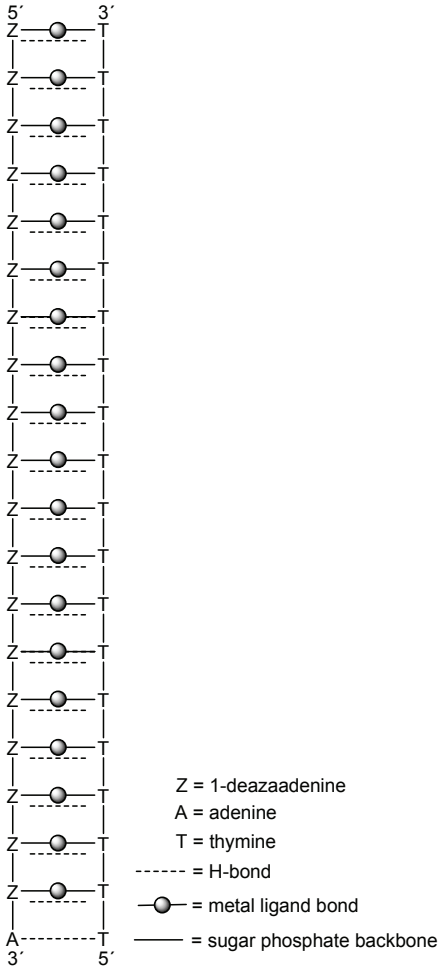

Figure VII: A possibly formed double helix through artificial Ag^+-mediated Z-T base pairs.

2 German Version

Das Ziel dieser Arbeit ist die Synthese von Oligonucleotiden, die neuartige künstliche Nucleobasen enthalten, welche die Ausbildung künstlicher und planarer Metallionen-vermittelter Basenpaare fördern. Durch den Aufbau dieser Basenpaare sollen die Wasserstoffbrückenbindungen und die π-Stapelwechselwirkungen entweder teilweise oder komplett durch kovalente Metall-Liganden Bindungen ersetzt werden ohne die Geometrie des Rückgrates zu beeinflussen. Durch die Synthese und Charakterisierung dieser neuartigen Systeme wurden Informationen über die Struktur und das Verhalten von Bindungspartnern studiert. Vier Systeme mit verschiedenen Koordinationsmodi ([3+1], [2+2], [1+1] und [1+1] + Wasserstoffbrückenbindung) werden beschrieben.

Kapitel I

Modellstrukturen mit 2,2´:6´,2´´-Terpyridin, einem Pd^{2+}- oder einem Pt^{2+}-Metallion und zwei verschiedenen monodentaten Liganden, 1-Methylimidazol und 1-Methyltetrazol, wurden synthetisiert und charakterisiert. In den Komplexen, die über eines der Metalle an das 1-Methylimidazol verknüpft sind, bindet dies, wie erwartet, über N3. Kristallstrukturen zeigen eindeutig, dass aus sterischen Gründen keine Planarität zwischen den Liganden vorhanden ist. Aus einer Kristallstruktur von [(trpy)Pt(1-mtetate)](ClO_4) geht hervor, dass das 1-Methyltetrazol nicht über N3, sondern über C5 an das Metall bindet. Die auch hier nicht vorhandene Planarität des Liganden wird diskutiert. Ein über C5 gebundenes 1-Methyltetrazol wurde auch für den Pd^{2+} Komplex gefunden, allerdings bindet es auch noch zusätzlich über N4 oder N3 an ein weiteres Pd^{2+}. Eine Bindung über C5 könnte möglicherweise durch einen veränderten pH Wert vermieden werden und offensichtlich könnte eine Bindung über N3 durch mögliche Wasserstoffbrücken zu einem planaren Komplex führen.

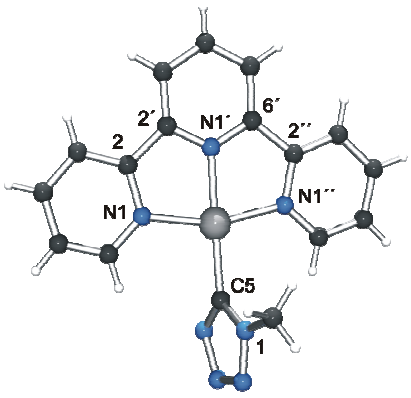

Abbildung I: Kristallstruktur von [(trpy)Pt(1-mtetate)](ClO_4).

Die N2- und N4-Positionen könnten mit H6 und H6´´ von den äußeren Ringen des 2,2´:6´,2´´-Terpyridin Wasserstoffbrücken ausbilden und somit ein planares System fördern. Dies wurde mit Hilfe von DFT Rechnungen gezeigt. Aus sterischen Gründen würde der Ligand eingebaut in einem Oligonucleotid wahrscheinlich über N3 binden. So kann man feststellen, dass Terpyridin und Tetrazol als künstliche Nucleobasen, eingebaut in gegenüberliegender Position in einem Oligonucleotid, ein sehr hoffnungsvolles System ergeben für metallmodifizierte Basenpaarungen.

Die Versuche, die unternommen wurden, um das 4´-Methyl-2,2´:6´,2´´-terpyridin Nucleosid zu synthetisieren, werden beschrieben. Zu diesem Zweck wurden verschiedene Ausgangsverbindungen hergestellt, wie das 4´-Methyl-2,2´:6´,2´´-terpyridin und das 4´-Bromomethyl-2,2´:6´,2´´-terpyridin. Diese Ausgangsverbindungen wurden dann in mehreren Versuchen mit verschieden Zuckern verknüpft. Die Synthese der C-glycosidischen Bindung war allerdings in keinem Fall erfolgreich und Gründe hierfür werden aufgezeigt und besprochen. Auch wird eine neue synthetische Route zum Zielmolekül vorgeschlagen, welche den Aufbau des Terpyridins an einer Zuckereinheit nach erfolgreicher Synthese der C-glycosidischen Bindung beinhaltet.

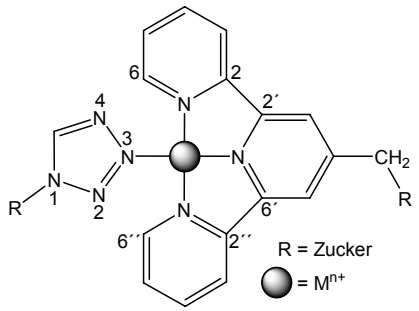

Abbildung II: Ein mögliches planares Metall-vermitteltes Basenpaar ([3+1]).

Kapitel II

Die Synthese von drei künstlichen Nucleosiden mit N-glycosidischen Bindungen, die in möglichen Metallionen-vermittelten Basenpaaren nützlich sein könnten, wird beschrieben. Das 1-Deazapurin-N7 Nucleosid, das 1-Deazapurin-N9 Nucleosid und das 1-Deazaadenin Nucleosid wurden synthetisiert und charakterisiert. Die Charakterisierung beinhaltet Kristallstrukturen von Nucleosiden und Modellstrukturen, Vergleiche mit DFT Rechnungen, die Bestimmung von pK_s Werten und Stabilitätskonstanten, Job-Plots und Titrationen mit Metallionen. Für alle drei Nucleoside konnte eine konkurrierende Protonierung ausgeschlossen werden.

Speziell für das 1-Deazapurin-N9 Nucleosid wurde ein stabiler 2:1 Komplex mit Hg^{2+} (ein linear koordinierendes Metallion) gefunden und durch eine Kristallstruktur von $[Hg(9\text{-MeDP})_2](NO_3)_2 \cdot H_2O$ bestätigt. Kristallstrukturen von den 1-Deazapurin Nucleosiden wurden erhalten und beschrieben. Die weiteren Synthesestufen der Nucleotide und der Oligonucleotide sowie deren Aufreinigung sind im Detail beschrieben und eventuelle Besonderheiten, wie die Säureempfindlichkeit der N-glycosidischen Bindung werden diskutiert. Kristallstrukturen von zahlreichen Zwischenstufen wurden erhalten und analysiert.

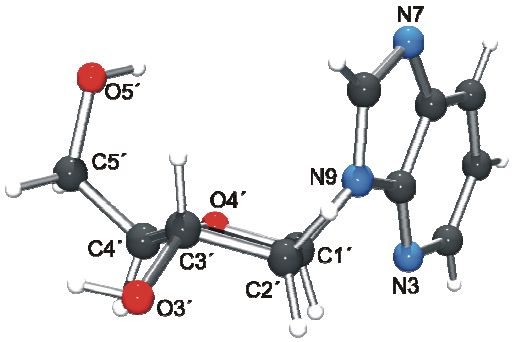

Abbildung III: Kristallstruktur von 1-Deazapurin-N9-β-2´-desoxyribonucleosid.

Das Erzeugen von Metallionen-vermittelten Basenpaaren mit einem synthetisierten 1-Deazapurin-N7 (X) enthaltenden Oligonucleotid war nicht erfolgreich. Mögliche Gründe werden benannt und diskutiert. Dies steht im Gegensatz zu den erhaltenen Daten mit einem synthetisierten 1-Deazapurin-N9 (Y) enthaltenden Oligonucleotid und Ag^+ (ein linear koordinierendes Metallion).

1-Deazapurin-N9 (Y) enthaltende Oligonucleotide zeigten Anzeichen für das Vorhandensein von Ag^+-vermittelten Basenpaaren. Y-A, Y-C, Y-G, Y-T und Y-Y Basenpaare in einem 15-mer mit 14 A-T Basenpaaren wurden untersucht. Für die Y-G und Y-C Basenpaare mit Ag^+ zeigte eine Erhöhung der Schmelztemperatur (um 11,3°C und 9,2°C) und die Kooperativität des Schmelzvorganges, dass möglicherweise ein Metallionen-vermitteltes Basenpaar erhalten werden konnte.

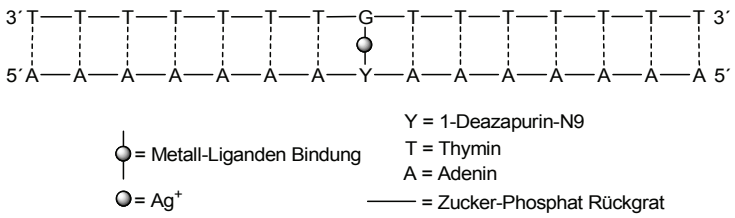

Abbildung IV: Ein mögliches Ag^+-vermitteltes Y-G Basenpaar in einem 15-mer.

Nach Zugabe von einem Äquivalent Ag^+ kann eine Schmelzpunkterhöhung für die Y enthaltenden Basenpaare beobachtet werden. Weitere Zugaben von Ag^+ erhöhen den Schmelzpunkt nur noch geringfügig. Dies schließt ein mögliches Binden am Rückgrat aus. Ohne Ag^+ hatten die natürlichen Basenpaare (A-T und C-G) eine höhere Schmelztemperatur als die Y enthaltenden Basenpaare. Allerdings zeigten die natürlichen Basenpaare durch die Zugabe von Ag^+ weder eine Schmelzpunkterhöhung, noch sonstige Änderungen im Schmelzverhalten. Die Ergebnisse der Schmelzkurven werden eingehend diskutiert und die Unterschiede analysiert.

Das Schmelzverhalten eines synthetisierten Oligonucleotids, $Y_{16}A$ (Y = 1-Deazapurine-N9-nucleosid), und eine mögliche Y-Y Basenpaarung mit Ag^+ wurden untersucht. Mittels CD-Spektren wurde herausgefunden, dass der Strang auch ohne Ag^+ eine geordnete Struktur einnimmt. Nach der Zugabe von einem halben Äquivalent Ag^+ wurde eine Schmelztemperatur von rund 43°C gemessen, die sich auch nach weiterer Zugabe nicht weiter erhöhte. Dies schließt ein mögliches Binden des Ag^+ am Rückgrat aus. Die nach Zugabe von Ag^+ beobachtete Hypochromizität wird im Detail besprochen. Auch erhöht sich die Kooperativität des Schmelzens. Allerdings ändert sich die Struktur (möglicherweise eine Doppelhelix) durch die Zugabe von Ag^+ nicht. Wahrscheinlich enthält jedes zweite Basenpaar ein Ag^+ wie es auch in Abbildung V gezeigt ist. Strukturen der Basenpaare und einer möglichen Doppelhelix werden vorgeschlagen und diskutiert.

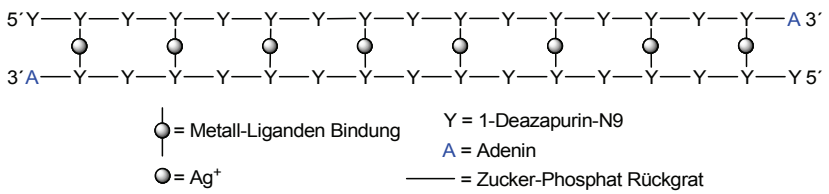

Abbildung V: Mögliche Struktur des $Y_{16}A$ nach der Zugabe von Ag^+.

Das Schmelzverhalten eines Oligonucleotids, welches 19 1-Deazaadenin Nucleoside (Z) und ein Adenin Nucleosid enthält, mit einem T_{20} unter Zugabe von Ag^+ wurde untersucht. Ohne Ag^+ wurde kein kooperatives Schmelzverhalten gefunden. Nach der Zugabe von einem Äquivalent Ag^+ erhält man eine Schmelztemperatur von rund 48°C. Eine weitere Zugabe an Ag^+ erhöht die Schmelztemperatur nicht, was darauf schließen lässt, dass Ag^+ an den Basen und nicht am Rückgrat bindet. Neben einem starken Anstieg der Kooperativität des Schmelzens, kann auch Hypochromizität beobachtet werden.

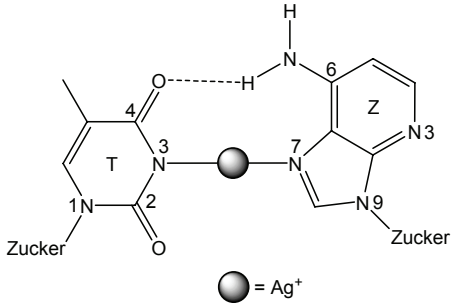

Abbildung VI: Eine mögliche Struktur eines Ag^+-vermittelten Z-T Basenpaares ([1+1] + Wasserstoffbrücke).

Eine mögliche Bindung über die Hoogsteen Seite von Z mit Thymin durch ein Ag^+ würde zu einer stabilen Doppelhelix führen, in der 19 Ag^+ in einer eindimensionalen Anordnung zu finden wären. Weitere Messungen, die eine größere Bandbreite an strukturellen Informationen zur Verfügung stellen würden, werden vorgeschlagen und erläutert.

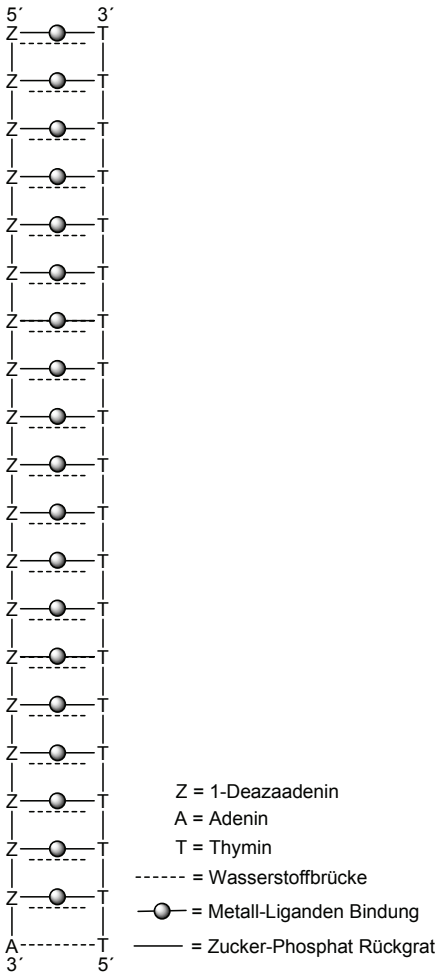

Abbildung VII: Mögliche Struktur einer Doppelhelix durch künstliche Ag^+-modifizierte Z-T Basenpaare.

F Appendix

1 Crystallographic Tables

Compound	[(trpy)Pt(1-mtet)](ClO_4) (**7**)
Empirical formula	$C_{17}H_{14}N_7O_4ClPt$
Molar weight (g/mol)	610.89
Crystal colour and habit	yellow stick
Solvent	H_2O
Space system	triclinic
Space group	P-1
Cell constants (Å and °)	a = 8.136(2) / α = 100.57(3)
	b = 10.592(2) / β = 91.00(3)
	c = 10.835(2) / γ = 94.40(3)
Cell volume (Å)	914.7(3)
Z	2
ρ_{calc} (g/cm)	2.218
μ (MoK_α) (1/mm)	7.860
F(000)	584
Temperature (K)	183(2)
θ range (°)	2.98-29.12
No. of reflections collected / observed	17970/14546
Absorption correction	numerical
No. of parameters refined	274
R_1 (observed data)	0.0382
wR_2 (observed data)	0.0949
GooF	1.054
Residual ρ_{min}, ρ_{max} (e/ Å^3)	-2.007, 2.106
Completion until θ = 29.12 (%)	92.2

Crystallographic table 1: [(trpy)Pt(1-mtet)](ClO_4) (**7**).

Compound	[(trpy)Pd(1-mimi)]$(ClO_4)_2$ (**10**)
Empirical formula	$C_{19}H_{17}N_5O_8Cl_2Pd$
Molar weight (g/mol)	620.69
Crystal colour and habit	orange cube
Solvent	H_2O
Space system	monoclinic
Space group	$P2_1/n$
Cell constants (Å and °)	a = 8.477(2)
	b = 10.529(2) / β = 92.98(3)
	c = 26.042(5)
Cell volume (Å)	2321.2(8)
Z	4
ρ_{calc} (g/cm)	1.776
μ (MoK_α) (1/mm)	1.086
F(000)	1240
Temperature (K)	183(2)
θ range (°)	3.04-27.10
No. of reflections collected / observed	5059/5059
Absorption correction	numerical
No. of parameters refined	357
R_1 (observed data)	0.0590
wR_2 (observed data)	0.1364
GooF	0.814
Residual ρ_{min}, ρ_{max} (e/ Å^3)	-1.366, 0.769
Completion until θ = 27.10 (%)	98.9

Crystallographic table 2: [(trpy)Pd(1-mimi)]$(ClO_4)_2$ (**10**).

Compound	[(trpy)Pt(1-mimi)]$(ClO_4)_2$ (**11**)
Empirical formula	$C_{19}H_{17}N_5O_8Cl_2Pt$
Molar weight (g/mol)	709.35
Crystal colour and habit	yellow stick
Solvent	H_2O
Space system	monoclinic
Space group	$P2_1/n$
Cell constants (Å and °)	a = 8.472(2)
	b = 10.703(2) / β = 93.53(3)
	c = 25.740(5)
Cell volume (Å)	2329.6(8)
Z	4
ρ_{calc} (g/cm)	2.023
μ (MoK_α) (1/mm)	6.309
F(000)	1368
Temperature (K)	183(2)
θ range (°)	3.05-28.28
No. of reflections collected / observed	5765/5765
Absorption correction	numerical
No. of parameters refined	365
R_1 (observed data)	0.0366
wR_2 (observed data)	0.0965
GooF	0.939
Residual ρ_{min}, ρ_{max} (e/ Å^3)	-1.127, 1.488
Completion until θ = 28.28 (%)	99.5

Crystallographic table 3: [(trpy)Pt(1-mimi)]$(ClO_4)_2$ (**11**).

Compound	$[Hg(9\text{-}MeDP)_2](NO_3)_2 \cdot H_2O$ (**24**)
Empirical formula	$C_{14}H_{16}HgN_8O_7$
Molar weight (g/mol)	608.94
Crystal colour and habit	colourless needles
Solvent	H_2O
Space system	monoclinic
Space group	$P2_1/c$
Cell constants (Å and °)	a = 5.4015(11)
	b = 20.467(4) / β = 97.00(3)
	c = 17.775(4)
Cell volume (Å)	1950.4(7)
Z	4
ρ_{calc} (g/cm^3)	2.074
μ (MoK_α) (1/mm)	7.948
F(000)	1168
Temperature (K)	293(2)
θ range (°)	3.20-27.5
No. of reflections collected / observed	14611/4429
Absorption correction	SADABS
No. of parameters refined	335
R_1 (observed data)	0.032
wR_2 (observed data)	0.042
GooF	0.979
Residual ρ_{min}, ρ_{max} (e/ Å^3)	-0.603, 0.618
Completion until θ = 27.5 (%)	99.2

Crystallographic table 4: $[Hg(9\text{-}MeDP)_2](NO_3)_2 \cdot H_2O$ (**24**).

Compound	1-deazapurine-N9-β-2´-deoxyribonucleoside (**28b**)
Empirical formula	$C_{11}H_{13}N_3O_3$
Molar weight (g/mol)	235.24
Crystal colour and habit	colourless blocks
Solvent	cyclohexane / THF
Space system	orthorhombic
Space group	$P2_12_12_1$
Cell constants (Å and °)	a = 7.1639(11)
	b = 14.921(3)
	c = 20.1672(18)
Cell volume (Å)	2155.7(6)
Z	8
ρ_{calc} (g/cm)	1.450
μ (MoK_α) (1/mm)	0.108
F(000)	992
Temperature (K)	150(2)
θ range (°)	3.02-25.41
No. of reflections collected / observed	2303/2281
Absorption correction	none
No. of parameters refined	385
R_1 (observed data)	0.0295
wR_2 (observed data)	0.0449
GooF	0.593
Residual ρ_{min}, ρ_{max} (e/ Å^3)	-0.176, 0.155
Completion until θ = 25.41 (%)	99.6

Crystallographic table 5: 1-deazapurine-N9-β-2´-deoxyribonucleoside (**28b**).

Compound	1-deazapurine-N7-β-2´-deoxyribonucleoside (**29b**)
Empirical formula	$C_{11}H_{13}N_3O_3$
Molar weight (g/mol)	235.24
Crystal colour and habit	colourless blocks
Solvent	cyclohexane / THF
Space system	orthorhombic
Space group	$C222_1$
Cell constants (Å and °)	a = 7.256(2)
	b = 21.920(5)
	c = 13.741(4)
Cell volume (Å)	2185.5(10)
Z	8
ρ_{calc} (g/cm)	1.430
μ (MoK_α) (1/mm)	0.106
F(000)	992
Temperature (K)	298(2)
θ range (°)	2.96-25.35
No. of reflections collected / observed	1158/1151
Absorption correction	none
No. of parameters refined	181
R_1 (observed data)	0.0347
wR_2 (observed data)	0.0476
GooF	0.758
Residual ρ_{min}, ρ_{max} (e/ Å^3)	-0.106, 0.159
Completion until θ = 25.35 (%)	99.2

Crystallographic table 6: 1-deazapurine-N7-β-2´-deoxyribonucleoside (**29b**).

Compound	1,3-deazapurine-β-2´-deoxyribonucleoside (**30**)
Empirical formula	$C_{12}H_{14}N_2O_3$
Molar weight (g/mol)	234.25
Crystal colour and habit	colourless block
Solvent	CH_3OH
Space system	monoclinic
Space group	$P2_1$
Cell constants (Å and °)	a = 5.8146(5)
	b = 7.8927(14) / β = 94.019(8)
	c = 12.6224(18)
Cell volume (Å)	577.85(35)
Z	2
ρ_{calc} (g/cm)	1.346
μ (MoK_α) (1/mm)	0.098
F(000)	248
Temperature (K)	298(2)
θ range (°)	3.05-25.35
No. of reflections collected / observed	1138/1134
Absorption correction	none
No. of parameters refined	197
R_1 (observed data)	0.0274
wR_2 (observed data)	0.0538
GooF	0.918
Residual ρ_{min}, ρ_{max} (e/ Å^3)	-0.105, 0.111
Completion until θ = 25.35 (%)	99.9

Crystallographic table 7: 1,3-deazapurine-β-2´-deoxyribonucleoside (**30**).

Compound	1-deaza-N3-oxidepurine (**35**)
Empirical formula	$C_6H_9N_3O_3$
Molar weight (g/mol)	171.15
Crystal colour and habit	colourless sticks
Solvent	H_2O
Space system	Orthorhombic
Space group	Pbcn
Cell constants (Å and °)	a = 10.7699(19)
	b = 6.8914(9)
	c = 20.693(18)
Cell volume (Å^3)	1535.9(4)
Z	8
ρ_{calc} (g/cm)	1.480
μ (MoK_α) (1/mm)	1.029
F(000)	720
Temperature (K)	183(2)
θ range (°)	2.92-64.29
No. of reflections collected / observed	4723/968
Absorption correction	numerical
No. of parameters refined	121
R_1 (observed data)	0.0685
wR_2 (observed data)	0.1738
GooF	1.082
Residual ρ_{min}, ρ_{max} (e/ Å^3)	-0.284, 0.243
Completion until θ = 55.94 (%)	96.8

Crystallographic table 8: 1-deaza-N3-oxidepurine (**35**).

Compound	1-deaza-6-nitropurine (**37**)
Empirical formula	$C_6H_4N_4O_2$
Molar weight (g/mol)	164.13
Crystal colour and habit	yellow blocks
Solvent	H_2O
Space system	monoclinic
Space group	$P2_1/c$
Cell constants (Å and °)	a = 11.684(2)
	b = 9.5750(19) / β = 116.53(3)
	c = 7.2052(14)
Cell volume (Å^3)	721.2(2)
Z	4
ρ_{calc} (g/cm)	1.512
μ (MoK_α) (1/mm)	0.119
F(000)	336
Temperature (K)	298(2)
θ range (°)	3.58-26.51
No. of reflections collected / observed	6047/1483
Absorption correction	none
No. of parameters refined	125
R_1 (observed data)	0.0531
wR_2 (observed data)	0.0994
GooF	1.011
Residual ρ_{min}, ρ_{max} (e/ Å^3)	-0.217, 0.191
Completion until θ = 26.51 (%)	99.3

Crystallographic table 9: 1-deaza-6-nitropurine (**35**).

Compound	1-deaza-(6-benzoylamino)-purine-N9-β-2´-deoxyribonucleoside · H_2O (**42I**)
Empirical formula	$C_{18}H_{20}N_4O_5$
Molar weight (g/mol)	372.38
Crystal colour and habit	colourless block
Solvent	iso-propanol
Space system	orthorhombic
Space group	$P2_12_12_1$
Cell constants (Å and °)	a = 6.9486(7)
	b = 9.0272(12)
	c = 27.091(3)
Cell volume (Å)	1699.3(3)
Z	4
ρ_{calc} (g/cm^3)	1.456
μ (MoK_α) (1/mm)	0.108
F(000)	784
Temperature (K)	150(2)
θ range (°)	3.01-25.32
No. of reflections collected / observed	1822/868
Absorption correction	none
No. of parameters refined	306
R_1 (observed data)	0.0303
wR_2 (observed data)	0.0399
GooF	0.705
Residual ρ_{min}, ρ_{max} (e/ Å^3)	-0.162, 0.130
Completion until θ = 25.32 (%)	99.8

Crystallographic table 10: 1-deaza-(6-benzoylamino)-purine-N9-β-2´-deoxyribonucleoside · H_2O (**42I**).

Compound	1-deaza-(6-benzoylamino)-purine-N9-β-2´-deoxyribonucleoside · CH_3OH (**42II**)
Empirical formula	$C_{19}H_{22}N_4O_5$
Molar weight (g/mol)	386.41
Crystal colour and habit	colourless blocks
Solvent	CH_3OH
Space system	monoclinic
Space group	$P2_1$
Cell constants (Å and °)	a = 7.860(2)
	b = 9.194(3) / β = 105.055(16)
	c = 13.385(3)
Cell volume (Å)	934.0(4)
Z	2
ρ_{calc} (g/cm)	1.374
μ (MoK_α) (1/mm)	0.101
F(000)	408
Temperature (K)	298(2)
θ range (°)	3.15-25.37
No. of reflections collected / observed	1802/1797
Absorption correction	none
No. of parameters refined	258
R_1 (observed data)	0.0276
wR_2 (observed data)	0.0385
GooF	0.562
Residual ρ_{min}, ρ_{max} (e/ Å^3)	-0.114, 0.097
Completion until θ = 25.37 (%)	98.1

Crystallographic table 11: 1-deaza-(6-benzoylamino)-purine-N9-β-2´-deoxyribonucleoside · CH_3OH (**42II**).

2 References

(1) Watson, J. D.; Crick, F. H. C. Molecular structure of nucleic acids: a structure for deoxyribose nucleic acid. *Nature* **1953**, *171*, 737-738.

(2) Wilkins, M. H.; Stokes, A. R.; Wilson, H. R. Molecular structure of deoxypentose nucleic acids. *Nature* **1953**, *171*, 738-740.

(3) Franklin, R. E.; Gosling, R. G. Molecular configuration in sodium thymonucleate. *Nature* **1953**, *171*, 740-741.

(4) Bruice, P. Y. *Organic Chemistry*; 2nd ed.; Prentice-Hall, Inc.: New Jersey, 1998; 1256.

(5) Alberts, B.; Johnson, A.; Lewis, J.; Raff, M.; Roberts, K. et al. *Molekularbiologie der Zelle*; Wiley-VCH: Weinheim, 2004.

(6) Breuer, H. *dtv-Atlas zur Chemie*; Deutscher Taschenbuch Verlag: München, 1994.

(7) Müller, J. Metals in Complex Nucleic Acid Structures; Universität Dortmund: Germany, WS 2005/2006.

(8) Hoogsteen, K. Crystal and Molecular Structure of a Hydrogen-Bonded Complex between 1-Methylthymine and 9-Methyladenine. *Acta Crystallographica* **1963**, *16*, 907-908.

(9) Hoogsteen, K. The Structure of Crystals Containing a Hydrogen-Bonded Complex of 1-Methylthymine and 9-Methyladenine. *Acta Crystallographica* **1959**, *12*, 822-823.

(10) Lu, Y. New Transition-Metal-Dependent DNAzymes as Efficient Endonucleases and as Selective Metal Biosensors. *Chem. Eur. J.* **2002**, *8*, 4588-4596.

(11) Gaster, J.; Marx, A. Tuning Single Nucleotide Discrimination in Polymerase Chain Reactions (PCRs): Synthesis of Primer Probes Bearing Polar 4´-C-Modifications and Their Application in Allele-Specific PCR. *Chem. Eur. J.* **2005**, *11*, 1861-1870.

(12) Leumann, C. J. Tuning Molecular Recognition of RNA and DNA via Sugar Modifications. *Chimia* **2005**, *59*, 776-779.

(13) Hatano, A.; Tanaka, K.; Shiro, M.; Shionoya, M. Synthesis of nucleic acid mimics designed for a metal-induced strand formation on DNA. *Tetrahedron* **2002**, *58*, 2965-2972.

(14) Chiba, J. Y.; Tanaka, K.; Ohshiro, Y.; Miyake, R.; Hiraoka, S. et al. Artificial nucleosides possessing metal binding sites at the 3' and 5'-positions of the deoxyribose moieties. *J. Org. Chem.* **2003**, *68*, 331-338.

(15) Höbartner, C.; Rieder, R.; Kreutz, C.; Puffer, B.; Lang, K. et al. Syntheses of RNAs with up to 100 Nucleotides Containing Site-Specific 2´-Methylseleno Labels for use in X-ray Crystallography. *J. Am. Chem. Soc.* **2005**, *127*, 12035-12045.

(16) Eschenmoser, A. Searching for Nucleic Acid Alternatives. *Chimia* **2005**, *59*, 836-850.

(17) Schoning, K. U.; Scholz, P.; Guntha, S.; Wu, X.; Krishnamuthy, R. et al. Chemical Etiology of Nucleic Acid Structure: the α-threofuranosyl-(3´-2´) oligonucleotide system. *Science* **2000**, *290*, 1347-1351.

(18) Zhang, L.; Peritz, A.; Meggers, E. A Simple Glycol Nucleic Acid. *J. Am. Chem. Soc.* **2005**, *127*, 4174-4175.

(19) Zhang, L.; Meggers, E. An Extremely Stable and Orthogonal DNA Base Pair with a Simplified Three-Carbon Backbone. *J. Am. Chem. Soc.* **2005**, *127*, 74-75.

(20) Christensen, U. B.; Pederson, E. B. Intercalating nucleic acids containing insertions of 1-*O*-(1-pyrenylmethyl)glycerol: stabilisation of dsDNA and discrimination of DNA over RNA. *Nucleic Acids Res.* **2002**, *30*, 4918-4925.

(21) Küsel, A.; Zhang, J.; Alvarino Gil, M.; Stückl, A. C.; Meyer-Klaucke, W. et al. Metal Binding Within a Peptide-Based Nucleobase Stack with Tuneable Double-Strand Topology. *Eur. J. Inorg. Chem.* **2005**, 4317-4324.

(22) Achim, C.; Franzini, R.; Watson, R. M.; Patra, G. K. Metal-containing modified peptide nucleic acids. *Abstracts of Papers of the American Chemical Society* **2004**, *227*, U403-U403.

(23) Popescu, D.-L.; Parolin, T. J.; Achim, C. Metal Incorporation in Modified PNA Duplexes. *J. Am. Chem. Soc.* **2003**, *125*, 6354-6355.

(24) Watson, R. M.; Skorik, Y. A.; Patra, G. K.; Achim, C. Influence of metal coordination on the mismatch tolerance of ligand-modified PNA duplexes. *J. Am. Chem. Soc.* **2005**, *127*, 14628-14639.

(25) Nielsen, P. E.; Egholm, M.; Berg, R. H.; Buchardt, O. Sequence-selective recognition of DNA by strand displacement with a thymine-substituted polyamide. *Science* **1991**, *254*, 1497-1500.

(26) Sessler, J. L.; Jayawickramarajah, J. Functionalized base-pairs: versatile scaffolds for self-assembly. *Chem. Commun.* **2005**, 1939-1949.

(27) Haaima, G.; Hansen, H. F.; Christensen, L.; Dahl, O.; Nielsen, P. E. Increased DNA binding and sequence discrimination of PNA oligomers containing 2,6-diamino-purine. *Nucleic Acids Res.* **1997**, *25*, 4639-4643.

(28) Constable, E. C.; Chaurin, V.; Housecroft, C. E.; Wirth, A. In-Strand Metallated Nucleic Acids - Novel Bioinorganic Constructs. *Chimia* **2005**, *59*, 832-835.

(29) Vasella, A. T. Oligonucleosides with Integrated Backbone and Base: Foldamers with a Novel Architecture. *Chimia* **2005**, *59*, 785-793.

(30) Wagenknecht, H.-A. Metallionen-vermittelte DNA-Basenpaarung und Anordnungen von Metallen in künstlicher DNA: auf dem Weg zu neuen Nanobauelementen. *Angew. Chem.* **2003**, *115*, 3322-3324.

(31) Shionoya, M.; Tanaka, K. Artificial metallo-DNA: a bio-inspired approach to metal array programming. *Current Opinion in Chemical Biology* **2004**, *8*, 592-597.

(32) Hunziker, J.; Mathis, G. DNA with Artificial Base Pairs. *Chimia* **2005**, *59*, 780-784.

(33) Liu, H.; Gao, J.; Maynard, L.; Saito, Y. D.; Kool, E. T. Toward a New Genetic System with Expanded Dimensions: Size-Expanded Analogues of Deoxyadenosine and Thymidine. *J. Am. Chem. Soc.* **2004**, *126*, 1102-1109.

(34) Liu, H.; Gao, J.; Kool, E. T. Helix-Forming Properties of Size-Expanded DNA, an Alternative Four-Base Genetic Form. *J. Am. Chem. Soc.* **2005**, *127*, 1396-1402.

(35) Lee, A. H. F.; Kool, E. T. A New Four-Base Genetic Helix, yDNA, Composed of Widened Benzopyrimidine. *J. Am. Chem. Soc.* **2005**, *127*, 3332-3338.

(36) Gao, J.; Liu, H.; Kool, E. T. Expanded-Size in Naturally Sized DNA: Evaluation of Steric Effects in Watson-Crick Pairing. *J. Am. Chem. Soc.* **2004**, *126*, 11826-11831.

(37) Ishiyama, K.; Smyth, G. E.; Ueda, T.; Masutomi, Y.; Ohgi, T. et al. Homo-*N*-oligonucleotides (N1/N9-C1´ Methylene Bridge Oligonucleotides): Nucleic Acids with Left-Handed Helicity. *J. Am. Chem. Soc.* **2004**, *126*, 7476-7485.

(38) Crey-Desbiolles, C.; Lhomme, J.; Dumy, P.; Kotera, M. 3-Nitro-3-deaza-2´-deoxyadenosine as a Versatile Photocleavable 2´-Deoxyadenosine Mimic. *J. Am. Chem. Soc.* **2004**, *126*, 9532-9533.

(39) Greco, N. J.; Tor, Y. Simple Fluorescent Pyrimidine Analogues Detect the Presence of DNA Abasic Sites. *J. Am. Chem. Soc.* **2005**, *127*, 10784-10785.

(40) Okamoto, A.; Tanaka, K.; Fukuta, T.; Saito, I. Design of Base-Discriminating Fluorescent Nucleoside and Its Application to T/C SNP Typing. *J. Am. Chem. Soc.* **2003**, *125*, 9296-9297.

(41) Okamoto, A.; Tanaka, K.; Saito, I. Rational Design of a DNA Wire Possessing an Extremely High Hole Transport Ability. *J. Am. Chem. Soc.* **2003**, *125*, 5066-5071.

(42) Seela, F.; Lindner, M.; Glacon, V.; Lin, W. Q. Pyrazolo[3,4-d][1,2,3]triazine DNA: Synthesis and base pairing of 7-deaza-2,8-diaza-2 '-deoxyadenosine. *J. Org. Chem.* **2004**, *69*, 4695-4700.

(43) Lai, J. L.; Kool, E. T. Fluorous Base-Pairing Effects in a DNA Polymerase Active Site. *Chem. Eur. J.* **2005**, *11*, 2966-2971.

(44) Lai, J. L.; Kool, E. T. Selective Pairing of Polyfluorinated DNA Bases. *J. Am. Chem. Soc.* **2004**, *126*, 3040-3041.

(45) Zahn, A.; Brotschi, C.; Leumann, C. J. Pentafluorophenyl-Phenyl Interactions in Biphenyl-DNA. *Chem. Eur. J.* **2005**, *11*, 2125-2129.

(46) Gao, J.; Strässler, C.; Tahmassebi, D.; Kool, E. T. Libraries of Composite Polyfluors Built from Fluorescent Deoxyribosides. *J. Am. Chem. Soc.* **2002**, *124*, 11590-11591.

(47) Gao, J.; Watanabe, S.; Kool, E. T. Modified DNA Analogues That Sense Light Exposure with Color Changes. *J. Am. Chem. Soc.* **2004**, *126*, 12748-12749.

(48) Matsuda, S.; Henry, A. A.; Schultz, P. G.; Romesberg, F. E. The Effect of Minor-Groove Hydrogen-Bond Acceptors and Donors on the Stability and Replication of Four Unnatural Base Pairs. *J. Am. Chem. Soc.* **2003**, *125*, 6134-6139.

(49) Francis, A. W.; Helquist, S. A.; Kool, E. T.; David, S. D. Probing the Requirements for Recognition and Catalysis in Fpg and MutY with Nonpolar Adenine Isosteres. *J. Am. Chem. Soc.* **2003**, *125*, 16235-16242.

(50) Langenegger, S. M.; Bianke, G.; Tona, R.; Häner, R. DNA Mimics Containing Non-Nucleosidic Base Surrogates. *Chimia* **2005**, *59*, 794-797.

(51) Zimmermann, N.; Meggers, E.; Schultz, P. G. A second-generation copper(II)-mediated metallo-DNA-base pair. *Bioorg. Chem.* **2004**, *32*, 13-25.

(52) Switzer, C.; Sinha, S.; Kim, P. H.; Heuberger, B. D. A Purine-like Nickel(II) Base Pair for DNA. *Angew. Chem.* **2005**, *117*, 1553-1556.

(53) Clever, G. H.; Polborn, K.; Carell, T. Ein hochgradig DNA-Duplex-stabilisierendes Metall-Salen-Basenpaar. *Angew. Chem.* **2005**, *117*, 7370-7374.

(54) Tanaka, K.; Shionoya, M. Synthesis of a Novel Nucleoside for Alternative DNA Base Pairing through Metal Complexation. *J. Org. Chem.* **1999**, *64*, 5002-5003.

(55) Shionoya, M.; Tanaka, K. Synthetic Incorporation of Metal Compexes into Nucleic Acids and Peptides Directed toward Functionalized Molecules. *Bull. Chem. Soc. Jpn.* **2000**, *73*, 1945-1954.

(56) Meggers, E.; Holland, P. L.; Tolman, W. B.; Romesberg, F. E.; Schultz, P. G. A Novel Copper-Mediated DNA Base Pair. *J. Am. Chem. Soc.* **2000**, *122*, 10714-10715.

(57) Tanaka, K.; Tasaka, M.; Cao, H.; Shionoya, M. An approach to metal-assisted DNA base pairing: novel β-*C*-nucleosides with a 2-aminophenol or a catechol as the nucleobase. *Eur. J. Pharm. Sci.* **2001**, *13*, 77-83.

(58) Atwell, S.; Meggers, E.; Spraggon, G.; Schultz, P. G. Structure of a Copper-Mediated Base Pair in DNA. *J. Am. Chem. Soc.* **2001**, *123*, 12364-12367.

(59) Weizman, H.; Tor, Y. Oligo-ligandosides: a DNA mimetic approach to helicate formation. *Chem. Commun.* **2001**, 453-454.

(60) Weizman, H.; Tor, Y. 2,2´-Bipyridine Ligandoside: A Novel Building Block for Modifying DNA with Intra-Duplex Metal Complexes. *J. Am. Chem. Soc.* **2001**, *123*, 3375-3376.

(61) Tanaka, K.; Tasaka, M.; Cao, H.; Shionoya, M. Toward Nano-assembly of Metals Through Engineered DNAs. *Supramolecular Chemistry* **2002**, *14*, 225-261.

(62) Tanaka, K.; Yamada, Y.; Shionoya, M. Formation of Silver(I)-Mediated DNA Duplex and Triplex through Alternative Base Pair of Pyridine Nucleobases. *J. Am. Chem. Soc.* **2002**, *124*, 8802-8803.

(63) Zimmermann, N.; Meggers, E.; Schultz, P. G. A Novel Silver(I)-Mediated DNA Base Pair. *J. Am. Chem. Soc.* **2002**, *124*, 13684-13685.

(64) Mancin, F.; Chin, J. An Artificial Guanine that Binds Cytidine through the Cooperative Interaction of Metal Coordination and Hydrogen Bonding. *J. Am. Chem. Soc.* **2002**, *124*, 10946-10947.

(65) Switzer, C.; Shin, D. A pyrimidine-like nickel(II) DNA base pair. *Chem. Commun.* **2005**, 1342-1344.

(66) Tanaka, K.; Tengeiji, A.; Kato, T.; Toyama, N.; Shionoya, M. A Discrete Self-Assembled Metal Array in Artificial DNA. *Science* **2003**, *299*, 1212-1213.

(67) Tanaka, K.; Tengeiji, A.; Kato, T.; Toyama, N.; Shiro, M. et al. Efficient Incorporation of a Copper Hydroxypyridone Base Pair in DNA. *J. Am. Chem. Soc.* **2002**, *124*, 12494-12498.

(68) Rakitin, A.; Aich, P.; Papadopoulos, C.; Kobzar, Y.; Vedeneev, A. S. et al. Metallic Conduction through Engineered DNA: DNA Nanoelectronic Building Blocks. *Phys. Rev. Lett.* **2001**, *86*, 3670-3673.

(69) Robertson, N.; McGowan, C. A. A comparison of potential molecular wires as components for molecular electronics. *Chem. Soc. Rev.* **2003**, *32*, 96-103.

(70) Carell, T.; Behrens, C.; Gierlich, J. Electrontransfer through DNA and metal-containing DNA. *Org. Biomol. Chem.* **2003**, *1*, 2221-2228.

(71) Koren, A. O.; Gaponik, P. N. Selective N(2) Alkylation of Tetrazole and 5-Substituted Tetrazoles by Alcohols. *Chem. Heterocycl. Compd.* **1990**, 1366-1377.

(72) Bergtrup, M.; Larsen, P. Alkylation, Acylation and Silylation of Azoles. *Acta Chem. Scand.* **1990**, 1050-1057.

(73) Annibale, G.; Brandolisio, M.; Pitteri, B. New Routes for the Synthesis of Chloro-(diethylenetriamine)platinum(II)chloride and Chloro(2,2´:6´,2´´-terpyridine)platinum(II)chloride dihydrate. *Polyhedron* **1995**, 451-453.

(74) Drew, D.; Doyle, J. R. Cyclic diolefin complexes of platinum and palladium. *Inorg. Synth.* **1990**, *28*, 346-349.

(75) Müller, J.; Freisinger, E.; Lax, P.; Megger, D.; Polonius, F.-A. Interaction of Pd(II) and Pt(II) complexes of terpyridine with 1-methylazoles: a combined experimental and density functional study. *Inorg. Chim. Acta, accepted for publication*.

(76) Cosar, S.; Janik, M. B. L.; Flock, M.; Freisinger, E.; Farkas, E. et al. Mono- and di-nuclear complexes of (trpy)M^{II} (M = Pd, Pt) with the model nucleobase 1-methylcytosine. Crystal structure and NMR solution studies. *J. Chem. Soc., Dalton Trans.* **1999**, 2329-2336.

(77) Lax, P. Nucleobase-Quartette und ihre Wechselwirkungen mit Metallen und Pt(II)-Komplexen. In *(vorgelegte) Dissertation*; Universität Dortmund: Germany, 2006.

(78) Armspach, D.; Constable, E. C.; Diederich, F.; Housecroft, C. E.; Nierengarten, J.-F. Bucky Ligands: Synthesis, Ruthenium(II) Complexes, and Electrochemical Properties. *Chem. Eur. J.* **1998**, *4*, 723-733.

(79) Potts, K. T.; Usifer, D. A.; Guadalupe, A.; Abruna, H. D. 4-Vinyl-, 6-Vinyl-, and 4´-Vinyl-2,2´:6´,2´´-terpyridinyl Ligands: Their Synthesis and Electrochemistry of Their Transition-Metal Coordination Complexes. *J. Am. Chem. Soc.* **1987**, *109*, 3961-3967.

(80) Wichai, U.; Woski, S. A. Disiloxane-Protected 2-Deoxyribonolactone as an Efficient Precursor to 1,2-Dideoxy-1-β-aryl-D-ribofuranoses. *Org. Lett.* **1999**, *1*, 1173-1175.

(81) Wichai, U.; Woski, S. A. An Improved Route to 1,2-dideoxy-β-1-phenyl-D-ribofuranose. *Bioorg. Med. Chem. Lett.* **1998**, *8*, 3465-3468.

(82) Reese, C. B.; Wu, Q. Conversion of 2-deoxy-D-ribose into 2-amino-5-(2-deoxy-β-D-ribofuranosyl)pyridine, 2´-deoxypseudouridine, and other C-(2´-deoxyribonucleosides). *Org. Biomol. Chem.* **2003**, *1*, 3160-3172.

(83) Padilla-Tosta, M. E.; Lloris, J. M.; Martinez-Manez, R.; Benito, A.; Soto, J. et al. Bis(terpyridyl)-Ruthenium(II) Units Attached to Polyazacycloalkanes as Sensing Fluorescent Receptors For Transition Metal Ions. *Eur. J. Inorg. Chem.* **2000**, 741-748.

(84) Collin, J.-P.; Anthony, H.; Heitz, V.; Odobel, F.; Sauvage, J.-P. Photoinduced Electron- and Energy-Transfer Processes Occuring within Porphyrin-Metal-Bisterpyridyl Conjugates. *J. Am. Chem. Soc.* **1994**, *116*, 5679-5690.

(85) Acevedo, O. L.; Andrews, R. S. Synthesis of Propane-2,3-diol Combinatorial Monomers. *Tetrahedron Letters* **1996**, *37*, 3931-3934.

(86) Heller, M.; Schubert, U. S. Multi-functionalized 2,2´:6´,2´´-Terpyridines. *Synlett* **2002**, *5*, 751-754.

(87) Heller, M.; Schubert, U. S. Functionalized 2,2´-Bipyridines and 2,2´:6´,2´´-Terpyridines via Stille-Type Cross-Coupling Procedures. *J. Org. Chem.* **2002**, *67*, 8269-8272.

(88) Lützen, A.; Hapke, M. Synthesis of 5-Substituted 2,2´-Bipyridines from Substituted 2-Chloropyridines by a Modified Negishi Cross-Coupling Reaction. *Eur. J. Org. Chem.* **2002**, 2292-2297.

(89) Savage, S. A.; Smith, A. P.; Fraser, C. L. Efficient Synthesis of 4-, 5-, and 6-Methyl-2,2´-bipyridine by a Negishi Cross-Coupling Strategy Followed by High-Yield Conversion to Bromo- and Chloromethyl-2,2´-bipyridines. *J. Org. Chem.* **1998**, *63*, 10048-10051.

(90) Schubert, U. S.; Eschbaumer, C.; Heller, M. Stille-Type Cross-Coupling - An Efficient Way to Various Symmetrically and Unsymmetrically Substituted Methyl-Bipyridines: Toward New ATRP Catalysts. *Org. Lett.* **2000**, *2*, 3373-3376.

(91) Mack, A. G.; Suschitzky, H.; Wakefield, B. J. Polyhalogenoaromatic Compounds. Part39. Synthesis of the Bromo- and Iodo-tetrachloropyridines. *J. Chem. Soc., Perkin Trans. 1* **1978**, *6*, 1472-1474.

(92) Müller, J.; Böhme, D.; Lax, P.; Morell Cerda, M.; Roitzsch, M. Metal Ion Coordination to Azole Nucleosides. *Chem. Eur. J.* **2005**, *11*, 6246-6253.

(93) Seela, F.; T., W. Hoogsteen-Duplex: Synthesis and Base Pairing of Oligonucleotides Containing 1-Deaza-2´deoxyadenosine. *Helv. Chim. Acta* **1994**, *77*, 1485-1499.

(94) Wu, Y.; Fa, M.; Tae, E. L.; Schultz, P. G.; Romesberg, F. E. Enzymatic Phosphorylation of Unnatural Nucleosides. *J. Am. Chem. Soc.* **2002**, *124*, 14626-14630.

(95) Narukulla, R.; Xu, Y.-Z.; Shuker, D. E. Synthesis, characterization and properties of potentially mutagenic novel DNA bases of natural origin. *Abstracts of Papers of the American Chemical Society, 228th ACS National Meeting* **2004**, TOXI-105.

(96) Müller, J.; Polonius, F.-A.; Roitzsch, M. [Hg(9-methyl-1-deazapurine)$_2$]$(NO_3)_2 * H_2O$: a complex with a distorted hexagonal bipyramidal metal ion coordination sphere. *Inorg. Chim. Acta* **2005**, *358*, 1225-1230.

(97) Sletten, E.; Nerdal, W. Interaction of Mercury with Nucleic Acids and Their Components. *Metal Ions in Biological Systems*; Marcel Dekker, Inc.: New York, 1997; pp 479-501.

(98) Grdenic, D. The structural chemistry of mercury. *Q. Rev. Chem. Soc.* **1965**, *19*, 303-328.

(99) Onyido, I.; Norris, A. R.; Buncel, E. Biomolecule-Mercury Interactions: Modalities of DNA Base-Mercury Binding Mechanisms. Remediation Strategies. *Chem. Rev.* **2004**, *104*, 5911-5929.

(100) Simpson, R. B. Association Constants of Methylmercuric and Mercuric Ions with Nucleosides. *J. Am. Chem. Soc.* **1964**, *86*, 2059-2065.

(101) Kosturko, L. D.; Folzer, C.; Stewart, R. F. The Crystal and Molecular Structure of a 2:1 Complex of 1-Methylthymine-Mercury(II). *Biochemistry* **1974**, *13*, 3949-3952.

(102) Zamora, F.; Sabat, M.; Lippert, B. A bis(9-methyladeninium) complex of Hg(II) with a highly irregular coordination geometry: [Hg(9-MeAH-*N7*)$_2$(H_2O)$(NO_3)_3$]ClO_4. *Inorg. Chim. Acta* **1998**, *267*, 87-91.

(103) Graves, B. J.; Hodgson, D. J. Metal Ion Interactions with 8-Azapurines. Synthesis and Structure of Dichlorobis(8-azaadenine)mercury(II) and Tetraaquabis(8-azahypoxanthinato)mercury(II). *Inorg. Chem.* **1981**, *20*, 2223-2229.

(104) Norris, A. R.; Kumar, R. ^{199}Hg NMR Correlations in Methylmercury(II) Complexes of Nucleic Acid Constituents and Their Analogs. *Inorg. Chim. Acta* **1984**, *93*, L63-L65.

(105) Menzer, S.; Hillgeris, E. C.; Lippert, B. $HgCl_2$ coordination to guanine derivatives: structural and spectroscopic studies on the interactions with 9-ethylguanine, 1,9-dimethylguanine and 2-amino-6-methoxy-9-methylpurine (6,9-dimethylguanine). *Inorg. Chim. Acta* **1993**, *211*, 221-226.

(106) Antonini, I.; Cristalli, G.; Franchetti, P.; Grifantini, M.; Martelli, S. et al. Deaza Analogues of Adenosine as Inhibitors of Blood Platelet Aggregation. *J. Pharm. Sci.* **1984**, *73*, 366-368.

(107) Petrow, V.; Saper, J. Some 5-Azaquinoxalines and 4-Azabenziminazoles. *J. Chem. Soc.* **1948**, 1389-1392.

(108) Middleton, R. W.; Wibberley, G. Synthesis of Imidazo[4,5-*b*]- and [4,5-*c*]pyridines. *J. Heterocyclic Chem.* **1980**, *17*, 1757-1760.

(109) Gonnella, N. C.; Roberts, J. D. Studies of Tautomerism of Purine and the Protonation of Purine and Its 7- and 9-methyl Derivatives by Nitrogen-15 Nuclear Magnetic Resonance Spectroscopy. *J. Am. Chem. Soc.* **1982**, *104*, 3162-3164.

(110) Itoh, T.; Ono, K.; Sugawara, T.; Mizuno, Y. Studies on the Chemical Synthesis of Potential Antimetabolites. 30. Regioselective Introduction of a Chlorine Atom into the Imidazo[4,5-*b*]pyridine Nucleus (1). *J. Heterocyclic Chem.* **1982**, *19*, 513-517.

(111) Itoh, T.; Kitano, S.; Mizuno, Y. Synthetic Studies of Potential Antimetabolites. XIII. Synthesis of 7-Amino-3-β-D-ribofuranosyl-3*H*-imidazo[4,5-*b*] pyridine (1-deazaadenosine) and Related Nucleosides (1a). *J. Heterocyclic Chem.* **1972**, *9*, 465-470.

(112) Mizuno, Y.; Ikehara, M.; Itoh, T.; Saito, K. Studies on Condensed Systems of Aromatic Nitrogenous Series. XXII. Structural Studies of β-D-Ribofuranosylimidazopyridines. *J. Org. Chem.* **1963**, *28*, 1837-1841.

(113) Wenzel, T.; Seela, F. Synthesis of 6-Substituted 1-Deazapurine 2´-Deoxyribonucleosides. *Helv. Chim. Acta* **1996**, *79*, 169-178.

(114) Müller, J.; Drumm, M.; Boudvillain, M.; Leng, M.; Sletten, E. et al. Parallel-stranded DNA with Hoogsteen base pairing stabilized by a *trans*-$[Pt(NH_3)_2]^{2+}$ cross-link: characerization and conversion into a homodimer and a triplex. *J. Biol. Inorg. Chem.* **2000**, *5*, 603-611.

(115) Lüth, M. S.; Freisinger, E.; Glahé, F.; Lippert, B. Mixed Adenine, Guanine Nucleobase Quartets: Metal-Modified Forms of an Open U and a Closed Rectangle. *Inorg. Chem.* **1998**, *37*, 5044-5045.

(116) Müller, J.; Zangrando, E.; Pahlke, N.; Freisinger, E.; Randaccio, L. et al. Affinity of the Iminooxo Tautomer Anion of 1-Methylcytosine in *trans*-$[Pt(NH_3)_2(1\text{-MeC-}N4)_2]^{2+}$ for Heterometals. *Chem. Eur. J.* **1998**, *4*, 397-405.

(117) Canty, A. J.; Deacon, G. B. The van der Waals Radius of Mercury. *Inorg. Chim. Acta* **1980**, *45*, L225-L227.

(118) Kleywegt, G. J.; Wiesmeijer, W. G. R.; Van Driel, G. J.; Driessen, W. L.; Reedijk, J. et al. Unidentate versus Symmetrically and Unsymmetrically Bidentate Nitrate Co-ordination in Pyrazole-containing Chelates. The Crystal and Molecular Structures of (Nitrato-*O*)[tris(3,5-dimethylpyrazole-1-yl-methyl)amine]copper(II) Nitrate, (Nitrato-*O*,*O*')[tris(3,5-dimethylpyrazole-1-yl-methyl)amine]nickel(II) Nitrate, and (Nitrato-*O*)(nitrato-*O*,*O*')[tris(3,5-dimethylpyrazole-1-yl-methyl)amine]cadmium(II). *J. Chem. Soc., Dalton Trans.* **1985**, 2177-2184.

(119) Viossat, B.; Khodadad, P.; Rodier, N. Structure of aqua(4-aza-1-azoniabicyclo[2.2.2]octane)trinitratocadmium(II), $Cd(C_6H_{13}N_2)(H_2O)(NO_3)_3$. *Acta Crystallogr.* **1984**, *C40*, 24-28.

(120) Nardelli, M.; Pelizzi, C.; Pelizzi, G.; Tarasconi, P. Chemical and structural aspects of silver-triphenylarsine complexes and silver-tin complex salts. *J. Chem. Soc., Dalton Trans.* **1985**, 321-331.

(121) Pelizzi, C.; Pelizzi, G.; Tarasconi, P. Synthesis and crystal and molecular structure of a silver tin complex salt, $[Ag(PPh_3)_4][SnPh_2(NO_3)_2(Cl,NO_3)]$. *J. Organomet. Chem.* **1984**, *277*, 29-35.

(122) Bhat, C. C. 2-Deoxy-3,5-di-*O*-*p*-toluoyl-D-*erythro*-pentosyl Chloride. *Synthetic Procedures in Nucleic Acid Chemistry*; Wiley: New York, 1968; pp 521-522.

(123) Hoffer, M. α-Thymidin. *Chem. Ber.* **1960**, *93*, 2777-2781.

(124) Rolland, V.; Kotera, M.; Lhomme, J. Convenient preparation of 2-Deoxy-3,5-di-O-*p*-toluoyl-α-D-*erythro*-pentofuranosyl chloride. *Synth. Comm.* **1997**, *27*, 3505-3511.

(125) Montgomery, J. A.; Hewson, K. 1-Deaza-6-methylthiopurine Ribonucleoside. *J. Med. Chem.* **1966**, *9*, 354-357.

(126) de Roos, K. B.; Salemink, C. A. Deazapurine Derivatives. VIII. Synthesis of 7-substituted 3-β-D-ribofuranosylimidazo[4,5-*b*] pyridines: 1-deazaadenosine and related compounds. **1971**, *90*, 654-662.

(127) Gerbersmann, O. Zur Verwendung von Benzimidazol-Nukleosid in metallmodifizierten Oligonukleotiden. In *Diplomarbeit*; der Universität Dortmund, 2005.

(128) Markley, J. L.; Bax, A.; Arata, Y.; Hilbers, C. W.; Kaptein, R. et al. Recommendations for the Presentation of NMR Structures of Proteins and Nucleic Acids. *Pure & Appl. Chem.* **1998**, *70*, 117-142.

(129) Catalan, J.; Claramunt, R. M.; Elguero, J.; Laynez, J.; Menendez, M. et al. Basicity and Acidity of Azoles - the Annelation Effect in Azoles. *J. Am. Chem. Soc.* **1988**, *110*, 4105-4111.

(130) Kapinos, L. E.; Song, B.; Sigel, H. Metal ion-coordinating properties of imidazole and derivatives in aqueous solution: interrelation between complex stability and ligand basicity. *Inorg. Chim. Acta* **1998**, *280*, 50-56.

(131) Gabryszewski, M. The complexing behaviour of some alkyl and amino derivatives of 1,2,4-triazole in aqueous solution. *Pol. J. Chem.* **1992**, *66*, 1067-1075.

(132) Ostrovskii, V. A.; Koldobskii, G. I.; Shirokova, N. P.; Poplavskii, V. S. Acid-Base Properties Of 5-Substituted Tetrazoles. *Chem. Heterocycl. Compd.* **1981**, 412-416.

(133) Lippert, B. Alterations of Nucleobase pK_a Values upon Metal Coordination: Origins and Consequences. *Progress in Inorganic Chemistry*; Wiley-VCH: Weinheim, 2005; pp 385-447.

(134) Connors, K. A. *Binding Constants. The Measurement of Molecular Complex Stability*; Wiley: New York, 1987.

(135) Job, P. Recherches Sur La Formation De Complexes Nineraux En Solution, Et Sur Leur Stabilite. *Ann. Chim.* **1928**, *9*, 113-203.

(136) Fielding, L. Determination of association constants (K-a) from solution NMR data. *Tetrahedron* **2000**, *56*, 6151-6170.

(137) Likussar, W.; Boltz, D. F. Theory of Continuous Variations Plots and a New Method for Spectrophotometric Determination of Extraction and Formation Constants. *Analytical Chemistry* **1971**, *43*, 1265-1266.

(138) Hynes, M. J. Eqnmr - a Computer-Program for the Calculation of Stability-Constants from Nuclear-Magnetic-Resonance Chemical-Shift Data. *J. Chem. Soc., Dalton Trans.* **1993**, 311-312.

(139) Lenarcik, B.; Maciejewski, W. Complex Forming Capacity of Benzimidazole and 4-azabenzimidazole in Aqueous Solutions. *Pol. J. Chem.* **1981**, *55*, 31-38.

(140) Rettig, S. J.; Sanchez, V.; Storr, A.; Thompson, R. C.; Trotter, J. Polybis(4-azabenzimidazolato)-iron(II) and cobalt(II) 3-D single diamond-like framework materials which exhibit spin canting and ferromagnetic ordering at low temperatures. *J. Chem. Soc., Dalton Trans.* **2000**, 3931-3937.

(141) Seela, F.; Wenzel, T. 1,7-Dideaza-2´-deoxyadenosine: Building Blocks for Solid-Phase Synthesis and Secondary Structure of Base-Modified Oligodeoxyribonucleotides. *Helv. Chim. Acta* **1992**, *75*, 1111-1122.

(142) Seela, F.; Wenzel, T. Oligodeoxyribonucleotides Containing 4-Aminobenzimidazole in Place of Adenine: Solid-Phase Synthesis and Base Pairing. *Helv. Chim. Acta* **1995**, *78*, 833-846.

(143) Seela, F.; Leonard, P. N^7-DNA: Base-Pairing Properties of N^7-(2´-Deoxy-β-D-erythro-pentofuranosyl)-Substituted Adenine, Hypoxanthine, and Guanine in Duplexes with Parallel Chain Orientation. *Helv. Chim. Acta* **1998**, *81*, 2244-2263.

(144) Seela, F.; Debelak, H.; Usman, N.; Burgin, A.; Beigelman, L. 1-Deazaadenosine: synthesis and activity of base-modified hammerhead ribozymes. *Nucleic Acids Res.* **1998**, *26*, 1010-1018.

(145) Seela, F.; Becher, G. Pyrazolo[3,4-*d*]pyrimidine nucleic acids: adjustment of dA-dT to dG-dC base pair stability. *Nucleic Acids Res.* **2001**, *29*, 2069-2078.

(146) Debalek, H. Deazapurin-Nucleoside und Oligonucleotide: Synthese, Basenpaarung und katalytische Aktivität. In *Doktorarbeit*; an der Universität Osnabrück, 2001; pp 93.

(147) Böhme, D.; Düpre, N. persönliche Mitteilung, 2006.

(148) Ono, A.; Togashi, H. Highly selective Oligonucleotide-Based Sensor for Mercury(II) in Aqueous Solutions. *Angew. Chem.* **2004**, *116*, 4400-4402.

(149) Frøystein, N. Å.; Sletten, E. Interaction of Mercury(II) with the DNA Dodecamer CGCGAATTCGCG. A ^{1}H and ^{15}N NMR Study. *J. Am. Chem. Soc.* **1994**, *116*, 3240-3250.

(150) Kuklenyik, Z.; Marzilli, L. G. Mercury(II) Site-Selective Binding to a DNA Hairpin. Relationship of Sequence-Dependent Intra- and Interstrand Cross-Linking to the Hairpin-Duplex Conformational Transition. *Inorg. Chem.* **1996**, *35*, 5654-5662.

(151) Miyake, Y.; Togashi, H.; Tashiro, M.; Yamaguchi, H.; Oda, S. et al. Mercury^{II}-Mediated Formation of Thymine-Hg^{II}-Thymine Base Pairs in DNA Duplexes. *J. Am. Chem. Soc.* **2006**, *128*, 2172-2173.

(152) Gray, D. M.; Hung, S.-H.; Vaughan, M. R. Circular Dichroism Spectroscopy of DNA. *Methods in Enzymology*; Academic Press, Inc.: San Diego New York Boston London Sydney Tokyo Toronto, 1992; pp 389-406.

(153) Gray, D. M.; Hung, S.-H.; Johnson, K. H. Absorption and Circular Dichroism Spectroscopy of Nucleic Acid Duplexes and Triplexes. *Methods in Enzymology*; Academic Press, Inc.: San Diego New York Boston London Sydney Tokyo Toronto, 1995; pp 19-34.

(154) Ho, H.-A.; Bera-Aberem, M.; Leclerc, M. Optical Sensors Based on Hybrid DNA/Conjugated Polymer Complexes. *Chem. Eur. J.* **2005**, *11*, 1718-1724.

(155) Jain, P. C.; Chattejee, S. K.; Anand, N. Potential Purine Antagonists: Part VII-Synthesis of 3-β-D-Ribofuranosyl-7-aminoimidazo(4,5-*b*)pyridine (1-Deazaadenosine). *Indian J. Chem.* **1966**, *4*, 403-405.

(156) Cristalli, G.; Franchetti, P.; Grifantini, M.; Vittori, S.; Bordoni, T. et al. Improved Synthesis and Antitumor Activity of 1-Deazaadenosine. *J. Med. Chem.* **1987**, *30*, 1686-1688.

(157) Watson, D. G.; Sweet, R. M.; Marsh, R. E. Crystal and Molecular Structure of Purine. *Acta Cryst.* **1965**, *19*, 573-580.

(158) Müller, J.; Gil Bardaji, E.; Polonius, F.-A. 6-Nitro-1-deazapurine. *Acta Crystallogr.* **2006**, *E62*, o223-o225.

(159) Cristalli, G.; Vittori, S.; Eleuteri, A.; Grifantini, M.; Volpini, R. et al. Purine and 1-Deazapurine Ribonucleosides and Deoxyribonucleosides: Synthesis and Biological Activity. *J. Med. Chem.* **1991**, *34*, 2226-2230.

(160) Devlin, T. A.; Lacrosaz-Rouanet, E.; Vo, D.; Jebaratnam, D. J. Glycosylation Reactions of 6-Nitro-1,3-dideazapurine and 6-Nitro-1-deazapurine. *Tetrahedron Letters* **1995**, *36*, 1601-1604.

(161) Itoh, T.; Sugawara, T.; Mizuno, Y. A Novel Synthesis of 1-Deazaadenosine. *Heterocycles* **1982**, *17*, 305-309.

(162) Seela, F.; Wenzel, T. 1-Deaza-2´-deoxyadenosine: Phosphonate and Phosphoramidite Building Blocks for Solid-phase Oligonucleotide Synthesis. *Heterocycles* **1993**, *36*, 237-242.

(163) Jenkins, S. R.; Holly, F. W.; Robins, R. K. 4-Amino-1-(β-D-ribofuranosyl)benzimidazole. *J. Med. Chem.* **1968**, *11*, 910.

(164) Seela, F.; Debelak, H.; Reuter, H.; Kastner, G.; Mikhailopulo, I. A. Different Conformations of 1-Deazaadenosine and its 2´-Deoxyribonucleoside in the Solid State and in Solution. *Tetrahedron* **1999**, *55*, 1295-1308.

(165) Frisch, M. J.; Trucks, G. W.; Schlegel, H. B.; Scuseria, G. E.; Robb, M. A. et al. *Gaussian 98, Revision A.7*; Gaussian, Inc.: Pittsburgh PA.

(166) Mikhailopoulo, I. A.; Kalinichenko, E. N.; Podkopaeva, T. L.; Wenzel, T.; Rosemeyer, H. et al. Synthesis of 1-Deazaadenosine Analogues of (2´-5´) ApApA. *Nucleos. Nucleot.* **1996**, *15*, 445-464.

(167) Seela, F.; Wenzel, T.; Debelak, H. Hoogsteen-Duplex DNA: Synthesis and Base Pairing of Oligo-deoxynucleotides Containing 1-Deaza-2´deoxyadenosine. *Nucleos. Nucleot.* **1995**, *14*, 957-960.

(168) Ohkubo, A.; Sakamoto, K.; Miyata, K.; Taguchi, H.; Seio, K. et al. Convenient synthesis of N-unprotected deoxynucleoside 3 '-phosphoramidite building blocks by selective deacylation of N-acylated species and their facile conversion to other N-functionalized derivatives. *Organic Letters* **2005**, *7*, 5389-5392.

(169) Seela, F.; Debalek, H. Parallel-Stranded DNA Formed by 1-Deazaadenine or 7-Deazaguanine Homo Base Pairs Incorporated in the Duplex of 5´-d[(G-A)$_7$-G]. *Collection of Symposium Series* **1999**, *2*, 316-319.

(170) Lumry, R.; Smith, E. L.; Glantz, R. R. Kinetics of Carboxypeptidase Action. I. Effect of Various Extrinsic Factors on Kinetic Parameters. *J. Am. Chem. Soc.* **1951**, *73*, 4330-4340.

(171) Martin, R. B. Deuterated water effects on acid ionization constants. *Science* **1963**, *139*, 1198-1203.

(172) Otwinowsky, Z.; Minor, W. DENZO and SCALEPACK. *Methods Enzymol* **1997**, *276*, 307.

(173) Sheldrick, G. M. *SHELXTL-PLUS (VMS)*; Siemens Analytical X-ray Instruments: Madison, WI.

(174) Sheldrick, G. M. *SHEL-97, Program for the Refinement of Crystal Structures*; University of Göttingen: Germany.

(175) Farrugia, L. J. Windows programs for the solution, refinement and analysis of single crystal X-ray diffraction data. *J. Appl. Cryst.* **1999**, *32*, 837.

3 List of the Compounds Discussed in this Thesis

Synthesised Compounds

(**1**) 1-methylimidazole (1-mimi)

(**2**) 1-methyltetrazole (1-mtet)

(**3**) 2-methyltetrazole (2-mtet)

(**4**) $[(trpy)PdCl]Cl \cdot 2H_2O$

(**5**) $[(trpy)PtCl]Cl \cdot 2H_2O$

(**6**) $[(trpy)_2Pd_2(1\text{-mtetate})](ClO_4)_3$

(**7**) $[(trpy)Pt(1\text{-mtetate})](ClO_4)$

(**8**) $[(trpy)Pd(2\text{-mtet})](ClO_4)_2$

(**9**) $[(trpy)Pt(2\text{-mtet})](ClO_4)_2$

(**10**) $[(trpy)Pd(1\text{-mimi})](ClO_4)_2$

(**11**) $[(trpy)Pt(1\text{-mimi})](ClO_4)_2$

(**12**) 3-methylpentanedioic acid

(**13**) dimethyl 3-methylpentanedioate

(**14**) 1,5-bis(2-pyridyl)-3-methylpentane-1,5-dione

(**15**) 4´-methyl-2,2´:6´,2´´-terpyridine

(**16**) disiloxane-protected 2-deoxyribonolactone

(**17**) 4´-carboxyaldehyde-2,2´:6´,2´´-terpyridine

(**18**) 4´-hydroxymethyl-2,2´:6´,2´´-terpyridine

(**19**) 4´-bromomethyl-2,2´:6´,2´´-terpyridine

(**20**) DMTr-(S)-glycidol

(**21**) 1-deazapurine

(**22**) 1-deaza-9-methylpurine

(**23**) 1-deaza-7-methylpurine

(**24**) $[Hg(1\text{-deaza-9-methylpurine})_2](NO_3)_2 \cdot H_2O$

(**25**) Hoffer´s chlorosugar

(**26b** and **26a**) 1-deazapurine-N9-β(α)-[2´-deoxy-3´,5´-di-O-(p-toluoyl)-ribonucleoside

(**27b** and **27a**) 1-deazapurine-N7-β(α)-[2´-deoxy-3´,5´-di-O-(p-toluoyl)-ribonucleoside

(**28b** and **28a**) 1-deazapurine-N9-β(α)-2´-deoxyribonucleoside (**Y**)

(**29b** and **29a**) 1-deazapurine-N7-β(α)-2´-deoxyribonucleoside (**X**)

(**30**) 1,3-deazapurine-β-2´deoxyribonucleoside

(**31**) 1-deazapurine N9-β-[2´-deoxy-5´-O-(4,4´-dimethoxytrityl)-ribonucleoside]

(**32**) 1-deazapurine N7-β-[2´-deoxy-5´-O-(4,4´-dimethoxytrityl)-ribonucleoside]

(**33**) 1-deazapurine-N9-β-[2´-deoxy-3´-O-(2-cyanoethyl)-N,N-diisopropylphosphoramidite-5´-O-(4,4´-dimethoxytrityl)-ribonucleoside]

(**34**) 1-deazapurine-N7-β-[2´-deoxy-3´-O-(2-cyanoethyl)-N,N-diisopropylphosphoramidite-5´-O-(4,4´-dimethoxytrityl)-ribonucleoside]

(**35**) 1-deaza-N3-oxidepurine $\cdot H_2O$

(**36**) 1-deaza-N3-oxide-6-nitropurine

(**37**) 1-deaza-6-nitropurine

(**38b** and **38a**) 1-deaza-6-nitropurine-N9-β(α)-[2´-deoxy-3´,5´-di-O-(p-toluoyl)-ribonucleoside

(**39**) 1-deaza-6-nitropurine-N9-β-2´-deoxyribonucleoside

(**40**) 1-deazaadenine-N9-β-2´-deoxyribonucleoside (**Z**)

(**41**) 1-deaza-6-aminopurine

(**42**) 1-deaza-(6-benzoylamino)-purine-N9-β-[2´-deoxyribonucleoside] $\cdot H_2O$

(**43**) 1-deaza-(6-benzoylamino)-purine-N9-β-[2´-deoxy-5´-O-(4,4´-dimethoxytrityl)-ribonucleoside]

(**44**) 1-deaza-(6-benzoylamino)-purine-N9-β-[2´-deoxy-3´-O-(2-cyano-ethyl)-N,N-diisopropylphosphoramidite-5´-O-(4,4´-dimethoxy-trityl)-ribonucleoside]

(**45**) 1-deaza-(6-methoxyacetylamino)-purine-N9-β-[2´-deoxyribo-nucleoside] · 0.5H_2O

(**46**) 1-deaza-(6-methoxyacetylamino)-purine-N9-β-[2´-deoxy-5´-O-(4,4´-dimethoxytrityl)-ribonucleoside]

(**47**) 1-deaza-(6-methoxyacetylamino)-purine-N9-β-[2´-deoxy-3´-O-(2-cyanoethyl)-N,N-diisopropylphosphoramidite-5´-O-(4,4´-dimethoxytrityl)-ribonucleoside]

Oligonucleotides

(**a**) 5´-d(AAA AAA A**XX X**TT TTT TT)

(**b**) 5´-d(AAA AAA A**XX XX**T TTT TTT)

(**c**) 5´-d(AAA AAA A**X**A AAA AAA)

(**d**) 5´-d(TTT TTT T**X**T TTT TTT)

X = 1-deazapurine-N7-β(α)-2´-deoxyribonucleoside (**29b** and **29a**)

(**e**) 5´-d(C**YY YY**G)

(**f**) 5´-d(CGC G**Y**A T**Y**C GCG)

(**g**) 5´-d(AAA AAA A**Y**A AAA AAA)

(**h**) 5´-d(TTT TTT T**Y**T TTT TTT)

(**i**) 5´-d(**YYY YYY YYY YYY YYY Y**A)

(**j**) 5´-d(TTT TTT TTT TTT TTT TT)

Y = 1-deazapurine-N9-β(α)-2´-deoxyribonucleoside (**28b** and **28a**)

(**k**) 5´-d(A**ZZ ZZZ ZZZ** A)

(**l**) 5´-d(A**Z**A **Z**A**Z** A**Z**A)

(**m**) 5´-d(**ZZZ ZZZ ZZZ ZZZ ZZZ ZZZ Z**A)

(**n**) 5´-d(TTT TTT TTT TTT TTT TTT TT)

Z = 1-deazaadenine-N9-β-2´-deoxyribonucleoside (**40**)

4 Curriculum Vitae

Zur Person

Name	Polonius, Fabian-Alexander
Adresse	Rote Becker Str. 29 44141 Dortmund
Geburtsdatum	24.11.1980
Geburtsort	Hamburg
Eltern	Prof. Dr. med. Michael-J. Polonius, Klinikdirektor i. R. Gudrun Polonius-Neubert Ärztin
Nationalität	deutsch
Familienstand	ledig

Ausbildung

Promotion	seit 08/2002	Promotion Universität Dortmund Fachbereich Chemie, Prof. Dr. B. Lippert
Diplomarbeit	01-05/2002	BASF AG/ Ludwigshafen (Verfahrenstechnik/ Dr. M. Klumpe) „Improved Quinoline Synthesis“
Studium	1998-2002	Master of Chemistry (Industrial) University of Durham, U.K. College of St. Hild & St. Bede
	2001-2002	Durham University Athletic Union Representative of the College
	2001	full colours awarded by the College
	2000	half colours awarded by the College
Schule	1996-1998	Stowe School Buckingham, U.K.
	Leistungsfächer	Mathematik, Physik, Chemie
	1997-1998	Prefect of Stowe School
	1990-1996	Stadtgymnasium Dortmund
	1986-1990	Kerschensteiner Grundschule Dortmund

Praktika

2000	3 Wochen	Max-Planck Institut für Molekulare Physiologie Dortmund (Forschung)
1999	8 Wochen	Promacon Dr. Schirm AG/ Dortmund (Herstellung von Düngemitteln)
1998	5 Wochen	Krupp Uhde/ Dortmund (Chemie Anlagenbau)
1998	4 Wochen	Max-Planck Institut für Molekulare Physiologie/ Dortmund
1997	4 Wochen	Forschungslabor Bayer AG/ Wuppertal (Physikalische Chemie/ Analytik)

Besondere Kenntnisse

EDV-Kenntnisse	Microsoft Office, Chem Office, Mes Trec, Isotope, Origin Pro 7.0, Corel Draw
Fremdsprachen	Bilingual Englisch/ Deutsch Spanisch (Grundkentnisse)

Engagement

Sport		Ski- & Snowboard, Wandern, Klettern, Hockey
	1994-2004	Ehrenamtlicher Damen, Herren & Jugend-Trainer & Betreuer (TSC Eintracht Dortmund / Stowe School Buckingham, U.K./ St. Hild & St. Bede Hockey Club, U.K.)
Musik		Klavier